AD-A189 715　MODEL SELECTION FOR THE MULTIPLE MODEL ADAPTIVE　　1/4
　　　　　　　　ALGORITHM FOR IN-FLIGHT SIMULATION(U) AIR FORCE INST OF
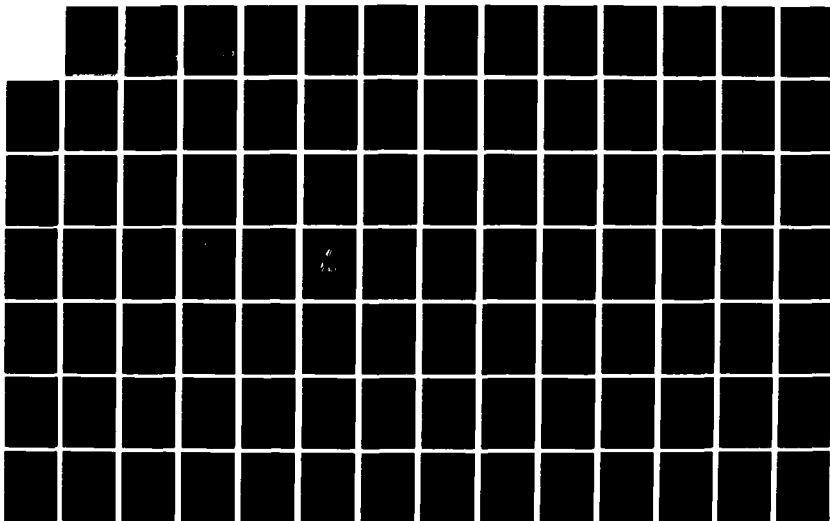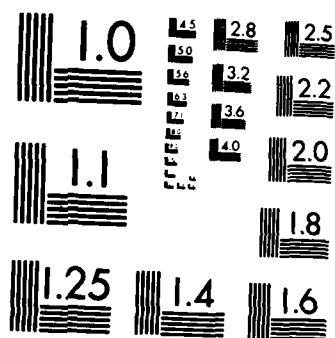　　　　　　　　TECH WRIGHT-PATTERSON AFB OH　J R MATHES DEC 87
UNCLASSIFIED　AFIT/GE/ENG/87D-40　　　　　　　　F/G 1/1　　　NL
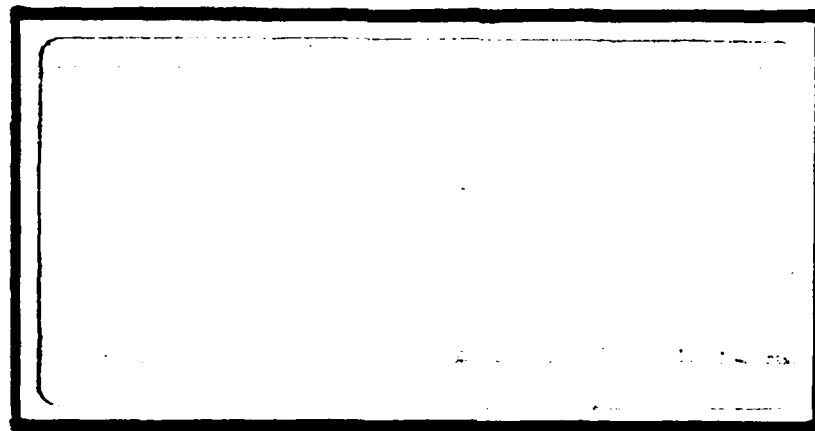
MICROCOPY RESOLUTION TEST CHART
NATIONAL BUREAU OF STANDARDS-1963-A

AD-A189 715

DTIC
ELECTE
MAR 0 7 1988
H

DEPARTMENT OF THE AIR FORCE
AIR UNIVERSITY
AIR FORCE INSTITUTE OF TECHNOLOGY

Wright-Patterson Air Force Base, Ohio

AFIT/GE/ENG/87D-40

MODEL SELECTION FOR THE MULTIPLE
MODEL ADAPTIVE ALGORITHM FOR
IN-FLIGHT SIMULATION

THESIS

James R. Matthes, Jr.
Captain, USAF

AFIT/GE/ENG/87D-40

DTIC
ELECTE
S
MAR 0 7 1988
H
D

AFIT/GE/ENG/87D-40

MODEL SELECTION FOR THE MULTIPLE

MODEL ADAPTIVE ALGORITHM FOR

IN-FLIGHT SIMULATION

THESIS

Presented to the Faculty of the School of Engineering

of the Air Force Institute of Technology

Air University

In Partial Fulfillment of the

Requirements for the Degree of

Master of Science in Electrical Engineering

James R. Matthes, Jr., B.S.

Captain, USAF

December 1987

Acknowledgments

The thesis represents the culmination of my AFIT experience. This effort was accomplished to a large degree by depriving myself of one of my favorite recreational pursuits -- sleep. Being cognizant of my limited ability, I realize that without the guidance and suggestions of my peers and professors this effort would have not been possible.

My special thanks are extended to the AFIT faculty members who patiently and expertly guided me through this research effort. The technical knowledge, suggestions, and dedication of my thesis advisor Professor John J. D'Azzo were instrumental in the success of this thesis. I also wish to express thanks to Professor Peter S. Maybeck for whom I have the utmost respect. His tireless reviews of the thesis drafts provided many constructive technical improvements to my thesis and enhanced my understanding of the material presented in this document.

Gratitude is also due to Captain Julio Velez and Lieutenant Tom Berens. The many stimulating and enlightening discussions we had were enjoyable and were an invaluable addition to this thesis.

ii

Table of Contents

List of Figures

List of Tables

AFIT/GE/ENG/87D-40

ABSTRACT

This thesis extends the research accomplished by Capt
Pineiro and Lt Berens in the area of adaptive algorithm
implementation. Specifically, this thesis explores the
performance characteristics of the multiple model estimation
algorithm and how they influence the selection of aircraft
models to allow the parameter adaptive control system to
maintain tracking performance over a desired portion of the
flight envelope. The aircraft dynamic equations used are
those of the AFTI/F-16 and the control law design is based
on the method developed by Professor Porter.

Numerous fixed gain simulations are presented in order
to determine the performance robustness to plant variations
of selected flight conditions. From these simulations,
performance or robustness boundaries for each nominal flight
condition are determined. Data is then generated to ascer-
tain the effect on the control surfaces' responses of re-
placing the nominal model of a performance boundary with
another model within the same boundary. That leads to the
determination of the critical factors to be considered in

choosing an aircraft model to represent a specific set of performance boundaries.

Following the determination of what factors are important in establishing performance bounds for a fixed gain system, model selection for the multiple model algorithm is evaluated. In attempting to select a set of aircraft models that would ensure an acceptable level of tracking performance over the desired flight envelope, several two-, three, and four-model configurations are examined. Each configuration is evaluated to determine the amount of overlap of performance bounds required for proper tracking performance, the amount of the flight envelope that is covered, and control surface performance.

After selecting a set of aircraft models that results in the best overall system response, the effect of adjusting the control law gains on the performance of the multiple model estimation algorithm is evaluated. By assuming that all states are accessible, sensor noise is then added to each of the longitudinal states to study how noise impacts model selection. A set of models that produces acceptable tracking performance over the desired flight envelope and the most immunity to sensor noise is then selected.

MODEL SELECTION FOR THE MULTIPLE
MODEL ADAPTIVE ALGORITHM FOR
IN-FLIGHT SIMULATION

1. Introduction

1.1 Overview

There are a large number of estimation and control
problems where algorithm design and implementation are de-
pendent on the modeling and evaluation of uncertain para-
meters. One such problem was analyzed by Capt Luis Pineiro
in his thesis, Parameter Adaptive Model Following For In
Flight Simulation (1). Pineiro's thesis documented the fact
that parameter adaptive control techniques can be implemen-
ted to allow a specific system to maintain a desired level
of tracking performance in the presence of plant parameter
changes. Lt Thomas Berens continued Pineiro's research by
implementing a multiple model algorithm (2) as the primary
parameter estimation technique. This estimation algorithm
allows the system to maintain tracking performance when the
plant has deviated considerably from the nominal condition.
This thesis extends Beren's research by investigating the
performance characteristics of the multiple model algorithm

1

and how they affect the selection of aircraft models that
will yield a desired level of tracking performance over a
specific portion of the flight envelope.

1.2 Background

Using the techniques developed by Professor Brian Porter
(3;4;5;6;7;8), Pineiro developed an adaptive, fast sampling
control law to compensate for changing aircraft parameters
of the Advanced Fighter Technology Integration F-16 (AFTI/F-
16) operating in a model following configuration. This
technique involved the use of on-line, recursive, step re-
sponse matrix identifiers to update the control law gains as
needed to account for plant parameter variations. Pineiro's
research was limited to the linearized, longitudinal, rigid
body dynamics of the AFTI/F-16 using perturbation equations
of motion at a nominal flight condition of 10,000 feet
altitude and Mach 0.9 (1).

In order to keep the computational loading and conver-
gence time to a minimum, Pineiro allowed only a small number
of parameters to be estimated (only four parameters were
adjustable out of 20) while retaining an accurate represen-
tation of the plant. The remaining parameters that were not
among those to be estimated were fixed at values representa-

tive of the current flight condition. The results of Pinei-

ro's research documented the fact that parameter-adaptive

control techniques can be implemented to allow a specific

system to maintain a desired level of tracking performance

in the presence of plant parameter changes (produced by

large changes in the stability derivatives)(1).

Capt Pineiro recommended that analysis of this research

area continue with the parameter adaptive algorithm extended

to include a multiple model estimator (1). In his thesis,

Lt Berens implemented such an estimation algorithm. The

multiple model algorithm implementation can be approached by

assuming that the uncertain parameters take on discrete

values within a possible range of parameter values. For

each flight condition a complete system model is designed

which produces an estimate of the selected parameters. Fol-

lowing the design of a bank of system models, each model is

weighted by the probability of that particular model being

correct and averaged with the outputs of all other models

(9).

1.3 Problem Statement

The purpose of this thesis is to extend the research

accomplished by Capt Pineiro and Lt Berens in the area of adaptive algorithm implementation. Specifically, this thesis explores the performance characteristics of the multiple model estimation algorithm, how they influence the selection of aircraft models, and how well they allow the system to maintain tracking performance over a desired portion of the flight envelope.

1.4 Summary of Current Knowledge

This section summarizes the current knowledge that is pertinent to this thesis effort. The areas of in-flight simulators, adaptive control, and multiple model adaptive estimation are examined in the *following paragraphs.*

1.4.1 In-Flight Simulators. An in-flight simulator is an aircraft that is able to fly with the same characteristics as another aircraft. While flying the simulator, the pilot actually experiences the flying qualities and feel of the aircraft that is being simulated (10).

The in-flight simulator has become an extremely important tool in the aircraft research and development process. As the cost of developing aircraft has increased, the benefits of in-flight simulation have become more pronounced.

4

In-flight simulation provides the capability to fly aircraft systems prior to committing to the full scale or production phases of the acquisition process. Another area in which the simulator has been extremely helpful is the area of experimental testing of aircraft. Investigations into flight control systems, aircraft flying qualities, and system integration have been addressed in detail with the advent of the in-flight simulator (11).

An advanced in-flight simulator designated as the Variable-Stabilty In-Flight Simulator Test Aircraft (VISTA) will be developed by the USAF. VISTA will be a high performance, supersonic, six degree of freedom simulator based on a two place fighter aircraft. By having a variable stability system, VISTA will be able to support a diverse range of aeronautical research in the fields of flight controls, handling qualities, and flying characteristics. It will also have the ability to simulate current, modified, or new aircraft (11).

Because VISTA will be able to operate over a large range of flight conditions, wide variations in the aircraft stability derivatives will be possible. Jones and Porter have shown that degradation in closed loop-system behavior will

5

inevitably occur in the case of large plant parameter chan-
ges and a fixed control law (3). To ensure that the simula-
tion is not degraded substantially due to inaccurate stabil-
ity derivatives, a model-following mode of operation may be
used. The term model-following means that the response
characteristics of the host aircraft are tailored to 'fol-
low' the responses of the simulated aircraft as generated by
a computer model (12).

1.4.2 Adaptive Control. Hartman and Krebs (13) have shown
that adaptive control is a method of maintaining desired
tracking performance throughout the flight envelope. In his
research, Pineiro's main objective was to implement a para-
meter adaptive control law that would compensate for the
degraded simulation performance that occurs when the sta-
bility derivatives of the host aircraft take on values which
have deviated considerably from the expected nominal values
(1).

The area of adaptive control has become an area of great
current interest in automatic control research. The reason
for this is that adaptive control is a technique that pro-
poses solutions when the system varies with time in a manner
that is not totally specifiable a-priori. This is in

contrast to the manner in which most automatic control

techniques afford solutions to time invariant systems (14).

The main benefit of adaptive control is that the system

parameters can be adjusted on-line as the system environment

changes. Hagglund (14) stated in his doctoral thesis, New

Estimation Techniques For Adaptive Control,

> The idea of adaptive control is to automate the
> analysis and design. Hence, an adaptive controller
> does not only control the process, but it also
> collects information about the process behaviour
> from the control signals and the measured output
> signals. Based on this information, or analysis,
> the controller parameters are adjusted on-line.

There are numerous schemes reported in the litera-

ture for parameter adaptive control, three of which are gain

scheduling, model reference control, and self tuning regula-

tors (15).

The actual concept of gain scheduling started with the

development of flight control systems. In fact, it is the

predominant method used in current aircraft to handle varia-

tions of parameters in flight control systems. Mach number

and dynamic pressure are measured and used as scheduling

variables. When the scheduling variables have been chosen,

the control parameters are evaluated at a number of opera-

ting conditions using an acceptable design method. The draw-
backs of gain scheduling are that it is an open loop compen-
sation method (no feedback is provided to correct for an
incorrect schedule, resulting in gains being implemented
which could degrade system performance or even result in
system instability) and the design is time consuming (15).

Model reference adaptive controllers try to obtain a
control behavior close to that of a reference model for a
given input signal. The disadvantage of this type of adap-
tive control is that if a fixed reference model is used, the
system will approach the behavior of the reference model as
opposed to the behavior of a proper model at the current
operating condition. The advantage of the model reference
system is that, when the operating condition is near the
fixed reference model and the input is one for which the
system has been designed, quick adaptation is possible
(16).

Another method of adaptively adjusting the parameters of
a system is to use a self tuning regulator (15), also refer-
red to as a parameter adaptive controller. It should be
noted that self tuning regulators are one form of a parame-
ter adaptive controller and are not equivalent to that

8

entire class. A block diagram of the self tuning regulator

used by Pineiro is shown in Figure 1-1 (1). The adaptive

controller has three different parts, the first of which

(see Figure 1-1) is the ordinary feedback loop formed by the

control algorithm (regulator) and the aircraft dynamics

(process). The input and output of the process are fed into

a parameter estimator which performs on-line estimation of
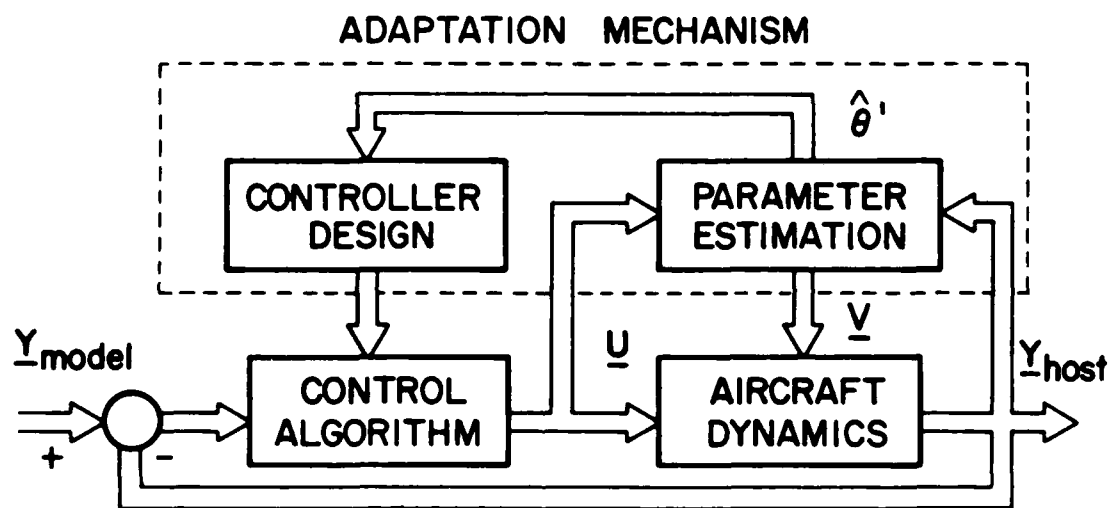
Figure 1-1. Parameter Adaptive Control System (1)

the parameters of the process. The estimated parameters are

then used to modify the controller gains by a design calcu-

lation. The term adaptation mechanism refers to the parame-

ter estimator and the design calculation (14). The host

aircraft dynamics for the adaptive controller designed by

Pineiro were the linearized, longtitudinal, rigid body dyna-

mics of the Advanced Fighter Technology Integration F-16 (AFTI/F-16). The signals that were used as tracking references (Y model in Figure 1-1) were the elevators and flaperons and the adaptive system outputs (Y host in Figure 1-1) were flight path angle and pitch rate (1).

The control algorithm and controller design that were implemented by Pineiro were the techniques developed by Professor Brian Porter (3;4;5;6;7;8). Porter and Jones have shown that on-line recursive identifiers can be used to provide updated step response matrices. Inclusion of these updated step response matrices in a digital proportional plus integral control law, results in highly effective adaptive digital set point tracking controllers for multivariable plants (3). Using these design techniques, Pineiro developed an adaptive control law to compensate for changing aircraft parameters of the AFTI/F-16 operating in a model following configuration. This technique involved the use of on-line, recursive, step response matrix identifiers to update the control law gains as needed to account for plant parameter variations.

As shown in Figure 1, the parameter adaptive controller also contains a recursive parameter estimator. Many estima-

tion schemes have been used, including stochastic approxima-
tion, least squares, extended and generalized least squares,
instrumental variables, extended Kalman filtering, and the
maximum likelihood method (15). A summary of the different
estimation methods is given in Ljung and Sodestrom (17).
The parameter identification algorithm used by Pineiro was a
modified recursive least squares algorithm developed by
Hagglund (1).

1.4.3 Multiple Model Adaptive Estimation (MMAE). In his
research, Berens continued Pineiro's effort by extending the
parameter adaptive algorithm to include a multiple model
estimator (2). MMAE is especially beneficial when the ap-
plication has parameters that can undergo large changes such
as is the case with the stability derivatives of the host
aircraft of an in-flight simulator (18). Multiple model
adaptation has been successfully applied to numerous prob-
lems including flight control problems (19).

Multiple model implementation can be approached by as-
suming that the uncertain parameters can take on discrete
values within a possible range of parameter values. A
complete system model is designed for each flight condition,

11

resulting in a bank of n system models. Based upon the

characteristics of the residuals generated for each of the n

system models, the correctness of each of the estimated

parameters is calculated iteratively from the conditional

probability for each of the n system models being the best

model to use. The conditional probability is determined

using the past measurement history. The closer the value of

the conditional probability is to one, the more weight is

placed on that given model's parameter estimates being cor-

rect. The parameter estimate of each system model is weight-

ed by the value of its probability, and the adaptive parame-

ter estimate is determined by the probabilistically weighted

average of all the system model outputs (9;18).

1.5 Assumptions

The assumptions in this thesis are those typically

adopted when using linearized longitudinal perturbation

equations. These assumptions are those used by Pineiro and

Berens and are listed below.

* The aircraft is a rigid body with constant mass.

* The atmosphere is fixed with respect to the earth.

12

* The earth's surface is an inertial reference frame.

* Linearization about an operating condition is valid for preliminary aircraft models.

* Aerodynamics are constant for Mach and altitude.

1.6 Approach

Using the control law design parameters and commanded inputs of flight path angle and pitch rate as given by Pineiro, numerous fixed gain simulations were accomplished in order to determine the performance robustness to plant variations, of selected flight conditions. From these simulations, performance or robustness boundaries for each nominal flight condition were determined. Data was then generated to ascertain the effect on the control surfaces' responses of replacing the nominal model of a performance boundary with another model within the same boundary on the control surfaces responses. That led to the determination of the critical factors to be considered in choosing an aircraft model to represent a specific set of performance bounds.

Following the determination as to what factors were important in establishing performance bounds for a fixed gain system, model selection for the multiple model algo-

13

rithm was evaluated. In attempting to select a set of aircraft models that would ensure an acceptable level of tracking performance over the desired flight envelope, several two-, three-, and four-model configurations were examined. (The term model configuration refers to the number of models that were explicitly implemented in the multiple model algorithms). Each configuration was evaluated to determine the amount of overlap of performance bounds required for proper tracking performance, the region of the flight envelope that was covered, and control surface performance.

After selecting a set of aircraft models that resulted in the best overall system response (discussed in a later section), the effect of adjusting the control law gains on the performance of the multiple model estimation algorithm was evaluated. By assuming that all states were accessible, sensor noise was then added to each of the longitudinal states to study how noise impacts model selection. A set of models that produced acceptable tracking performance over the desired flight envelope and the most immunity to sensor noise was then selected.

1.7 Overview

The material in this thesis begins in Chapter 2 with a description of the AFTI/F-16 and a presentation of the mathematical aircraft model. The actuator model is also discussed in Chapter 2. Chapter 3 contains a brief description of the multivariable design theory developed by Professor Brian Porter of the University of Salford, England. The multiple model estimation algorithm is discussed in Chapter 4 and model selection criteria are presented in Chapter 5. Chapter 6 presents the simulation results, and a discussion of conclusions and recommendations for future study is found in Chapter 7.

2. Aircraft Description and Models

2.1 AFTI/F-16 Description

Because the VISTA is still in the process of being developed and the aircraft dynamic equations are not available, the Advanced Fighter Technology Integration (AFTI)/F-16 was used as the host aircraft for the parameter adaptive control system. The reason for this choice is the anticipated similarity of the AFTI and proposed VISTA. The AFTI/F-16 aircraft, shown in Figure 2-1, is an F-16A air superiority fighter modified to be a testbed for evaluating new aircraft technologies (20). These modifications include the addition of two vertical canards which are mounted on the engine inlet, control surfaces that allow independent motion of the trailing edge flaps and independent motion of the horizontal tail halves, and a redundant, digital fly-by-wire flight control system. The AFTI/F-16's mission is very important in that the technologies tested on it may be incorporated in the Air Force's future fighter aircraft.

The unaugmented AFTI/F-16 aircraft is statically unstable in the longitudinal axis for subsonic flight. The reason this condition exists is that the center of gravity
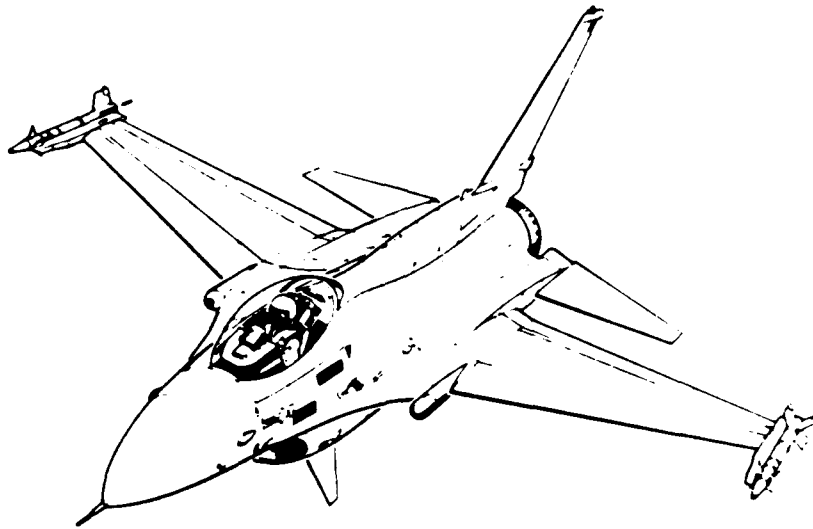
Figure 2-1. The AFTI/F-16

is located behind the aircraft's center of pressure. The

instability, manifested by an unstable short period mode,

allows the aircraft to withstand higher load factors and

reduces drag,thereby enhancing maneuverability. Additional-

ly, the aircraft has a lightly damped dutch roll mode.

Therefore, the flight control system has a twofold purpose:

to stabilize the aircraft longitudinally and to improve the

dutch roll damping (20).

In addition to being able to perform conventional ma-

neuvers such as pitching longitudinally, rolling laterally,

and turning with zero sideslip, the AFTI/F-16 can also

perform unconventional maneuvers that require decoupling of

the aircraft's modes of responses. These unconventional

maneuvers include pitch-pointing, yaw-pointing, and lateral

and longitudinal translation. Conventional and decoupled maneuvers can also be blended, which gives the AFTI/F-16 an even wider array of possible maneuvers (20).

The control surfaces that are used to maneuver the AFTI/F-16, as well as the definitions of positive surface deflections, are shown in Figure 2-2. The surfaces include left and right horizontal tail halves, left and right flaperons, left and right canards, and the rudder. The horizontal tail halves have a dual function in that they can be deflected symmetrically as elevators to pitch the aircraft, or they can be deflected asymmetrically to augment rolling. Likewise, the flaperons can be deflected symmetrically to function as conventional flaps or asymmetrically to function as ailerons to control roll. The canards can be used in a snow plow configuration to function as a speedbrake or they can be used to provide sideforces on the aircraft. As in a conventional aircraft, the rudder is used for yawing. The surfaces used in this thesis are shown in heavy black in Figure 2-2 and include the left and right tail halves and the left and right flaperons.
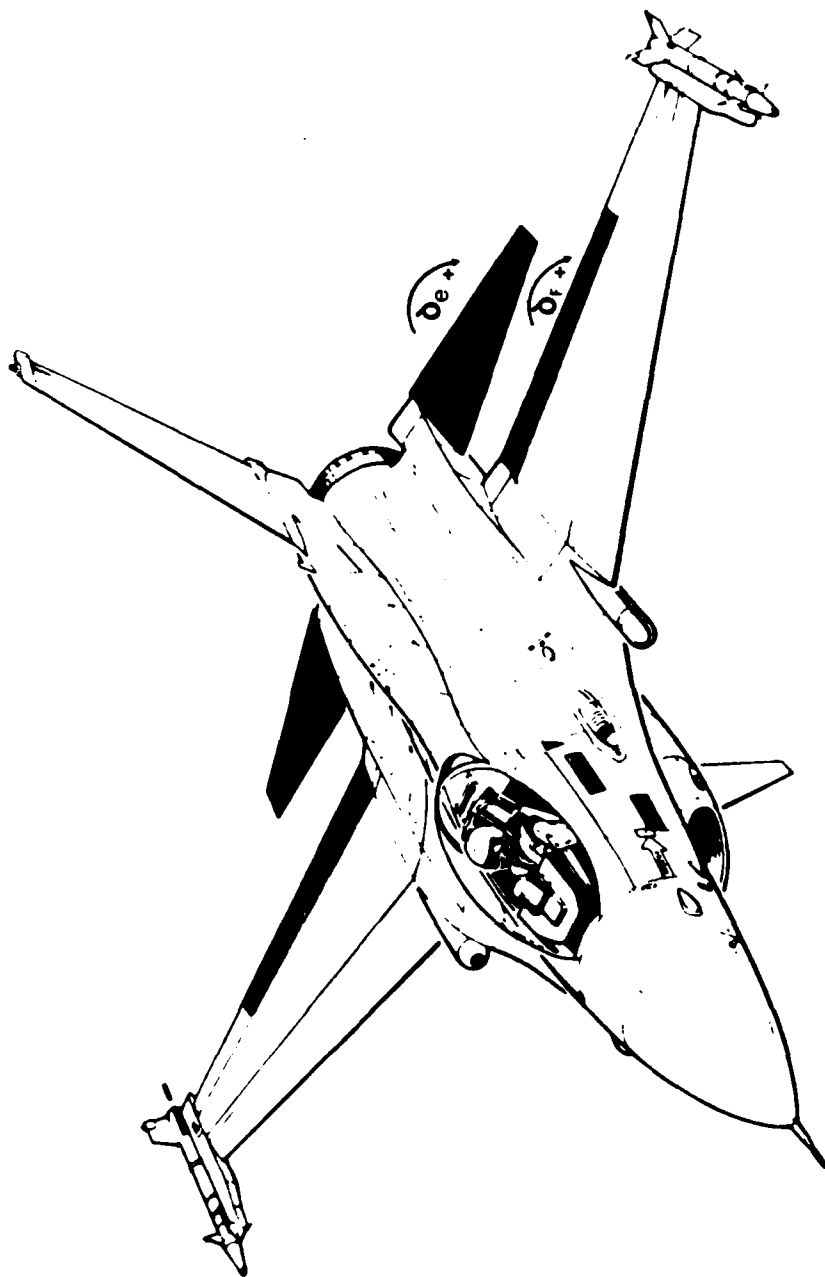
Figure 2-2. AFTI/F-16 Control Surfaces and Definition of Positive Deflections

2.2 Aircraft Models

2.2.1 State Space Model.
The aircraft is modeled by a set
of first order differential equations in the state space
form

$$\dot{\underline{x}} = \underline{A}\underline{x} + \underline{B}\underline{u} \qquad (2-1)$$

The state equations are perturbation equations about a trim
condition and are derived from the aircraft equations of
motion which consist of forces at the center of gravity and
moments with reference to the body axis. Detailed deriva-
tions of the longitudinal state perturbation equations used
in this thesis are presented in a thesis by Barfield (21).

Equation (2-2) shows the longitudinal axis state space
model for the AFTI/F-16. The primed terms in Equation (2-2)
are dimensionalized derivatives (Appendix A) in the body

$$
\begin{bmatrix} \dot{\theta} \\ \dot{u} \\ \dot{\alpha} \\ \dot{q} \end{bmatrix}
=
\begin{bmatrix} 0 & 0 & 0 & 1 \\ X'_\theta & X'_u & X'_\alpha & X'_q \\ Z'_\theta & Z'_u & Z'_\alpha & Z'_q \\ M'_\theta & M'_u & M'_\alpha & M'_q \end{bmatrix}
\begin{bmatrix} \theta \\ u \\ \alpha \\ q \end{bmatrix}
+
\begin{bmatrix} 0 & 0 \\ X'_{\delta e} & X'_{\delta f} \\ Z'_{\delta e} & Z'_{\delta f} \\ M'_{\delta e} & M'_{\delta f} \end{bmatrix}
\begin{bmatrix} \delta e \\ \delta f \end{bmatrix}
\qquad (2-2)
$$

where

20

θ is pitch angle

u is forward velocity

α is angle of attack

q is pitch rate

δ_e is the total elevator where both horizontal tail halves deflect symmetrically

δ_f is the total flap where both flaperons deflect symmetrically

axis. The definition of the body axis along with the positive directions of forces, moments, and angles are found in Figure 2-3.

A Flight Dynamics Laboratory aerodynamic data package for the AFTI/F-16 was used to obtain linearized aerodynamic coefficients and dimensionalized derivatives by trimming the aircraft at various flight conditions. Aircraft weight and inertias were common to all flight conditions and were also provided by the program (see Appendix A).

This thesis is concerned with that portion of the flight envelope which ranges in altitude from 10,000 to 38,000 feet and from 0.25 to 0.9 in Mach number. This portion of the flight envelope is shown graphically in Figure 2-4. The specific flight conditions considered in the envelope of interest are listed in Table 2-1. The
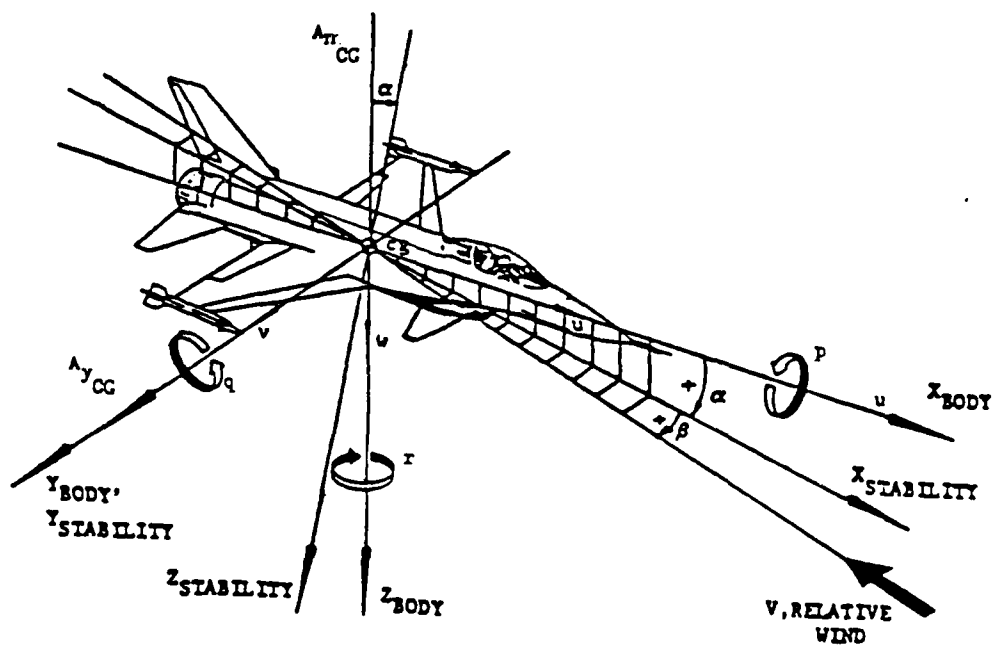
Figure 2-3. Positive Directions of Forces, Moments,
and Angles in Body Reference Frame

22
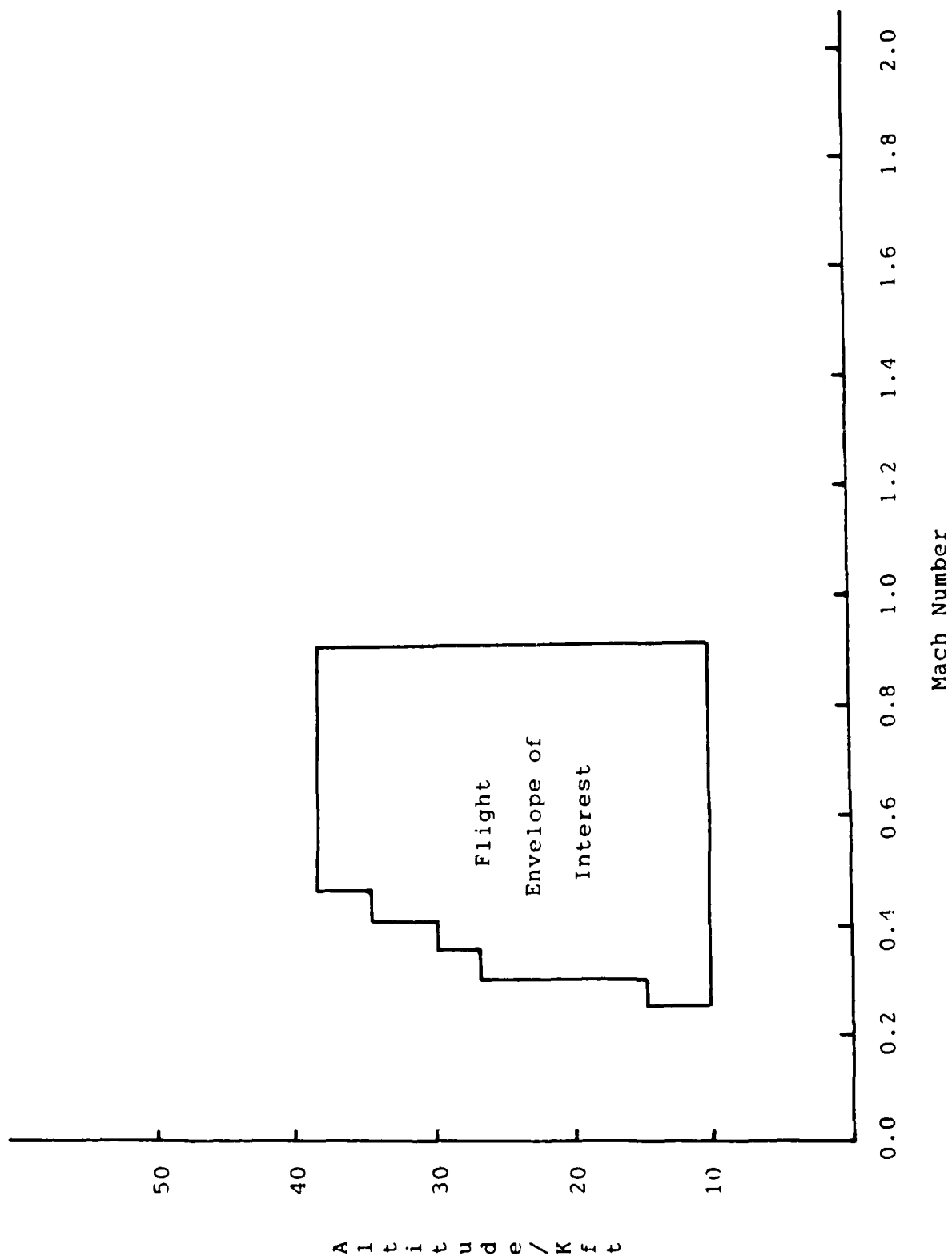
Figure 2-4. Flight Envelope of Interest

23

Table 2-1.

Flight Conditions of Interest

Alt (kft)	Mach No.	Alt (kft)	Mach No.	Alt (kft)	Mach No.
38	0.45	26	0.40	18	0.85
38	0.50	26	0.45	18	0.90
38	0.55	26	0.50	14	0.25
38	0.60	26	0.55	14	0.30
38	0.65	26	0.60	14	0.35
38	0.70	26	0.65	14	0.40
38	0.75	26	0.70	14	0.45
38	0.80	26	0.75	14	0.50
38	0.85	26	0.80	14	0.55
38	0.90	26	0.85	14	0.60
34	0.40	26	0.90	14	0.65
34	0.45	22	0.30	14	0.70
34	0.50	22	0.35	14	0.75
34	0.55	22	0.40	14	0.80
34	0.60	22	0.45	14	0.85
34	0.65	22	0.50	14	0.90
34	0.70	22	0.55	10	0.25
34	0.75	22	0.60	10	0.30
34	0.80	22	0.65	10	0.35
34	0.85	22	0.70	10	0.40
34	0.90	22	0.75	10	0.45
30	0.35	22	0.80	10	0.50
30	0.40	22	0.85	10	0.55
30	0.45	22	0.90	10	0.60
30	0.50	18	0.30	10	0.65
30	0.55	18	0.35	10	0.70
30	0.60	18	0.40	10	0.75
30	0.65	18	0.45	10	0.80
30	0.70	18	0.50	10	0.85
30	0.75	18	0.55	10	0.90
30	0.80	18	0.60		
30	0.85	18	0.65		
30	0.90	18	0.70		
26	0.30	18	0.75		
26	0.35	18	0.80		

24

longitudinal dimensionalized derivatives for each of the
flight conditions listed in Table 2-1 have been obtained
using the Flight Dynamics Laboratory's AFTI/F-16 aerodynamic
data package. A state space model for each flight condition
is formed by inserting the proper dimensionalized deriva-
tives into Equation (2-1). Appendix A presents the state
space models for each of the flight conditions.

An output vector, $\underline{y}$, is defined for the model in Equa-
tion (2-1) in order to command desired maneuvers. The
output vector is added to the state space aircraft model
with an output matrix, $\underline{C}$. The aircraft model state and
output equations then take the form of

$$\dot{\underline{x}} = \underline{A}\underline{x} + \underline{B}\underline{u} \qquad (2-3)$$

$$\underline{y} = \underline{C}\underline{x}$$

The output vector used in this study is the same vector as
that used by Pineiro (1) and Berens (2) in which flight path
angle and pitch rate are commanded. Flight path angle is
given by

$$\gamma = \theta - \alpha \qquad (2-4)$$

Because pitch angle, pitch rate, and angle of attack

25

are state variables, flight path angle and pitch rate are easily included in the model by placing unit elements with the proper signs in the appropriate positions in the $\underline{C}$ matrix. This results in an output equation

$$
\begin{bmatrix} \gamma \\ q \end{bmatrix} = \begin{bmatrix} 1 & 0 & -1 & 0 \\ 0 & 0 & 0 & 1 \end{bmatrix} \begin{bmatrix} \Theta \\ u \\ \alpha \\ q \end{bmatrix}
\tag{2-5}
$$

2.2.2 Autoregressive Difference Equation Model.

The AFTI/F-16 plant state and output equations of Equation (2-3) may be discretized for a sampling period T by using the relationships

$$
\begin{bmatrix} \Phi_{11} & \Phi_{12} \\ \Phi_{21} & \Phi_{22} \end{bmatrix} = \exp \left[\begin{bmatrix} \underline{A}_{11} & \underline{A}_{12} \\ \underline{A}_{21} & \underline{A}_{22} \end{bmatrix} T \right]
\tag{2-6}
$$

and

$$
\begin{bmatrix} \underline{\Psi}_1 \\ \underline{\Psi}_2 \end{bmatrix} = \int_0^T \exp \left[\begin{bmatrix} \underline{A}_{11} & \underline{A}_{12} \\ \underline{A}_{21} & \underline{A}_{22} \end{bmatrix} t \right] \begin{bmatrix} 0 \\ \underline{B}_2 \end{bmatrix} dt
\tag{2-7}
$$

The resulting sampled data state and output equations become

26

$$
\begin{bmatrix} \underline{x}_1\{(k+1)T\} \\ \underline{x}_2\{(k+1)T\} \end{bmatrix} = \begin{bmatrix} \Phi_{11} & \Phi_{12} \\ \Phi_{21} & \Phi_{22} \end{bmatrix} \begin{bmatrix} \underline{x}_1(kT) \\ \underline{x}_2(kT) \end{bmatrix} + \begin{bmatrix} \Psi_1 \\ \Psi_2 \end{bmatrix} \underline{u}(kT) \qquad (2\text{-}8)
$$

and

$$
\underline{y}(kT) = [\underline{C}_1 \qquad \underline{C}_2] \begin{bmatrix} \underline{x}_1(kT) \\ \underline{x}_2(kT) \end{bmatrix} \qquad (2\text{-}9)
$$

Pineiro showed (Appendix B) that the input-output relation-
ship of Equations (2-8) and (2-9) can be expressed in terms
of an Nth order autoregressive vector difference equation of
the form

$$
\underline{y}(kT) = \underline{B}_1 \underline{u}\{(k-1)T\} - \underline{A}_1 \underline{y}\{(k-1)T\} + \ldots\ldots\ldots \qquad (2\text{-}10)
$$
$$
+ \underline{B}_n \underline{u}\{(k-N)T\} - \underline{A}_n \underline{y}\{(k-N)T\} + \underline{e}(kT)
$$

or equivalently

$$
\underline{y}(kT) = \underline{\Upsilon}^T \underline{\Theta}(kT) + \underline{e}(kT) \qquad (2\text{-}11)
$$

where the equation error vector $\underline{e}(kT)$ is assumed to be a
zero-mean Gaussian white-noise vector with covariance $\underline{A}_e$,
$\underline{\Upsilon}(k^T) \in R^{m \times \ell}$ is a matrix of past values of $\underline{y}$ and $\underline{u}$, the
matrices $\underline{A}_i \in R^{m \times m}$ $(1=1,2,\ldots,N)$, $\underline{B}_i \in R^{m \times m}$ $(i=1,2,\ldots,N)$
and the vector $\underline{\Theta} \in R^{\ell}$ are the parameters of the Nth order
difference equation, m is equal to the number of inputs and

ℓ is equal to the number of parameters in the difference

equation. For the case AFTI/F-16 longitudinal aircraft

model of Equation (2-3), the parameter vector $\underline{\Theta}$ consists

of a column vector of 20 elements which are unique for a

given flight condition.

2.3 Actuator Model

Consideration of control surface position and rate

limits is important in the design of a realistic control

system. The actuator transfer function model for both the

elevator and the flaperon surfaces are first order models of

the form

$$T_{actuator}(s) = \frac{44}{(s+44)} \qquad (2-12)$$

The control surface position and rate limits used in this

study are those given in Pineiro's thesis and are found in

Table 2-2. The position limits assume that the elevator and

flaperon have a trimmed position of zero degrees. Due to

the fact that each flight condition has a different nonzero

trim value of elevator and flaperon position, the surface

position limits are adjusted accordingly for each point.

28

Table 2-2.

Control Surface Position and Rate Limits

Surface	Position Limit (deg)	Rate Limit (deg/sec)
Elevators	+25	90
Flaperons	+20 −23	78

The position limits for each flight condition are found in Appendix C.

2.4 Summary

This section presents the mathematical development of the equations describing the AFTI/F-16. The AFTI/F-16 is chosen as the plant due to the non-availibility of similar equations for the VISTA. The autoregressive difference equation representing an equivalent state space representation of the aircraft is also presented, along with the flight conditions considered in this thesis.

3. Control Law Algorithm

3.1 Introduction

This chapter describes the control algorithm that is implemented in the parameter adaptive control system as shown in Figure 1-1. The control law should be such that the plant is able to follow the time response generated by a computer model of the vehicle being simulated. The multi-variable control algorithm used in this thesis is that developed by Professor Brian Porter of the University of Salford, England. Porter's method employs output feedback with high-gain error-actuated controllers. Output feedback may be advantageous since state variables may be difficult to measure.

3.2 Model Following Technique (1)

One method of achieving in-flight simulation is through the implementation of the model following concept (12). A model following in-flight simulation scheme uses the signals from the evaluation pilot's cockpit as inputs to an aircraft computer which simulates the equations of motion of the desired aircraft. The output of the same aircraft computer

is comprised of the time histories that describe the responses of the simulated aircraft to the inputs from the evaluation pilot. The variable stability system has the responsibility of manuevering the control surfaces of the host aircraft so that the aircraft response at the pilot's station is the same as those of the emulated airplane. Obviously, achieving satisfactory model following performance depends on having an accurate knowledge of the host aircraft's stability derivatives.

The dynamics of the host vehicle can be represented by a differential equation of the form

$$\dot{\underline{x}}_h(t) = \underline{A}_h \underline{x}_h(t) + \underline{B}_h \underline{u}_h(t) \qquad (3-1)$$

and the dynamics of the vehicle to be simulated can be represented by

$$\dot{\underline{x}}_m(t) = \underline{A}_m \underline{x}_m(t) + \underline{B}_m \underline{u}_m(t) \qquad (3-2)$$

where $\underline{A}_h$, $\underline{A}_m$, $\underline{B}_h$, $\underline{B}_m$ are matrices that contain the stability derivatives, $\underline{x}_h$ and $\underline{x}_m$ are the states of the respective differential equations, $\underline{u}_h$ and $\underline{u}_m$ are the required control surface deflection, and the subscripts h and m signify the host and model aircraft, respectively.

31

By substituting the states and the rate of change of the states of the model into Equation (3-1), a control law for exact model following can be obtained by solving for the control input $\underline{u}_h(t)$:

$$\dot{\underline{x}}_m(t) = \underline{A}_h \underline{x}_m(t) + \underline{B}_h \underline{u}_h(t) \tag{3-3}$$

Assuming $\underline{B}_h$ is invertible and solving for $\underline{u}_h(t)$ leads to

$$\underline{u}_h(t) = \underline{B}_h^{-1} \dot{\underline{x}}_m(t) - \underline{B}_h^{-1} \underline{A}_h \underline{x}_m(t) \tag{3-4}$$

$$\underline{u}_h(t) = \underline{K}_1 \dot{\underline{x}}_m(t) - \underline{K}_2 \underline{x}_m(t) \tag{3-5}$$

From Equations (3-4) and (3-5) it can be seen that the control inputs to the host aircraft are defined in terms of the states of the model and the first derivative of those states. Also, Equations (3-4) and (3-5) show that accurate stability derivatives are required to have good model following performance. As shown in Figure 3-1, the states and
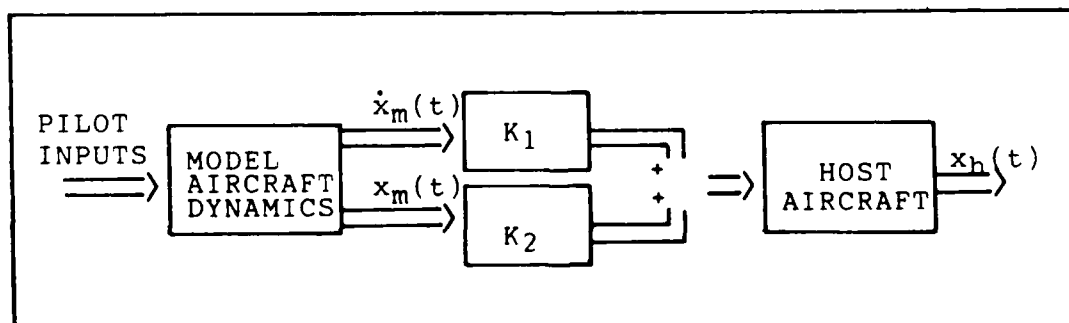
Figure 3-1. Explicit Model Following System (1)

32

rates of change of the states are available from
the variable stability system's computer that contains the
model aircraft dynamics.

Figure 3-2 shows an improved explicit model following
system. Notice that there is a feedback loop containing a
gain matrix $\underline{K}_h$ around the plant. The purpose of this feed-
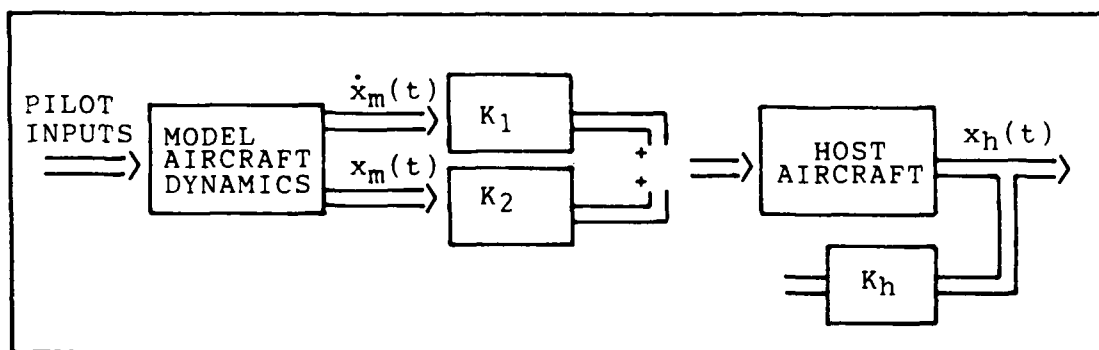
Figure 3-2. Improved Explicit Model Following System (1)

back loop is to reduce the sensitivity of the explicit model
following system (see Figure 3-1) to plant parameter varia-
tions.

With the inclusion of the feedback loop the feedforward
gains become

$$\underline{K}_1 = \underline{B}_h^{-1} \tag{3-6}$$

$$\underline{K}_2 = \underline{B}_h^{-1}\underline{A}_h - \underline{K}_h \tag{3-7}$$

33

If

$$\underline{K}_h \quad >> \quad \underline{B}_h^{-1} \underline{A}_h \qquad\qquad (3\text{-}8)$$

then the feedback loop becomes increasingly tighter which makes the system less dependent on $\underline{K}_1$ (less sensitive to plant parameter variations).

3.3 Porter's Control Law (1)

The multivariable control law used in this thesis to achieve model following was developed by Professor Brian Porter. Porter developed a control law that can be used to make the plant follow the responses generated by a computer model of the vehicle to be simulated. This section presents Porter's control law.

The host aircraft in this thesis is completely con-trollable and observable, and is described by the continuous time state space model

$$\dot{\underline{x}}(t) = \underline{A}\,\underline{x}(t) + \underline{B}\,\underline{u}(t) \qquad\qquad (3\text{-}9)$$

$$\underline{y}(t) = \underline{C}\,\underline{x}(t) \qquad\qquad (3\text{-}10)$$

where

$\underline{A}$ = continuous plant matrix (n x n)

34

$\underline{B}$ = continuous input control matrix (n x m)
having a rank "m"

$\underline{C}$ = continuous output matrix (ℓ x n)

$\underline{y}$ = output vector with ℓ outputs

$\underline{u}$ = input vector with m inputs

$\underline{x}$ = state variable vector with n states

For the linearized, longitudinal dynamics of the AFTI/F-16, the state variable vector has 4 states as described in Chapter 2:

Θ = pitch

u = forward velocity

α = angle of attack

q = pitch rate

The input vector consists of 2 inputs

δ_e = elevator

δ_f = flaperons

The 2 elements of the output vector are

γ = flight path angle

q = pitch rate

In using Porter's design method, it is desirable to
partition the state equations so that $\underline{B}_2$ and $\underline{C}_2$ are square
$(m \times m)$ and $(\ell \times \ell)$ matrices, respectively. This process
yields

$$\begin{bmatrix} \dot{\underline{x}}_1(t) \\ \dot{\underline{x}}_2(t) \end{bmatrix} = \begin{bmatrix} \underline{A}_{11} & \underline{A}_{12} \\ \underline{A}_{21} & \underline{A}_{22} \end{bmatrix} \begin{bmatrix} \underline{x}_1(t) \\ \underline{x}_2(t) \end{bmatrix} + \begin{bmatrix} 0 \\ \underline{B}_2 \end{bmatrix} \underline{u} \qquad (3-11)$$

and

$$\underline{y}(t) = [\underline{C}_1 \quad \underline{C}_2] \begin{bmatrix} \underline{x}_1(t) \\ \underline{x}_2(t) \end{bmatrix} \qquad (3-12)$$

where it is required that the number of inputs to the system
equal the number of outputs, $m = \ell$. This requirement ensures
that the column dimension of $\underline{B}$ equals the row dimension of
$\underline{C}$. In equation (3-12) the elements associated with $\underline{x}_1(t)$
and $\underline{x}_2(t)$ are

$$\underline{x}_1(t) = [\; \Theta \;] \qquad (3-13)$$

$$\underline{x}_2(t) = [\; u \; \alpha \; q \;] \qquad (3-14)$$

The plant of Equations (3-11) and (3-12) is defined as
regular if the matrix, $\underline{CB}$, has full rank "m". The input
output configuration of this thesis provides for a regular
design. For regular plants with stable transmission zeros,

36

the control law is a discrete proportional-plus-integral

(PI) output feedback control law (see Figure 3-3) expressed

as

$$\underline{u}(kT) = (1/T) [\underline{K}_1 \underline{e}(kT) + \underline{K}_2 \underline{z}(kT)] \qquad (3-15)$$

and

$$\underline{u}(t) = \underline{u}(kT) \text{ for } t \in [kT, (k+1)T] \qquad (3-16)$$

where

$\underline{r}(kT)$ is the sampled reference tracking signal

k is an integer

$T = (1/f)$ is the sampling period

$\underline{K}_1$ and $\underline{K}_2$ are the (m x m) controller matrices

$\underline{e}(kT)$ is the error vector $[\underline{e}(kT) = \underline{r}(kT) - \underline{y}(kT)]$

$\underline{z}(kT)$ is the digital integral of the error vector
$[\underline{z}((k+1)T) = \underline{z}(kT) + T\underline{e}(kT)]$

When $\underline{CB}$ does not have full rank, the plant is

labeled as irregular and a proportional-plus integral-plus

derivative (PID) controller structure may be implemented

(6;7).

3.3.1 Fixed Gain Controller Matrices.

The continuous time state equations given in Equations

(3-11) and (3-12) can be discretized for the sampling period

37
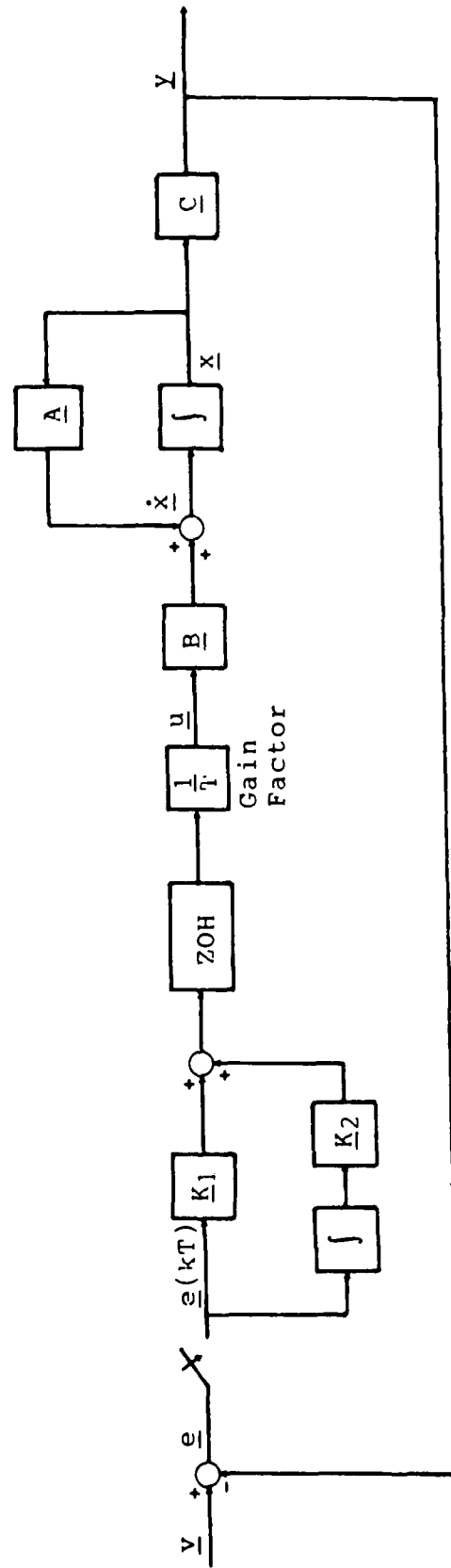
Figure 3-3. System Block Diagram - Discrete Design

38

T by using

$$\begin{bmatrix} \underline{\Phi}_{11} & \underline{\Phi}_{12} \\ \underline{\Phi}_{21} & \underline{\Phi}_{22} \end{bmatrix} = \exp\left\{ \begin{bmatrix} \underline{A}_{11} & \underline{A}_{12} \\ \underline{A}_{21} & \underline{A}_{22} \end{bmatrix} T \right\} \qquad (3\text{-}17)$$

and

$$\begin{bmatrix} \underline{\Psi}_1 \\ \underline{\Psi}_2 \end{bmatrix} = \int_0^T \exp\left\{ \begin{bmatrix} \underline{A}_{11} & \underline{A}_{12} \\ \underline{A}_{21} & \underline{A}_{22} \end{bmatrix} t \right\} \begin{bmatrix} 0 \\ \underline{B}_2 \end{bmatrix} dt \qquad (3\text{-}18)$$

The resulting sampled data state and output equations for the plant are

$$\begin{bmatrix} \underline{x}_1\{(k+1)T\} \\ \underline{x}_2\{(k+1)T\} \end{bmatrix} = \begin{bmatrix} \underline{\Phi}_{11} & \underline{\Phi}_{12} \\ \underline{\Phi}_{21} & \underline{\Phi}_{22} \end{bmatrix} \begin{bmatrix} \underline{x}_1(kT) \\ \underline{x}_2(kT) \end{bmatrix} + \begin{bmatrix} \underline{\Psi}_1 \\ \underline{\Psi}_2 \end{bmatrix} \underline{u}(kT) \qquad (3\text{-}19)$$

and

$$\underline{y}(kT) = [\underline{C}_1 \quad \underline{C}_2] \begin{bmatrix} \underline{x}_1(kT) \\ \underline{x}_2(kT) \end{bmatrix} \qquad (3\text{-}20)$$

The augmented closed-loop state and output equations for the control law of equation (3-15) are (8)

$$\begin{bmatrix} \underline{z}\{(k+1)T\} \\ \underline{x}_1\{(k+1)T\} \\ \underline{x}_2\{(k+1)T\} \end{bmatrix} = \begin{bmatrix} \underline{I}_m & -T\underline{C}_1 & -T\underline{C}_2 \\ f\underline{\Psi}_1\underline{K}_2 & \underline{\Phi}_{11}-f\underline{\Psi}_1\underline{K}_1\underline{C}_1 & \underline{\Phi}_{12}-f\underline{\Psi}_1\underline{K}_1\underline{C}_2 \\ f\underline{\Psi}_2\underline{K}_2 & \underline{\Phi}_{21}-f\underline{\Psi}_2\underline{K}_1\underline{C}_2 & \underline{\Phi}_{22}-f\underline{\Psi}_2\underline{K}_1\underline{C}_2 \end{bmatrix} \begin{bmatrix} \underline{z}(kT) \\ \underline{x}_1(kT) \\ \underline{x}_2(kT) \end{bmatrix}$$

$$+ \begin{bmatrix} T\underline{I}_m \\ f\underline{\Psi}_1\underline{K}_1 \\ f\underline{\Psi}_2\underline{K}_1 \end{bmatrix} \underline{r}(kT) \qquad (3\text{-}21)$$

and

$$\underline{y}(kT) = [\underline{0} \quad \underline{C}_1 \quad \underline{C}_2] \begin{bmatrix} \underline{z}(kT) \\ \underline{x}_1(kT) \\ \underline{x}_2(kT) \end{bmatrix} \quad (3-22)$$

A transformation block diagonalizes equations (3-21) and (3-22) as

$$\begin{bmatrix} \bar{\underline{x}}_1\{(k+1)T\} \\ \bar{\underline{x}}_2\{(k+1)T\} \end{bmatrix} = \begin{bmatrix} \bar{\underline{A}}_1 & \underline{0} \\ \underline{0} & \bar{\underline{A}}_4 \end{bmatrix} \begin{bmatrix} \bar{\underline{x}}_1(kT) \\ \bar{\underline{x}}_2(kT) \end{bmatrix} + \begin{bmatrix} \bar{\underline{B}}_1 \\ \bar{\underline{B}}_2 \end{bmatrix} \underline{r}(kT) \quad (3-23)$$

$$\underline{y}(kT) = [\bar{\underline{C}}_1 \quad \bar{\underline{C}}_2] \begin{bmatrix} \bar{\underline{x}}_1(kT) \\ \bar{\underline{x}}_2(kT) \end{bmatrix} \quad (3-24)$$

where

$$\bar{\underline{x}}_1(kT) = \begin{bmatrix} \underline{z}(kT) \\ \underline{x}_1(kT) \end{bmatrix} \quad (3-25)$$

$$\bar{\underline{x}}_2(kT) = \underline{x}_2(kT) \quad (3-26)$$

$$\bar{\underline{C}}_1 = [\underline{K}_1^{-1}\underline{K}_2 , \quad \underline{0}] \quad (3-27)$$

$$\bar{\underline{C}}_2 = \underline{C}_2 \quad (3-28)$$

$$\bar{\underline{A}}_1 = \begin{bmatrix} \underline{I}_m - T\underline{K}_1^{-1}\underline{K}_2 & \underline{0} \\ T\underline{A}_{12}\underline{C}_2^{-1} \underline{K}_1^{-1} \underline{K}_2 & \underline{I}_{n-m} + \underline{A}_{11}T - T\underline{A}_{12}\underline{C}_2^{-1} \underline{C}_1 \end{bmatrix} \quad (3-29)$$

$$\bar{\underline{B}}_1 = \begin{bmatrix} \underline{0} \\ T\underline{A}_{12}\underline{C}_2^{-1} \end{bmatrix} \quad (3-30)$$

$$\bar{\underline{A}}_4 = [\underline{I}_m - \underline{B}_2\underline{K}_1\underline{C}_2] \quad (3-31)$$

$$\bar{\underline{B}}_2 = [\underline{B}_2\underline{K}_1] \quad (3-32)$$

40

As the sampling frequency is increased, the closed-loop transfer function takes on the asymptotic form (23)

$$\underline{G}(z) = \underline{G}_1(z) + \underline{G}_2(z) \qquad (3-33)$$

where z is the discrete transform operator and

$$\underline{G}_1(z) = \bar{\underline{C}}_1(z\underline{I}_n - \underline{I}_n - T\underline{A}_o)^{-1}T\underline{B}_o \qquad (3-34)$$

$$\underline{G}_2(z) = \bar{\underline{C}}_2(z\underline{I}_m - \underline{I}_m - \underline{A}_4)^{-1}\underline{B}_4 \qquad (3-35)$$

with

$$\underline{A}_o = \begin{bmatrix} \underline{K}_1^{-1}\underline{K}_2 & 0 \\ \underline{A}_{12}\underline{C}_2^{-1}\underline{K}_1^{-1}\underline{K}_2 & \underline{A}_{11} - \underline{A}_{12}\underline{C}_2^{-1}\underline{C}_1 \end{bmatrix} \qquad (3-36)$$

$$\underline{B}_o = \begin{bmatrix} 0 \\ \underline{A}_{12}\underline{C}_2^{-1} \end{bmatrix} \qquad (3-37)$$

$$\underline{A}_4 = \begin{bmatrix} -\underline{B}_2\underline{K}_1\underline{C}_2 \end{bmatrix} \qquad (3-38)$$

In Equations (3-33), (3-34), and (3-35), $\underline{G}_1(z)$ and $\underline{G}_2(z)$ are the slow and fast mode transfer functions respectively. The slow modes contain two sets of eigenvalues Z_1 and Z_2 which are given by the equations

$$Z_1 = \{z \in C: \det\{z\underline{I}_m - \underline{I}_m + T\underline{K}_1^{-1}\underline{K}_2\} = 0\} \qquad (3-39)$$

$$Z_2 = \{z \in C: \det\{z\underline{I}_{n-m} - \underline{I}_{n-m} - T\underline{A}_{11} + T\underline{A}_{12}\underline{C}_2^{-1}\underline{C}_1\} = 0\} \qquad (3-40)$$

41

The fast mode eigenvalues are given by

$$Z_3 = \{z \in C: \det\{z\underline{I}_m - \underline{I}_m + \underline{C}_2\underline{B}_2\underline{K}_1\} = 0\} \qquad (3-41)$$

Because of the form of $\underline{A}_o$, $\underline{B}_o$, and $\underline{C}_1$, the eigenvalues of $\underline{A}_o$ are uncontrollable or unobservable. Therefore, as the sampling frequency increases, the slow transfer function asymptotically approaches zero and the overall system transfer function contains only the fast modes, as given in $\underline{G}_2(z)$, which can be expressed in the equivalent form

$$G(z) = \underline{G}_2(z) = (z\underline{I}_m - \underline{I}_m + \underline{C}_2\underline{B}_2\underline{K}_1)^{-1}\underline{C}_2\underline{B}_2\underline{K}_1 \qquad (3-42)$$

The desired fixed gain controller matrices $\underline{K}_1$ and $\underline{K}_2$ are then given by

$$\underline{K}_1 = [\underline{C}_2\underline{B}_2]^{-1}\underline{\xi} \qquad (3-43)$$

$$\underline{K}_2 = \rho\underline{K}_1 \qquad (3-44)$$

where ρ is a positive scalar greater than zero and assigns the ratio of proportional to integral control, and $\underline{\xi}$ is a diagonal tuning matrix. The diagonal elements of $\underline{\xi}$ determine the weighting effect of a particular error signal on the respective control input. Hence, selection of the di-

42

agonal weighting matrix elements can be altered to achieve desired tracking characteristics.

3.3.2 Adaptive Controller Matrices.

To avoid performance degradation in the presence of large plant parameter variations, Porter has shown (3;4;5;6;7) that by incorporating fast on-line recursive identifiers which provide updated step-response matrices, satisfactory response characteristics can be acheived. The significance of using the step response matrix is that it can be obtained from real time input-output measurements to reflect the current characteristics of the plant, thus forming the basis for an adaptive system.

The discrete step response matrix is defined as (4)

$$\underline{H}(T) = \int_0^T \underline{C} \exp(\underline{A}t) \underline{B} \, dt \qquad (3-45)$$

For small sampling periods $\underline{H}(T) \cong T\underline{CB}$, and the control law design equation becomes

$$\underline{u}(kT) = \bar{\underline{K}}_1 \underline{e}(kT) + \bar{\underline{K}}_2 \underline{z}(kT) \qquad (3-46)$$

where

$$\bar{\underline{K}}_1 = \underline{H}^{-1}(T)\underline{\xi} \qquad (3-47)$$

$$\bar{\underline{K}}_2 = \rho \bar{\underline{K}}_1 \qquad (3-48)$$

43

Equations (3-47) and (3-48) show that for the case of
plants with variable parameters, updated step response ma-
trices need to be provided to the control-law design equa-
tions. This requirement can be achieved due to the fact
that the step response matrix can be obtained from real time
input-output data reflecting the current plant. Thus, by
using the step response matrix, an adaptive control system
can be designed to track plants with variable parameters.
The elements of the step response matrix for the control law
equation (3-47) can be obtained by expressing the state and
output equations ((3-19) and (3-20)) as an Nth order autore-
gressive difference equation, as shown in Chapter 2, of the
form

$$\underline{y}(kT) = \underline{B}_1 \{\underline{u}(k-1)T\} - \underline{A}_1 \underline{y}\{(k-1)T\} + \ldots$$
$$+ \underline{B}_n \underline{u}\{(k-N)T\} - \underline{A}_n \underline{y}\{(k-N)T\} + \underline{e}(kT) \qquad (3-49)$$

or

$$\underline{y}(kT) = \Upsilon^T(kT)\underline{\theta} + \underline{e}(kT) \qquad (3-50)$$

where the equation error vector $\underline{e}(kT)$ is assumed to be a
zero-mean Gaussian white-noise vector, $\Upsilon^T(kT) \in R^{m \times l}$ is the
measurement matrix consisting of past values of $\{\underline{y}_k\}$ and

44

$\{\underline{u}_k\}$, the matrices $\underline{A}_i \in R^{m \times m}$ (i=1,2,...N), $\underline{B}_i \in R^{m \times m}$ (i=1,2,..N), and the vector $\underline{\theta} \in R^l$ are the parameters of the Nth order difference equation.

It can be shown that, by using the definition of the step response matrix, the following equation can be derived

$$\underline{H}(T) = \underline{B}_1 \cong TC\underline{B} \qquad (3-51)$$

Equation (3-51) clearly shows that by identifying $\underline{B}_1$ in real-time using input-output data, updated step-response matrix estimates can be provided for the control law design equation, (3-47). From Equation (3-49), it can be seen that $\underline{B}_1$ can be identified as a set of parameters in the parameter vector $\underline{\theta}$.

3.4 Summary

This chapter briefly presents the concept of model following in-flight simulation and discusses a control law design technique that can be used to accomplish model following. The design technique discussed is the Porter method, and both fixed gain and adaptive controller gains matrices are presented. Finally, the method of adaptively updating the controller gain matrices via the parameters of

45

an autoregressive difference equation are presented. The

next chapter discusses in detail the parameter estimation

algorithm used in this thesis.

4. Parameter Estimation

4.1 Introduction

This chapter details the algorithm, used in this thesis, that allows the process parameters to be identified. Due to the fact that the stability derivatives change as the aircraft operates through varying flight conditions, a parameter identification algorithm is required that estimates the time varying parameter vector $\underline{\Theta}(t)$. In his thesis, Pineiro incorporated a modified recursive least squares algorithm developed by Hagglund (14) to account for time varying parameters. In order to minimize the number of parameters to be identified, Pineiro fixed some parameters that were not used in the control law and were assumed to be constant about a nominal flight condition. Thus, the number of parameters estimated by the estimation algorithm was reduced to four.

In an attempt to decrease the parameter estimation convergence time required to estimate the complete set of plant model parameters, Berens (2) implemented a multiple model algorithm parameter estimation technique in lieu of the modified recursive least squares algorithm used by Pineiro.

47

The algorithm discussed in this chapter and used in this
thesis is the multiple model parameter estimation technique
which was presented by Wittenmark (24) and implemented by
Berens. The manner in which models are to be selected for
the multiple model algorithm, to provide satisfactory track-
ing performance in the flight envelope of interest, is the
primary emphasis of this thesis.

4.2 Multiple Model Algorithm

The multiple model adaptive algorithm is a parameter
estimation technique which can yield satisfactory parameter
estimates over a desired parameter space. By selecting a
discrete number of parameter values that are dispersed
throughout the region of expected parameter space and incor-
porating them as a-priori data, the multiple model estima-
tion algorithm provides a method of discriminating which of
the a-priori models is nearest to the true parameter value.

The multiple model algorithm defines the parameter
vector as a random variable whose conditional probability
density function can be approximated as a weighted sum of
Dirac delta functions. The weights that are associated with

48

each of the a-priori models are dependent on the fit of a given model to the current real-world condition and are updated from modeling errors generated for each candidate model.

As is discussed earlier, the parameter vector, $\underline{\Theta}(kT)$, is composed of the coefficients of an autoregressive difference equation. Each flight condition has a parameter vector associated with it and hence becomes the source of the a-priori information required by the multiple model algorithm. The candidate model parameter vectors are designated as

$$\underline{\Theta}_i(kT) \quad i = 1,2,\ldots N \qquad (4-1)$$

where N is the number of candidate models being considered.

One method of estimating $\underline{\Theta}(kT)$ is to form a weighted sum of a-priori models as given by the equation

$$\underline{\Theta}(kT) = \sum_{i=1}^{N} a_i(kT)\underline{\Theta}_i(kT) \qquad (4-2)$$

where $a_i(kT)$ is a weighting factor associated with a particular candidate model. The conditions on the weighting factors are given by

$$0 \le a_i(kT) \le 1 \qquad (4-3)$$

49

and

$$\sum_{i=1}^{N} a_i(kT) = 1 \qquad (4-4)$$

From the above equations, estimating the parameter vector $\underline{\Theta}(kT)$ becomes a matter of properly choosing the weighting factors, $a_i(kT)$, associated with each candidate model, which in turn are dependent on the fit of the associated model.

Iserman and Lachman (25) present a list of quantities that give information as to which candidate model parameter vector, $\underline{\Theta}_i(kT)$, provides the best fit of the parameter vector associated with the actual flight condition. These quantities include

1) The parameter covariance matrices

$$\underline{P}_i(kT) = E\{(\underline{\Theta}(kT) - \underline{\Theta}_i(kT))(\underline{\Theta}(kT) - \underline{\Theta}_i(kT))^T\}, \; \underline{P}_i(kT) \in R^{m \times m}$$
$$\text{for } i=1,2,\ldots$$

2) The covariance of the prediction error

$$\underline{A}_{ie}(kT) = E\{\underline{e}_i(kT)\underline{e}_i^T(kT)\}, \; \underline{A}_{ie}(kT) \in R^{m \times m}$$

3) The autocorrelation function

$$\underline{\psi}_{ee}(kT,\tau) = E\{\underline{e}_i(kT)\underline{e}_i^T(kT+\tau)\}, \; \underline{\psi}_{ee}(kT,\tau) \in R^{m \times m}$$

4) The crosscorrelation function

$$\underline{\psi}_{ue}(kT,\tau) = E\{\underline{u}(kT)\underline{e}_i^T(kT+\tau)\}, \; \underline{\psi}_{ue}(kT,\tau) \in R^{m \times m}$$

50

As shown in this thesis, the multiple model algorithm as given by Wittenmark (24) utilizes the variance of the prediction error as the method of determining the best model fit.

The multiple model algorithm (9,18,19,24) provides a method of blending a-priori information with parameter estimation to formulate a weighting factor for each candidate model. As stated earlier, this approach views $\underline{\Theta}(kT)$ as a random vector that has a conditional probability density function approximated as a weighted sum of Dirac delta functions. The quantities that affect the shape of the approximated probability density function are the mean vector, covariance and the weighting factors associated with each of the individual models of the multiple model algorithm.

The mean of each individual distribution is the a-priori model parameter values themselves. The covariance of each distribution is the corresponding parameter covariance matrix, $\underline{P}_i(kT)$, which, as shown later, does not need to be directly estimated. The weighting factors, $a_i(kT)$, are selected via a Bayesian approach and are calculated based on the assumption that the residuals of the best fitting model

to the true model are zero mean white Gaussian. This obser-
vation can be used to test which model best fits the input/
output data. Assuming an a-priori distribution, $p(\underline{\theta}_i | \underline{y}(0))$,
for each model (if there is no a-priori knowledge the as-
sumption can be made that all models are equally probable,
i.e. $p(\underline{\theta}_i | \underline{y}(0))=1/N$, a conditional probability can be
calculated and updated following a measurement by the equa-
tions as given by Wittenmark (24)

$$p(\underline{\theta} | \underline{y}(kT)) = p(\underline{\theta} | \underline{y}(kT), \underline{y}(k-1)T) \qquad (4-5)$$

$$= \frac{p(\underline{y}(kT) | \underline{\theta}, \underline{y}((k-1)T)) p(\underline{\theta} | \underline{y}((k-1)T))}{p(\underline{y}(kT) | \underline{y}((k-1)T))} \qquad (4-6)$$

where

$$p(\underline{y}(kT) | \underline{\theta}, \underline{y}((k-1)T)) = (2\pi \underline{A}_{ie}(kT))-1/2 * E \qquad (4-7)$$

and

$$E = \exp\{-.5\underline{e}_i^T(kT)(\underline{A}_{ie}(kT))^{-1}\underline{e}_i(kT)\}$$

Therefore the weighting coefficients, $a_i(kT)$, take the form
of

$$a_i(kT)=Ca_i((k-1)T)[\underline{A}_{ie}(kT)]^{-1/2}\exp\{-.5\underline{e}_i^T(kT)(\underline{A}_{ie})^{-1}\underline{e}_i(kT)\}$$
$$(4-8)$$

where C is a normalization factor, such that

$$\sum_{i=1}^{N} \{a_i(kT)\} = 1 \tag{4-9}$$

$$\underline{\Theta}(kT) = \sum_{i=1}^{N} \{a_i(kT)\underline{\Theta}_i(kT)\} \tag{4-10}$$

and $\underline{e}_i$ is the residual generated by the ith model and $\underline{A}_{ie}$ is the prediction error covariance. Multiple model algorithm weighting coefficient update equations similar to those presented above are given by Maybeck (9) and Andersson (26).

4.2.1 Prediction Error. To define the error associated with a specific candidate model (the ith model), the prediction error or residual is defined from Equation (2-11) as

$$\underline{e}_i(kT) = \underline{y}(kT) - \Upsilon^T(kT)\underline{\Theta}_i(kT) \tag{4-11}$$

The parameter error is defined as

$$\Delta\underline{\Theta}_i(kT) = \underline{\Theta}_i(kT) - \underline{\Theta}(kT) \tag{4-12}$$

where $\underline{\Theta}(kT)$ is the best fitting model parameter vector. By incorporating Equation (4-12) into Equation (4-11), the prediction error becomes

$$\underline{e}_i(kT) = \underline{y}(kT) - \Upsilon^T(kT)\underline{\Theta}(kT) - \Upsilon^T(kT)\Delta\underline{\Theta}_i(kT) \tag{4-13}$$

The first two terms on the right hand side of Equation

(4-13) represent the error introduced by actuator and sensor

noise as well as the error due to linear approximation

errors. The third term is an additional modeling error term

induced by the model not being the best fitting model.

4.2.2 __ Prediction_Error_Covariance.__ As can be seen in

Equation (4-8), the multiple model algorithm as given by

Wittenmark (24) utilizes the covariance of the prediction

error as the method of determining the best model fit.

Berens (2) showed that an estimate of the prediction error

covariance is given by

$$A_{ie}(kT) \sim (1/k)(\sum_{ii=1}^{k} e_i(ii)*e_i^T(ii)) \qquad (4-14)$$

Equation (4-14) is an ergodic approximation to the true

ensemble average and assumes e_i is zero-mean.

The prediction error covariance of systems with gene-

ralized inputs is slowly time varying. Old values of

$A_{ie}(kT)$ are discarded exponentially by replacing Equation

(4-14) with a recursive fading memory filter (9),

$$\underline{A}_{ie}(kT) \sim j \, \underline{A}_{ie}((k-1)T) + (1-j)\underline{e}_i(kT)\underline{e}_i^T(kT) \quad (4-15)$$

54

where

$$0 < j < 1$$

Small j corresponds to short memory and j large corresponds
to long memory.

The performance of Equation (4-15) is restricted by the
fact that the prediction error covariance, $\underline{A}_{ie}(kT)$, is as-
sumed to vary slowly with time. When the time varying
assumption is violated, the performance of Equation (4-15)
can be enhanced by low pass filtering of the input, $\underline{u}(kT)$,
and the output, $\underline{y}(kT)$ (discussed in Section 4.3). From
Equations (4-11) and (4-14), it can be seen that $\underline{A}_{ie}(kT)$ is
a function of $\Upsilon(kT)$. It is shown earlier that $\Upsilon(kT)$ is
formed entirely of past values of $\underline{u}(kT)$ and $\underline{y}(kT)$. There-
fore, by reducing the high frequency variation in $\underline{u}(kT)$ and
$y(kT)$ via low pass filtering, high frequency variation in
$\underline{A}_{ie}(kT)$ is also reduced.

4.3 Multiple Model Parameter Estimator

The multiple model parameter estimator which incor-
porates a-priori information for use in in-flight simulation
is shown in Figure 4-1 (9). As discussed earlier, the a-

priori information is in the form of a set of autoregressive

difference equation model parameters which describe the air-

craft operating at a specific flight condition. Figure 4-1

shows that the a-priori information is stored in a bank of

parallel secondary, or elemental, estimators. Each of the
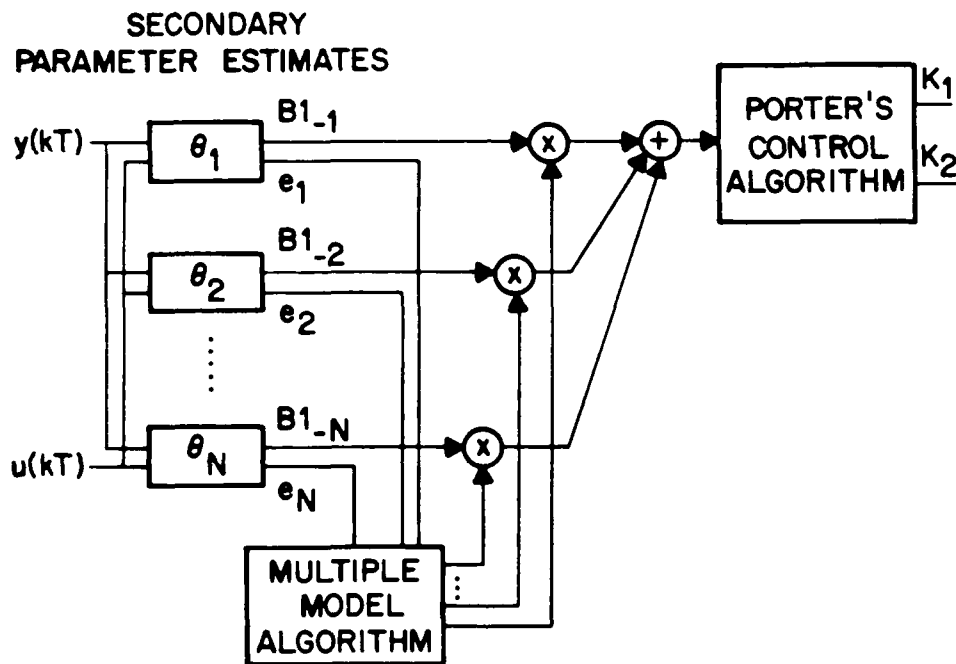
Figure 4-1. Multiple Model Parameter Estimator

secondary estimators is also referred to as a model in the

bank and is designed for a specific flight condition. The

prediction error from each of the secondary estimators is

used by the multiple model algorithm to form a primary (also

referred to as adaptive or composite) estimate of the best

fitting model parameters. The primary estimates are then

used to update the control law gains.

The secondary parameter estimation task can be accomplished by incorporating one of several different recursive estimation techniques such as recursive least squares or Hagglund's algorithm. The number of parameters to be estimated by the recursive parameter estimation routine is also a design option. The secondary estimator may be chosen to estimate all, some (as in Pineiro's simulation), or none of the parameters.

A number of problems become apparent if the secondary parameter estimators are allowed to update all the parameters recursively at every sampling period. As the number of inputs, outputs, and the order of the autoregressive difference equation increases, the computational effort may become impractical due to long convergence and computation time. Also, as the number of parameters to be updated increases, the system requires more excitation for parameter convergence (17).

To reduce the computational effort afforded by full scale secondary parameter estimation and to decrease the convergence time, the secondary estimators may be allowed to estimate part of the parameter vector while the remaining

57

parameters are assumed to be fixed at a nominal flight condition. At times, this assumption may not be satisfactory and in fact it may preclude convergence to the proper model.

Secondary parameter estimation can be avoided altogether by leaving all of the parameters in each secondary estimator fixed at a nominal flight condition. This method requires relatively little computational effort and provides good estimates of the parameter vector, especially when a robust control law is being implemented. Fixed secondary parameter estimation is the method incorporated in this thesis.

Three filters are incorporated into the system shown in Figure 1-1 to smooth variations in the parameter estimates. The first is a digital band pass filter which filters $y(k)$ and $\underline{u}(k)$. The low frequency components of the input-output signals must be removed to reduce parameter estimate bias, while high frequency signal components are removed to smooth input excitation (27). The filter is implemented as a sixth-order butterworth digital bandpass filter (2,28). A second non-linear filter is added to the weighting coefficients within the multiple model algorithm. The purpose of this filter is to smooth sudden changes in the model proba-

bilities that could result in destabilizing rapid changes in the primary parameter estimates. Therefore, the rate at which the weighting coefficients can change in a given sampling period is controlled by a rate limiting filter (2). The third filter is a low pass filter that filters the primary parameter estimates before they are implemented by the control law.

4.4 Summary

This chapter presents the multiple model estimation algortihm that was used in this thesis. The equations used to evaluate the weighting coefficients for the correctness of candidate models are presented as well as the overall implementation of the multiple model adaptive estimator. The next chapter presents important factors to be considered when selecting models for the multiple model estimation algorithm in the context of achieving desired tracking performance over a desired parameter space.

5. Model Selection Criteria

5.1 Introduction

Because the aircraft can maneuver through a continuum of different flight conditions, an infinite number of state space system models of the aircraft are possible. The large number of system models that would be required to characterize all sets of potential parameters could not be implemented in a realistic control system due to the computational burden that would be imposed as well as having a limited amount of computer memory available. To alleviate this situation, the multiple model algorithm with a discrete set of system models to represent the region of selected parameter space can be implemented. (The parameter space for this thesis is defined in Chapter 2 and is shown in Figure 2-4.) Selecting a discrete number of models to represent a continuous parameter space means that the actual values of the parameters do not correspond exactly to one of the models but are close to one. Therefore, the models must be 'close' enough to one another to ensure that the selected model is indeed representative of the actual flight condition.

However, the system models cannot be 'too close' or

difficulties occur with the multiple model algorithm. If the system models are such that the difference between measurement data and the model predicted values is not significant for more than one model, then selection of the 'proper' model cannot take place. As shown in Chapter 4, the multiple model algorithm generates a residual for each of the system models which is then passed on to be processed by the hypothesis conditional probability computation (see Figure 4-1). The algorithm performance depends on the fact that system models that are not representative of the current flight condition have large residuals, while those models that are near the true flight condition have small residuals. Therefore, it can be seen that a careful choice of system models must be made. The selected models must be close, but not too close. This chapter presents the criteria upon which model placement was based to allow the multiple model algorithm to select the model nearest the actual flight condition.

5.2 Performance Boundaries

The performance of an actual physical system can only be approximated by an appropriate mathematical model. The degree that a mathematical model represents an actual system

61

to depends on the model uncertainties that are present at a given instant in time. These model uncertainties can arise in several ways, including parameter variations or incorrectly modeled dynamics. Both stability and satisfactory performance are of prime concern in the face of these modelling uncertainties (29).

In designing a feedback control system, a model (referred to as the nominal model) must be selected from the set of available models to represent the plant's behavior. When a design has been performed with a specific nominal model, it is obvious that modelling errors are present when there is any deviation of the plant model from the nominal design model. A system is labeled as robust with respect to these modelling errors when the feedback control system remains stable when the nominal plant model is replaced by another plant without altering the controller (21).

Banda and Ridgely (29) point out that there are two types of robustness; stability robustness and performance robustness. Stability robustness occurs when the closed-loop system remains stable in the presence of plant variations. Performance robustness is present when the performance of the closed-loop system is acceptable in the face of

such variations. This chapter is primarily concerned with the issue of performance robustness.

Obviously, if a single control system possesses enough performance robustness, the entire flight envelope shown in Figure 2-4 could be approximated with a single nominal model. In any case, a given nominal model has a region of performance robustness that is associated with it as shown in Figure 5-1. This performance robustness region indicates that satisfactory system performance is achieved when the nominal plant is replaced by any plant model within the
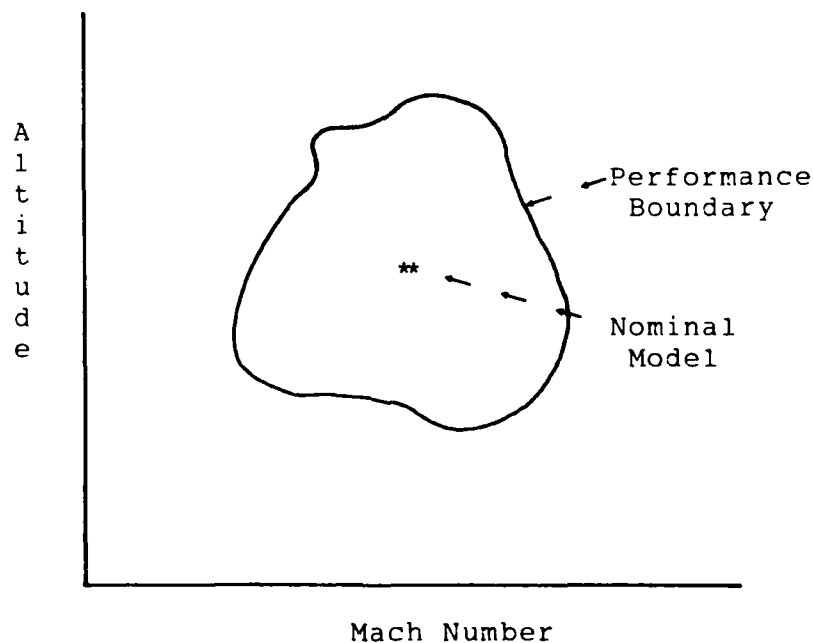
Figure 5-1. Region of Performance Robustness

region encompassed by the performance boundary (see Figure 5-1).

Recall that an aircraft state space model can be represented by a autoregressive difference equation

$$y(kT) = \underline{\Upsilon}^T(kT)\underline{\Theta}(kT) + \underline{e}(kT) \qquad (5-1)$$

where $\underline{\Theta}$ contains the parameters of the difference equation. In Chapter 3, it is shown that the control law gains are given by

$$\underline{K}_1 = \underline{H}^{-1}(T)\xi \qquad (5-2)$$

$$\underline{K}_2 = \rho\,\underline{K}_1 \qquad (5-3)$$

where the step response matrix is

$$\underline{H}(T) = \underline{B}_1 \qquad (5-4)$$

and $\underline{B}_1$ can be identified as a subset of the parameter vector $\underline{\Theta}$. Each flight condititon has a unique parameter vector associated with it and hence a unique step response matrix. Therefore, it can be, seen from Equations (5-2) and (5-3), that each model has a specific set of gains associated with it (assuming the tuning matrix $\underline{\xi}$ and the parameter ρ remain

64

constant).

In determining a performance boundary for a specific nominal model, the control law gains remain fixed at the values that are determined by the nominal model's parameter vector. By replacing the nominal plant model with other models and driving the closed-loop system with the commanded inputs outlined in Chapter 2, the performance boundary can be established for a given performance criteria. Hence, plant models that are outside the performance boundary fail to meet the desired performance criteria, while those models inside the boundary yield acceptable closed-loop performance.

The performance criteria used in this thesis are the criteria found in the VISTA statement-of-work and are also the criteria used by Pineiro and Berens. The criteria for tracking performance require that the average response error absolute value should not exceed the average absolute value of ten percent of the reference signal. The time-average response error absolute value is given by

$$1/t \int_{0.01}^{t} (\text{cmd input} - \text{output}) \, dt \qquad (5\text{-}5)$$

where

$$t = time$$

$$cmd\ input = commanded\ input$$

The time-average value of ten percent of the reference

signal is

$$1/t \int_{0.01}^{t} 0.1 * cmd\ input\ dt \qquad (5-6)$$

For satisfactory closed-loop tracking response to be

accomplished over the flight envelope of interest, the per-

formance boundaries of the required number of models must

overlap as shown in Figure 5-2. This requirement is due to

the fact that if the operating point lies outside the per-

formance boundaries, the multiple model algorithm assigns

probabilites to the respective models that result in control

law gains that cause the closed loop system to not meet the

performance criteria. From Figure 5-2, it can be seen that

there is a minimum number of models that will result in the

performance boundaries totally covering the desired flight

envelope. This thesis addresses the formation of perfor-

mance boundaries, the number of models required to yield
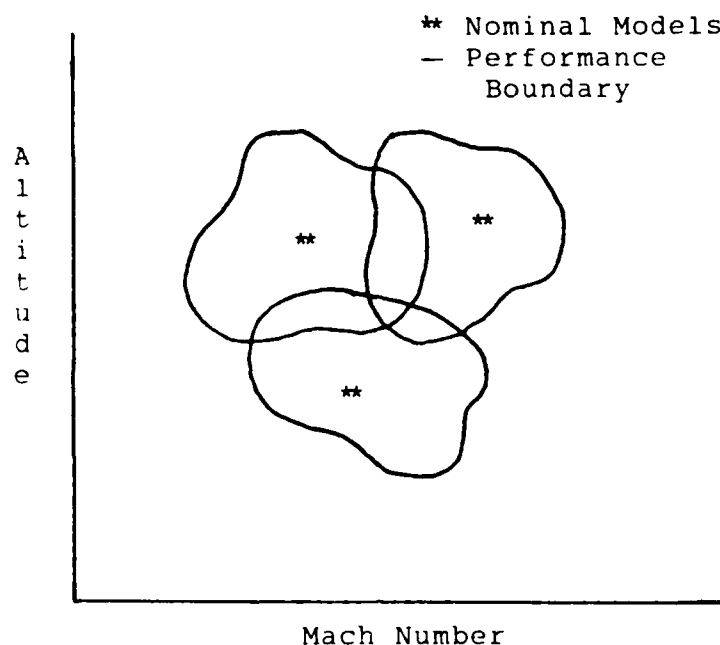
Figure 5-2.   Overlapping of Performance Boundaries

acceptable tracking performance over the flight envelope,

and the amount of overlapping of the performance boundaries

that the multiple model algorithm requires.

5.3 Sensor Noise Effects

By simple algebraic manipulation of the autoregressive

difference equation, it was shown in Chapter 4 that the

prediction error is defined as

$$\underline{e}(kT) = y(kT) - \underline{\Upsilon}^{T}(kT)\underline{\theta}(kT) \qquad (5-7)$$

Therefore, the prediction error covariance becomes

$$E(\underline{e}(kT)\underline{e}^T(kT)) = \underline{A}_e \qquad (5-8)$$

If the operating point of a fixed gain system (de-
scribed above) is the nominal plant model, then the predic-
tion error variance (assuming no sensor noise) is due to the
modeling error introduced when representing a continuous
system with an autoregressive difference equation. When
sensor noise is present, then the prediction error variance
is composed of the linear approximation errors just men-
tioned and the error introduced by addition of the sensor
noise.

As shown in Chapter 4, the multiple model algorithm
assigns a conditional probability to each candidate model
based on the calculated value of each model's prediction
error covariance. When selecting a model as the best model
to represent the current plant dynamics from a set of candi-
date models, the prediction error covariance is composed of
three error terms. These error terms are the errors intro-
duced by sensor noise and linear approximation (as for the
fixed gain case), as well as a modelling error term induced
by the model not being the best fitting model. Therefore,

for the multiple model case, the prediction error covariance
becomes

$$\underline{A}_{ie} = \underline{A}_e + \underline{A}_n + \underline{A}_{im} \qquad (5-9)$$

where

$\underline{A}_{ie}$ is the total error covariance associated
with the ith candidate model

A_e is the error covariance introduced
by linear approximation

A_n is the error covariance introduced
by the addition of sensor noise

$\underline{A}_{im}$ is the error covariance introduced
by a model not being the best fitting model

It can be seen from Equation (5-9) that, in order for
each candidate model to have a distinct prediction error
covariance, the third term on the right hand side of the
equal sign must be the dominant term. If the error asso-
ciated with the sensor noise becomes the dominant term, it
will mask the modelling error for each of the candidate
models. In essence, a large sensor noise causes the re-
siduals generated for each candidate model to be the same
and not distinct. Therefore, proper model se
occur.

The above discussion results in

AD-A189 715   MODEL SELECTION FOR THE MULTIPLE MODEL ADAPTIVE   2/4
               ALGORITHM FOR IN-FLIGHT SIMULATION(U) AIR FORCE INST OF
               TECH WRIGHT-PATTERSON AFB OH   J R MATHES DEC 87
UNCLASSIFIED   AFIT/GE/ENG/87D-40   F/G 1/1   NL
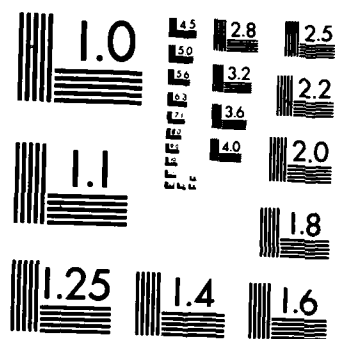
MICROCOPY RESOLUTION TEST CHART

NATIONAL BUREAU OF STANDARDS-1963-A

ty which must be satisfied in order for the multiple model

algorithm to be able to distinguiush one model from another.

$$A_e + A_{im} >> A_n \qquad (5-10)$$

Assuming that the linear approximation error term is small,

equation (5-10) becomes

$$A_{im} >> A_n \qquad (5-11)$$

Equation (5-11) shows that, for a given level of sensor

noise, there is a minimum spacing between models that is

necessary for the multiple model algorithm to determine the

proper model. This is shown graphically in Figure 5-3.

Figure 5-3 shows that if a second model is placed in the

region where the sensor noise would mask the residuals, then

proper model selection cannot occur. Therefore, there is a

region that is not acceptable for placement of models subse-

quent to the placement of an initial model (determined by

sensor noise level). On the other hand, when models are

placed such that the modelling errors dominate the sensor

noise, proper model selection can be made. Additionally,

Equation (5-11) shows that the farther apart the candidate

models are spaced, the more noise resistant the multiple

70

── Noise Boundary
   (determined for given
   level of sensor noise)
** Nominal Operating Point

1. $A_{im} > A_n$

Altitude

**
2. $A_n > A_{im}$

1. Region where get substantial model-
ing error. Acceptable region for place-
ment of subsequent model.

2. Region where sensor noise would mask
residuals. Unacceptable region for place-
ment of subsequent model.

Mach Number
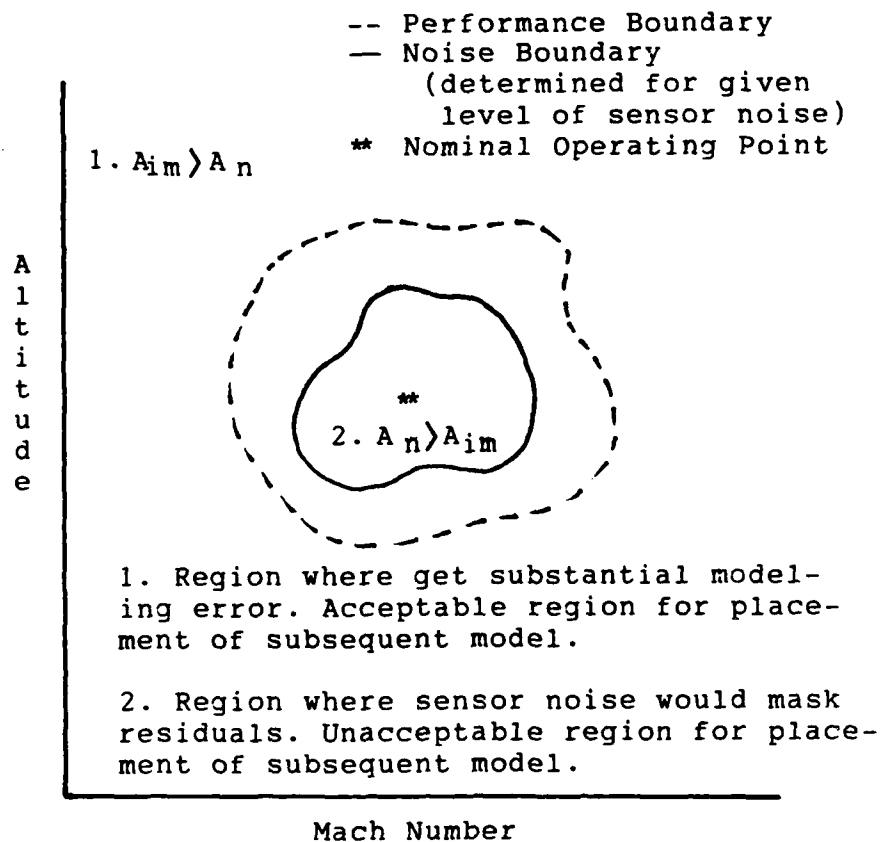
Figure 5-3.   Noise Effects on Model Selection

model algorithm becomes.   This thesis addresses the issues

just discussed by investigating how model selection for the

multiple model algorithm is affected by the addition of

sensor noise.

5.4 Summary

This chapter presents the factors considered in this

thesis for selecting models for the multiple model algo-

rithm.   Specifically, the concept of establishing perfor-

mance boundaries using fixed gain simulations is discussed,
showing how overlapping boundaries can be used to establish
desired tracking performance over a given set of flight
conditions. Sensor noise effects are also shown to be a
factor to be considered when selecting a discrete number of
aircraft models for the multiple model algorithm.

6.   Simulation Setup and Results

6.1   Simulation Setup

The parameter adaptive simulation software used in this thesis was developed by Pineiro and Berens. Figure 6-1 shows the top level description of the parameter adaptive system simulation package conducted with the aid of MATRIX$_x$ control design software and its System Build simulation tool. The block in Figure 6-1 that is labeled ADAPT2 implements the multiple model parameter estimation algorithm and also performs the design calculations of updating the control law gains $\underline{K}_1$ and $\underline{K}_2$. The block labled CTRL accepts the updated control law gains and implements the control law equations that are presented in Equations (3-47) and (3-48) with a sampling time, T, of 0.01 second. The block labled A/C implements the longitudinal linearized dynamics of the AFTI/F-16 as presented in Chapter 2. The A/C block also implements actuator dynamics and includes nonlinearities such as rate and position limits. The block labled SEN2 allows sensor noise to be added to the longitudinal states as desired. For a more detailed presentation of each of the blocks in Figure 6-1 consult Beren's thesis (2).

73

Editing : MODFOL (Continuous)
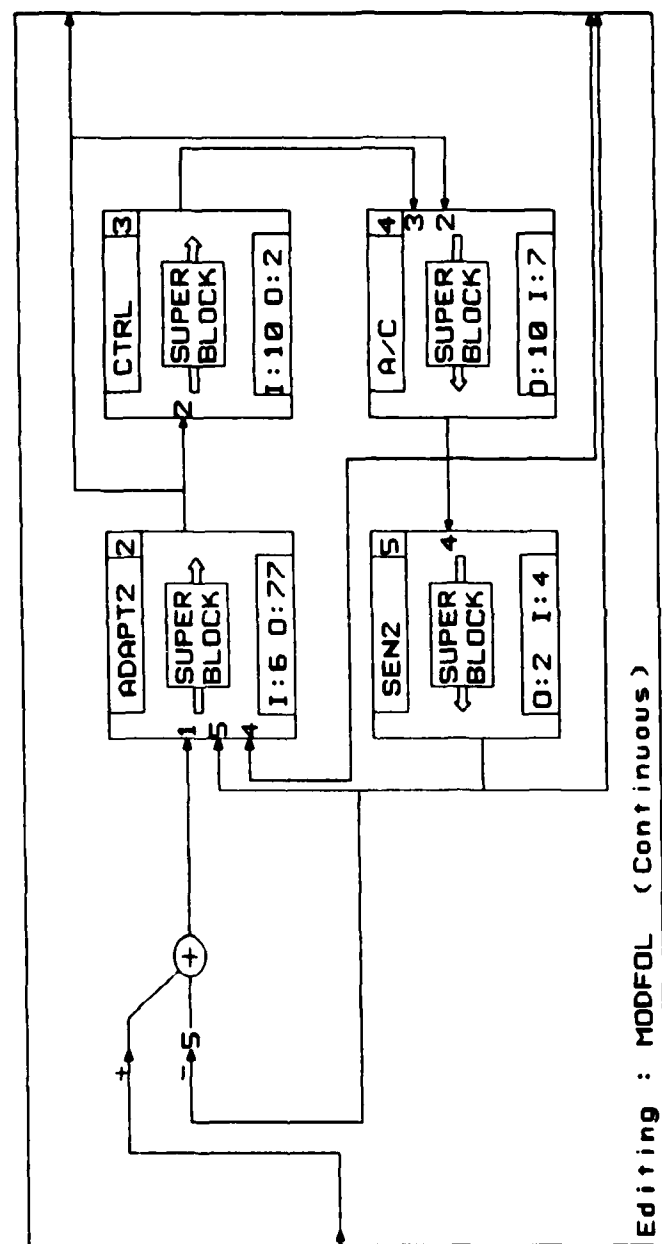
Figure 6-1. Top Level Description of Parameter Adaptive Simulation Package

The reference tracking signals used are those that were implemented by Pineiro and Berens. The inputs were obtained from real-time, nonlinear simulation with elevators and flaperons as control surfaces and with flight path angle and pitch rate as outputs. The reference tracking signals are shown on Figures 6-2 and 6-3.

In preparation to run the simulations, several data files were created to input specific flight condition data along with the necessary control surface deflection limits into the parameter adaptive simulation software. These data files consist of the A and B matrices of the state space representation of a flight condition as presented in Appendix A, along with the elevator and flaperon position limits as listed in Appendix C. This flight condition data was then input using the $MATRIX_x$ System Build options into the block labled A/C as shown on Figure 6-1. In addition, several parameter vectors were created from the state space models using $MATRIX_x$. These parameter vectors were input as needed into the ADAPT2 block (see Figure 6-1) as the fixed secondary parameter estimator models of the multiple model parameter estimator algorithm (see Figure 4-2).

Time (Sec)
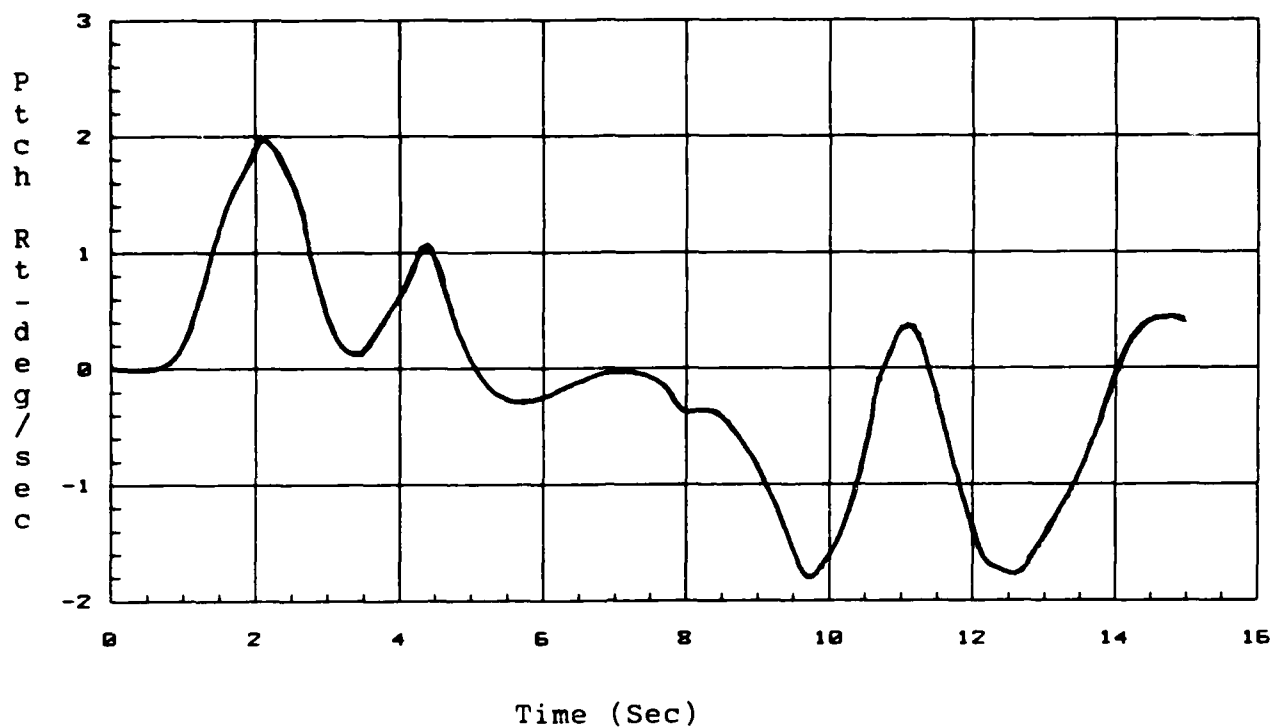
Figure 6-2.   Pitch Rate Input

Time (Sec)
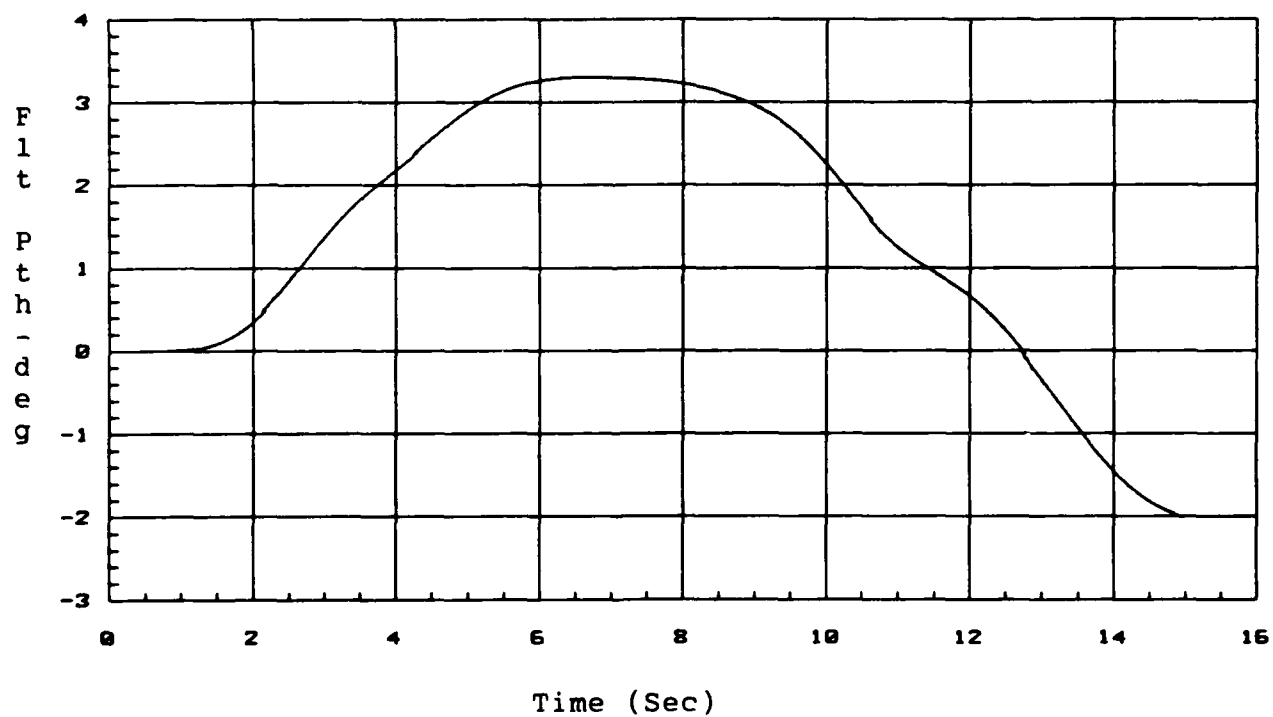
Figure 6-3.   Flight Path Angle Input

76

6.2 Simulation Results

6.2.1 Single Model Analysis

6.2.1.1 Performance Boundary Evaluation. In preparation

for determining the number of models and the spacing of

those models to obtain satisfactory tracking performance

over the desired flight envelope, fixed gain simulations

were run to determine the performance boundaries of a single

model. Recall that, as discussed in Chapter 5, by using the

performance criteria of Equations (5-5) and (5-6) perfor-

mance boundaries for a given model can be obtained by re-

placing the nominal state space aircraft model with another

aircraft model and running subsequent simulations. If the

performance criteria are satisfied, then the non-nominal

aircraft model yields satisfactory tracking performance with

the nominal models control law gains. This satisfactory

performance dictates that the off-nominal model is within

the performance boundary for the nominal model. Failure to

meet the performance criteria indicates that the off-nominal

model is outside of the nominal model performance boundary.

The first point chosen as a nominal aircraft model was

at the flight condition of 18,000 ft altitude and 0.45 Mach.

The parameter vector (Appendix D) was calculated and imple-

mented into parameter adaptive system for the purpose of

defining the control law gains via the step response matrix

for fixed gain simulations. The first simulation was run

with the nominal aircraft plant and the nominal gains. The

response of this simulation is shown on Figures 6-4 and 6-5.

Figure 6-4 plots the pitch rate input versus the output

response while Figure 6-5 shows a plot of the performance

index for this simulation. Figures 6-6 through 6-9 present

the elevator and flaperon positions and rates for this

simulation. From the data presented for this simulation, it

can be seen that the performance criteria are well satisfied

and that tracking response of the reference signal is very

good. It was noticed early in the simulations that the

pitch rate response was the critical response for the com-

manded inputs. The pitch rate response failed the perfor-

mance criteria well before the flight path angle response

for all simulations run. For this reason, only the pitch

rate responses are presented. Subsequent simulations were

made by replacing the nominal aircraft model with aircraft

models at the same altitude and decreased/increased Mach

number. Mach number was decreased/increased from the nomi-

nal point in increments of 0.05 until the resulting data
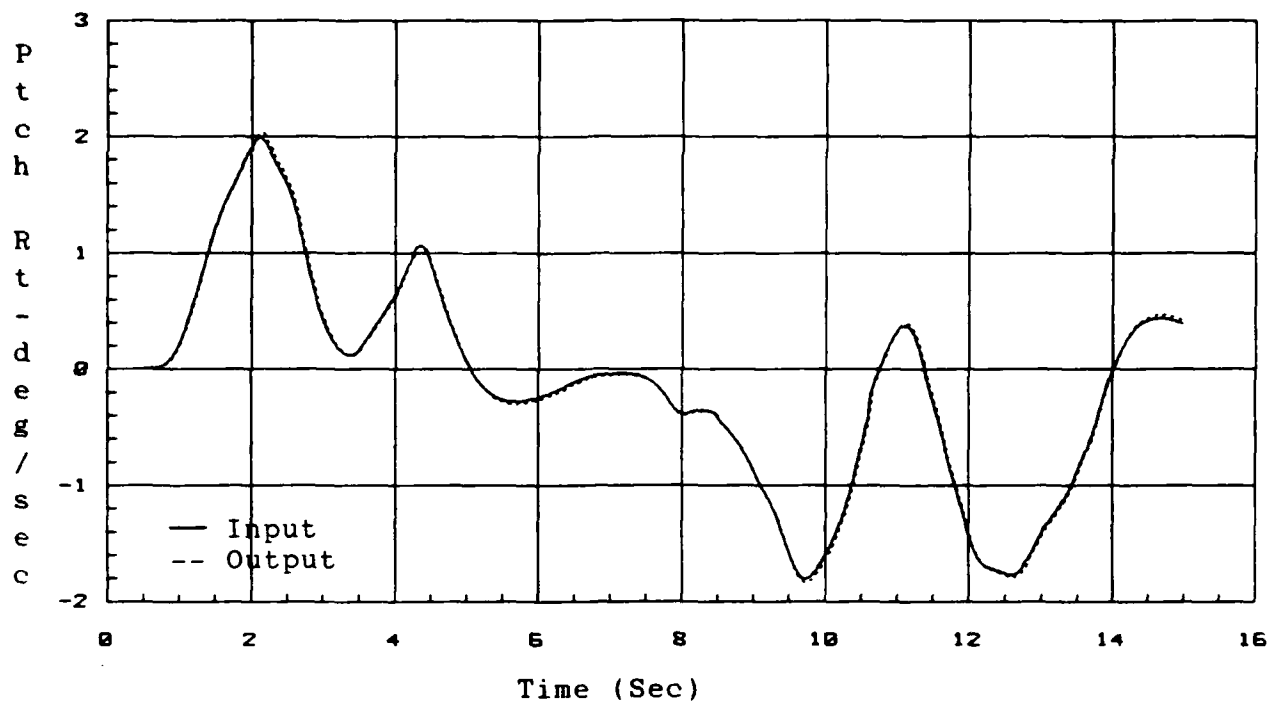
Figure 6-4.   Pitch Rate Response
Nominal Model: 18K 0.45M/Operating Point: 18K 0.45M
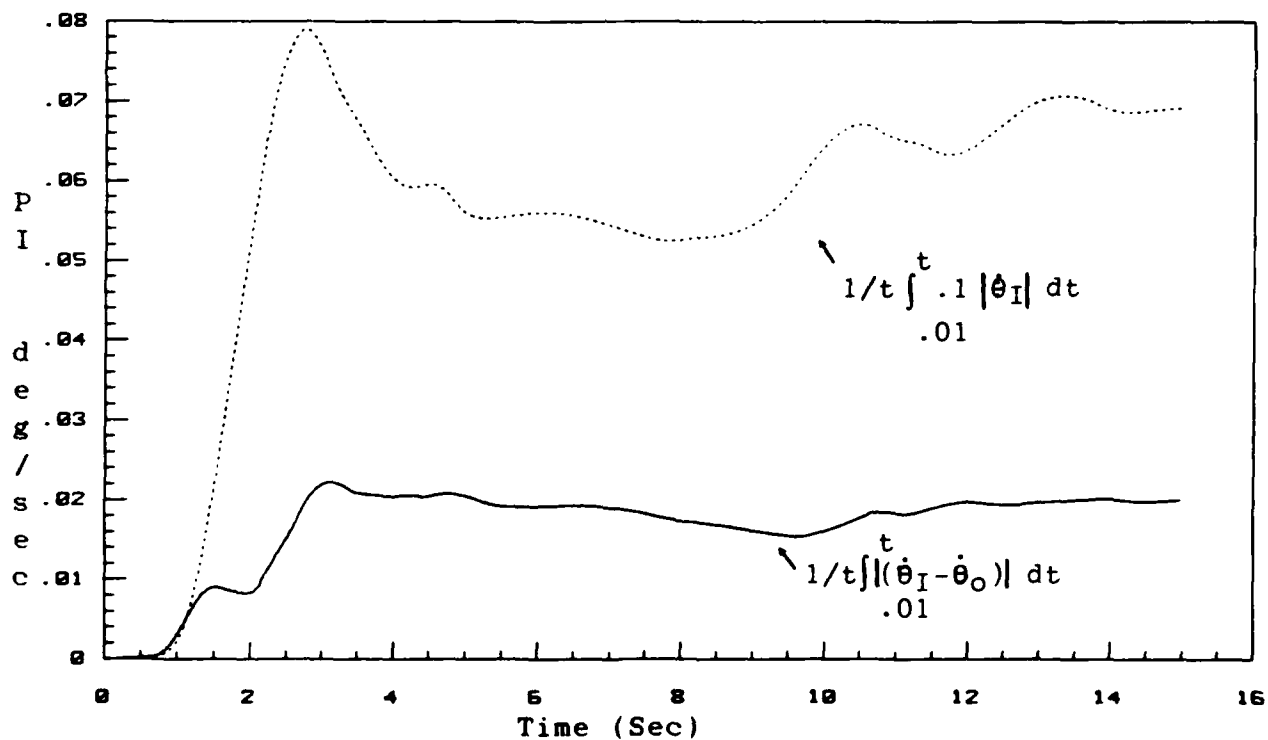
Figure 6-5.   Pitch Rate Performance Criterion
Nominal Model 18K 0.45M/Operating Point: 18K 0.45M

79
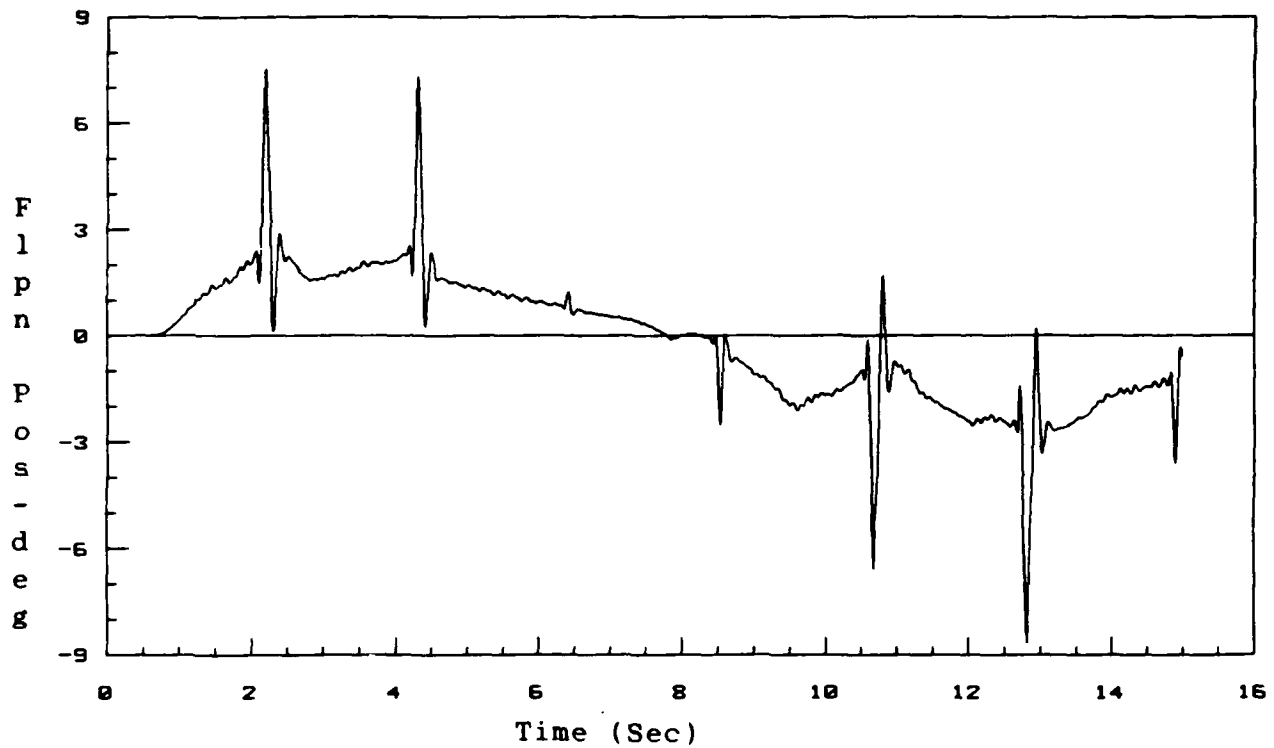
Figure 6-6.   Flaperon Position
Nominal Model: 18K 0.45M/Operating Point: 18K 0.45M
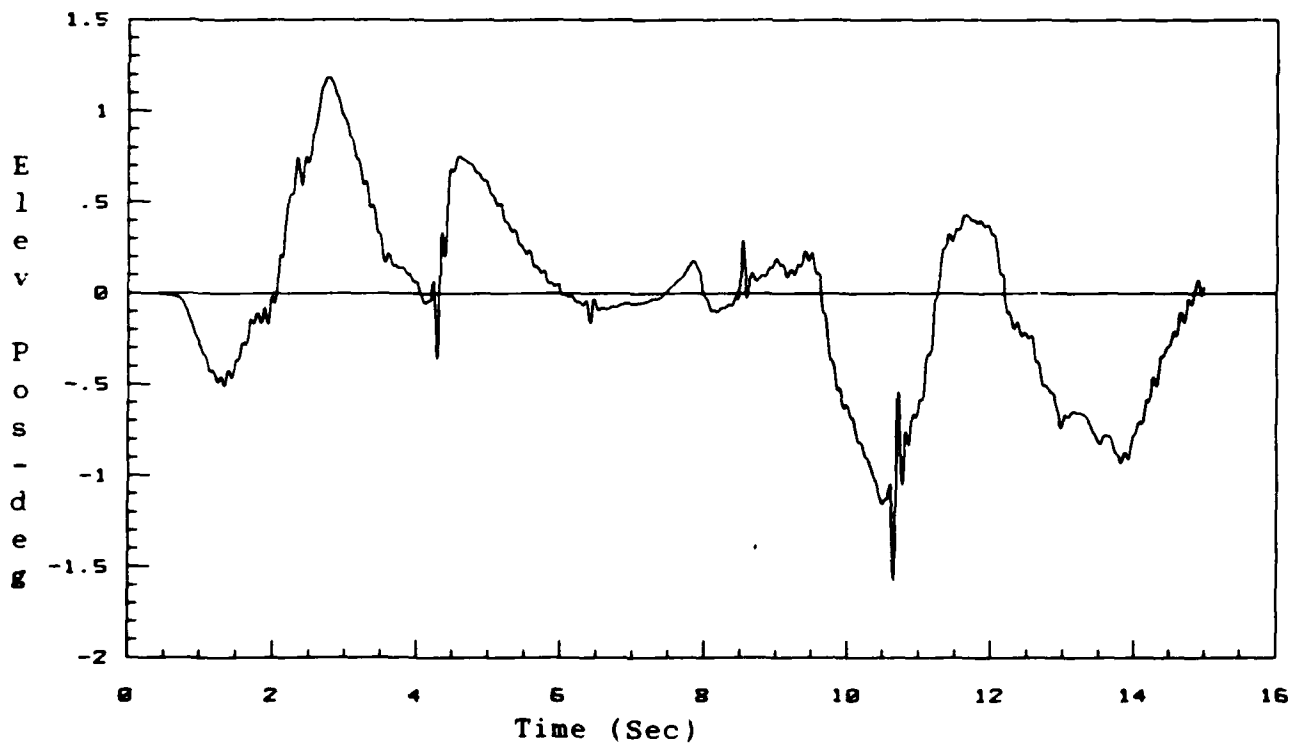
Figure 6-7.   Elevator Position
Nominal Model: 18K 0.45M/Operating Point: 18K 0.45M

80
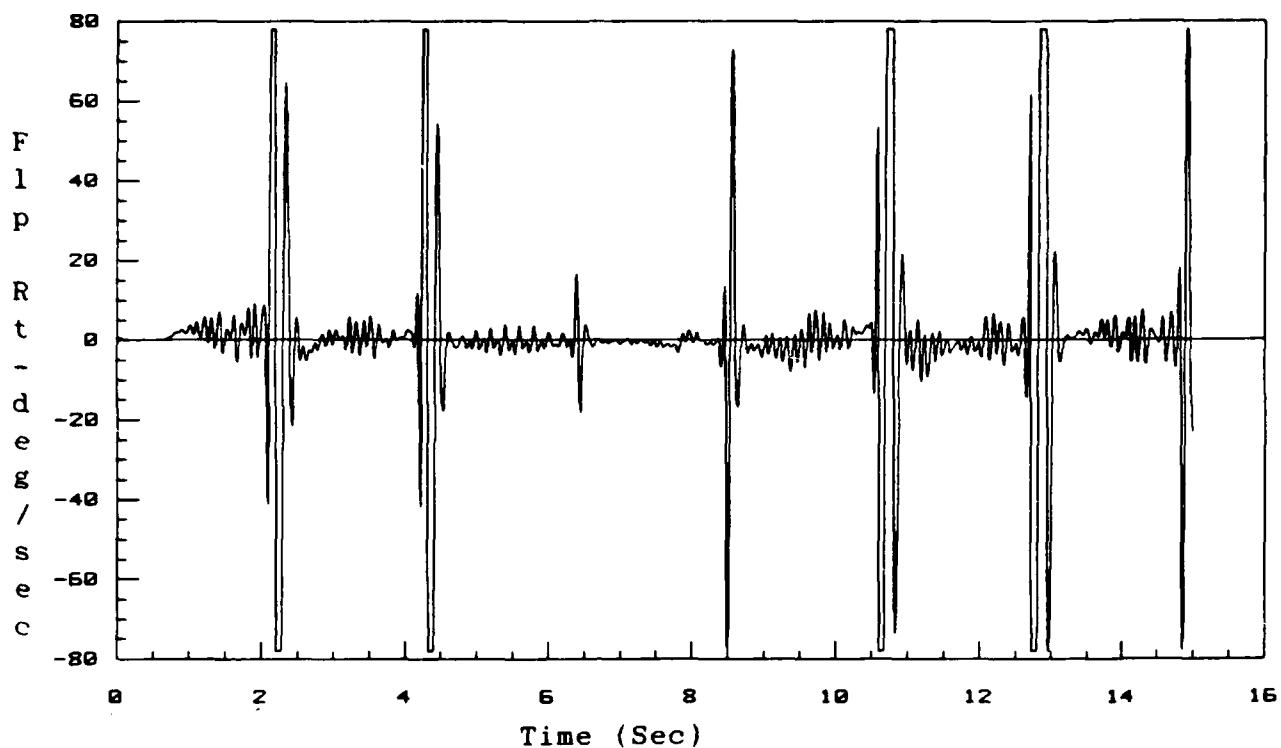
Figure 6-8.   Flaperon Rate
Nominal Model: 18K 0.45M/Operating Point: 18K 0.45M
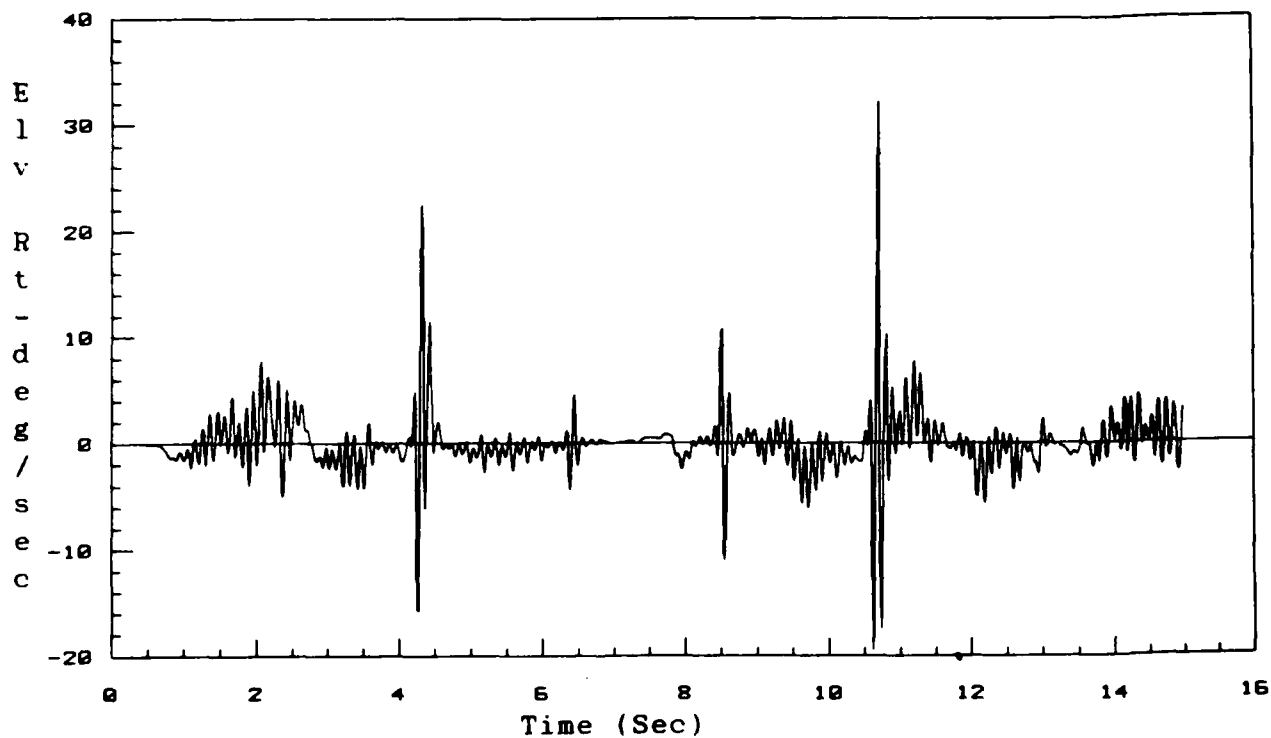
Figure 6-9.   Elevator Rate
Nominal Model: 18K 0.45M/Operating Point: 18K 0.45M

81

showed that the performance criteria had been violated.

Figures 6-10 through 6-15 present the data when the aircraft

model is set at 18,000 ft and 0.8 Mach. From the data, it

can be seen that the performance criteria is violated and

hence the model is outside the performance boundary for the

nominal model of 18,000 ft, 0.45 Mach.

Following the simulations at 18,000 ft, the control law

gains for the nominal plant were used with aircraft plant

models at altitudes of 10,000, 14,000, 22,000, 26,000,

30,000, 34,000 and 38,000 ft with Mach number varying from

0.25 to 0.9 in increments of .05. The flight conditions

that failed to meet the performance criteria are found in

Table 6-1. Using the data presented in Table 6-1, the

performance boundary for the 18,000 ft, 0.45 Mach nominal

point can be obtained and is shown on Figure 6-16. From

Figure 6-16, it can be seen that the performance boundary

encompasses the dynamic pressure line on which the nominal

plant resides. Figure 6-16 also shows that the upper and

lower limits of the performance boundary are contingent on

the differential of dynamic pressure between the nominal

model and the actual flight condition model.
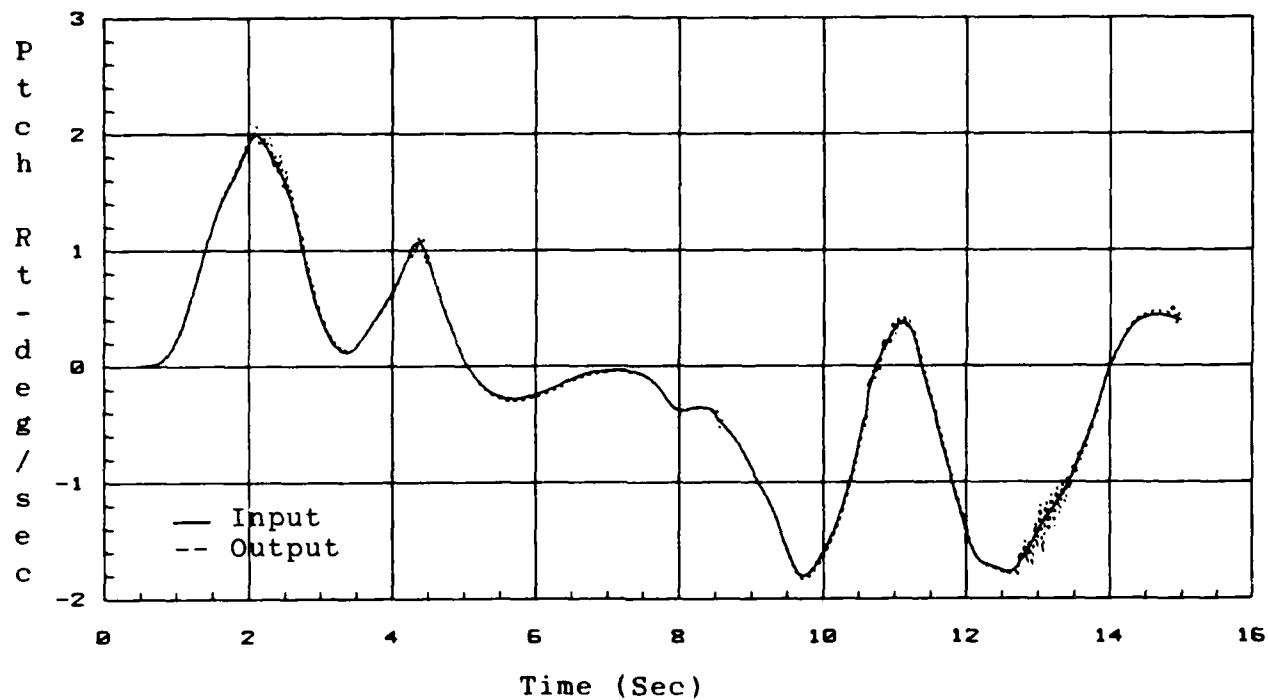
Figure 6-10. Pitch Rate Response
Nominal Model: 18K 0.45M/Operating Point: 18K 0.8M
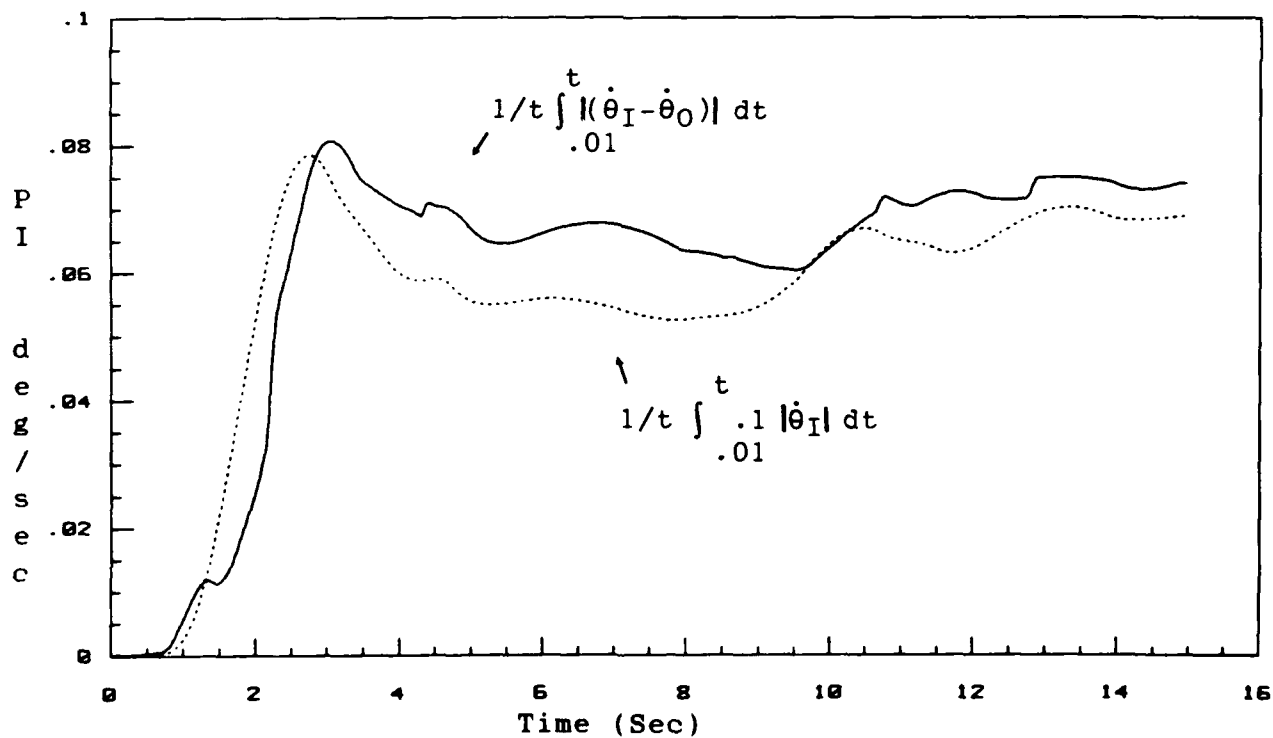
Figure 6-11. Pitch Rate Performance Criterion
Nominal Model: 18K 0.45M/Operating Point: 18K 0.8M

83
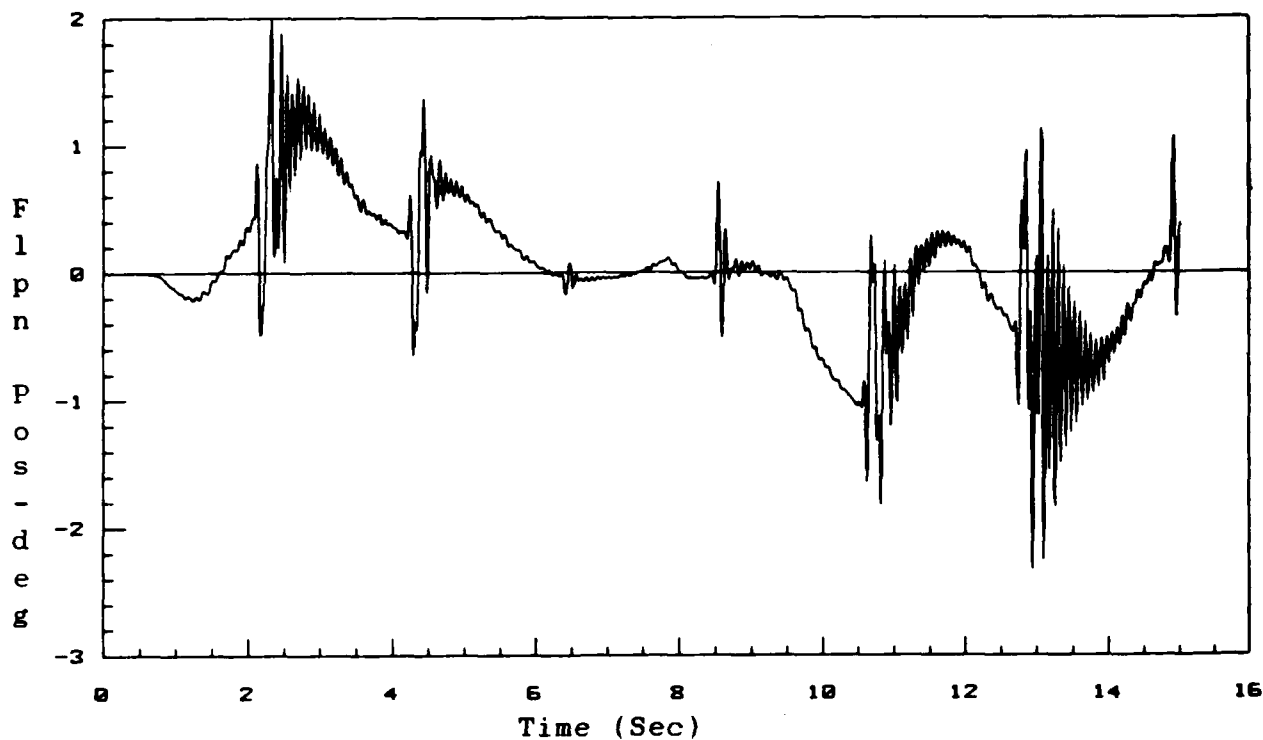
Figure 6-12.   Flaperon Position
Nominal Model: 18K 0.45M/Operating Point: 18K 0.8M
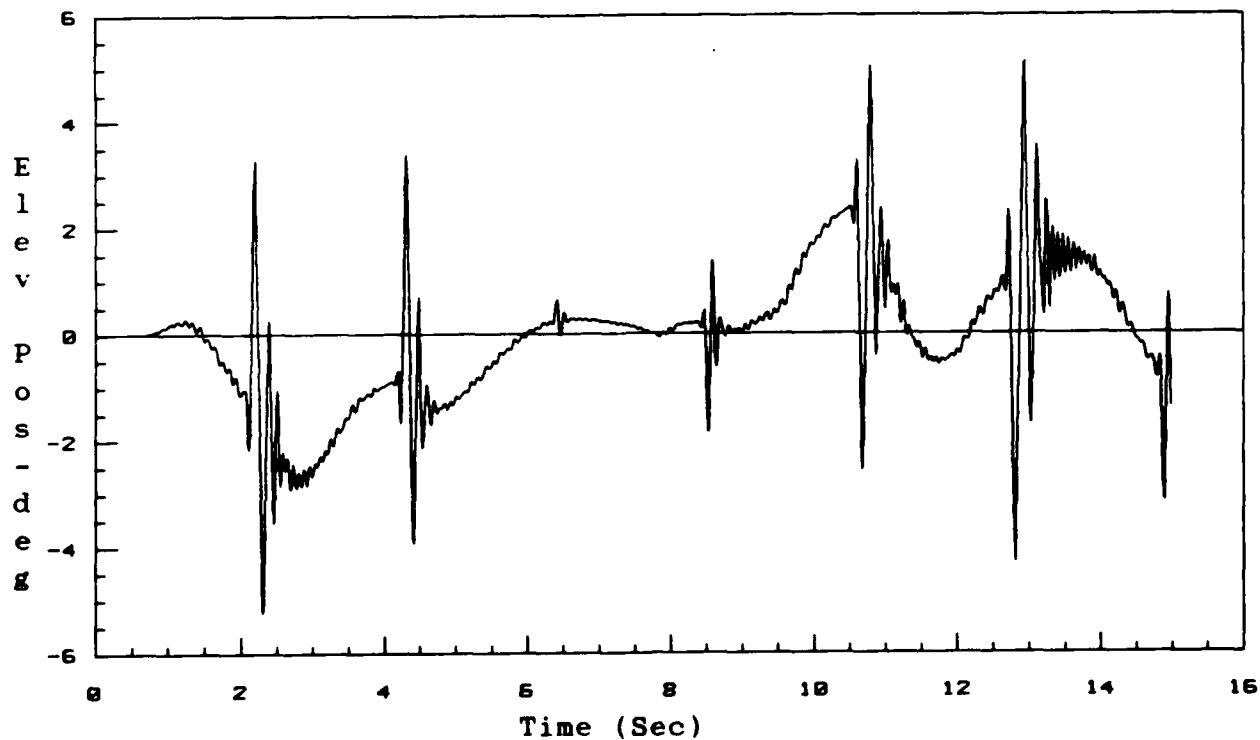
Figure 6-13.   Elevator Position
Nominal Model: 18K 0.45M/Operating Point: 18K 0.8M

84
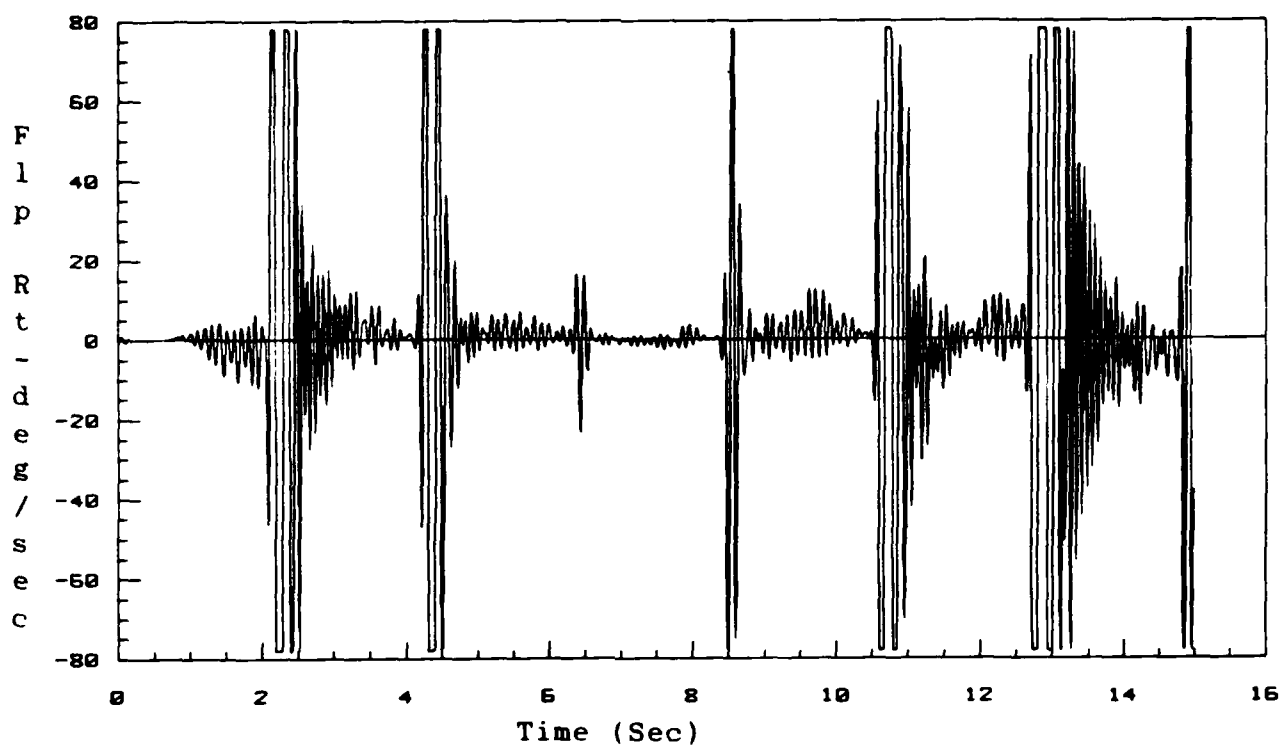
Figure 6-14. Flaperon Rate
Nominal Model: 18K 0.45M/Operating Point: 18K 0.8M
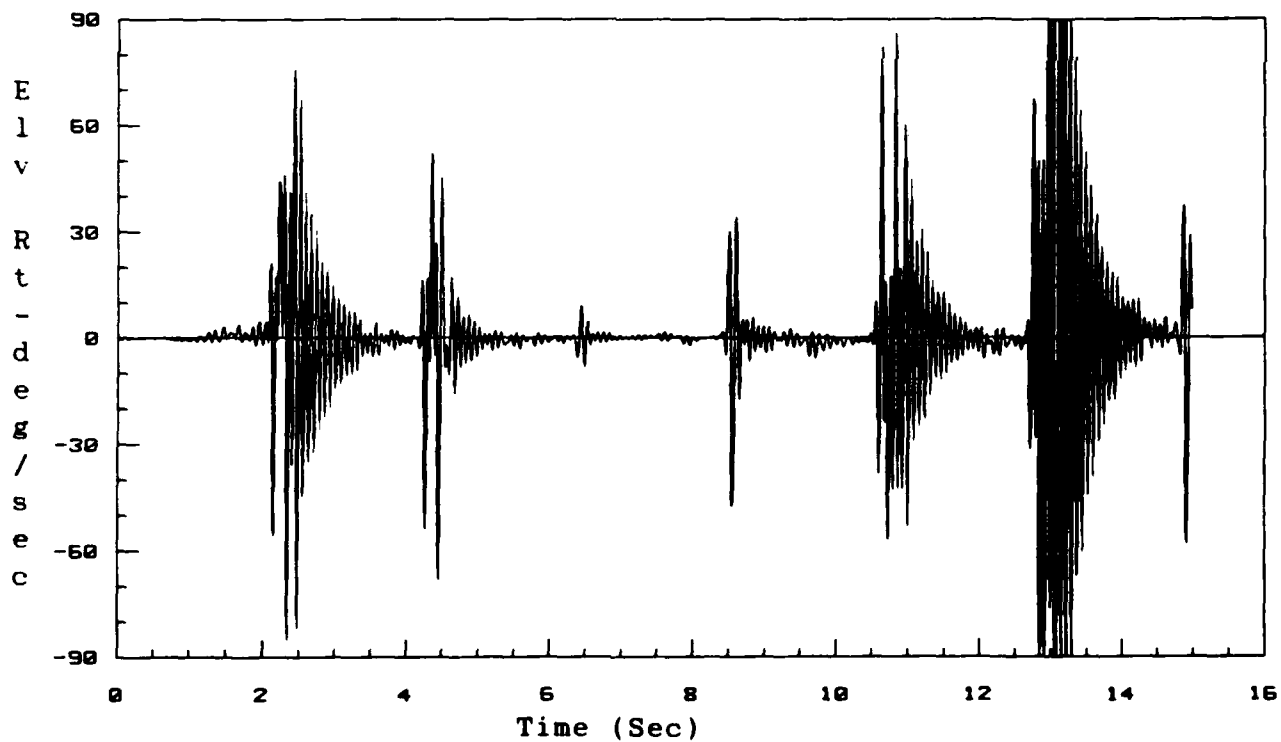
Figure 6-15. Elevator Rate
Nominal Model: 18K 0.45M/Operating Point: 18K 0.8M

85

Table 6-1

Flight Conditions Failing Performance Criteria
Nominal Flight Condition = 18,000 feet 0.45 Mach

Flight Conditions of Failure		
Altitude (Kft)	Mach Number	Dynamic Pressure
10	0.25	63.68
10	0.70	499.27
14	0.30	78.35
14	0.75	489.69
18	0.30	66.62
18	0.80	473.75
22	0.35	76.71
22	0.85	452.45
26	0.40	84.30
26	0.90	426.79
30	0.45	89.26
34	0.50	91.61
38	0.55	91.61

Due to the fact that the performance boundary above
seemed to be dependent on dynamic pressure, the next flight
condition was chosen so that the dynamic pressure was ap-
proximately the same as the 18,000 ft 0.45 Mach point. This
led to choosing the next flight condition at 38,000 ft, 0.7
Mach. Flight conditions that failed to meet the performance
criteria for this nominal flight condition are given in
Table 6-2 and the resulting performance boundary is presen-
ted on Figure 6-17. Comparing the performance boundaries of

Table 6-2

Flight Conditions Failing Performance Criteria
Nominal Flight Condition = 38,000 feet 0.7 Mach

Flight Conditions of Failure		
Altitude (Kft)	Mach	Dynamic Pressure
10	0.25	63.68
10	0.70	499.27
14	0.30	78.35
14	0.75	489.69
18	0.35	90.68
18	0.80	473.75
22	0.35	76.71
22	0.85	452.45
26	0.40	84.30
26	0.90	426.79
30	0.45	89.26
34	0.50	91.61
38	0.55	91.61

Figures 6-16 and 6-17 reveals that they are essentially the
same. This indicates that, from a performance criteria
standpoint, nominal models with approximately the same dyna-
mic pressure yield the same performance boundaries. Several
other performance boundaries were obtained for nominal mo-
dels with similar dynamic pressures. These flight condi-
tions along with the associated dynamic pressures are listed
in Table 6-3. The result of obtaining performance bounda-
ries for the flight conditions in Table 6-3 showed that, for

87
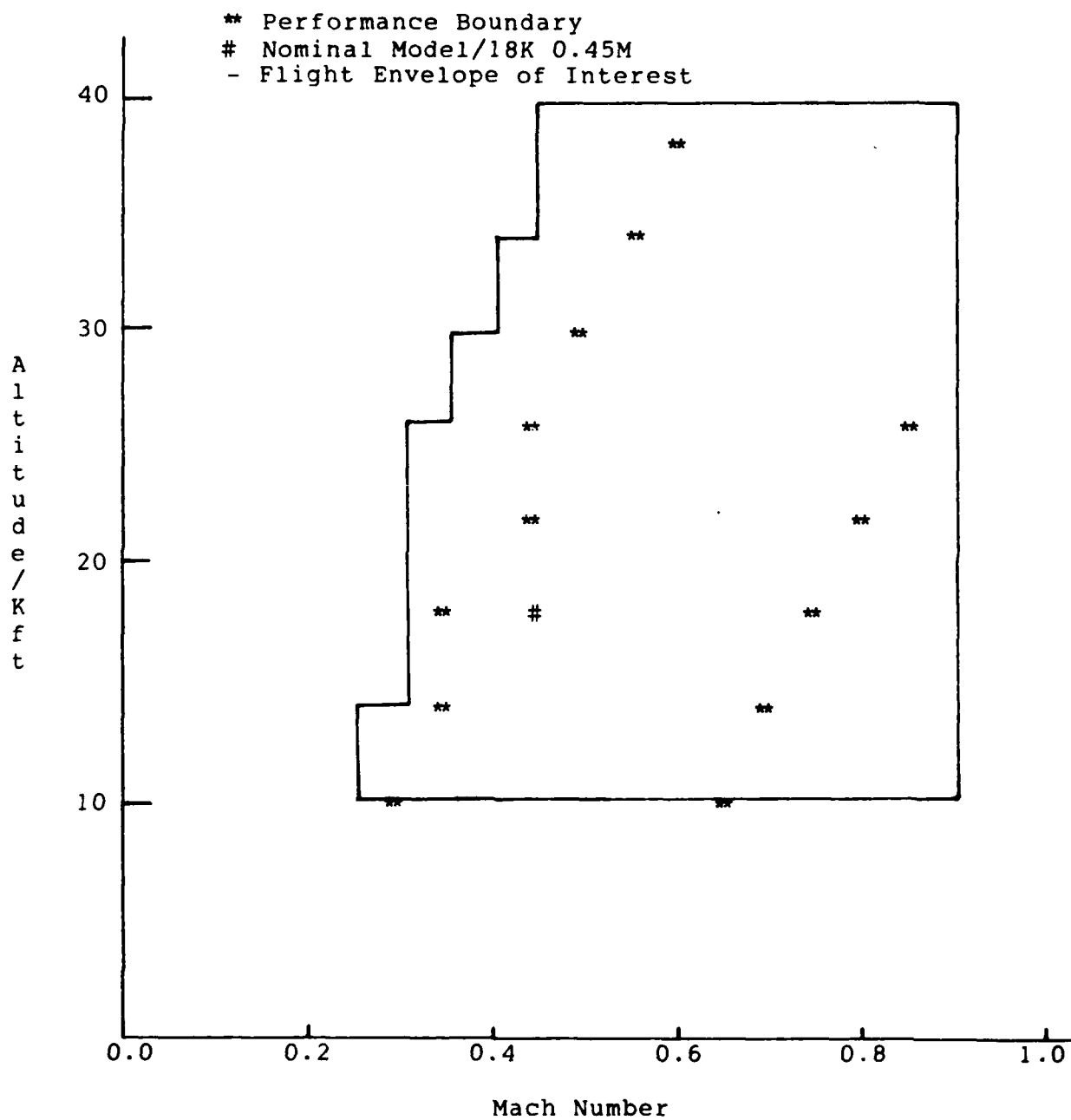
Figure 6-16.   Performance Boundary for
Nominal Model at 18K 0.45M
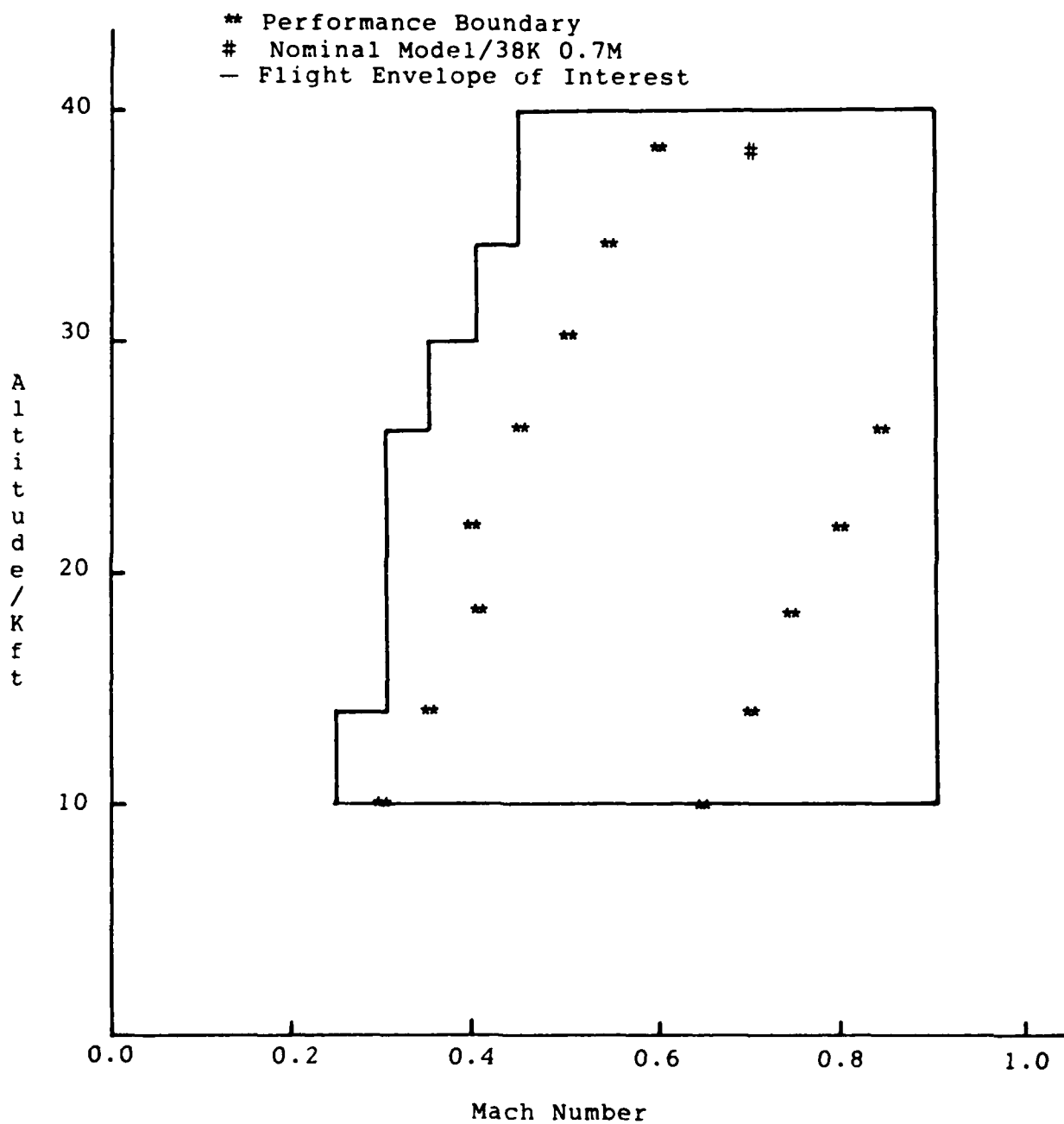
Figure 6-17. Performance Boundary for
Nominal Model at 38K 0.7M

Table 6-3.

Flight Conditions of Nominal Models With
Similar Dynamic Pressures

Case	Altitude (Kft)	Mach	Dynamic Pressure
1	22	0.65	264.58
	34	0.85	264.75
2	14	0.70	426.57
	26	0.90	426.79
3	26	0.50	131.73
	34	0.60	131.92
4	26	0.75	296.38
	34	0.90	296.82
5	30	0.50	110.19
	34	0.55	110.85
6	34	0.50	91.61
	38	0.55	91.61
7	34	0.75	206.12
	10	0.45	206.33
8	26	0.60	189.69
	22	0.55	189.43

each of the presented cases, models with similar dynamic

pressures yield the same set of performance boundaries.

Another point that became evident was that, when running a

fixed gain simulation, if the dynamic pressure of the air-

craft model differed significantly from that of the nominal

model the performance criteria would be violated.

The fact that aircraft models with similar dynamic pressures yield equivalent performance boundaries is also indicated by examining the equations for the dimensionalized derivatives of the aircraft state space model. Recall that the numbers generated by implementing the dimensionalized derivative equations are inserted directly into the A matrix of the aircraft state space model. By examining the dimensionalized derivative equations, it can be seen that dynamic pressure is present in all but one of the equations. Not only is dynamic pressure present in the dimensionalized derivative equations, it is also the dominant variable of the parameters that are not constant. Therefore, dynamic pressure can be seen to have a large influence on the equivalency of one aircraft model with another.

Upon comparing the fixed gain simulation data generated for the 18,000 ft altitude, 0.45 Mach and 38,000 ft altitude, 0.7 Mach flight conditions, an interesting observation was made. Although the performance boundaries were equivalent for both flight conditions, the responses of the control surfaces differed for equivalent simulations. As an example, consider the flight condition of 26,000 ft altitude

91

and 0.45 Mach. Figures 6-18 through 6-23 show the responses

for the case where the nominal model was 18,000 ft altitude,

0.45 Mach, and Figures 6-24 through 6-29 present data for

the case where the nominal model was 38,000 ft altitude and

0.7 Mach. Comparison of the elevator and flaperon surface

deflections for each nominal case shows that, although the

general responses are similar, the nominal model of 38,000

ft altitude and 0.7 Mach has noisier surface deflection

responses. The elevator deflection rates are much larger

for the 38,000 ft, 0.7 Mach case and the flaperon deflection

rates reach the rate limits more of the time. Because the

control surfaces respond differently for the same flight

conditions, the equivalence of one nominal model with ano-

ther is based on more than just dynamic pressure. If dyna-

mic pressure were the sole measure of model equivalence, not

only should the performance boundaries be the same for

nominal models with the same dynamic pressure, but the

surface deflections and rates should be also. This would

dictate that the eigenvalues of the A matrices of the nomi-

nal state space models and the control matrices be equal.

The eigenvalues for the 18,000 ft, 0.45 Mach and 38,000 ft,

0.7 Mach flight conditions are found in Table 6-4. From the

92
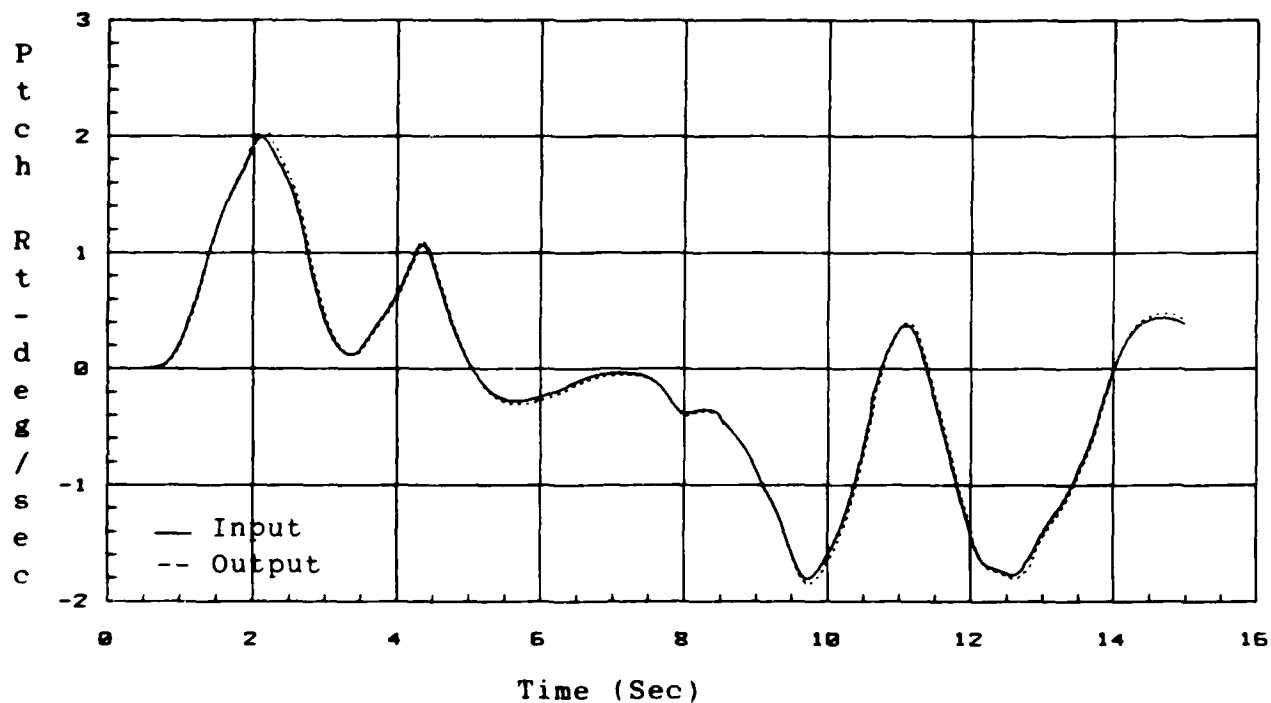
Figure 6-18. Pitch Rate Response
Nominal Model: 18K 0.45M/Operating Point: 26K 0.45M
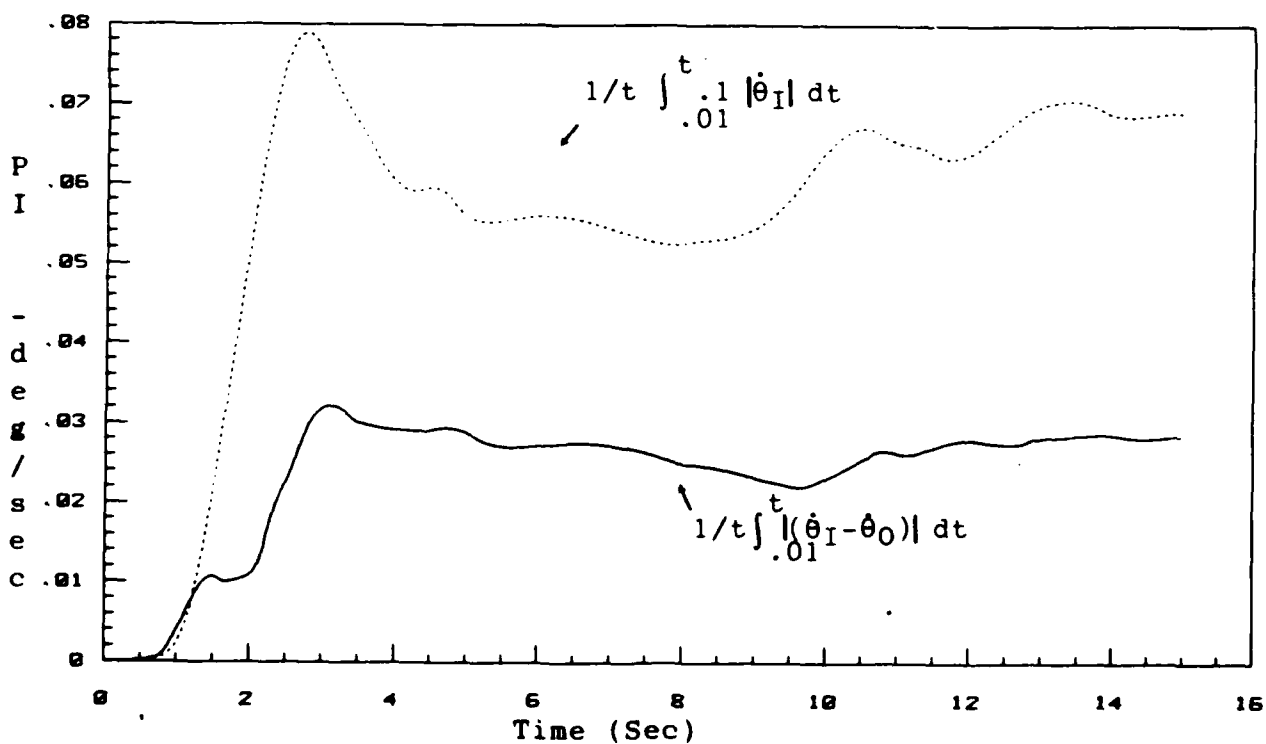
Figure 6-19. Pitch Rate Performance Criterion
Nominal Model: 18K 0.45M/Operating Point:26K 0.45M

93
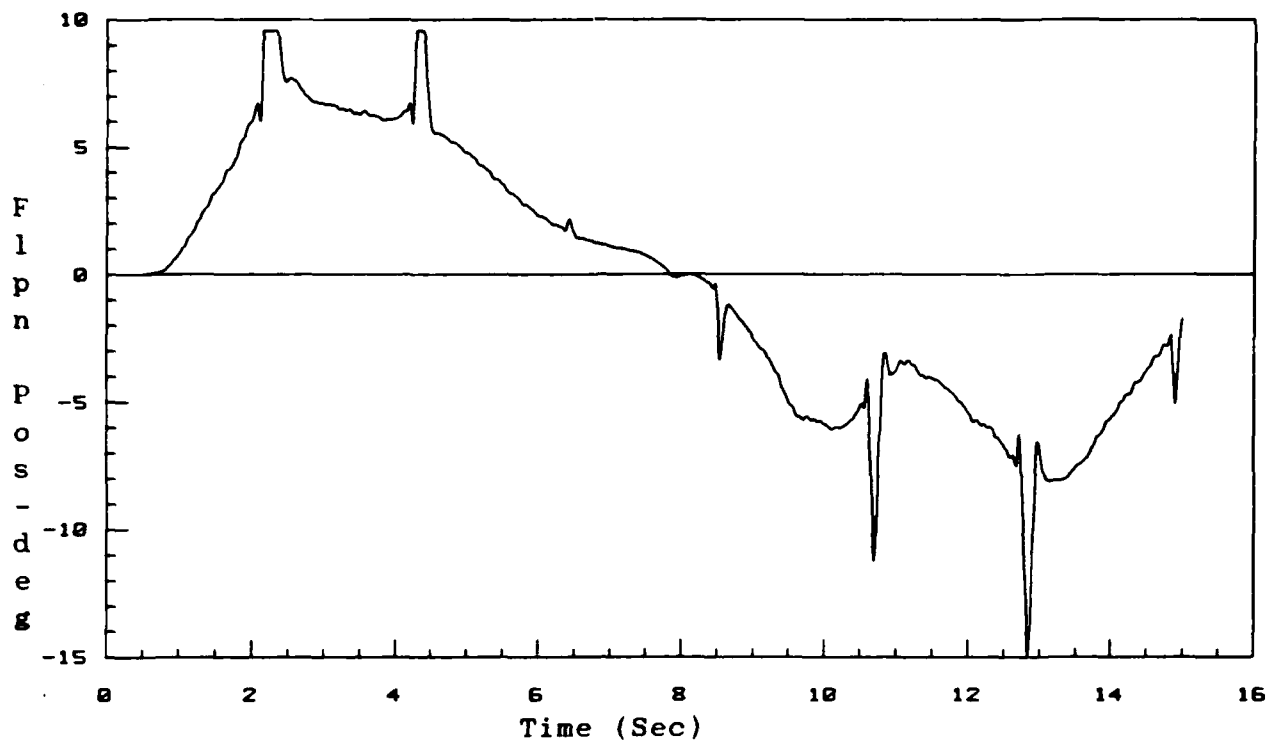
Figure 6-20. Flaperon Position
Nominal Model: 18K 0.45M/Operating Point: 26K 0.45M
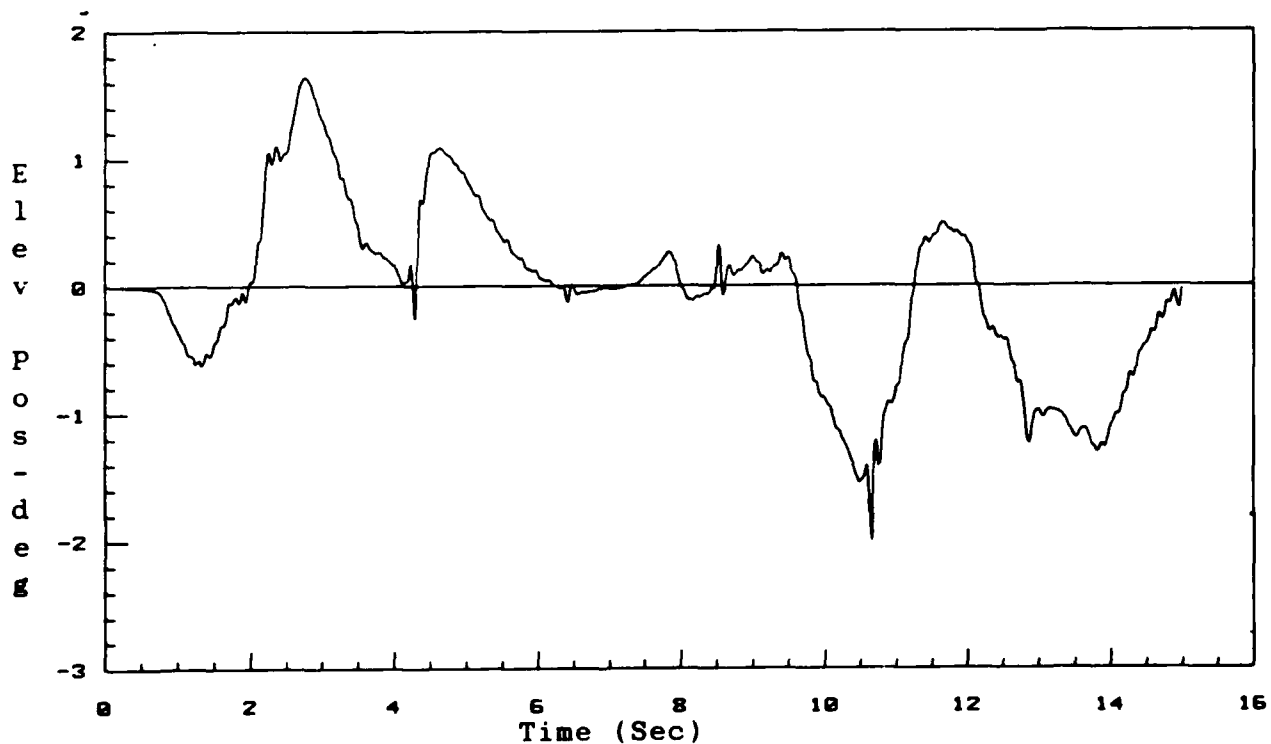
Figure 6-21. Elevator Position
Nominal Model: 18K 0.45M/Operating Point: 26K 0.45M

94
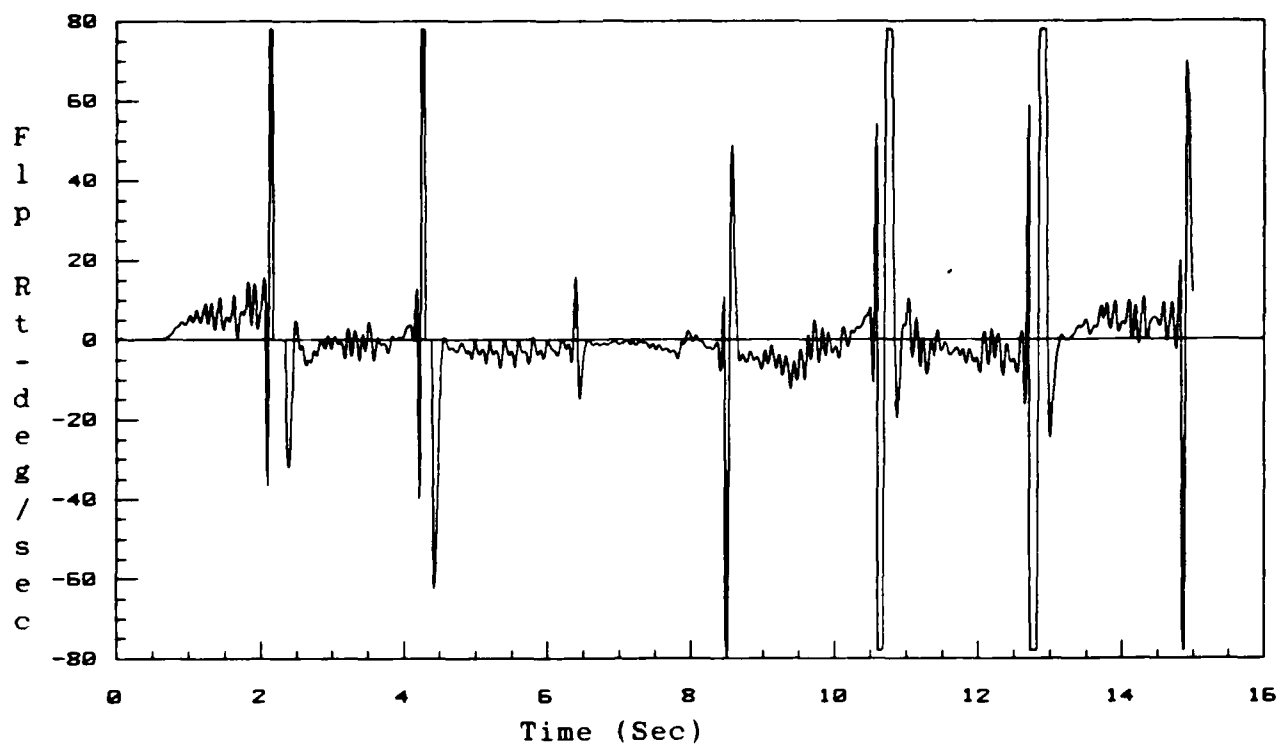
Figure 6-22. Flaperon Rate
Nominal Model: 18K 0.45M/Operating Point: 26K 0.45M
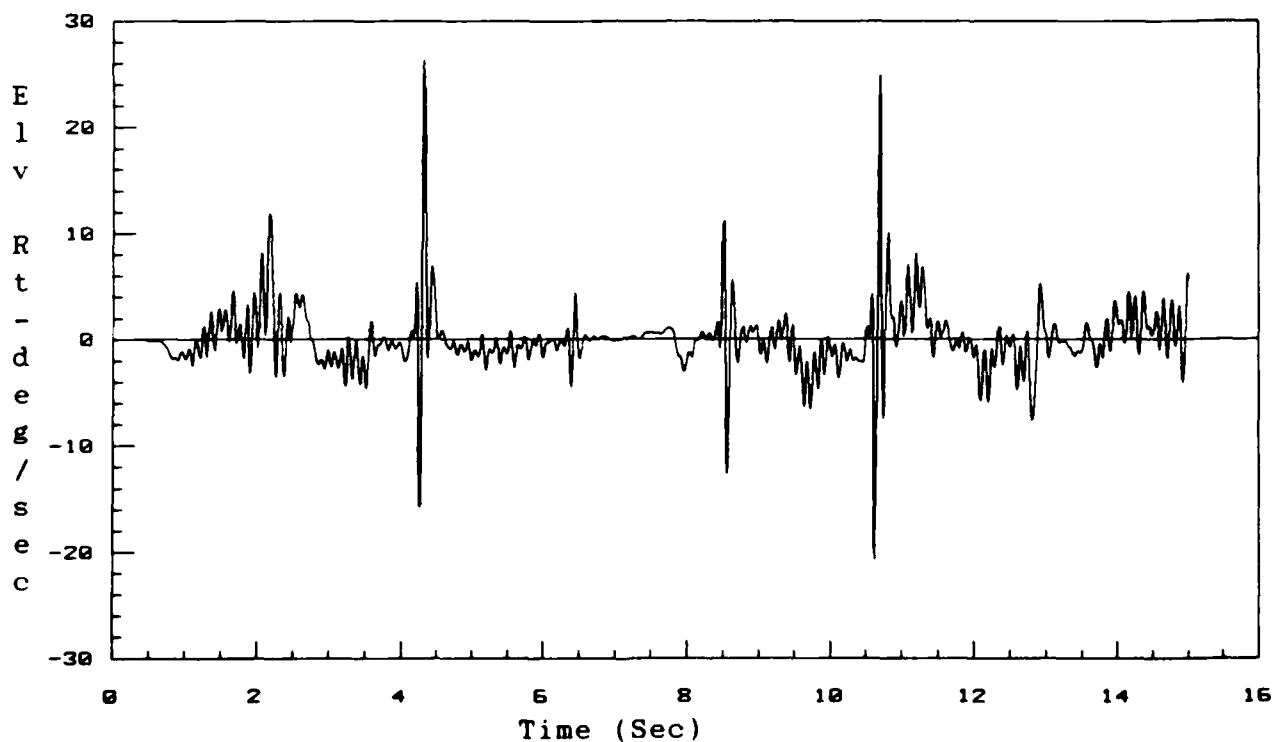
Figure 6-23. Elevator Rate
Nominal Model: 18K 0.45M/Operating Point: 26K 0.45M

95
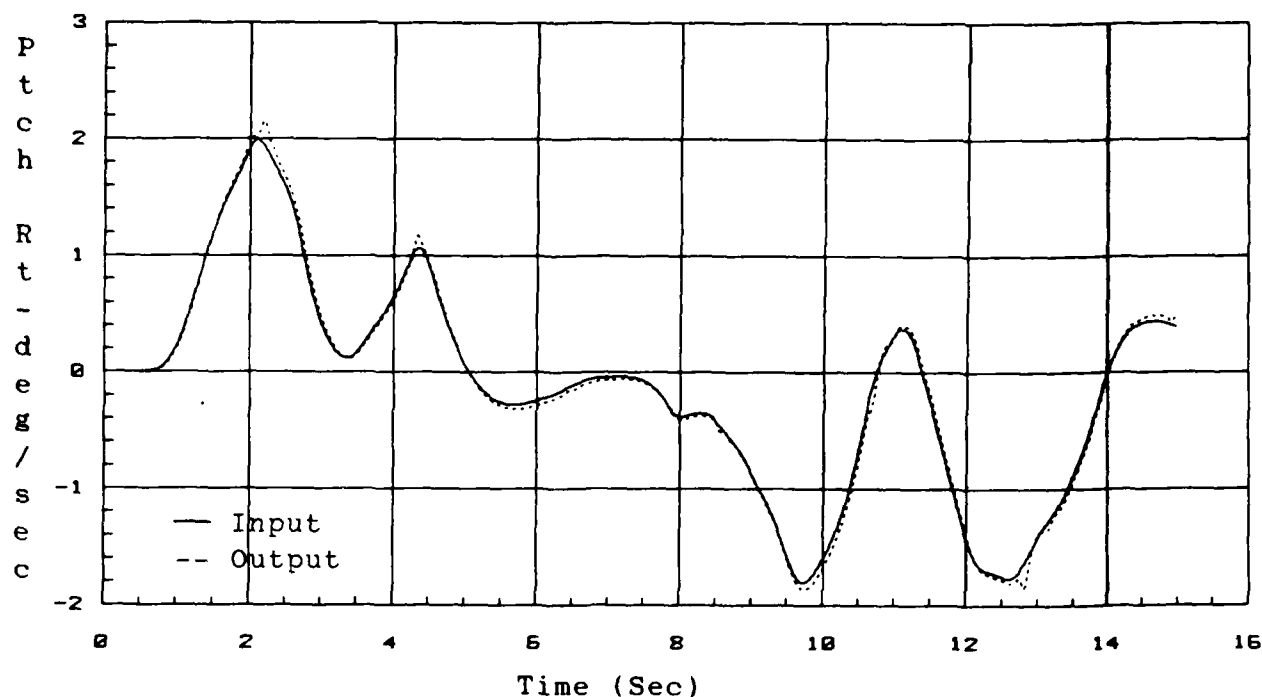
Figure 6-24.   Pitch Rate Response
Nominal Model: 38K 0.7M/Operating Point: 26K 0.45M
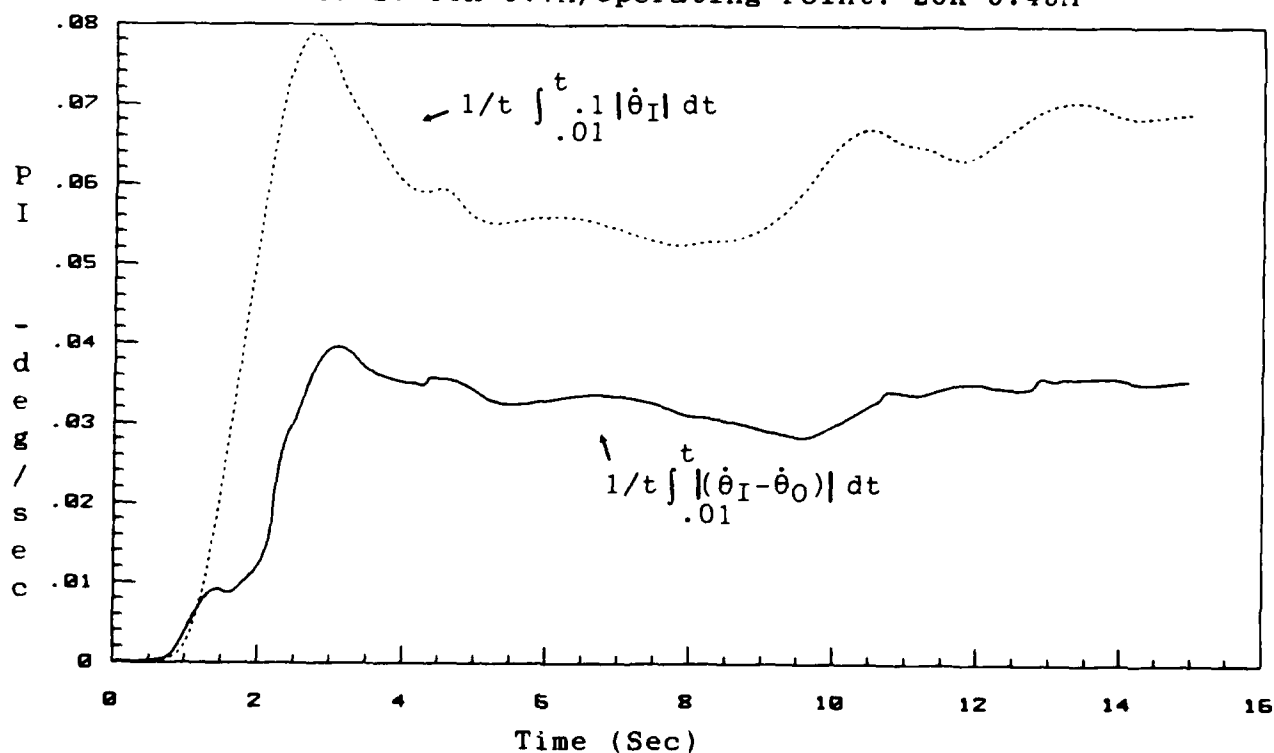
Figure 6-25.   Pitch Rate Performance Criterion
Nominal Model: 38K 0.7M/Operating Point: 26K 0.45M

96
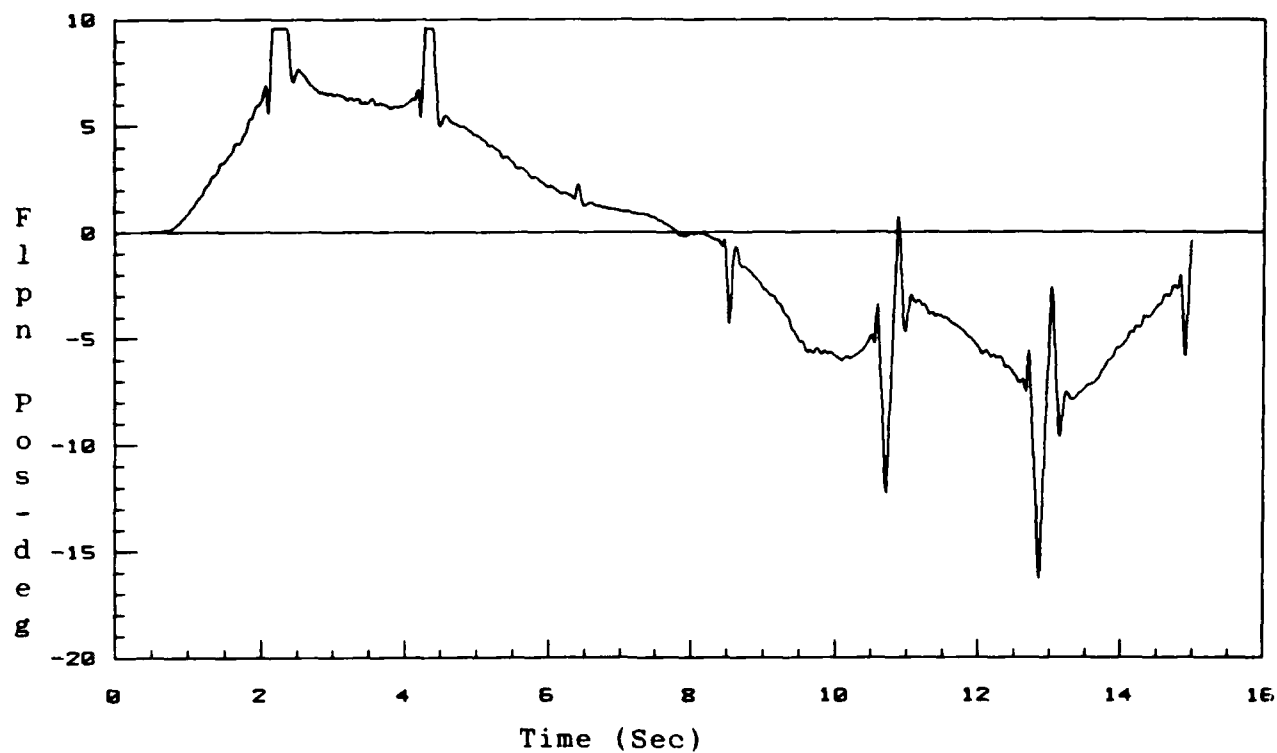
Figure 6-26. Flaperon Position
Nominal Model: 38K 0.7M/Operating Point: 26K 0.45M
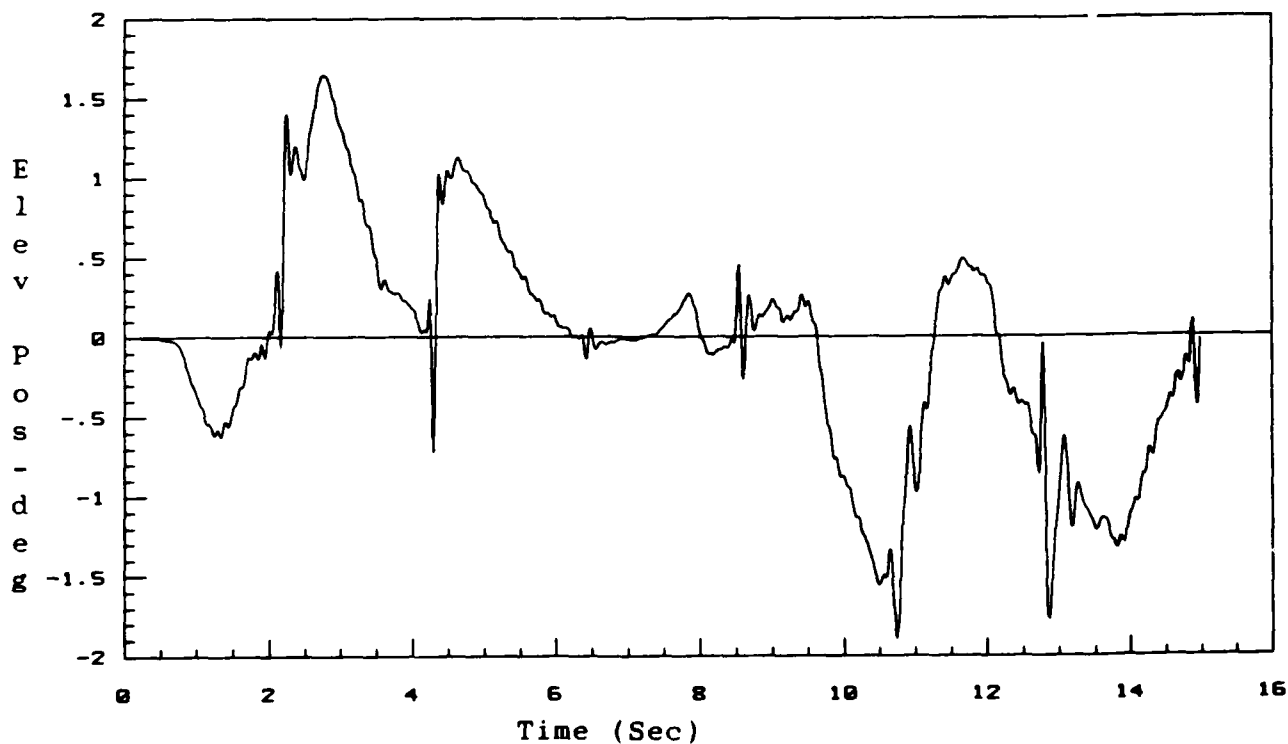
Figure 6-27. Elevator Position
Nominal Model: 38K 0.7M/Operating Point: 26K 0.45M

97
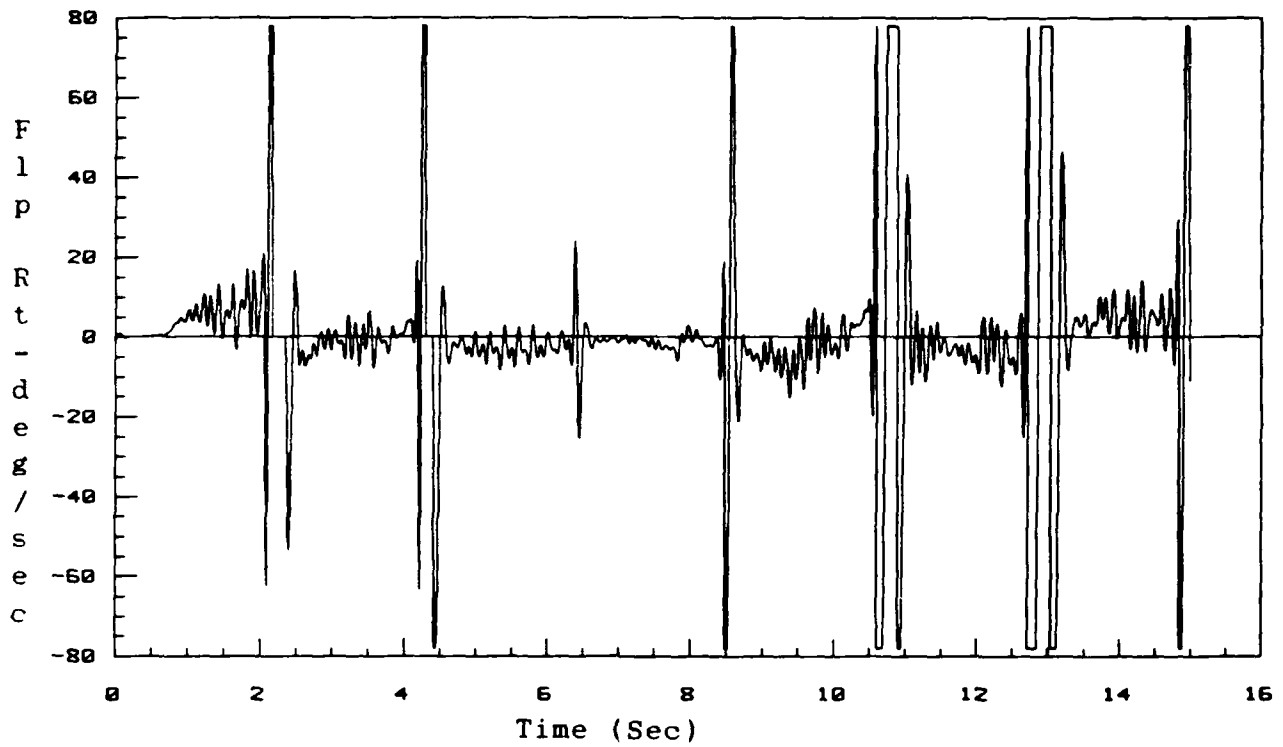
Figure 6-28.   Flaperon Rate
Nominal Model: 38K 0.7M/Operating Point: 26K 0.45M
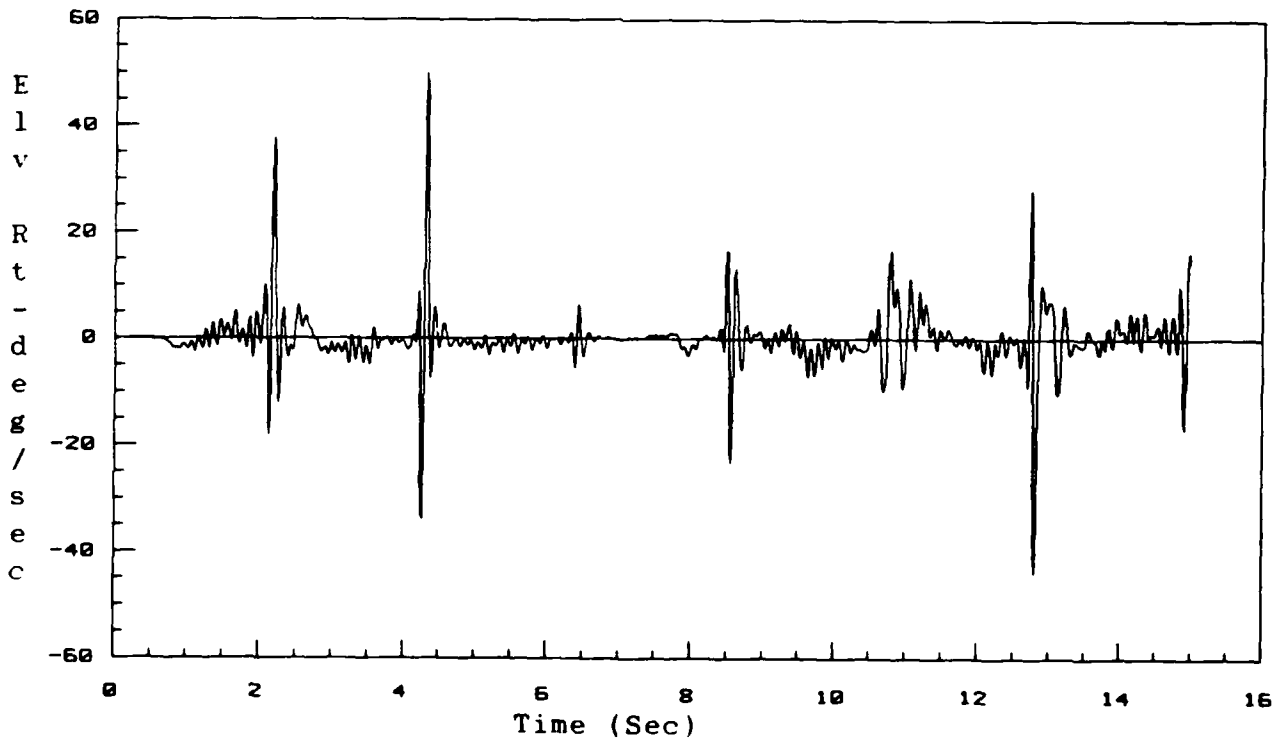
Figure 6-29.   Elevator Rate
Nominal Model: 38K 0.7M/Operating Point: 26K 0.45M

98

Table 6-4

Eigenvalues for the A Matrix of State Space Model

Flight Condition	Eigenvalues
38,000 ft	-0.01254387 + 0.09246732 i
0.7 Mach	-0.01254387 - 0.09246732 i
Dynamic	1.11849823 + 0.00000000 i
Pressure=148.4	-1.79023020 + 0.00000000 i
18,000 ft	-0.00386373 + 0.06747448 i
0.45 Mach	-0.00386373 - 0.06747448 i
Dynamic	-2.05216607 + 0.00000000 i
Pressure=149.9	1.11328404 + 0.00000000 i

data shown on Table 6-4, it is apparent that the eigenvalues

for the A matrices of flight conditions with similar values

of dynamic pressure are not equivalent. This conclusion was

further verified by examining the eigenvalues of the models

shown on Table 6-3. A comparison of the B matrices (see

Appendix A) for flight conditions with similar dynamic pres-

sures, shows they are not equivalent either.

The reason for the differences in the control surface

deflections for flight conditions with similar dynamic pres-

sures can be found in the aerodynamic data. When examining

the aerodynamic data obtained for the flight conditions of

18,000 ft, 0.45 Mach and 38,000 ft, 0.7 Mach, it was noted

that the trim values of angle of attack differed. Table

6-5 shows the angle of attack for each of the flight condi-

tions. Figure 6-30 shows that the lift coefficient varies

as the angle of attack changes. When the lift coefficient

changes, the stability derivatives associated with it

change, and hence so do the dimensionalized derivatives. The

pitching moment also changes as the lift coefficient chan-

ges. Therefore, the stability derivatives associated with

the pitching moment will differ also.

From the above discussion, it can be summarized that

there are some differences in the responses of the control

surfaces for models having the same dynamic pressure. Even

with these differences, model equivalency is primarily as-

sociated with dynamic pressure. This was shown by generating

Table 6-5

Angle of Attack for Nominal Flight Conditions

Flight Condition	Angle of Attack (deg)
38,000 ft 0.7 Mach Dynamic Pressure=148.4	5.11515
18,000 ft 0.45 Mach Dynamic Pressure=149.9	4.96835
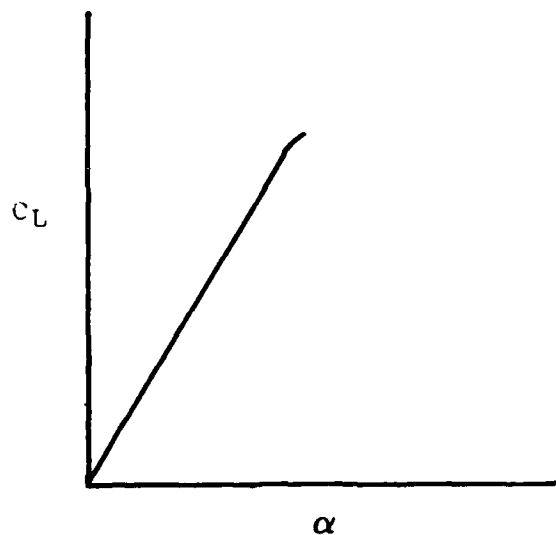
Figure 6-30. Lift Curve

performance boundaries for several pairs of models with
similar values of dynamic pressure (see Table 6-3) and
observing their similarity.

6.2.1.2 Control Surface Activity. The effects on the con-
trol surfaces of replacing a nominal model with plants
having increased/decreased Mach number and/or altitude can
be made clear by examining the changes in the aerodynamic
gain. For a given simulation, the system gain is composed of
the control law gains and the aerodynamic gain. The aerody-
namic gain is derived from the state space model for a

specific flight condition. As an example, the aerodynamic

gain for the flight condition of 30,000 ft and 1.2 Mach is

shown in the discussion to follow. Recall that the open

loop aircraft model is longitudinally unstable in the sub-

sonic region. The reason the flight condition chosen was in

the supersonic region is that the open loop plant is stable.

Therefore, the resulting transfer functions that were used

to calculate the aerodynamic gain will have all of the poles

in the left half plane.

The aerodynamic gains for the 30,000 ft, 1.2 Mach flight

condition were calculated for the following transfer func-

tions: q/δ_e, q/δ_f, α/δ_e, and α/δ_f. The state aircraft state

space model used was

$$
\begin{bmatrix} \dot{q} \\ \dot{\alpha} \end{bmatrix} = \begin{bmatrix} M'_q & M'_\alpha \\ Z'_q & Z'_\alpha \end{bmatrix} \begin{bmatrix} q \\ \alpha \end{bmatrix} + \begin{bmatrix} M_{\delta e} & M_{\delta f} \\ Z_{\delta e} & Z_{\delta f} \end{bmatrix} \begin{bmatrix} \delta_e \\ \delta_f \end{bmatrix} \qquad (6-1)
$$

and the output equation was

$$
\begin{bmatrix} q \\ \alpha \end{bmatrix} = \begin{bmatrix} 1 & 0 \\ 0 & 1 \end{bmatrix} \begin{bmatrix} q \\ \alpha \end{bmatrix} \qquad (6-2)
$$

The proper dimensionalized stability derivatives were ob-

tained and inserted into the state space model above. The

102

desired transfer functions were then obtained and are pre-
sented below:

$$q/\delta_e = \frac{-28.3423(s + 1.07441)}{s^2 + 1.725352s + 38.81511} \qquad (6-3)$$

$$q/\delta_f = \frac{-9.6179(s + .8210201)}{s^2 + 1.725352s + 38.81511} \qquad (6-4)$$

$$\alpha/\delta_e = \frac{-.1313(s + 213.8329)}{s^2 + 1.725352s + 38.81511} \qquad (6-5)$$

$$\alpha/\delta_f = \frac{-.1076(s + 88.84213)}{s^2 + 1.725352s + 38.81511} \qquad (6-6)$$

The steady state aerodynamic gains were calculated for the
transfer functions of Equations (6-3) through (6-6). The
aerodynamic gains for the above transfer functions are pre-
sented in Table 6-6.

Next, the steady state aerodynamic gains for a flight
condition at a different altitude were calculated. The
flight condition was 10,000 ft and 1.2 Mach. The transfer
functions for this flight condition were calculated as

103

Table 6-6

Aerodynamic Gains for Transfer Functions
of Equations (6-3) through (6-6)

Transfer Function	Magnitude of Gain
q/δ_e (Eq 6-3)	0.7845
q/δ_f (Eq 6-4)	0.2034
α/δ_e (Eq 6-5)	0.7237
α/δ_f (Eq 6-6)	0.2464

before and are presented in the following equations:

$$q/\delta_e = \frac{-60.5221(s + 2.150764)}{s^2 + 3.460089s + 80.19058} \tag{6-8}$$

$$q/\delta_f = \frac{-19.4011(s + 1.79332)}{s^2 + 3.460089s + 80.19058} \tag{6-9}$$

$$\alpha/\delta_e = \frac{-.259837(s + 229.2444)}{s^2 + 3.460089s + 80.19058} \tag{6-10}$$

$$\alpha/\delta_f = \frac{-.170677(s + 112.372)}{s^2 + 3.460089s + 80.19058} \tag{6-11}$$

As before, the steady state aerodynamic gains were calculated and are presented in Table 6-7. By comparing the aerodynamic gains of Table 6-6 and 6-7, it is seen that the gains for the pitch rate transfer functions are much larger for the altitude of 10,000 ft. The gains for the transfer functions with angle of attack as a parameter are approximately the same. Because this thesis uses pitch rate as a variable to be tracked, the fact that the aerodynamic gains for the higher altitude flight condition are larger is significant. Therefore, an increase in altitude results in an decreased aerodynamic gain and hence faster surface activity. Similar results were obtained when considering the

Table 6-7

Aerodynamic Gains for Transfer Functions
of Equations (6-8) through (6-11)

Transfer Function	Magnitude of Gain
q/δ_e (Eq 6-8)	1.6232
q/δ_f (Eq 6-9)	0.4339
α/δ_e (Eq 6-10)	0.7428
α/δ_f (Eq 6-11)	0.2392

effects on the aerodynamic gain when increasing Mach number. The data showed that, when Mach number and/or altitude increased, the aerodynamic gain decreased accordingly.

6.2.2 Two-Model Configurations

In determining the number of models required to allow the system with the multiple model algorithm to yield satisfactory tracking performance over the desired flight envelope, several two-model configurations were evaluated. The term "two-model configuration" refers to placing two aircraft models in the parallel bank to function as the secondary parameter estimators (see Figure 4-1). The two-model configuration evaluation consisted primarily of examining the amount the performance boundaries were required to overlap to yield proper tracking performance. The two models for each configuration were chosen on different dynamic pressure lines for the reasons discussed earlier. The two-model configurations are listed on Table 6-8.

The performance boundaries were determined as described previously for each of the configurations listed in Table 6-8. Figures 6-31 through 6-35 show the performance boundaries for each of the two-model configurations.

Table 6-8

Two Model Configurations

Configuration	Nominal Model Flight Conditions		
	Alt (Kft)	Mach	Dynamic Pressure
1	26	0.55	154.39
	18	0.80	473.75
2	10	0.50	254.73
	10	0.75	573.14
3	38	0.65	127.95
	10	0.65	430.50
4	10	0.50	254.73
	10	0.65	430.50
5	10	0.35	124.81
	10	0.75	573.14

From Figures 6-31 through 6-35 it is apparent that the flight envelope of interest can be encompassed by the union of the performance boundaries of two nominal models (depending on the position of the individual performance boundaries). However, in attempting to cover the desired flight envelope with two models, several observations were made as to the effects of model placement on the performance of the multiple model algorithm.

Due to the fact that the multiple model algorithm

107
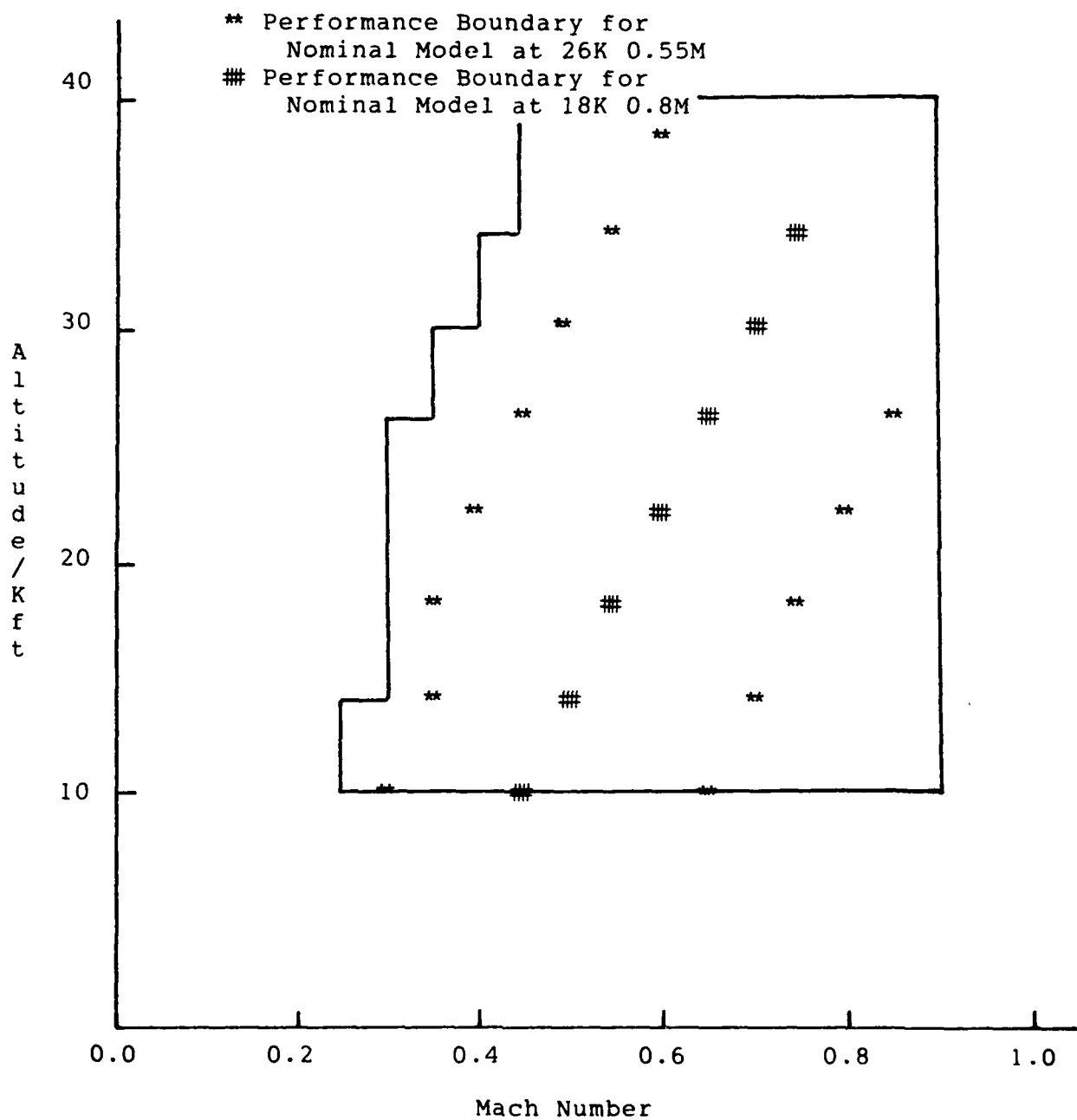
Figure 6-31.   Performance Boundaries
for Configuration 1
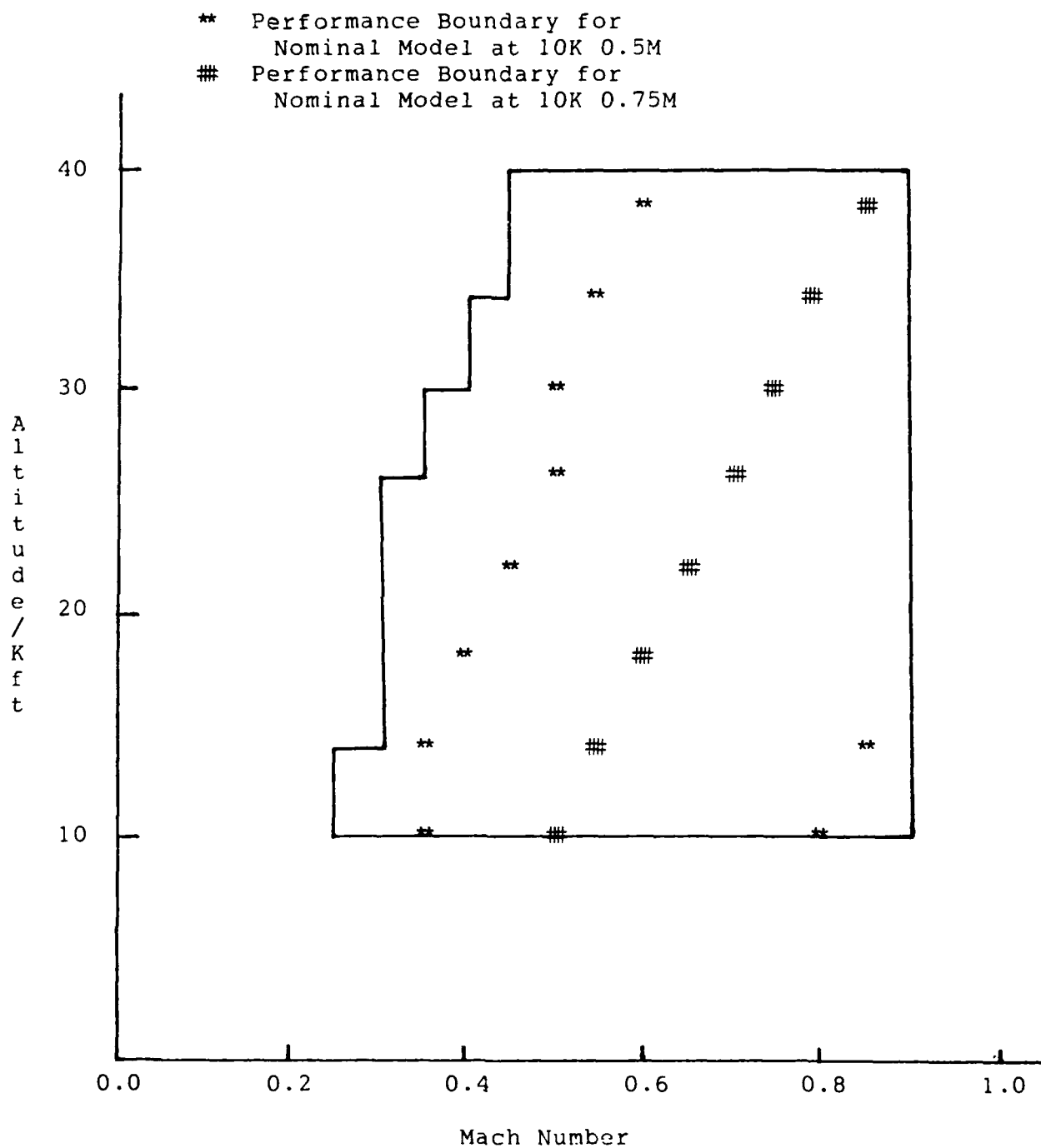
Figure 6-32.   Performance Boundaries
for Configuration 2
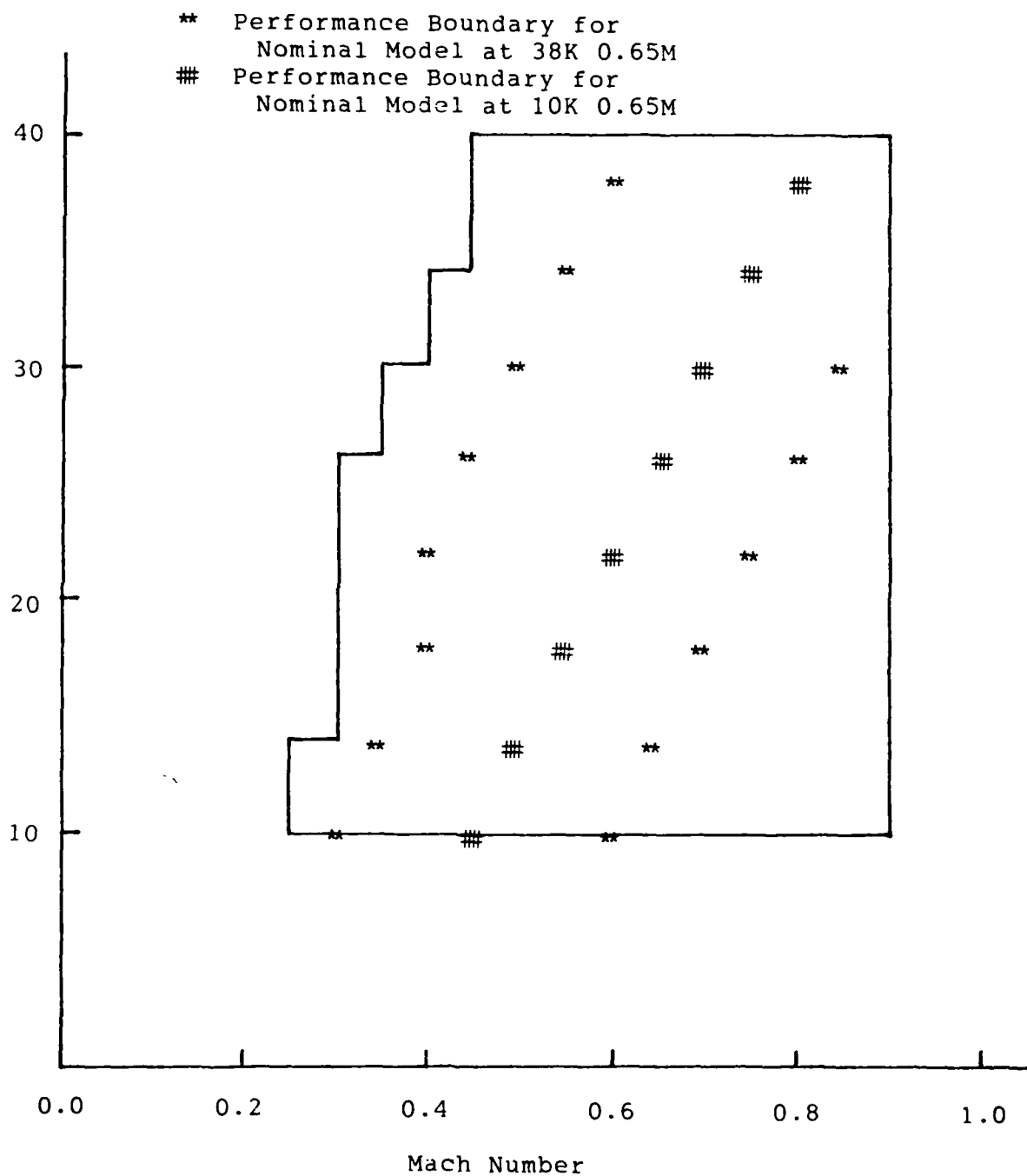
Figure 6-33.   Performance Boundaries
for Configuration 3
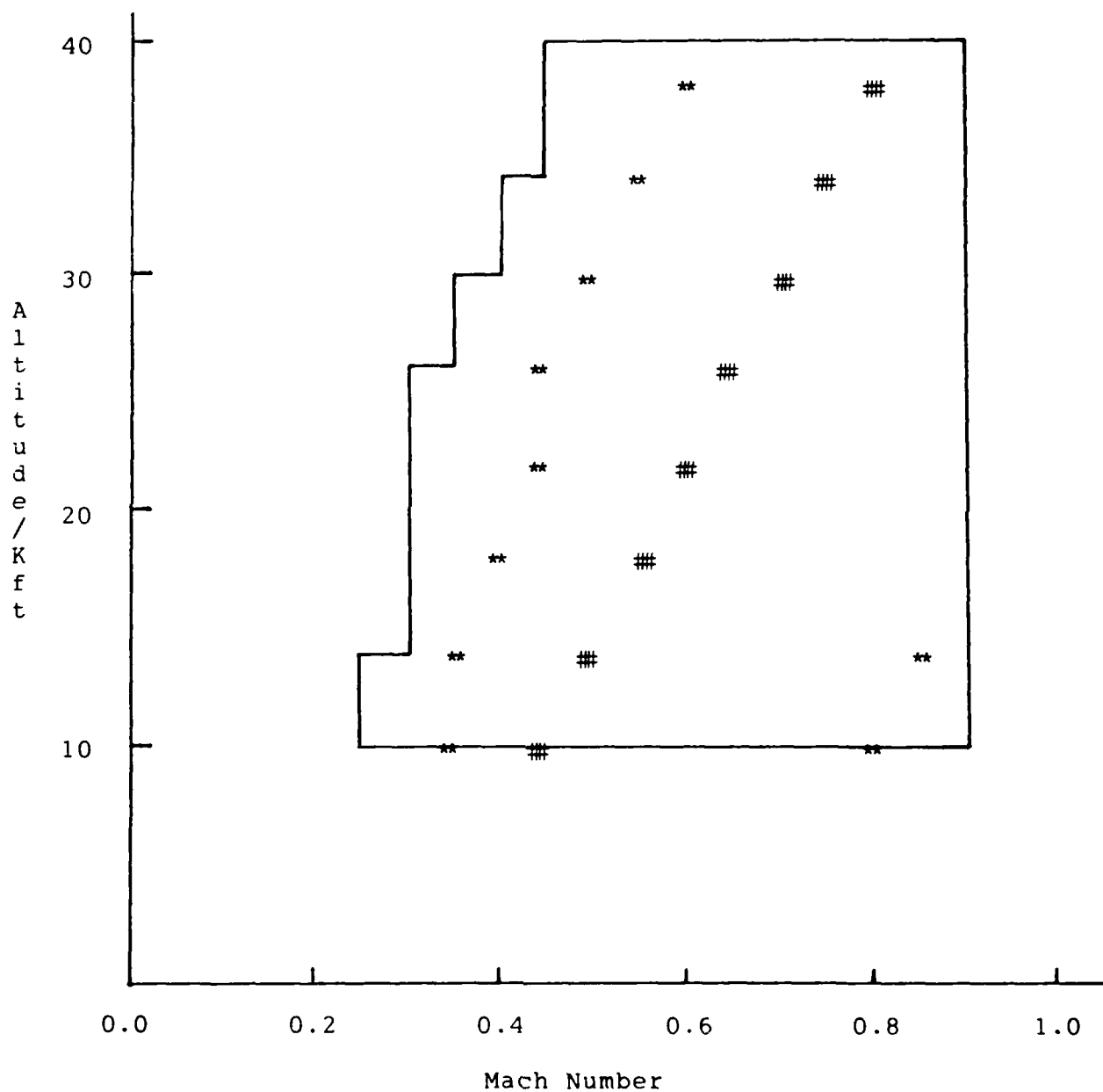
Figure 6-34. Performance Boundaries
for Configuration 4

111
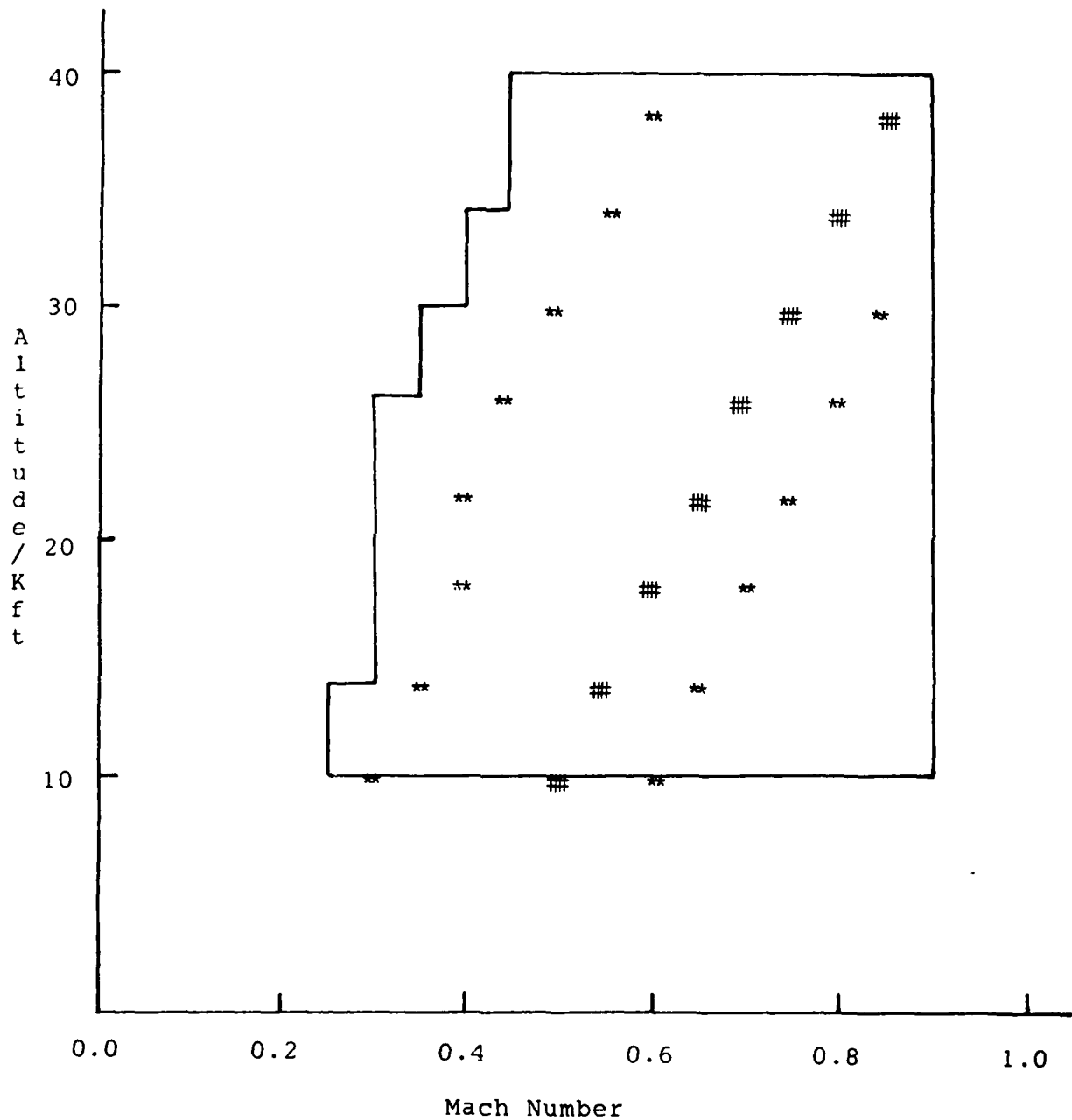
Figure 6-35.   Performance Boundaries
for Configuration 5

112

arrives at the estimated value of the $\underline{B}_1$ portion of the

parameter vector by a blending process of the hypothesis

probabilities (see Chapter 4), the amount of overlap of the

performance boundaries is important. Figures 6-36 through

6-44 show the significance of the overlap of the performance

boundaries. It is seen from Figures 6-36 through 6-44 that

although the operating point of each of the examples lies

within the performance boundaries (see Figures 6-32

through 6-34) the control law gains that were implemented

caused the performance criteria to be violated.

The reason that the performance criteria were violated,

was due to the manner in which the multiple model algorithm

was implemented. By looking at the plots of the hypothesis

probabilities (see Figures 6-38,41,44), it can be seen that

the multiple model algorithm calculated a probability of

approximately one for one of the two models, while the other

model was given a probability of approximately zero. If the

probabilties were exactly one and zero for the respective

cases, the time responses for the adaptive case would be the

same as those generated for the fixed gain case. The fact

that the responses were different for the adaptive versus

the fixed gain system showed that the probabilities were not

113
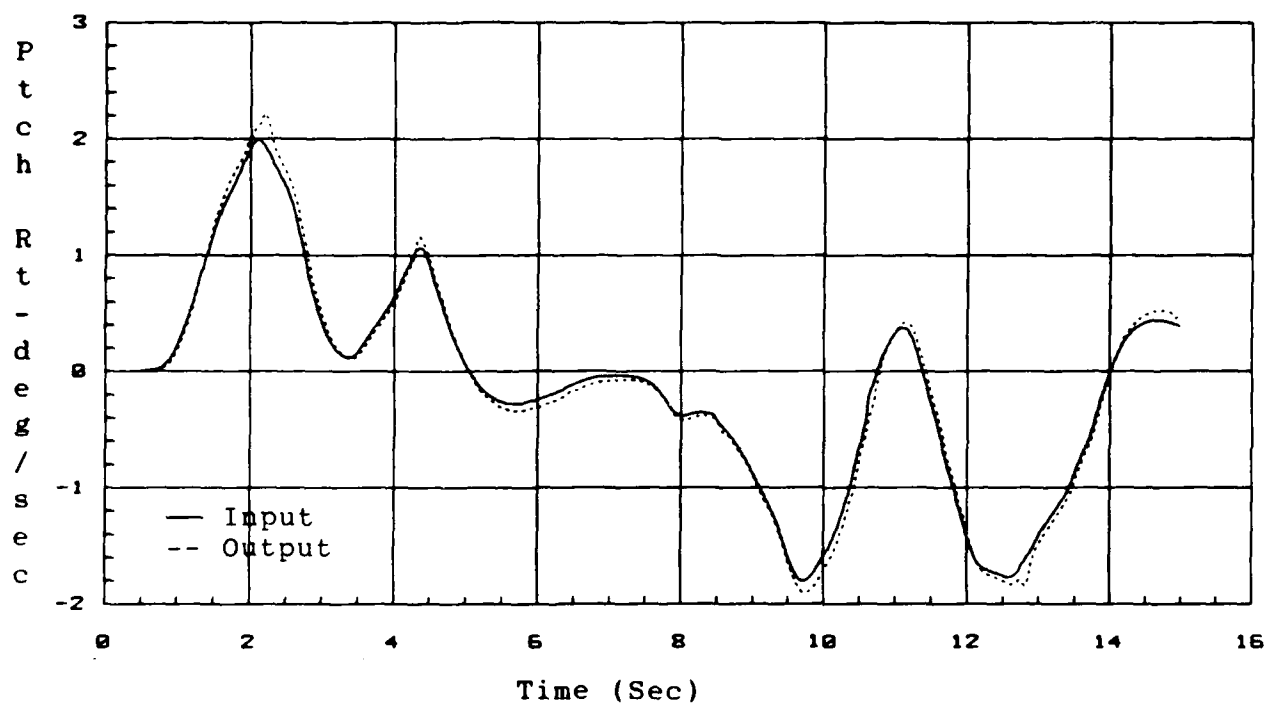
Figure 6-36. Pitch Rate Response
Configuration 2/Operating Point: 14K 0.35M
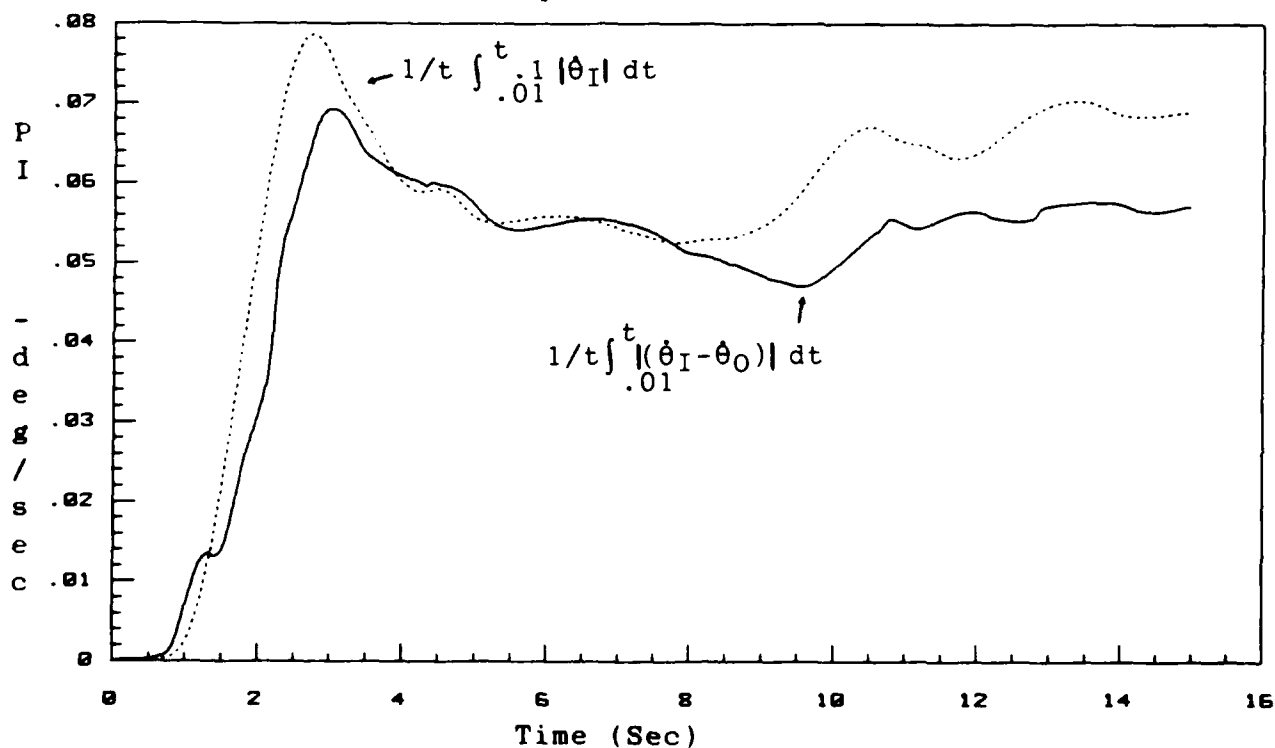
Figure 6-37. Pitch Rate Performance Criterion
Configuration 2/Operating Point: 14K 0.35M

114
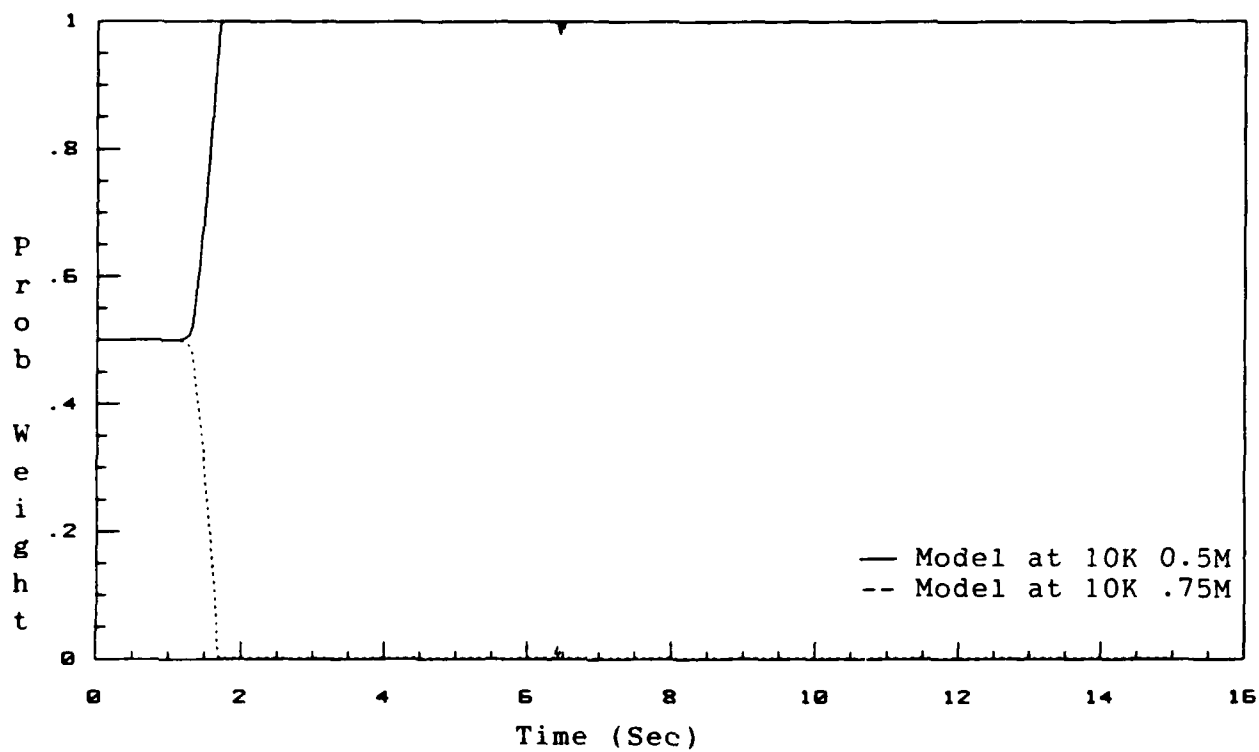
Figure 6-38.   Model Probability Weightings
Configuration 2/Operating Point: 14K 0.35M

115
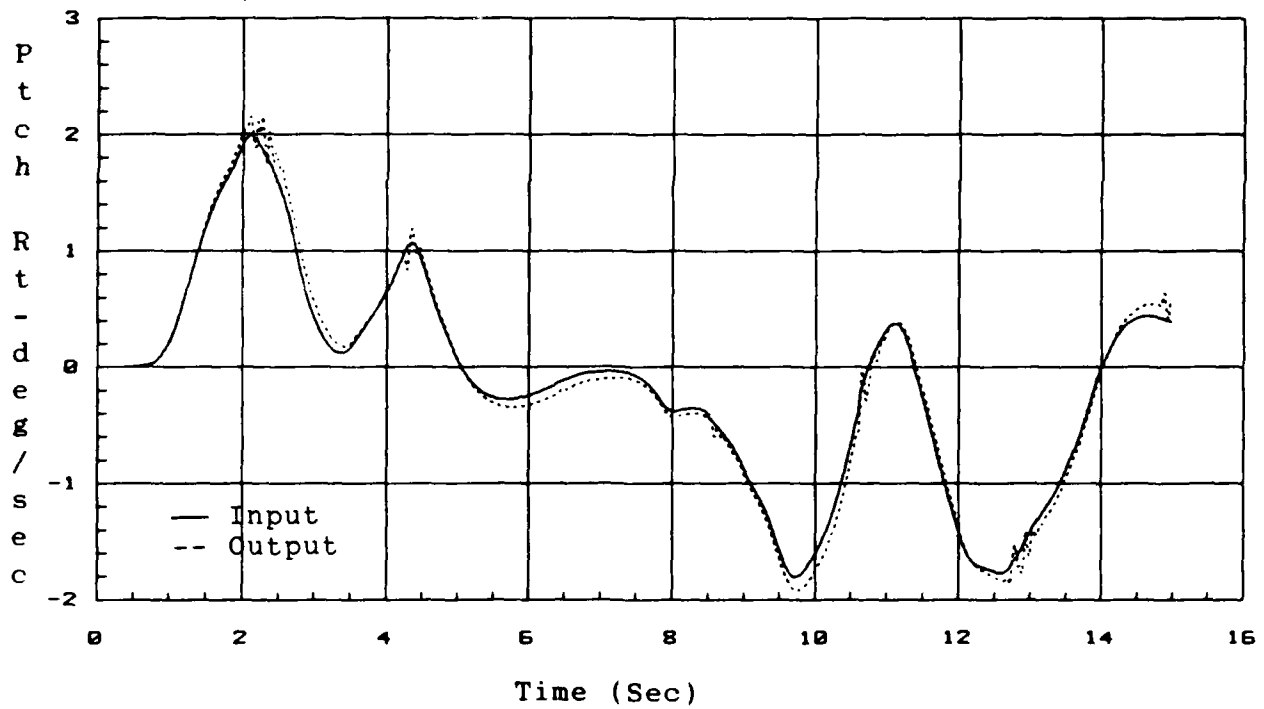
Figure 6-39.   Pitch Rate Response
Configuration 4/Operating Point: 14K 0.9M

$$1/t \int_{.01}^{t} |\dot{\theta}_I| \, dt$$

$$1/t \int_{.01}^{t} |(\dot{\theta}_I - \dot{\theta}_O)| \, dt$$
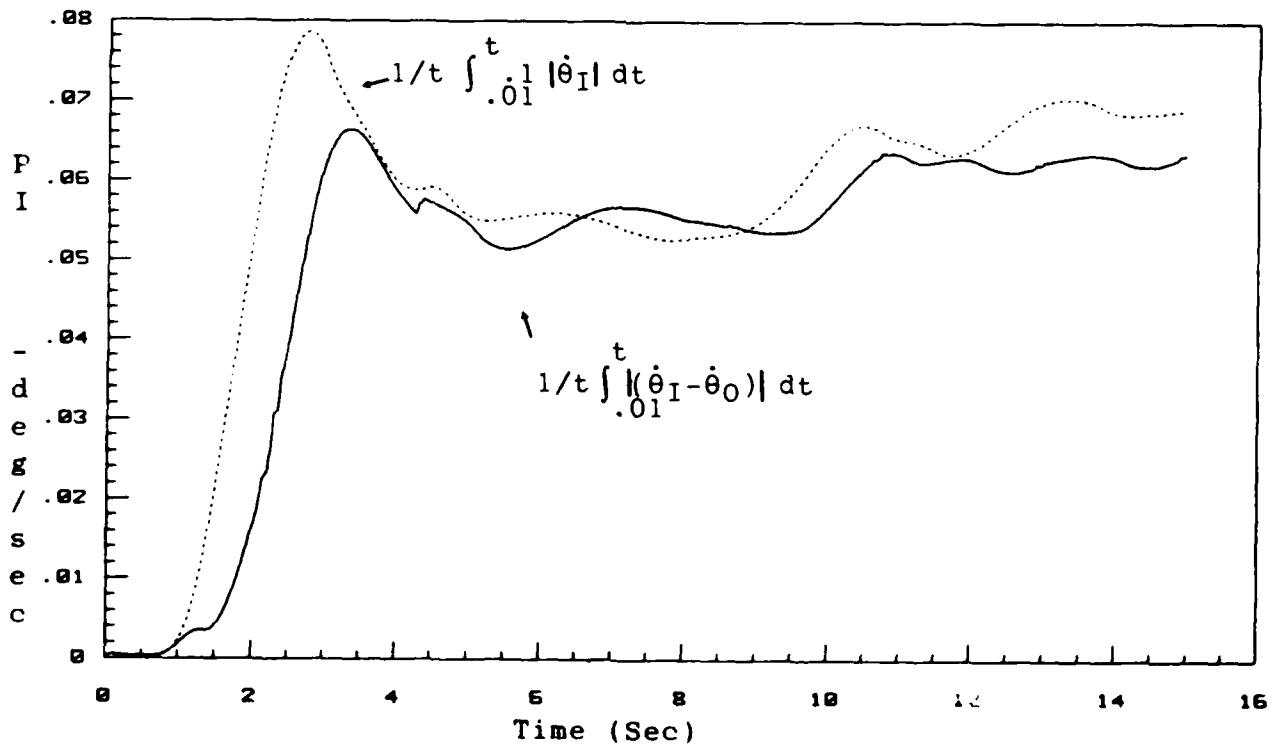
Figure 6-40.   Pitch Rate Performance Criterion
Configuration 4/Operating Point: 14K 0.9M

116
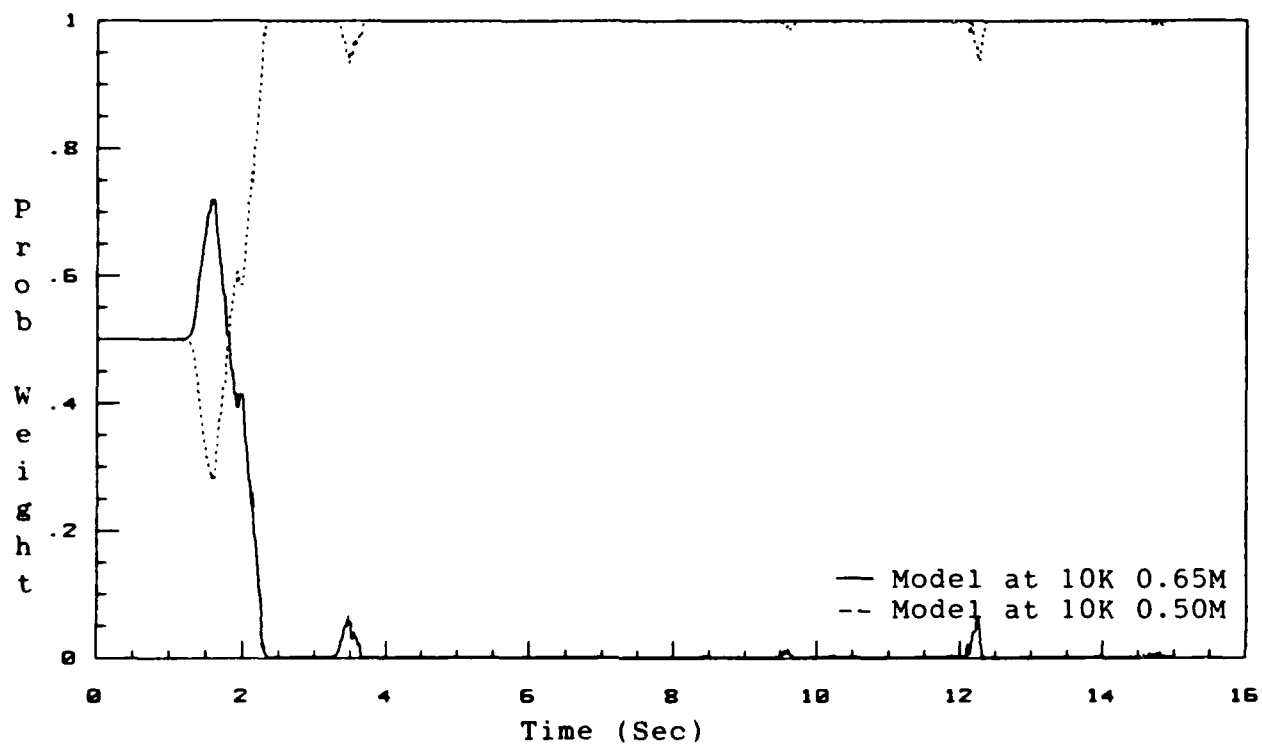
Figure 6-41. Model Probability Weightings
Configuration 4/Operating Point: 14K 0.9M
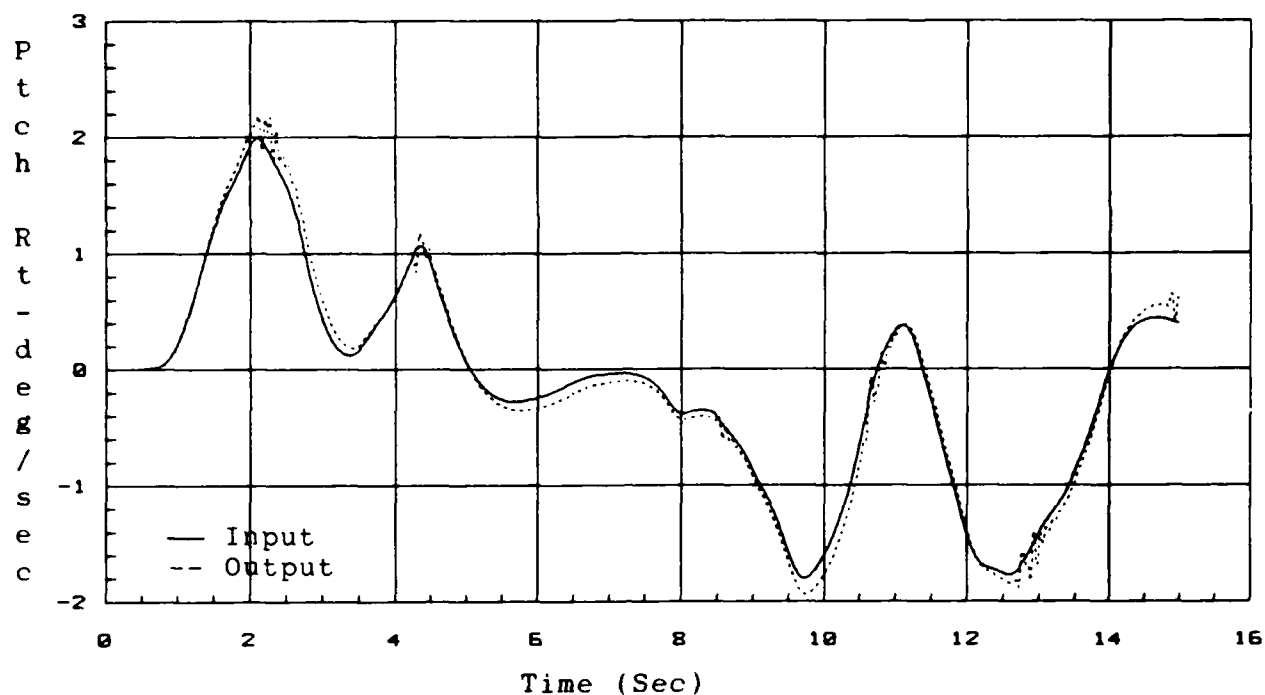
Figure 6-42. Pitch Rate Response
Configuration 3/Operating Point: 10K 0.9M
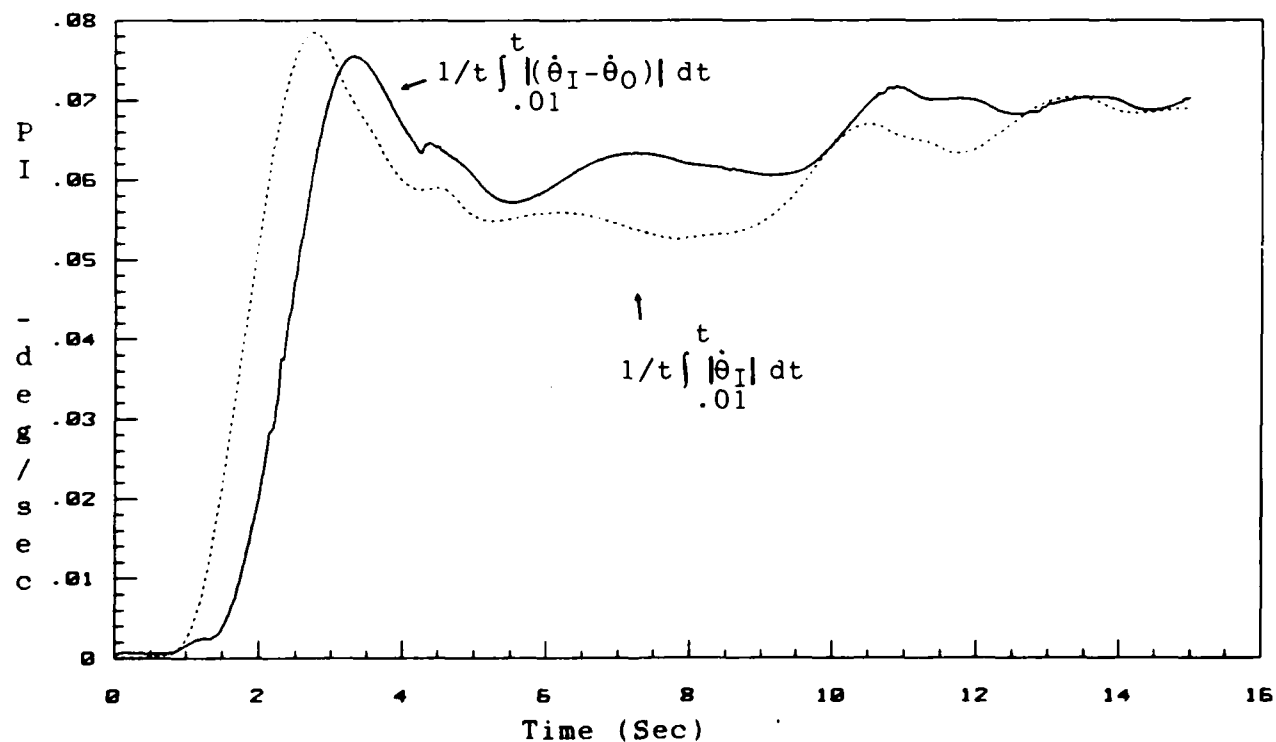
Figure 6-43. Pitch Rate Performance Criterion
Configuration 3/Operating Point: 10K 0.9M

118
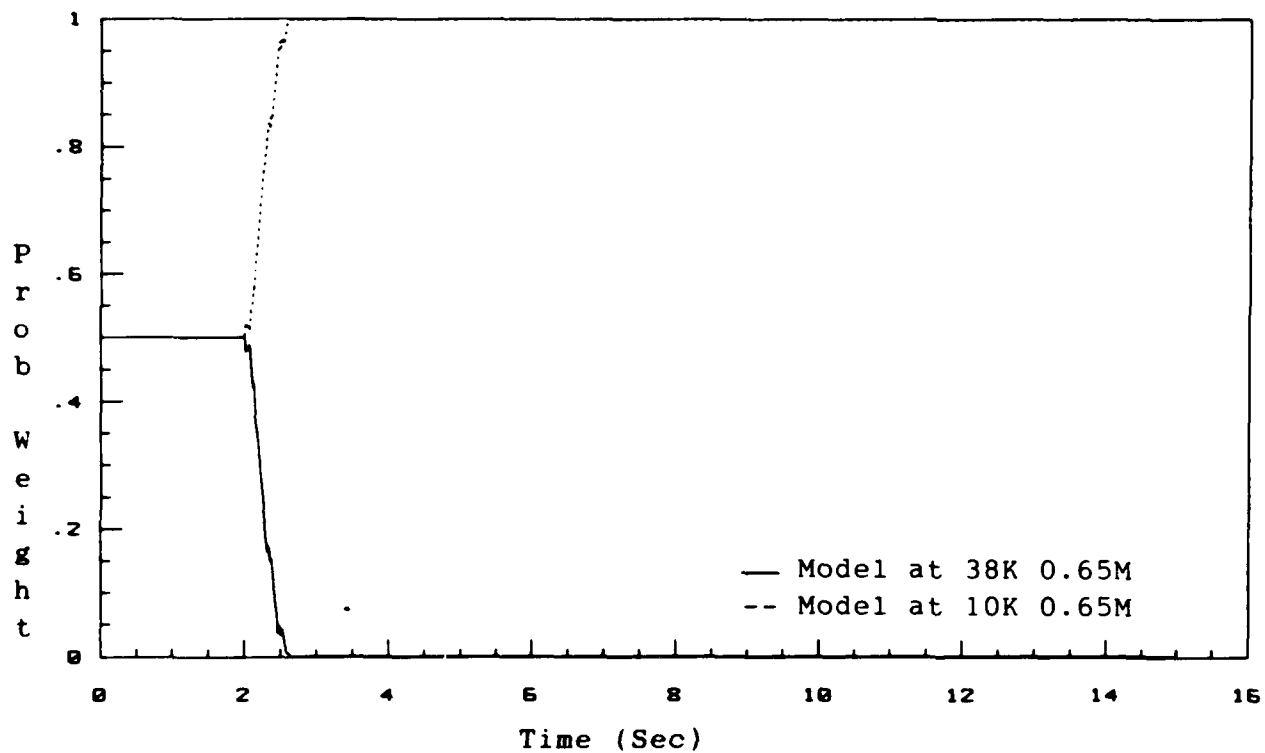
Figure 6-44.   Model Probability Weightings
Configuration 3/Operating Point: 10K 0.9M

119

exactly equal to one and zero.

The multiple model algorithm is implemented with a lower probability bound so the probability of any given candidate model will not be set to zero. The reason for this is that the multiple model algorithm is updated recursively and, if a candidate model's probability goes to zero, the contribution of that model will be eliminated from that point forward.

Lower bounding the candidate model probabilities means that every candidate model will have an effect on the control law gains to some degree. This means that, even if the operating point of the system is at a candidate model position the control law gains will differ slightly from the gains of the specific candidate model. When the candidate models are placed on constant dynamic pressure lines that are 'too far apart' and the operating point is close to the performance boundary of one of the models (see Figure 6-32) the gains may become such that the performance criteria is violated. By referring to Figure 6-32, it can be seen that the operating point is well outside the perfomance boundary of model 2 and on the boundary of model 1. Although model 1 has a high probability associated with it as

120

the correct model, by including the small contribution of the control law gains associated with model 2 the performance criteria was violated. This is shown in the data presented on Figures 6-36 through 6-38.

By running simulations with different values of the lower bound for the weighting factors, it was seen that there is an interplay between the amount of overlap required for the performance boundaries and the lower bound size. The smaller the value of the lower bound the less overlap was required of the performance boundaries (so that satisfactory tracking performance would be obtained for all the flight conditions within the union of the performance boundaries).

By using a lower bound value for the weighting factors of 0.01 it was determined that the candidate models need to be placed so that there is a sufficient amount of overlap between the performance boundaries. As shown on Figure 6-45, when the boundaries overlap it is preferable to have the boundary of one model well inside the performance boundary of the second model to minimize the problem discussed above. Also, the position of the candidate models that will cover the outer boundaries of the desired flight envelope

121
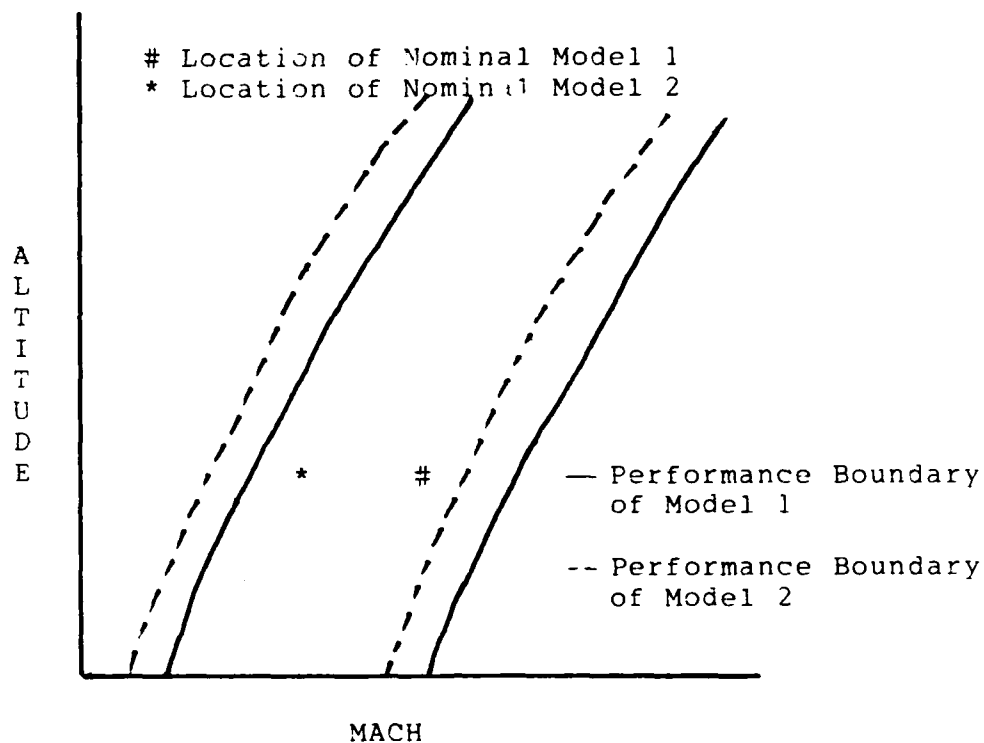
Figure 6-45. Performance Boundary Overlap

need to be placed so the outer boundaries of the flight

envelope are well inside the specific candidate models'

performance boundaries (see Figure 6-45). Because the model

placement requirements could be better achieved with three

models instead of two, several three-model configurations

were evaluated in an attempt to achieve the desired tracking

performance over the flight envelope of interest.

122

6.2.3 Three-Model Configurations

The three-model configurations that were evaluated are presented in Table 6-9. A graphical presentation of the three-model configurations are given in Figure 6-46. From the beginning of the three-model configuration evaluation, it was clear that the desired tracking performance could be obtained over the flight envelope of interest with three models.

The first three-model configurations that were evaluated were configurations 6, 7, and 8 (see Table 6-9). The models for configurations 6, 7, and 8, were chosen so that the values of dynamic pressures for the candidate models would be as close as possible with the data used for this thesis. The reason for doing this was to examine the effect of choosing different nominal models (with essentially the same dynamic pressures) on the multiple model algorithm's performance.

The performance boundaries for configurations 6, 7, and 8 are presented on Figures 6-47, 6-48, and 6-49. They show that the performance boundaries for each configuration are approximately the same. This equivalency of performance boundaries is due to the fact that each configuration con-

Table 6-9

Three-Model Configurations

Configuration	Nominal Model Flight Conditions		
	Alt (Kft)	Mach	Dynamic Pressure
6	38	0.65	127.95
	26	0.70	258.18
	10	0.75	573.14
7	30	0.50	110.19
	22	0.65	264.58
	14	0.80	557.18
8	10	0.35	124.81
	10	0.50	254.73
	10	0.75	573.14
9	22	0.45	126.81
	22	0.65	264.58
	22	0.90	507.24
10	10	0.35	124.81
	38	0.80	193.82
	10	0.75	573.14
11	10	0.35	124.81
	22	0.65	264.58
	10	0.75	573.14
12	10	0.35	124.81
	26	0.70	258.18
	10	0.75	573.14
13	22	0.45	126.81
	22	0.65	264.58
	10	0.75	573.14
14	22	0.45	126.81
	10	0.50	254.73
	10	0.75	573.14
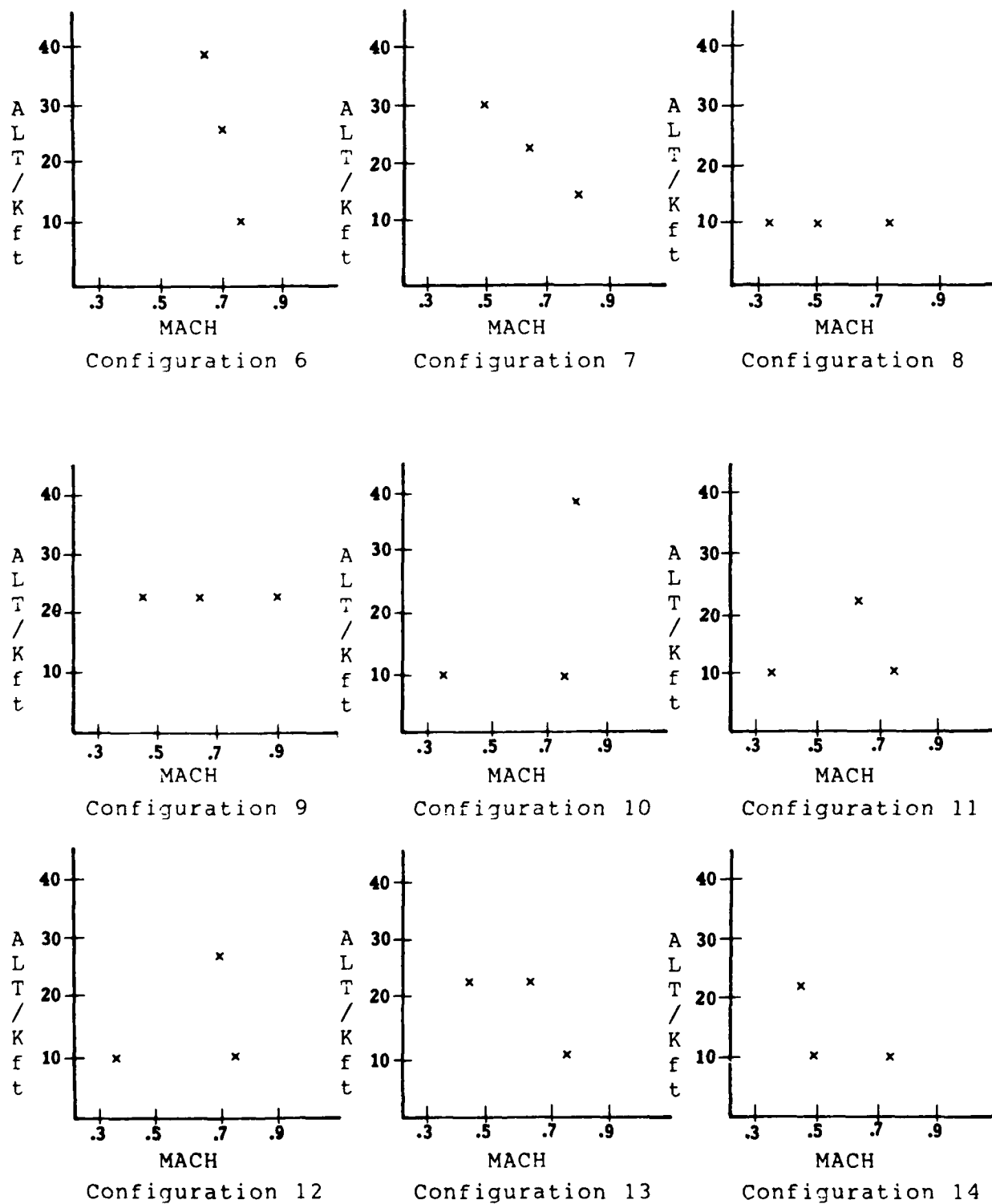
Figure 6-46. Three-Model Configurations

125
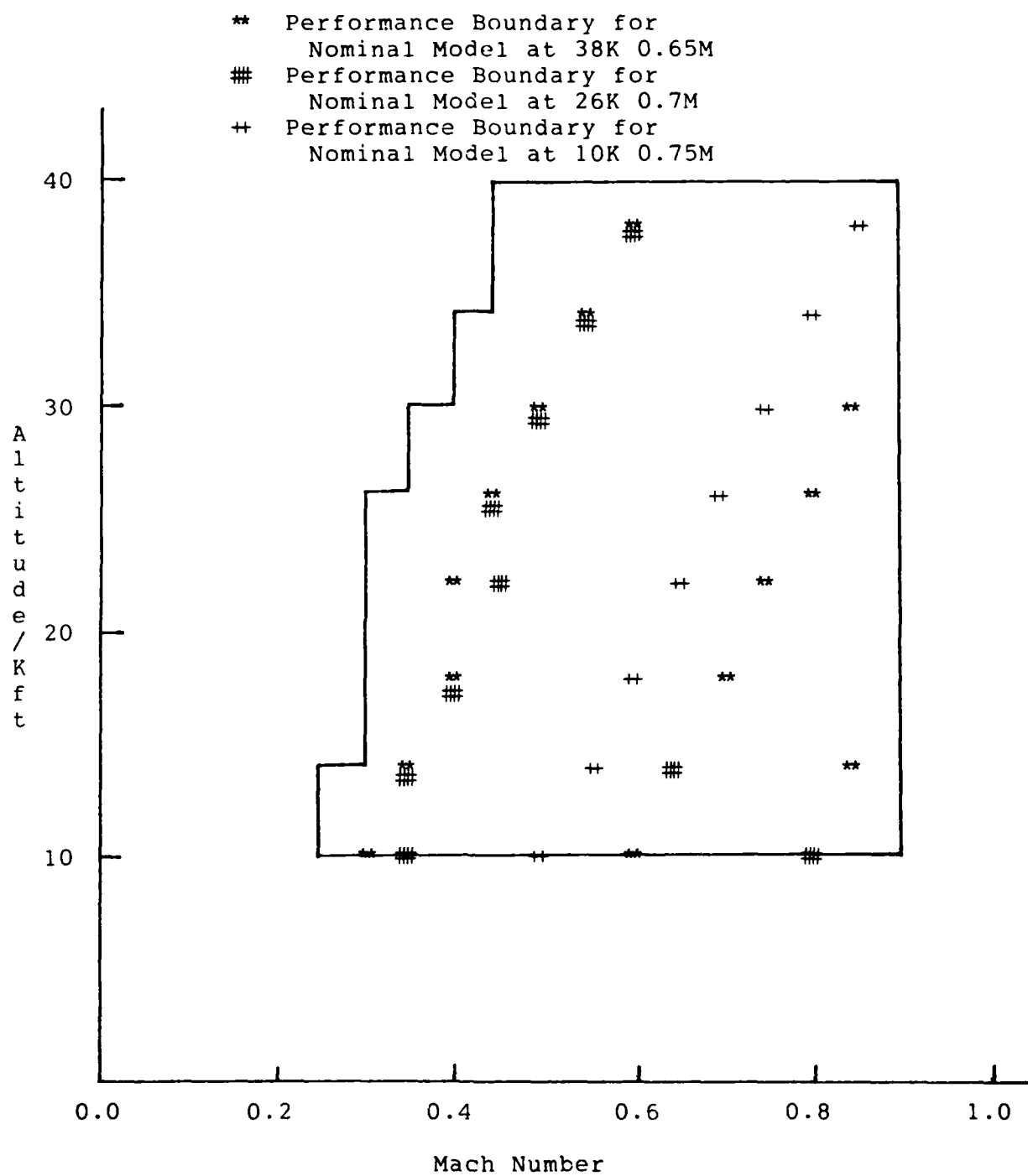
Figure 6-47. Performance Boundaries
for Configuration 6
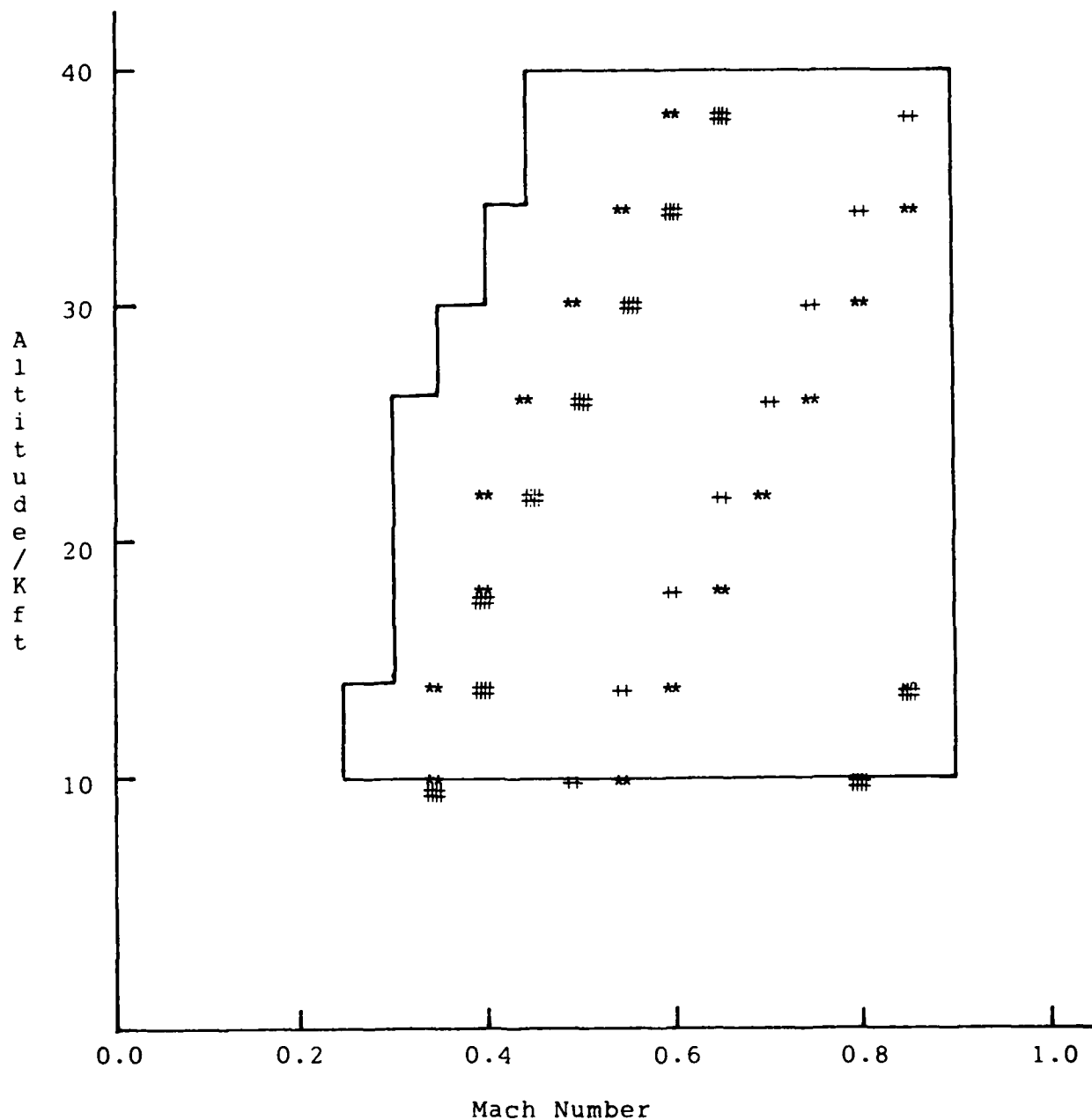
Figure 6-48.   Performance Boundaries
for Configuration 7
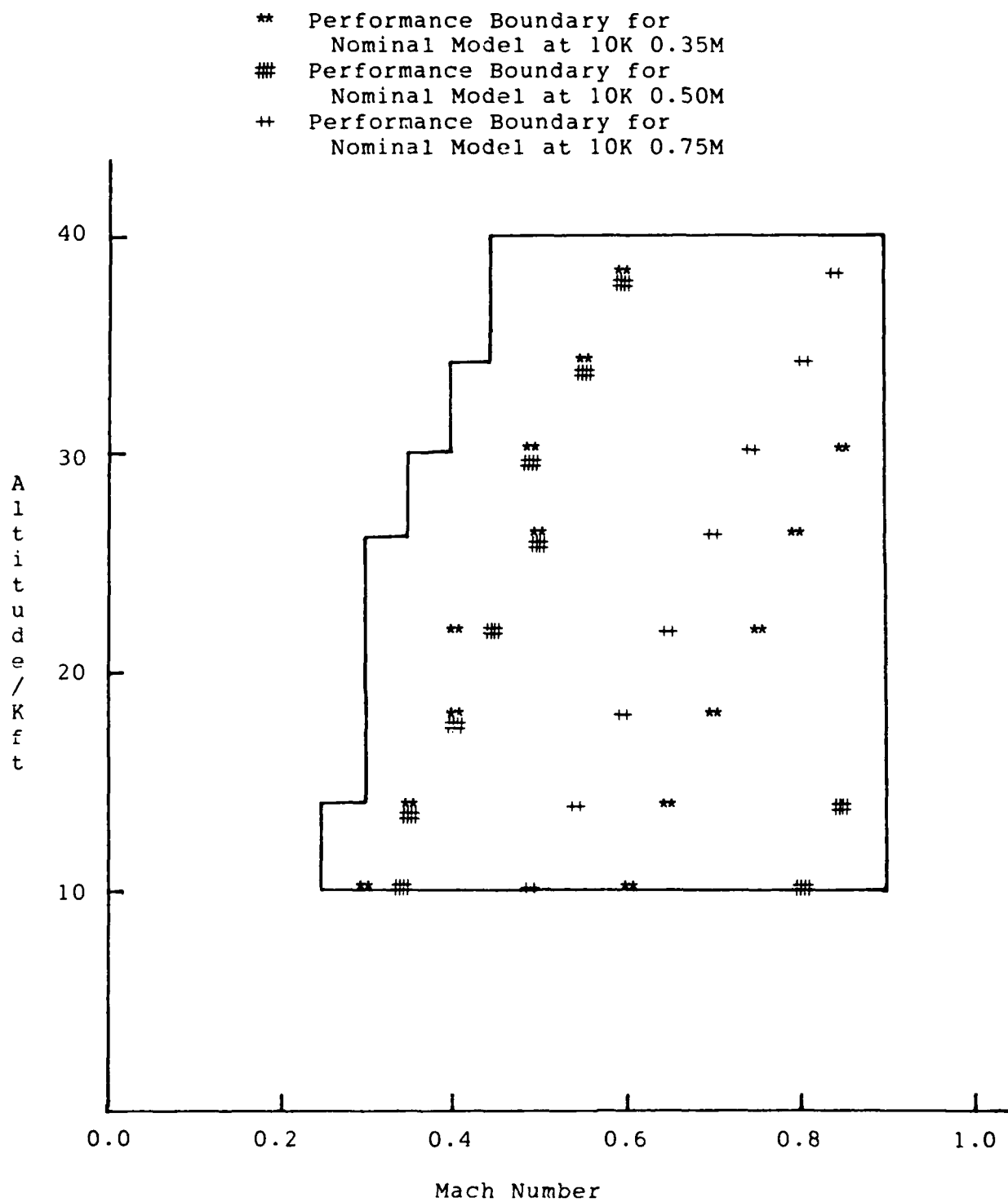
Figure 6-49. Performance Boundaries
for Configuration 8

sists of models with approximately the same dynamic pressures. The reason for the equivalency of the performance boundaries of models with the same dynamic pressure was discussed earlier in this chapter.

Following the establishment of the performance boundaries of configurations 6, 7, and 8, simulations were run using the multiple model algorithm for every flight condition in the flight envelope of interest. The results of those simulations are presented on Tables 6-10 through 6-12 and on Figures 6-50 through 6-52.

Figures 6-50 through 6-52 show graphically which model or models the multiple model algorithm selected as the model to represent the current flight condition. It should be pointed out that the performance criteria were met for every flight condition with the nominal models of configurations 6, 7, and 8. As an example of how the individual entries for each flight condition were determined for Figures 6-50 through 6-52, consider the flight condition 26,000 feet and 0.45 Mach for configuration 6. By looking at the plot of the conditional probabilities for the candidate models (see Figure 6-53), it can be seen that the probability of candidate model one (38,000 ft, 0.65 Mach) is above 0.9. There-

129

Table 6-10

Model Selection Data for Configuration 6

Operating Point			Candidate Model Deltas									Selected Model
			Model 1			Model 2			Model 3			
ALT	MACH	Q	ALT	MACH	Q	ALT	MACH	Q	ALT	MACH	Q	
10K	0.25	63.7	28K	0.40	64.3	16K	0.45	194.5	0	0.50	509.5	1
10K	0.30	91.7	28K	0.35	36.3	16K	0.40	166.5	0	0.45	481.4	1
10K	0.35	124.8	28K	0.30	3.1	16K	0.30	133.7	0	0.40	448.3	1
10K	0.30	163.0	28K	0.25	35.1	16K	0.30	95.2	0	0.35	410.1	2,1
10K	0.45	206.3	28K	0.20	78.3	16K	0.25	51.8	0	0.30	366.8	2
10K	0.50	254.7	28K	0.15	126.8	16K	0.20	3.5	0	0.25	318.4	2
10K	0.55	308.2	28K	0.10	180.3	16K	0.15	50.0	0	0.20	264.9	2
10K	0.60	366.8	28K	0.05	238.9	16K	0.10	108.6	0	0.15	206.3	2,3
10K	0.65	430.5	28K	0.00	302.6	16K	0.05	172.3	0	0.10	142.6	3,2
10K	0.70	499.3	28K	0.05	371.3	16K	0.00	241.1	0	0.05	73.9	3
10K	0.75	573.1	28K	0.10	445.2	16K	0.05	315.0	0	0.00	00.0	3
10K	0.80	652.2	28K	0.15	524.2	16K	0.10	393.9	0	0.05	78.9	3
10K	0.85	736.2	28K	0.20	608.2	16K	0.15	478.0	0	0.10	163.0	3
10K	0.90	825.3	28K	0.25	697.4	16K	0.20	567.1	0	0.15	252.2	3
14K	0.25	54.4	24K	0.40	73.4	12K	0.45	203.8	4K	0.50	518.7	1
14K	0.30	78.4	24K	0.35	49.6	12K	0.40	179.8	4K	0.45	494.8	1
14K	0.35	106.6	24K	0.30	21.3	12K	0.35	151.5	4K	0.40	466.5	1
14K	0.40	139.3	24K	0.25	11.3	12K	0.30	118.9	4K	0.35	433.9	1
14K	0.45	176.2	24K	0.20	48.3	12K	0.25	81.9	4K	0.30	396.9	2,1
14K	0.50	217.6	24K	0.15	89.7	12K	0.20	40.5	4K	0.25	355.5	2
14K	0.55	263.3	24K	0.10	135.4	12K	0.15	5.2	4K	0.20	309.8	2
14K	0.60	313.4	24K	0.05	185.5	12K	0.10	55.2	4K	0.15	259.7	2
14K	0.65	367.8	24K	0.00	239.9	12K	0.05	109.6	4K	0.10	205.3	2
14K	0.70	426.6	24K	0.05	298.6	12K	0.00	168.5	4K	0.05	146.6	3,2
14K	0.75	489.7	24K	0.10	361.7	12K	0.05	231.5	4K	0.00	83.5	3,2
14K	0.80	557.2	24K	0.15	429.2	12K	0.10	298.9	4K	0.05	15.9	3
14K	0.85	628.9	24K	0.20	501.0	12K	0.15	370.8	4K	0.10	55.8	3
14K	0.90	705.1	24K	0.25	577.2	12K	0.20	446.9	4K	0.15	132.0	3
18K	0.30	66.6	20K	0.35	61.3	8K	0.40	191.6	8K	0.45	506.5	1
18K	0.35	90.7	20K	0.30	37.3	8K	0.35	167.5	8K	0.40	482.5	1

130

Table 6-10 (cont.)

Model Selection Data for Configuration ...

Operating Point			Candidate Model Deltas									Selected Model
			Model 1			Model 2			Model 3			
ALT	MACH	Q	ALT	MACH	Q	ALT	MACH	Q	ALT	MACH	Q	Model
18K	0.40	118.4	20K	0.25	9.5	8K	0.30	139.7	8K	0.35	454.7	1
18K	0.45	149.9	20K	0.20	21.9	8K	0.25	108.2	8K	0.30	423.2	1
18K	0.50	185.1	20K	0.15	57.1	8K	0.20	73.1	8K	0.25	388.1	2,1
18K	0.55	223.9	20K	0.10	95.9	8K	0.15	34.3	8K	0.20	349.2	2
18K	0.60	266.5	20K	0.05	138.5	8K	0.10	8.3	8K	0.15	306.6	2
18K	0.65	312.8	20K	0.00	184.8	8K	0.05	54.6	8K	0.10	260.4	2
18K	0.70	362.7	20K	0.05	234.8	8K	0.00	104.5	8K	0.05	210.4	2
18K	0.75	416.4	20K	0.10	288.4	8K	0.05	158.2	8K	0.00	156.8	2,3
18K	0.80	473.8	20K	0.15	345.4	8K	0.10	215.2	8K	0.05	99.8	3,2
18K	0.85	534.8	20K	0.20	406.9	8K	0.15	276.6	8K	0.10	38.3	3
18K	0.90	599.6	20K	0.25	471.6	8K	0.20	341.4	8K	0.15	26.5	3
22K	0.30	56.4	16K	0.35	71.6	4K	0.40	201.8	12K	0.45	516.8	1
22K	0.35	76.7	16K	0.30	51.2	4K	0.35	181.5	12K	0.40	496.4	1
22K	0.40	100.2	16K	0.25	27.8	4K	0.30	58.0	12K	0.35	472.9	1
22K	0.45	126.8	16K	0.20	1.1	4K	0.25	131.4	12K	0.30	446.3	1
22K	0.50	156.6	16K	0.15	28.6	4K	0.20	101.6	12K	0.25	416.6	1
22K	0.55	189.4	16K	0.10	61.5	4K	0.15	68.8	12K	0.20	383.7	2,1
22K	0.60	225.4	16K	0.05	97.5	4K	0.10	32.7	12K	0.15	347.7	2
22K	0.65	264.6	16K	0.00	136.6	4K	0.05	6.4	12K	0.10	308.6	2
22K	0.70	306.9	16K	0.05	178.9	4K	0.00	48.7	12K	0.05	266.3	2
22K	0.75	352.2	16K	0.10	224.3	4K	0.05	94.1	12K	0.00	220.9	2
22K	0.80	400.8	16K	0.15	272.8	4K	0.10	142.6	12K	0.05	172.4	2,3
22K	0.85	452.5	16K	0.20	324.5	4K	0.15	194.3	12K	0.10	120.7	2,3
22K	0.90	507.2	16K	0.25	379.3	4K	0.20	249.1	12K	0.15	65.9	3,2
26K	0.30	47.4	12K	0.35	80.5	0	0.40	210.8	16K	0.45	525.7	1
26K	0.35	64.5	12K	0.30	63.4	0	0.35	193.6	16K	0.40	508.6	1
26K	0.40	84.3	12K	0.25	43.7	0	0.30	173.9	16K	0.35	488.8	1
26K	0.45	106.7	12K	0.20	21.3	0	0.25	151.5	16K	0.30	466.4	1
26K	0.50	131.7	12K	0.15	3.8	0	0.20	126.5	16K	0.25	441.8	1
26K	0.55	159.4	12K	0.10	31.4	0	0.15	98.8	16K	0.20	413.8	1

Table 6-10 (cont)

Model Selection Data for Configuration 6

Operating Point			Candidate Model Deltas									Selected Model
			Model 1			Model 2			Model 3			
ALT	MACH	Q	ALT	MACH	Q	ALT	MACH	Q	ALT	MACH	Q	
26K	0.60	189.7	12K	0.05	61.7	0	0.10	68.5	16K	0.15	383.5	2,1
26K	0.65	222.6	12K	0.00	94.7	0	0.05	35.6	16K	0.10	350.5	2
26K	0.70	258.2	12K	0.05	130.2	0	0.00	0.00	16K	0.05	315.0	2
26K	0.75	296.4	12K	0.10	168.4	0	0.05	38.2	16K	0.00	276.8	2
26K	0.80	337.2	12K	0.15	209.3	0	0.10	79.0	16K	0.05	235.9	2,3
26K	0.85	380.7	12K	0.20	252.7	0	0.15	122.5	16K	0.10	192.5	2,3
26K	0.90	426.8	12K	0.25	298.8	0	0.20	168.6	16K	0.15	146.4	2,3
30K	0.35	53.9	12K	0.30	74.0	4K	0.35	204.2	20K	0.40	519.1	1
30K	0.40	76.5	8K	0.25	51.4	4K	0.30	181.7	20K	0.35	496.6	1
30K	0.45	89.3	8K	0.20	38.7	4K	0.25	168.9	20K	0.30	483.9	1
30K	0.50	110.2	8K	0.15	17.7	4K	0.20	148.0	20K	0.25	462.9	1
30K	0.55	133.3	8K	0.10	5.4	4K	0.15	124.9	20K	0.20	439.8	1
30K	0.60	158.7	8K	0.05	30.7	4K	0.10	99.5	20K	0.15	414.5	1
30K	0.65	186.2	8K	0.00	58.3	4K	0.05	71.9	20K	0.10	386.9	1
30K	0.70	216.0	8K	0.05	88.0	4K	0.00	42.2	20K	0.05	357.2	1
30K	0.75	247.9	8K	0.10	119.9	4K	0.05	10.3	20K	0.00	325.2	1,2
30K	0.80	282.1	8K	0.15	154.1	4K	0.10	23.9	20K	0.05	291.1	2,1
30K	0.85	318.5	8K	0.20	190.5	4K	0.15	60.3	20K	0.10	254.7	2,1
30K	0.90	357.0	8K	0.25	229.1	4K	0.20	98.9	20K	0.15	216.1	2,3
34K	0.40	58.6	4K	0.25	69.3	8K	0.30	199.6	14K	0.35	514.5	2,3
34K	0.45	74.2	4K	0.20	53.8	8K	0.25	184.0	14K	0.30	498.9	1
34K	0.50	91.6	4K	0.15	36.3	8K	0.20	166.6	14K	0.25	481.5	1
34K	0.55	110.9	4K	0.10	17.1	8K	0.15	147.3	14K	0.20	462.3	1
34K	0.60	131.9	4K	0.05	4.0	8K	0.10	126.3	14K	0.15	441.2	1
34K	0.65	154.8	4K	0.00	26.9	8K	0.05	103.4	14K	0.10	418.3	1
34K	0.70	179.6	4K	0.05	51.6	8K	0.00	78.6	14K	0.05	393.6	1
34K	0.75	206.1	4K	0.10	78.2	8K	0.05	52.0	14K	0.00	367.0	1
34K	0.80	234.5	4K	0.15	106.6	8K	0.10	23.7	14K	0.05	338.6	2,1
34K	0.85	264.8	4K	0.20	136.8	8K	0.15	6.6	14K	0.10	308.4	2,1
34K	0.90	296.8	4K	0.25	168.9	8K	0.20	38.6	14K	0.15	276.3	2,3

132

Table 5-10 (cont)

Model Selection Data for Configuration 5

Operating Point			Candidate Model Deltas									Selected Model
			Model 1			Model 2			Model 3			
ALT	MACH	Q	ALT	MACH	Q	ALT	MACH	Q	ALT	MACH	Q	
38K	0.45	61.3	0	0.20	66.6	12K	0.25	196.9	18K	0.30	511.8	1
38K	0.50	75.7	0	0.15	52.2	12K	0.20	182.5	18K	0.25	497.4	1
38K	0.55	91.6	0	0.10	36.3	12K	0.15	166.5	18K	0.20	481.5	1
38K	0.60	109.0	0	0.05	18.9	12K	0.10	149.2	18K	0.15	464.1	1
38K	0.65	128.0	0	0.00	0.0	12K	0.05	130.2	18K	0.10	445.2	1
38K	0.70	148.4	0	0.05	20.0	12K	0.00	109.8	18K	0.05	424.7	1
38K	0.75	170.4	0	0.10	42.4	12K	0.05	87.8	18K	0.00	402.8	1
38K	0.80	193.8	0	0.15	65.9	12K	0.10	64.4	18K	0.05	379.3	1
38K	0.85	218.8	0	0.20	90.9	12K	0.15	39.4	18K	0.10	354.3	2,1
38K	0.90	245.3	0	0.25	117.4	12K	0.20	12.9	18K	0.15	327.8	2,1

Table 6-11

Model Selection Data for Configuration 7

Operating Point			Candidate Model Deltas									Selected Model
			Model 1			Model 2			Model 3			
ALT	MACH	Q	ALT	MACH	Q	ALT	MACH	Q	ALT	MACH	Q	
10K	0.25	63.7	4K	0.55	493.5	12K	0.40	200.9	20K	0.25	46.5	3
10K	0.30	91.7	4K	0.50	465.4	12K	0.35	172.9	20K	0.20	18.5	3
10K	0.35	124.8	4K	0.45	432.4	12K	0.30	139.8	20K	0.15	14.6	3
10K	0.40	163.0	4K	0.40	394.1	12K	0.25	101.6	20K	0.10	52.8	3,2
10K	0.45	206.3	4K	0.35	350.8	12K	0.20	58.3	20K	0.05	96.1	2
10K	0.50	254.7	4K	0.30	302.4	12K	0.15	9.9	20K	0.00	144.5	2
10K	0.55	308.2	4K	0.25	248.9	12K	0.10	43.6	20K	0.05	198.0	2
10K	0.60	366.8	4K	0.20	190.4	12K	0.05	102.2	20K	0.10	256.6	2,1
10K	0.65	430.5	4K	0.15	126.7	12K	0.00	165.9	20K	0.15	320.3	1,2
10K	0.70	499.3	4K	0.10	57.9	12K	0.05	234.7	20K	0.20	389.1	1
10K	0.75	573.1	4K	0.05	16.0	12K	0.10	308.6	20K	0.25	462.9	1
10K	0.80	652.1	4K	0.00	94.9	12K	0.15	387.5	20K	0.30	541.9	1
10K	0.85	736.2	4K	0.05	179.0	12K	0.20	471.6	20K	0.35	625.9	1
10K	0.90	825.3	4K	0.10	268.2	12K	0.25	560.7	20K	0.40	715.1	1
14K	0.25	54.5	0	0.55	502.8	8K	0.40	210.2	16K	0.25	55.8	3
14K	0.30	78.4	0	0.50	478.8	8K	0.35	186.2	16K	0.20	31.8	3
14K	0.35	106.6	0	0.45	450.5	8K	0.30	157.9	16K	0.15	3.6	3
14K	0.40	139.3	0	0.40	417.9	8K	0.25	125.3	16K	0.10	29.1	3
14K	0.45	176.3	0	0.35	380.9	8K	0.20	88.3	16K	0.05	66.1	2,3
14K	0.50	217.6	0	0.30	339.5	8K	0.15	46.9	16K	0.00	107.5	2
14K	0.55	263.3	0	0.25	293.9	8K	0.10	1.2	16K	0.05	153.2	2
14K	0.60	313.4	0	0.20	243.7	8K	0.05	48.8	16K	0.10	203.2	2
14K	0.65	367.8	0	0.15	189.4	8K	0.00	103.2	16K	0.15	257.6	2
14K	0.70	426.6	0	0.10	130.6	8K	0.05	161.9	16K	0.20	316.4	1,2
14K	0.75	489.7	0	0.05	67.5	8K	0.10	225.1	16K	0.25	379.5	1
14K	0.80	557.2	0	0.00	0.0	8K	0.15	292.6	16K	0.30	446.9	1
14K	0.85	629.0	0	0.05	71.8	8K	0.20	364.4	16K	0.35	518.8	1
14K	0.90	705.2	0	0.10	148.0	8K	0.25	440.6	16K	0.40	494.9	1
18K	0.30	66.6	4K	0.50	490.5	4K	0.35	198.0	12K	0.20	43.5	3
18K	0.35	90.7	4K	0.45	466.5	4K	0.30	173.9	12K	0.15	19.5	3

134

Table 6-11 (cont)

Model Selection Data for Configuration 7

Operating Point			Candidate Model Deltas								Selected Model
			Model 1			Model 2			Model 3		
ALT	MACH	Q	ALT	MACH	Q	ALT	MACH	Q	ALT	MACH	Q	
18K	0.40	118.4	4K	0.40	438.7	4K	0.25	146.1	12K	0.10	8.3	3
18K	0.45	149.9	4K	0.35	407.3	4K	0.20	114.7	12K	0.05	39.7	3
18K	0.50	185.1	4K	0.30	372.1	4K	0.15	79.5	12K	0.00	74.9	2,3
18K	0.55	223.9	4K	0.25	332.2	4K	0.10	40.7	12K	0.05	113.7	2
18K	0.60	26615	4K	0.20	399.7	4K	0.05	1.9	12K	0.10	156.3	2
18K	0.65	312.8	4K	0.15	244.4	4K	0.00	48.2	12K	0.15	202.6	2
18K	0.70	362.7	4K	0.10	194.5	4K	0.05	98.1	12K	0.20	252.5	2
18K	0.75	416.4	4K	0.05	140.8	4K	0.10	151.8	12K	0.25	306.2	2,1
18K	0.80	473.8	4K	0.00	83.4	4K	0.15	209.2	12K	0.30	363.6	1
18K	0.85	534.8	4K	0.05	22.3	4K	0.20	270.2	12K	0.35	424.6	1
18K	0.90	599.5	4K	0.10	42.4	4K	0.25	335.0	12K	0.40	489.4	1
22K	0.30	56.7	8K	0.50	500.8	0	0.35	208.2	8K	0.20	53.8	3
22K	0.35	76.7	8K	0.45	480.5	0	0.30	187.9	8K	0.15	33.5	3
22K	0.40	100.2	8K	0.40	457.0	0	0.25	164.4	8K	0.10	10.0	3
22K	0.45	126.8	8K	0.35	430.4	0	0.20	137.8	8K	0.05	16.6	3
22K	0.50	156.6	8K	0.30	400.6	0	0.15	108.0	8K	0.00	46.4	3
22K	0.55	189.4	8K	0.25	367.7	0	0.10	75.2	8K	0.05	79.2	2,3
22K	0.60	225.4	8K	0.20	331.7	0	0.30	39.1	8K	0.10	115.3	2
22K	0.65	264.6	8K	0.15	292.6	0	0.00	0.0	8K	0.15	154.4	2
22K	0.70	306.9	8K	0.10	250.3	0	0.05	42.3	8K	0.20	196.7	2
22K	0.75	352.3	8K	0.05	204.9	0	0.10	87.7	8K	0.25	242.1	2
22K	0.80	400.8	8K	0.00	156.4	0	0.15	136.2	8K	0.30	290.6	2,1
22K	0.85	454.5	8K	0.05	104.7	0	0.20	187.9	8K	0.35	342.3	1,2
22K	0.90	507.2	8K	0.10	49.9	0	0.25	242.7	8K	0.40	397.1	1
26K	0.30	47.4	12K	0.50	507.7	4K	0.35	217.2	4K	0.20	62.8	3
26K	0.35	64.6	12K	0.45	492.7	4K	0.30	200.3	4K	0.15	45.6	3
26K	0.40	84.3	12K	0.40	472.9	4K	0.25	180.3	4K	0.10	25.9	3
26K	0.45	106.7	12K	0.35	450.5	4K	0.20	157.9	4K	0.05	3.5	3
26K	0.50	131.7	12K	0.30	425.4	4K	0.15	132.9	4K	0.00	21.5	2
26K	0.55	159.4	12K	0.25	397.8	4K	0.10	105.2	4K	0.05	49.2	3

135

Table 6-11 (cont)

Model Selection Data for Configuration 7

Operating Point			Candidate Model Deltas									Selected Model
			Model 1			Model 2			Model 3			
ALT	MACH	Q	ALT	MACH	Q	ALT	MACH	Q	ALT	MACH	Q	
26K	0.60	189.7	12K	0.20	367.5	4K	0.05	74.9	4K	0.10	79.2	3,2
26K	0.65	222.6	12K	0.15	334.5	4K	0.00	41.9	4K	0.15	112.4	2
26K	0.70	258.2	12K	0.10	298.9	4K	0.05	5.4	4K	0.20	148.0	2
26K	0.75	296.4	12K	0.05	260.8	4K	0.10	31.8	4K	0.25	186.2	2
26K	0.80	337.2	12K	0.00	219.9	4K	0.15	72.6	4K	0.30	227.0	2,1
26K	0.85	380.7	12K	0.05	176.5	4K	0.20	116.1	4K	0.35	270.5	2,1
26K	0.90	426.8	12K	0.10	130.4	4K	0.25	162.2	4K	0.40	316.6	1,2
30K	0.35	53.9	16K	0.45	503.2	8K	0.30	210.6	0	0.15	56.2	3
30K	0.40	70.5	16K	0.40	486.6	8K	0.25	194.1	0	0.10	39.7	3
30K	0.45	89.3	16K	0.35	467.9	8K	0.20	175.3	0	0.05	20.9	3
30K	0.50	110.2	16K	0.30	446.9	8K	0.15	154.4	0	0.00	0.0	3
30K	0.55	133.3	16K	0.25	423.8	8K	0.10	131.3	0	0.05	23.1	3
30K	0.60	158.7	16K	0.20	398.5	8K	0.05	105.9	0	0.10	48.5	3
30K	0.65	186.2	16K	0.15	370.9	8K	0.00	78.4	0	0.15	76.0	3
30K	0.70	215.9	16K	0.10	341.2	8K	0.05	48.6	0	0.20	105.8	3,2
30K	0.75	247.9	16K	0.05	309.2	8K	0.10	16.7	0	0.25	137.7	2,3
30K	0.80	284.1	16K	0.00	275.1	8K	0.15	17.5	0	0.30	171.9	2
30K	0.85	318.5	16K	0.05	238.7	8K	0.20	53.9	0	0.35	208.3	2
30K	0.90	357.0	16K	0.10	200.1	8K	0.25	92.5	0	0.40	246.8	2,1
34K	0.40	58.6	20K	0.40	498.5	12K	0.25	205.9	4K	0.10	51.6	3
34K	0.45	74.2	20K	0.35	483.0	12K	0.20	190.4	4K	0.05	36.0	3
34K	0.50	91.6	20K	0.30	465.6	12K	0.15	172.9	4K	0.00	18.6	3
34K	0.55	110.9	20K	0.25	446.3	12K	0.10	153.7	4K	0.05	0.7	3
34K	0.60	131.9	20K	0.20	425.2	12K	0.05	132.7	4K	0.10	21.7	3
34K	0.65	154.8	20K	0.15	402.3	12K	0.00	109.8	4K	0.15	44.6	3
34K	0.70	179.6	20K	0.10	377.6	12K	0.05	85.0	4K	0.20	69.4	3
34K	0.75	206.1	20K	0.05	351.0	12K	0.10	58.5	4K	0.25	95.9	3
34K	0.80	234.5	20K	0.00	322.6	12K	0.15	30.1	4K	0.30	124.3	2,3
34K	0.85	264.8	20K	0.05	292.4	12K	0.20	0.2	4K	0.35	154.6	2,3
34K	0.90	296.8	20K	0.10	260.3	12K	0.25	32.2	4K	0.40	186.6	2,1

Table 6-11 (cont)

Model Selection Data for Configuration 7

Operating Point			Candidate Model Deltas									Selected Model
			Model 1			Model 2			Model 3			
ALT	MACH	Q	ALT	MACH	Q	ALT	MACH	Q	ALT	MACH	Q	
38K	0.45	61.3	24K	0.35	495.8	16K	0.20	203.3	8K	0.05	48.9	3
38K	0.50	75.7	24K	0.30	481.5	16K	0.15	188.9	8K	0.00	34.5	3
38K	0.55	91.6	24K	0.25	465.6	16K	0.10	172.9	8K	0.05	18.6	3
38K	0.60	109.0	24K	0.20	448.1	16K	0.05	155.6	8K	0.10	1.2	3
38K	0.65	127.9	24K	0.15	429.2	16K	0.00	136.6	8K	0.15	17.8	3
38K	0.70	148.4	24K	0.10	408.8	16K	0.05	116.2	8K	0.20	38.2	3
38K	0.75	170.4	24K	0.05	386.8	16K	0.10	94.2	8K	0.25	60.2	3
38K	0.80	193.8	24K	0.00	363.3	16K	0.15	70.8	8K	0.20	83.6	3
38K	0.85	218.8	24K	0.05	338.4	16K	0.20	45.8	8K	0.35	108.6	2,3
38K	0.90	245.3	24K	0.10	311.9	16K	0.25	19.3	8K	0.40	135.1	2,3

137

Table 6-12

Model Selection Data for Configuration 8

Operating Point			Candidate Model Deltas									Selected Model
			Model 1			Model 2			Model 3			
ALT	MACH	Q	ALT	MACH	Q	ALT	MACH	Q	ALT	MACH	Q	
10K	0.25	63.7	0	0.10	61.1	0	0.25	191.1	0	0.05	509.5	1
10K	0.30	91.7	0	0.05	33.1	0	0.20	163.0	0	0.45	481.4	1
10K	0.35	124.8	0	0.00	0.0	0	0.15	129.9	0	0.40	448.3	1
10K	0.40	163.0	0	0.05	38.2	0	0.10	91.7	0	0.35	410.1	1
10K	0.45	205.3	0	0.10	81.5	0	0.05	48.4	0	0.30	366.8	2
10K	0.50	254.7	0	0.15	129.9	0	0.00	0.0	0	0.25	318.4	2
10K	0.55	308.2	0	0.20	183.4	0	0.05	53.5	0	0.20	264.9	2
10K	0.60	366.8	0	0.25	242.0	0	0.10	112.1	0	0.15	206.3	2
10K	0.65	430.5	0	0.30	305.7	0	0.15	175.8	0	0.10	142.6	2,3
10K	0.70	499.3	0	0.35	374.5	0	0.20	244.5	0	0.05	73.9	3
10K	0.75	573.1	0	0.40	448.3	0	0.25	318.0	0	0.00	0.0	3
10K	0.80	652.1	0	0.45	527.3	0	0.30	397.4	0	0.05	79.0	3
10K	0.85	736.2	0	0.50	611.4	0	0.35	481.1	0	0.10	163.0	3
10K	0.90	825.3	0	0.55	701.5	0	0.40	570.6	0	0.15	252.2	3
14K	0.25	54.4	4K	0.10	70.4	4K	0.25	200.3	4K	0.50	518.7	1
14K	0.30	78.4	4K	0.05	46.5	4K	0.20	176.4	4K	0.45	494.8	1
14K	0.35	106.6	4K	0.00	18.2	4K	0.15	148.1	4K	0.40	466.5	1
14K	0.40	139.3	4K	0.05	14.5	4K	0.10	115.5	4K	0.35	433.9	1
14K	0.45	176.3	4K	0.10	51.5	4K	0.05	78.4	4K	0.30	396.9	1
14K	0.50	217.6	4K	0.15	92.8	4K	0.00	37.1	4K	0.25	355.5	2
14K	0.55	263.3	4K	0.20	138.5	4K	0.05	8.6	4K	0.20	309.8	2
14K	0.60	313.4	4K	0.25	188.6	4K	0.10	58.7	4K	0.15	259.7	2
14K	0.65	367.8	4K	0.30	242.0	4K	0.15	113.1	4K	0.10	205.3	2
14K	0.70	426.6	4K	0.35	301.8	4K	0.20	171.8	4K	0.05	146.6	2,3
14K	0.75	489.7	4K	0.40	364.9	4K	0.25	234.9	4K	0.00	83.5	3
14K	0.80	557.2	4K	0.45	432.4	4K	0.30	302.4	4K	0.05	15.9	3
14K	0.85	628.9	4K	0.50	504.2	4K	0.35	374.3	4K	0.10	55.8	3
14K	0.90	705.2	4K	0.55	580.3	4K	0.40	450.4	4K	0.15	132.0	3
18K	0.30	66.6	8K	0.05	58.2	8K	0.20	188.1	8K	0.45	506.5	1
18K	0.35	90.7	8K	0.00	34.1	8K	0.15	164.1	8K	0.40	482.5	1

138

Table 6-12 (cont)

Model Selection Data for Configuration 8

Operating Point			Candidate Model Deltas									Selected Model
			Model 1			Model 2			Model 3			
ALT	MACH	Q	ALT	MACH	Q	ALT	MACH	Q	ALT	MACH	Q	
18K	0.40	118.4	8K	0.05	6.4	8K	0.10	136.3	8K	0.35	454.7	1
18K	0.45	149.9	8K	0.10	25.1	8K	0.05	104.8	8K	0.30	423.2	1
18K	0.50	185.1	8K	0.15	60.3	8K	0.00	69.7	8K	0.25	388.1	1
18K	0.55	225.9	8K	0.20	99.1	8K	0.05	30.8	8K	0.20	349.2	2
18K	0.60	266.5	8K	0.25	141.7	8K	0.10	11.8	8K	0.15	306.7	2
18K	0.65	312.8	8K	0.30	187.9	8K	0.15	58.0	8K	0.10	260.4	2
18K	0.70	362.7	8K	0.35	237.9	8K	0.20	107.9	8K	0.05	210.4	2
18K	0.75	416.4	8K	0.40	291.6	8K	0.25	161.7	8K	0.00	156.8	2,3
18K	0.80	473.8	8K	0.45	348.9	8K	0.30	219.0	8K	0.05	99.4	3,2
18K	0.85	534.8	8K	0.50	410.0	8K	0.35	280.1	8K	0.10	38.3	3,2
18K	0.90	599.6	8K	0.55	474.8	8K	0.40	344.9	8K	0.15	26.5	3
22K	0.30	56.4	12K	0.05	68.5	12K	0.20	198.4	12K	0.45	516.8	1
22K	0.35	76.7	12K	0.00	48.1	12K	0.15	178.0	12K	0.40	496.4	1
22K	0.40	100.2	12K	0.05	24.6	12K	0.10	154.5	12K	0.35	472.9	1
22K	0.45	126.8	12K	0.10	2.0	12K	0.05	127.9	12K	0.30	446.3	1
22K	0.50	156.6	12K	0.15	31.8	12K	0.00	98.2	12K	0.25	416.6	1
22K	0.55	189.4	12K	0.20	64.6	12K	0.05	65.3	12K	0.20	383.7	1
22K	0.60	225.4	12K	0.25	100.6	12K	0.10	29.3	12K	0.15	347.7	2
22K	0.65	264.6	12K	0.30	139.8	12K	0.15	9.8	12K	0.10	308.6	2
22K	0.70	306.9	12K	0.35	182.0	12K	0.20	52.1	12K	0.05	266.3	2
22K	0.75	352.3	12K	0.40	227.4	12K	0.25	97.5	12K	0.00	220.9	2
22K	0.80	400.8	12K	0.45	275.9	12K	0.30	146.1	12K	0.05	172.4	2,3
22K	0.85	452.5	12K	0.50	327.6	12K	0.35	197.7	12K	0.10	120.7	2,3
22K	0.90	507.2	12K	0.55	382.4	12K	0.40	252.5	12K	0.15	65.9	3,2
26K	0.30	47.4	16K	0.05	77.4	16K	0.20	207.3	16K	0.45	525.7	1
26K	0.35	64.5	16K	0.00	60.3	16K	0.15	190.2	16K	0.40	508.6	1
26K	0.40	84.3	16K	0.05	40.5	16K	0.10	170.4	16K	0.35	488.8	1
26K	0.45	106.7	16K	0.10	18.1	16K	0.05	148.0	16K	0.30	466.4	1
26K	0.50	131.7	16K	0.15	6.9	16K	0.00	123.0	16K	0.25	441.4	1
26K	0.55	159.4	16K	0.20	34.6	16K	0.05	95.3	16K	0.20	413.8	1

Table 6-12 (cont)

Model Selection Data for Configuration 8

Operating Point			Candidate Model Deltas									Selected Model
ALT	MACH	Q	Model 1			Model 2			Model 3			
			Alt	MACH	Q	ALT	MACH	Q	ALT	MACH	Q	
26K	0.60	189.7	16K	0.25	64.8	16K	0.10	65.0	16K	0.15	383.5	1
26K	0.65	222.6	16K	0.30	97.8	16K	0.15	32.1	16K	0.10	350.5	1,2
26K	0.70	258.2	16K	0.35	133.4	16K	0.20	3.5	16K	0.05	314.9	2,1
26K	0.75	296.4	16K	0.40	171.6	16K	0.25	41.6	16K	0.00	276.8	2,1
26K	0.80	337.2	16K	0.45	212.4	16K	0.30	82.5	16K	0.05	235.9	2,1
26K	0.85	380.7	16K	0.50	255.9	16K	0.35	125.9	16K	0.10	192.5	2,3
26K	0.90	426.8	16K	0.55	301.9	16K	0.40	172.1	16K	0.15	146.4	2,3
30K	0.35	53.9	20K	0.00	70.8	20K	0.15	200.7	20K	0.40	519.2	1
30K	0.40	70.5	20K	0.05	54.3	20K	0.10	184.2	20K	0.35	502.6	1
30K	0.45	89.3	20K	0.10	35.5	20K	0.05	165.5	20K	0.30	483.9	1
30K	0.50	110.2	20K	0.15	14.6	20K	0.00	144.5	20K	0.25	462.9	1
30K	0.55	133.3	20K	0.20	8.5	20K	0.05	121.4	20K	0.20	439.8	1
30K	0.60	158.7	20K	0.25	33.9	20K	0.10	96.1	20K	0.15	414.5	1
30K	0.65	186.2	20K	0.30	61.4	20K	0.15	68.5	20K	0.10	386.9	1
30K	0.70	215.9	20K	0.35	91.2	20K	0.20	38.8	20K	0.05	357.2	1,2
30K	0.75	247.9	20K	0.40	123.1	20K	0.25	6.8	20K	0.00	325.2	1,2
30K	0.80	282.1	20K	0.45	157.3	20K	0.30	27.4	20K	0.05	291.1	2,1
30K	0.85	318.5	20K	0.50	193.7	20K	0.35	63.7	20K	0.10	254.7	2,1
30K	0.90	357.0	20K	0.55	232.2	20K	0.40	102.3	20K	0.15	216.1	2,3
34K	0.40	58.6	14K	0.05	66.2	14K	0.10	196.1	14K	0.35	514.5	1
34K	0.45	74.2	14K	0.10	50.6	14K	0.05	180.5	14K	0.30	498.9	1
34K	0.50	91.6	14K	0.15	33.2	14K	0.00	163.1	14K	0.25	41.5	1
34K	0.55	110.9	14K	0.20	14.0	14K	0.05	143.9	14K	0.20	462.3	1
34K	0.60	131.9	14K	0.25	7.1	14K	0.10	122.8	14K	0.15	441.2	1
34K	0.65	154.8	14K	0.30	30.1	14K	0.15	99.9	14K	0.10	418.3	1
34K	0.70	179.6	14K	0.35	54.7	14K	0.20	75.2	14K	0.05	393.6	1
34K	0.75	206.1	14K	0.40	81.3	14K	0.25	48.6	14K	0.00	367.0	1
34K	0.80	234.5	14K	0.45	109.3	14K	0.30	20.2	14K	0.05	338.6	2,1
34K	0.85	264.8	14K	0.50	139.9	14K	0.35	10.0	14K	0.10	308.4	2,1
34K	0.90	296.8	14K	0.55	172.0	14K	0.40	42.1	14K	0.15	276.3	2,1

Table 6-12 (cont)

Model Selection Data for Configuration 8

Operating Point			Candidate Model Deltas									Selected Model
			Model 1			Model 2			Model 3			
ALT	MACH	Q	ALT	MACH	Q	ALT	MACH	Q	ALT	MACH	Q	
38K	0.45	61.3	18K	0.10	63.5	18K	0.05	193.4	18K	0.30	511.8	1
38K	0.50	75.7	18K	0.15	49.1	18K	0.00	179.0	18K	0.25	497.4	1
38K	0.55	91.6	18K	0.20	33.2	18K	0.05	163.1	18K	0.20	481.5	1
38K	0.60	109.0	18K	0.25	15.8	18K	0.10	145.7	18K	0.15	464.1	1
38K	0.65	127.9	18K	0.30	3.1	18K	0.15	126.8	18K	0.10	445.2	1
38K	0.70	148.4	18K	0.35	23.6	18K	0.20	106.3	18K	0.05	424.7	1
38K	0.75	170.4	18K	0.40	45.5	18K	0.25	84.4	18K	0.00	402.8	1
38K	0.80	193.8	18K	0.45	69.0	18K	0.30	60.9	18K	0.05	379.3	1
38K	0.85	218.8	18K	0.50	94.0	18K	0.35	35.9	18K	0.10	354.3	1,2
38K	0.90	245.3	18K	0.55	120.5	18K	0.40	9.4	18K	0.15	327.8	1,2
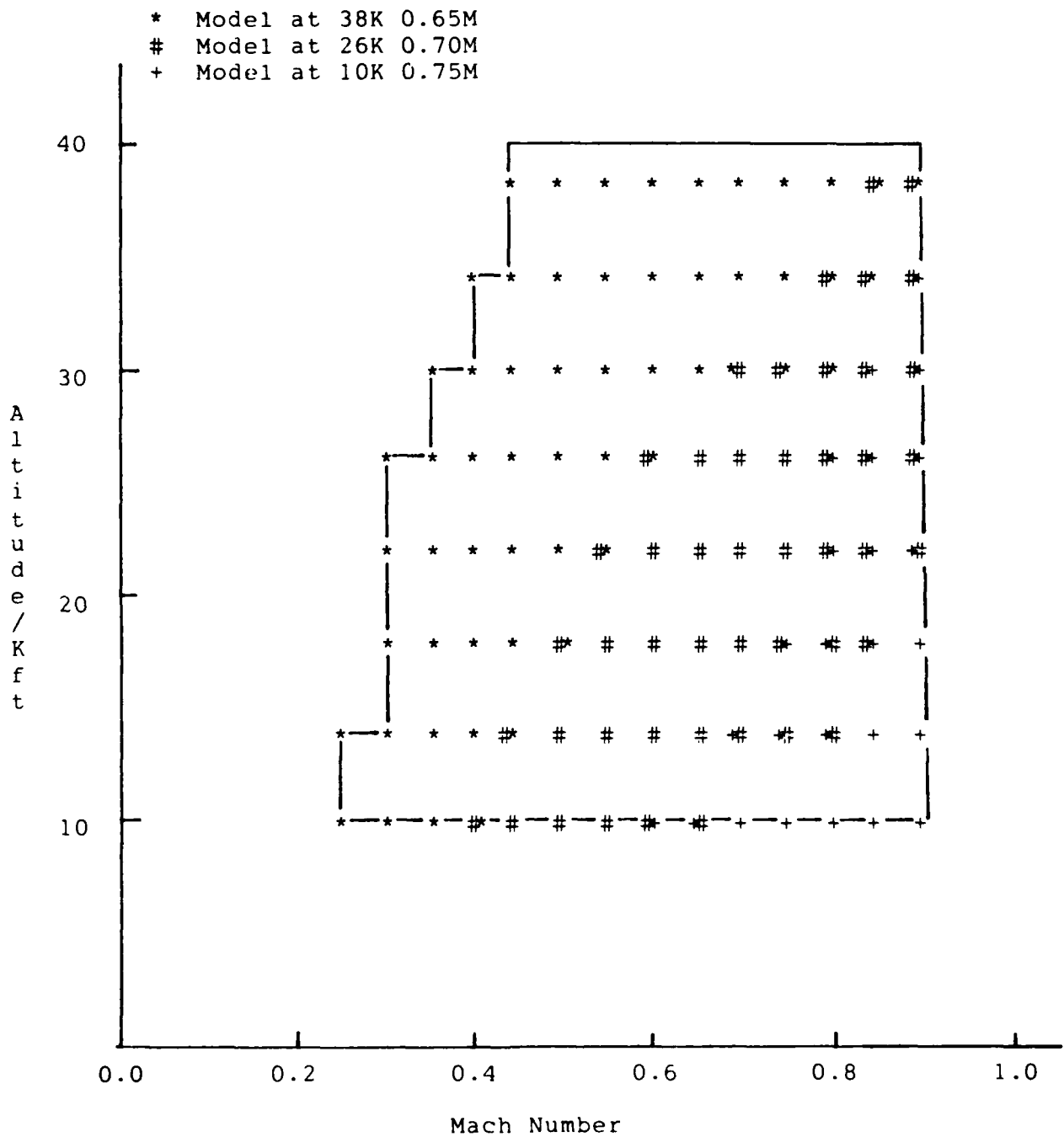
Figure 6-50. Model Selection Data
for Configuration 6

142
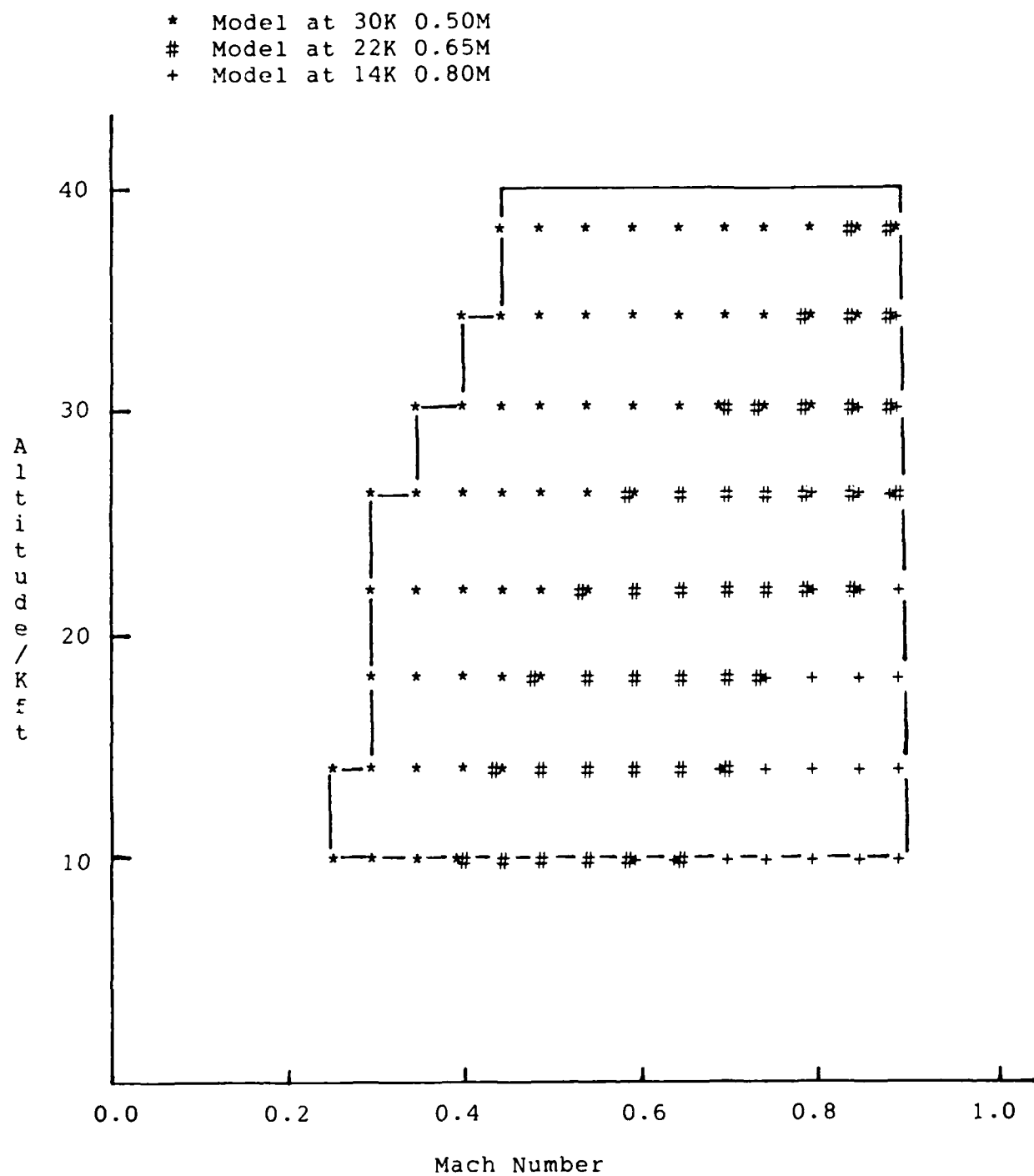
Figure 6-51. Model Selection Data
for Configuration 7

143
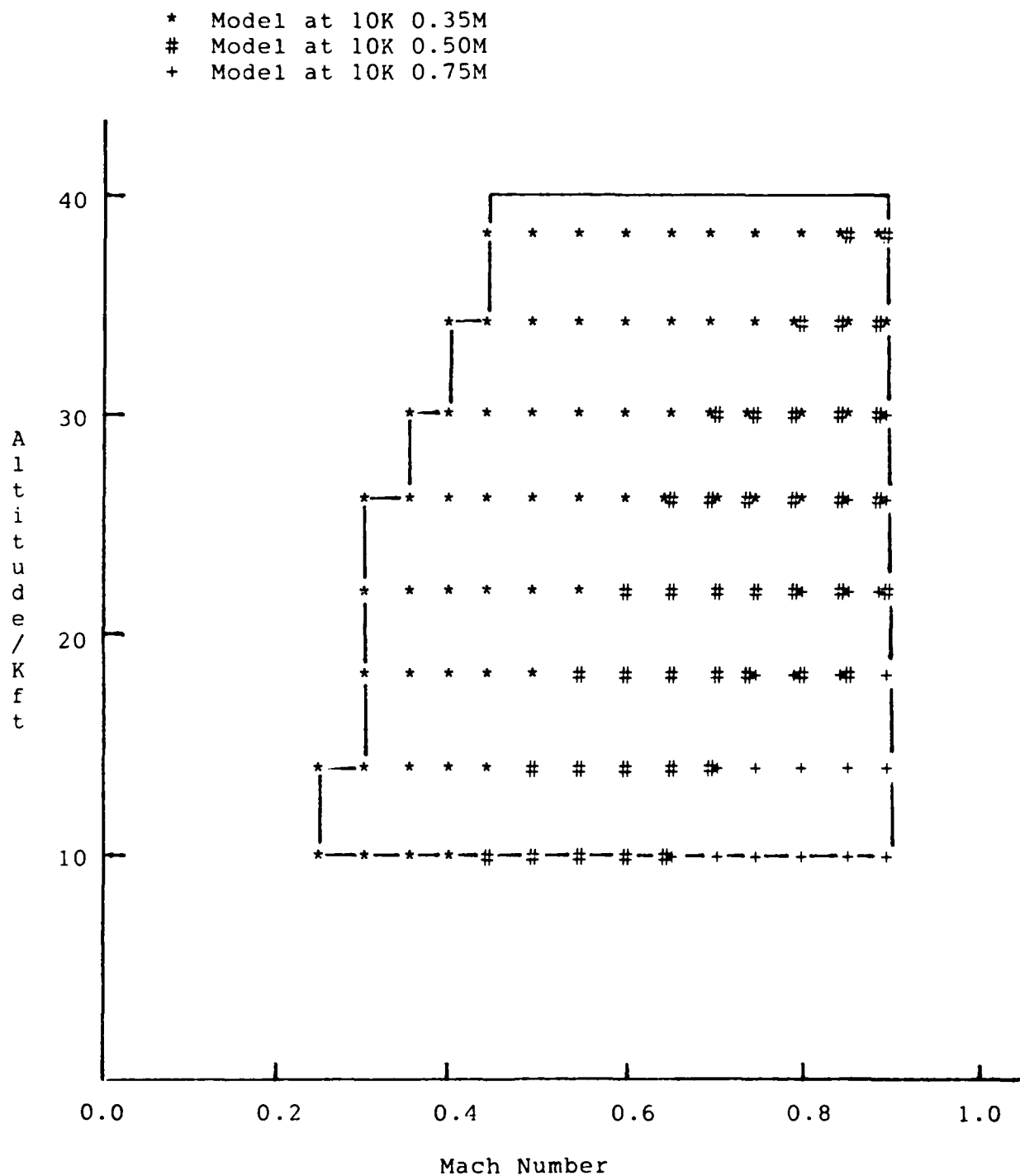
Figure 6-52. Model Selection Data
for Configuration 8

144
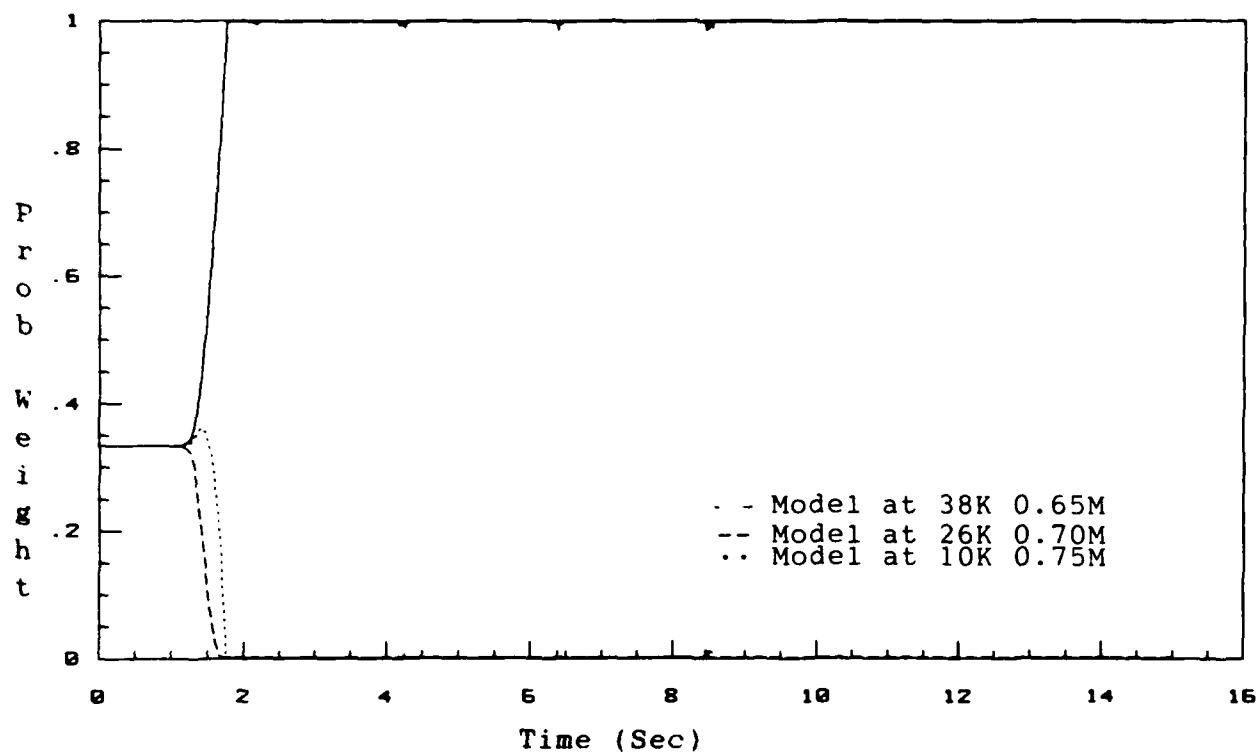
Figure 6-53. Model Probability Weightings
Configuration 6/Operating Point: 26K 0.45M

145

fore a * is placed at the flight condition of 26,000 feet, 0.45 Mach on Figure 6-50. If the conditional probability fell below 0.9 for a candidate model during the running of a simulation, then the two models with the highest probability were placed at the position of the flight condition of interest. As an example, the conditional probabilities for the flight condition of 26,000 feet, 0.65 Mach (configuration 8) are shown on Figure 6-54. Figure 6-54 shows that the conditional probability of model one falls below 0.9 and that the models with the most significant probabilities are models one and two, respectively. Therefore, a *# was placed on the location of the 26,000 feet, 0.65 Mach flight condition of Figure 6-52. This annotation delineated which candidate model(s) had the highest conditional probability at the given flight condition.

By comparing Figures 6-50 through 6-52, it can be seen that the multiple model algorithm performance was similar for configurations 6, 7, and 8. This similarity indicated that the conditional probability calculated for a candidate model was associated with dynamic pressure. Tables 6-10 through 6-12 show the candidate models that were selected as closest to the actual flight condition as well as the dif-

146
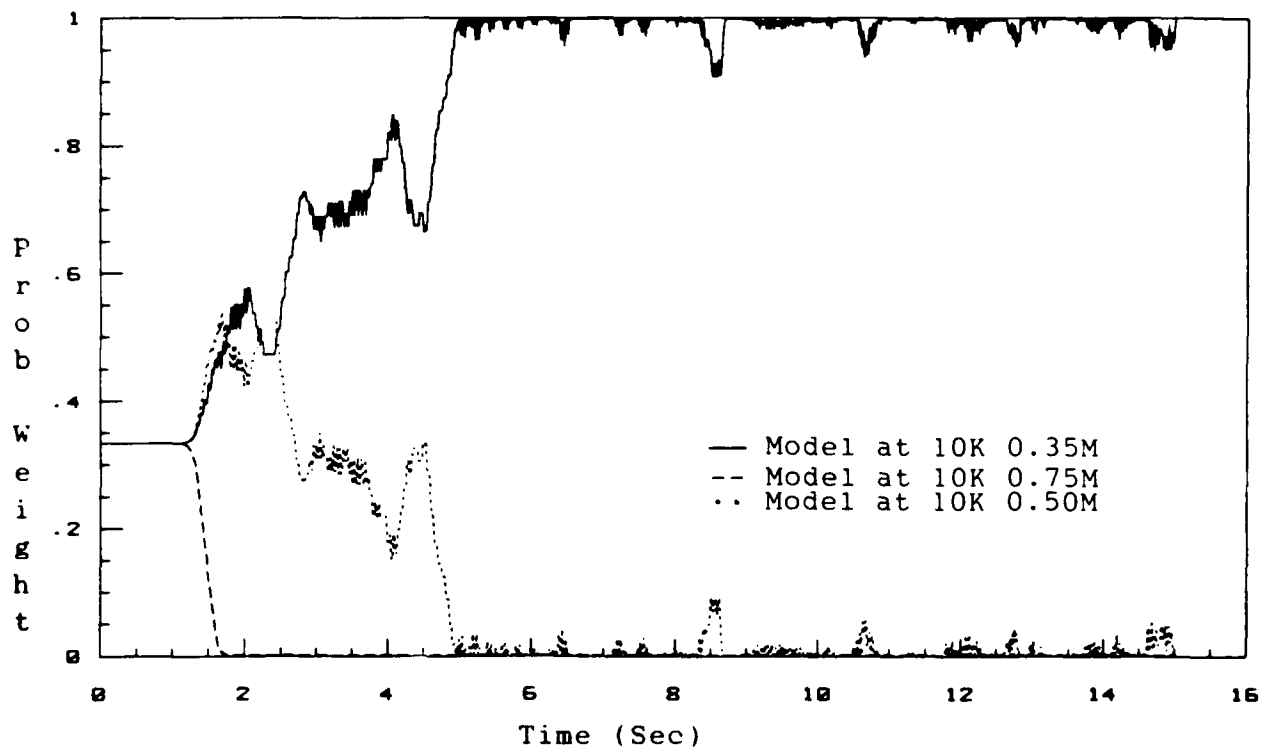
Figure 6-54.   Model Probability Weightings
Configuration 8/Operating Point: 26K 0.65M

ferences between the dynamic pressure of the flight condi-

tion and the candidate models. The data showed that, in

over ninety percent of the three hundred cases run, the

candidate model that received the highest conditional proba-

bility was the model with a dynamic pressure closest to the

dynamic pressure of the actual flight condition. Again,

this pointed out the fact that model equivalency is largely

dependent on dynamic pressure.

As just discussed, configurations 6, 7, and 8 all

yielded satisfactory tracking performance (from a perfor-

mance criteria standpoint) over the flight envelope of inte-

rest. However, when comparing the performance index respon-

ses of configurations 6, 7, and 8, it was determined that

configuration 8 resulted in the least tracking error for a

majority of the flight conditions. Table 6-13 presents a

representative sample of the performance index results for

configurations 6, 7, and 8. Configuration 6 had the largest

tracking error as determined by the performance index for

all of the flight conditions. As seen from Table 6-13,

configuration 8 was the best of the configurations labled as

6, 7, and 8 and configuration 6 was the least desirable.

In an effort to obtain a three-model configuration that

Table 6-13

Performance Index Comparison of Selected
Flight Conditions

Flight Condition		Configuration with Minimal Error		
Alt (Kft)	Mach	6	7	8
10	0.35			X
10	0.65			X
10	0.90		X	
14	0.35			X
14	0.65			X
14	0.90		X	
22	0.40			X
22	0.65			X
22	0.90		X	
26	0.45			X
26	0.65			X
26	0.90			X
30	0.50			X
30	0.90			X
38	0.60			X
38	0.90			X

yielded better performance than configuration 8, several

other three-model configutrations were examined. Specifi-

cally, these were configurations 9 through 14 as given on

Table 6-9. In each case, the overall performance

of configuration 8 proved to be the superior configuration.

Configuration 9 had performance index responses that

were very similar to those of configuration 8. Although

configuration 8 did have a minimal amount of error most of

149

the time, configuration 9 had less error at the low altitude/high Mach flight conditions. Configurations 11, 13, and 14 had performance index responses that were less than those for configuration 8 at 38,000 ft, 0.9 Mach. However, configuration 8 had better responses over the rest of the flight envelope. So, from a performance criteria standpoint, configuration 8 was the best configuration of those investigated with configuration 9 yielding similar performance.

In an effort to better the performance of configuration 8, a four-model configuration was evaluated with all of the models at 10,000 ft and Mach numbers of 0.35, 0.5, 0.75, and 0.9, respectively. However, the performance of this configuration was not any better than that afforded by the three models of configuration 8.

6.2.4 Control Law Gain Adjustment. In his thesis, Barfield (21) noted that although the Porter design technique yields exceptionally fast aircraft responses, many times this is achieved through large and extrememly fast surface movements. After a review of several applications of the design technique, it became apparent that for a given design, the

150

larger the control law gains, the faster the surface move-
ments. Reaching either the position limits or the rate
limits is a condition that should be avoided. Reaching a
position limit prevents the input command from being a-
chieved. Reaching rate limits results in the system becom-
ing nonlinear and can result in an increase in phase lag in
a feedback system. This phase lag increase has been shown
to cause loss of control in aircraft with a full authority
fly-by-wire system (21).

Recall, from Chapter 3, that the control law gains are
given by

$$\underline{K}_1 = \underline{H}^{-1}(T)\underline{\xi} \qquad (6-12)$$

$$\underline{K}_2 = \rho \, \underline{K}_1 \qquad (6-13)$$

where the diagonal weighting matrix, $\underline{\xi}$, can be altered to
achieve desired tracking characteristics and the parameter,
ρ, is a constant which assigns the ratio of proportional to
integral control.

For all of the simulations that were accomplished up to
this part of this thesis, the control law design parameters
that were implemented were those used by Pineiro and Berens.
The control law design parameters had the following values:

$$\underline{\xi} = \begin{bmatrix} 0.4 & 0.0 \\ 0.0 & 0.7 \end{bmatrix} \qquad (6-14)$$

and

$$\rho = 0.8 \qquad (6-15)$$

As is shown earlier, configuration 8 had satisfactory performance over the flight envelope of interest (from a performance index standpoint). However, for several of the flight conditions the rate limits were encountered for both the elevators and flaperons. In an effort to reduce the control surface activity for the multiple model algorithm, an investigation into the effects of altering the control law design parameters was performed.

To begin, the effects of altering the control law design parameters on the performance of a fixed gain simulation were investigated. The nominal flight condition chosen for this part of the analysis was 22,000 ft, 0.65 Mach. The responses for the fixed gain simulation using the control law design parameters values as shown above are shown Figures 6-55 through 6-60. As can be seen on Figure 6-60, the rate limits for the flaperons were encountered several times. For the reasons given above, this is a condition that should be avoided.

152

Figure 6-55.   Pitch Rate Response
Nominal Model: 22K 0.65M/Operating Point: 22K 0.65M
SIG1=0.4 SIG2=0.7 RHO=0.8

Figure 6-56.   Pitch Rate Performance Criterion
Nominal Model: 22K 0.65M/Operating Point: 22K 0.65M
SIG1=0.4 SIG2=0.7 RHO=0.8

153

Figure 6-57. Flaperon Position
Nominal Model: 22K 0.65M/Operating Point: 22K 0.65M
SIG1=0.4 SIG2=0.7 RHO=0.8

Figure 6-58. Elevator Position
Nominal Model: 22K 0.65M/Operating Point: 22K 0.65M
SIG1=0.4 SIG2=0.7 RHO=0.8

154

Figure 6-59. Flaperon Rate
Nominal Model: 22K 0.65M/Operating Point: 22K 0.65M
SIG1=0.4 SIG2=0.7 RHO=0.8

Figure 6-60. Elevator Rate
Nominal Model: 22K 0.65M/Operating Point: 22K 0.65M
SIG1=0.4 SIG2=0.7 RHO=0.8

Table 6-14 lists the simulations that were run subsequent to the initial 22,000 ft, 0.65 Mach simulation and the respective values of the control law design parameters. The entries labled Sigma 1 and Sigma 2 refer to the 1,1 and 2,2 elements of the diagonal weighting matrix, respectively while the term rho refers to the design parameter, ρ.

As can be seen from Table 6-14, simulations 1 and 2 were run with varying values of the parameter, ρ, simulations 3 through 6 were performed with different values of the 1,1 element of the weighting matrix, and simulations 7 through 9 were accomplished with different values of the 2,2 element of the weighting matrix.

Table 6-14

Design Parameter Values for Simulations
at 22,000 ft, 0.65 Mach

Simulation Number	Control Law Design Parameters		
	Sigma 1	Sigma 2	Rho
1	0.40	0.70	0.40
2	0.40	0.70	0.10
3	0.80	0.70	0.80
4	0.20	0.70	0.80
5	0.10	0.70	0.80
6	0.05	0.70	0.80
7	0.40	1.50	0.80
8	0.40	0.35	0.80
9	0.40	0.10	0.80

Decreasing the parameter, ρ, resulted in an increase in the tracking error as shown on the performance index responses. Figures 6-61 through 6-66 present the simulation results when the parameter, ρ, was set to 0.4 (simulation 1 on Table 6-14). By comparing the responses of the elevators and flaperons for the original simulation and those of simulation 1, it can be seen that there is little difference in control surface performance. Therefore, decreasing the ratio of proportional to integral control results in an increase in the tracking error as determined by the performance index while resulting in minimal changes in the control surface performances.

Figures 6-67 through 6-72 present the responses for simulation 3 on Table 6-14. As shown on Figure 6-68, increasing the value of Sigma 1 resulted in an increase in the performance error. Also, the increase in Sigma 1 resulted in the control surfaces becoming more active as evidenced by the deflection rates. The negative aspect of this is that the control surfaces spent a larger amount of time at the rate limit. Conversely, reducing Sigma 1 as in simulation 5 (see Figures 6-73 through 6-78) resulted in a performance error that was essentially the same as that of the original

157
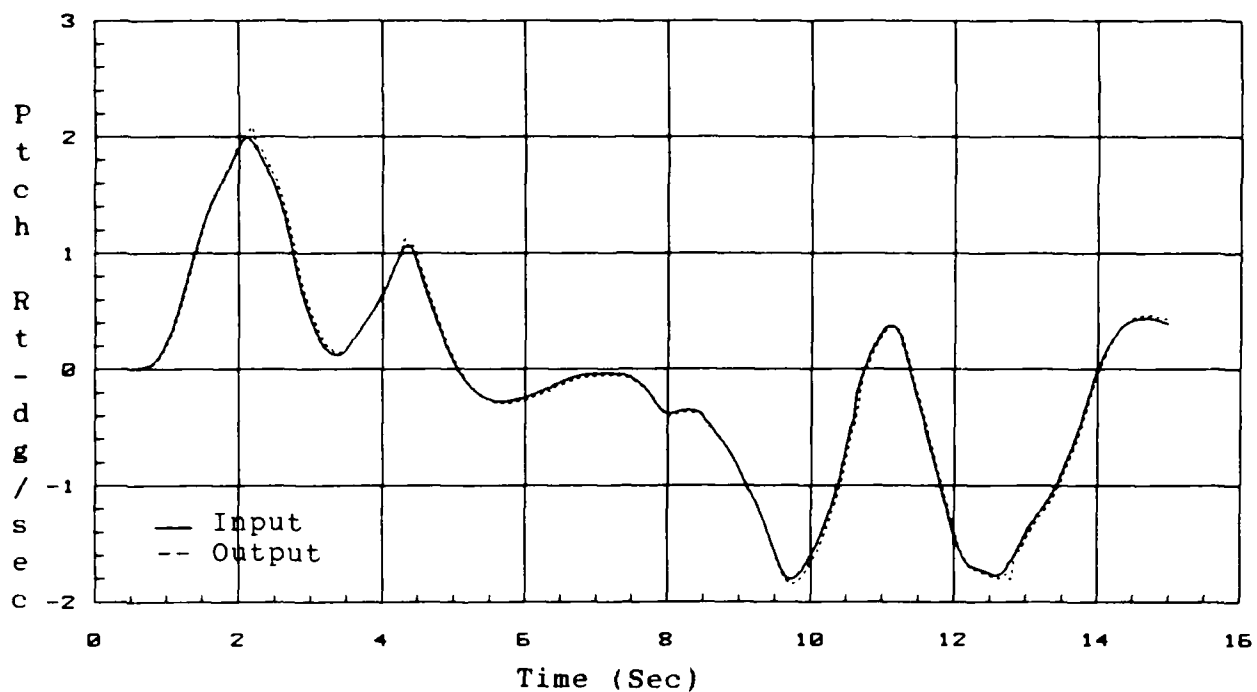
Figure 6-61.   Pitch Rate Response
Nominal Model: 22K 0.65M/Operating Point: 22K 0.65M
SIG1=0.4 SIG2=0.7 RHO=0.4
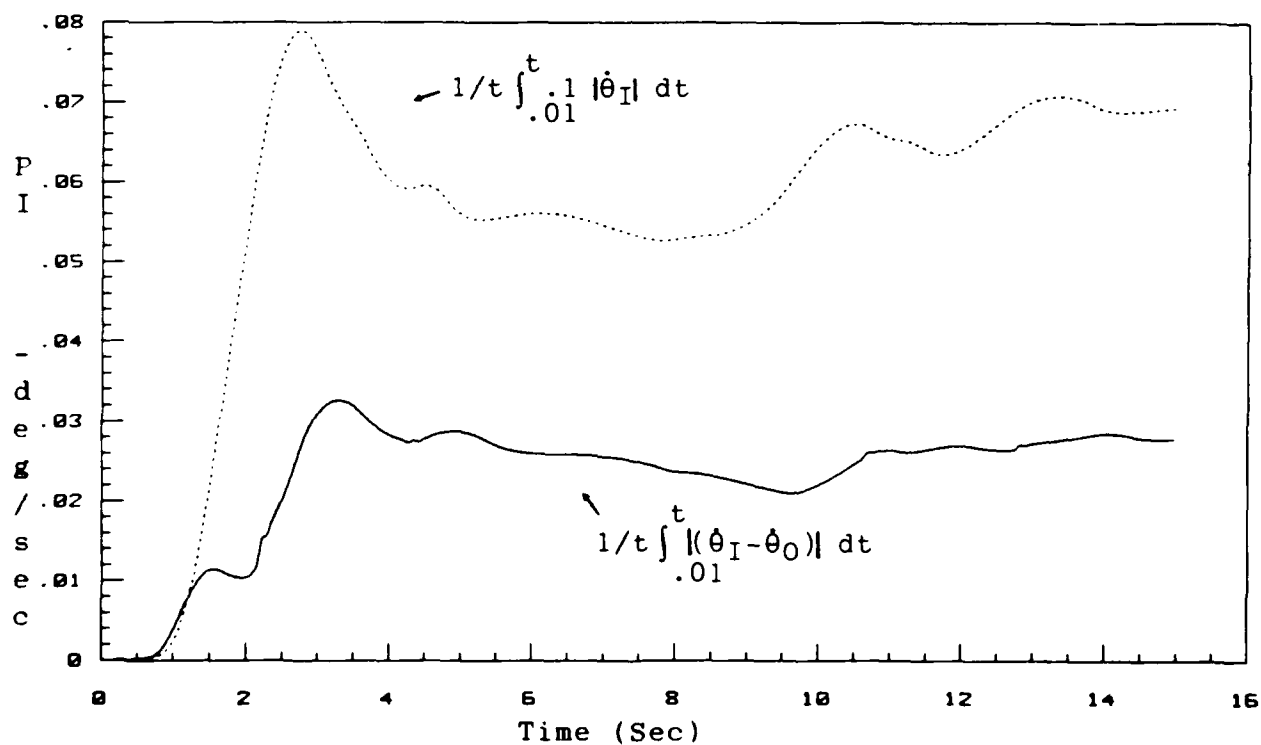
Figure 6-62.   Pitch Rate Performance Criterion
Nominal Model: 22K 0.65M/Operating Model: 22K 0.65M
SIG1=0.4 SIG2=0.7 RHO=0.4

158

Figure 6-63.   Flaperon Position
Nominal Model: 22K 0.65M/Operating Point: 22K 0.65M
SIG1=0.4 SIG2=0.7 RHO=0.4
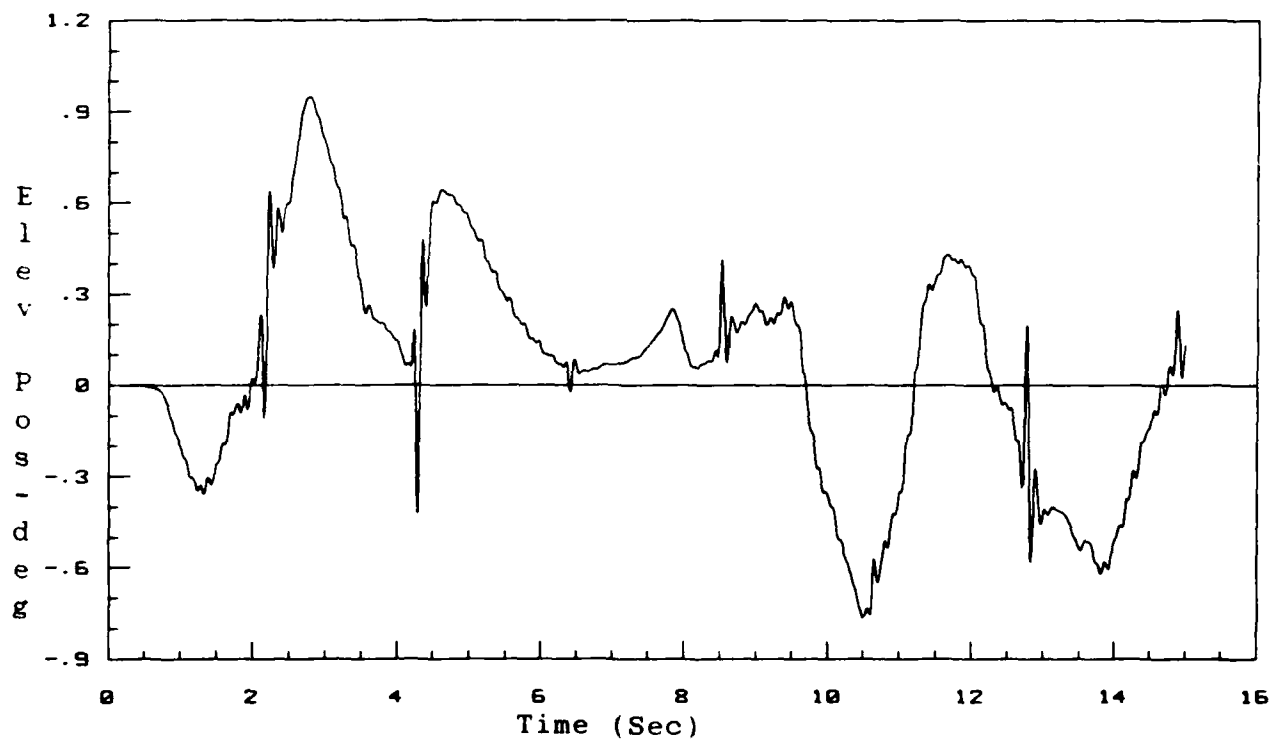
Figure 6-64.   Elevator Position
Nominal Model: 22K 0.65M/Operating Point: 22K 0.65M
SIG1=0.4 SIG2=0.7 RHO=0.4

159
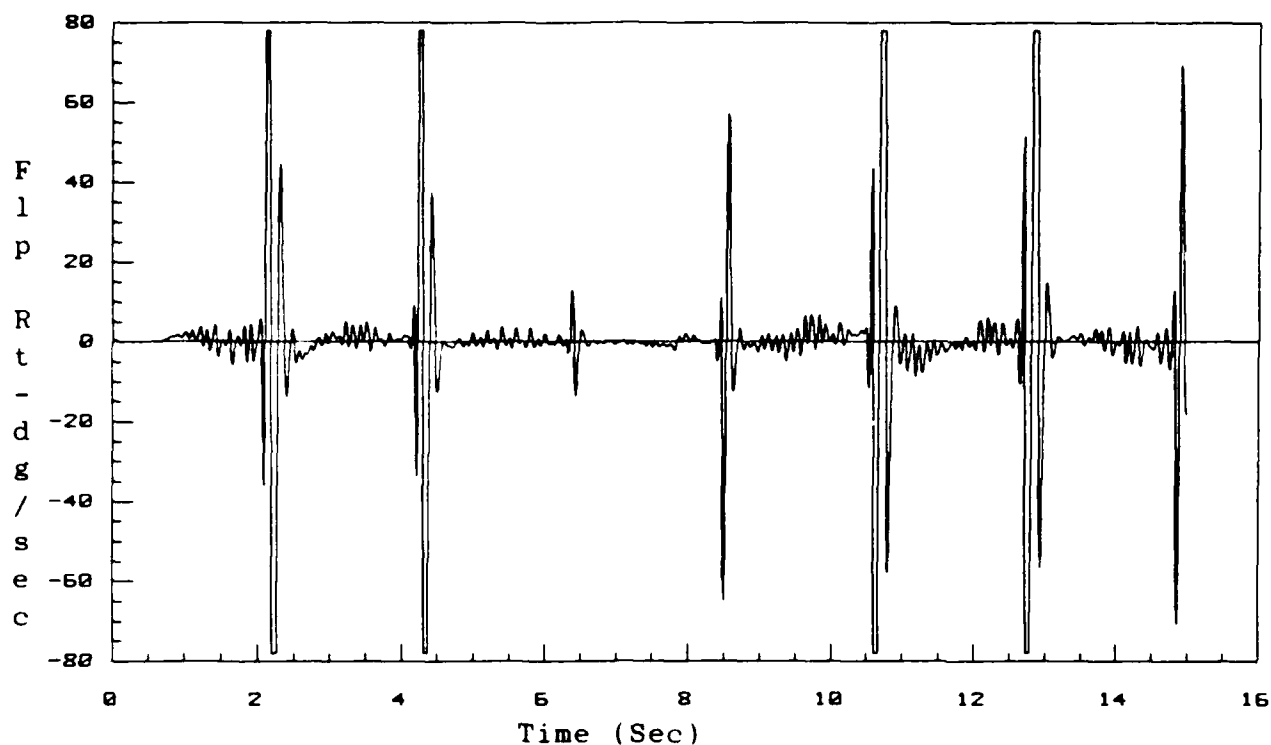
Figure 6-65.   Flaperon Rate
Nominal Model: 22K 0.65M/Operating Point: 22K 0.65M
SIG1=0.4 SIG2=0.7 RHO=0.4
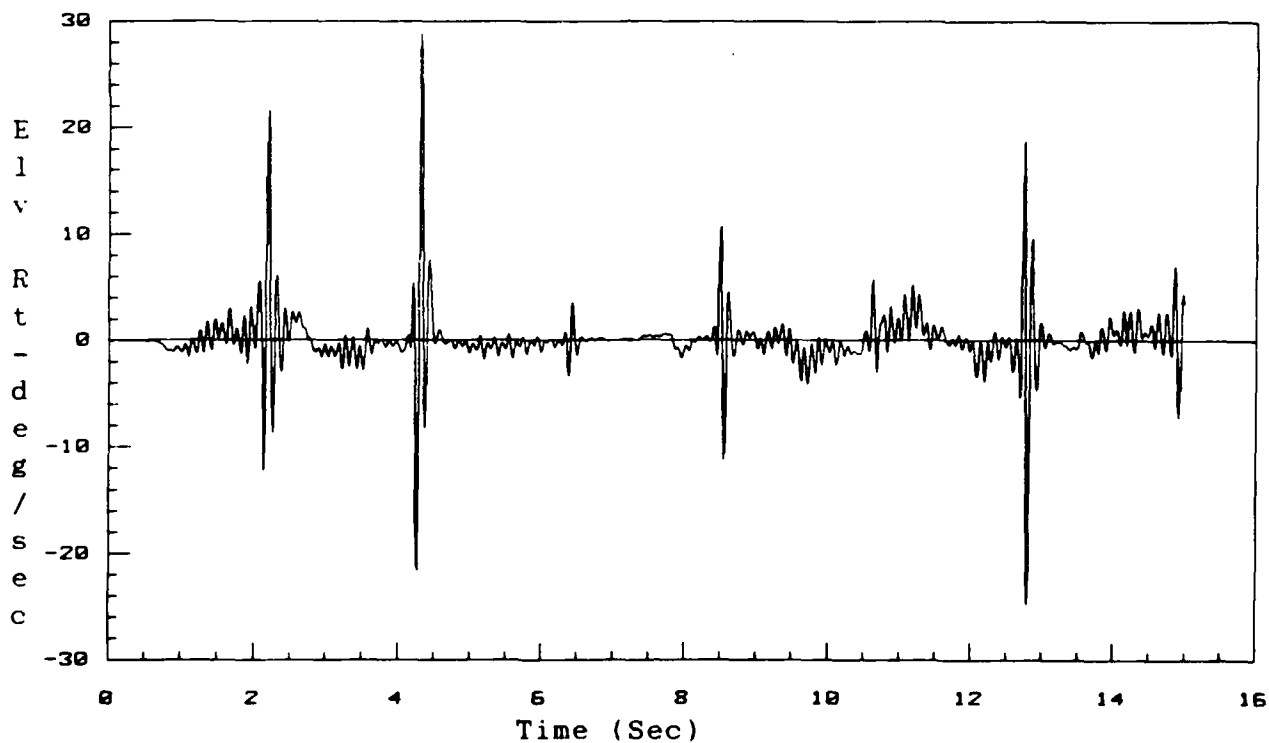
Figure 6-66.   Elevator Rate
Nominal Model: 22K 0.65M/Operating Point: 22K 0.65M
SIG1=0.4 SIG2=0.7 RHO=0.4

160
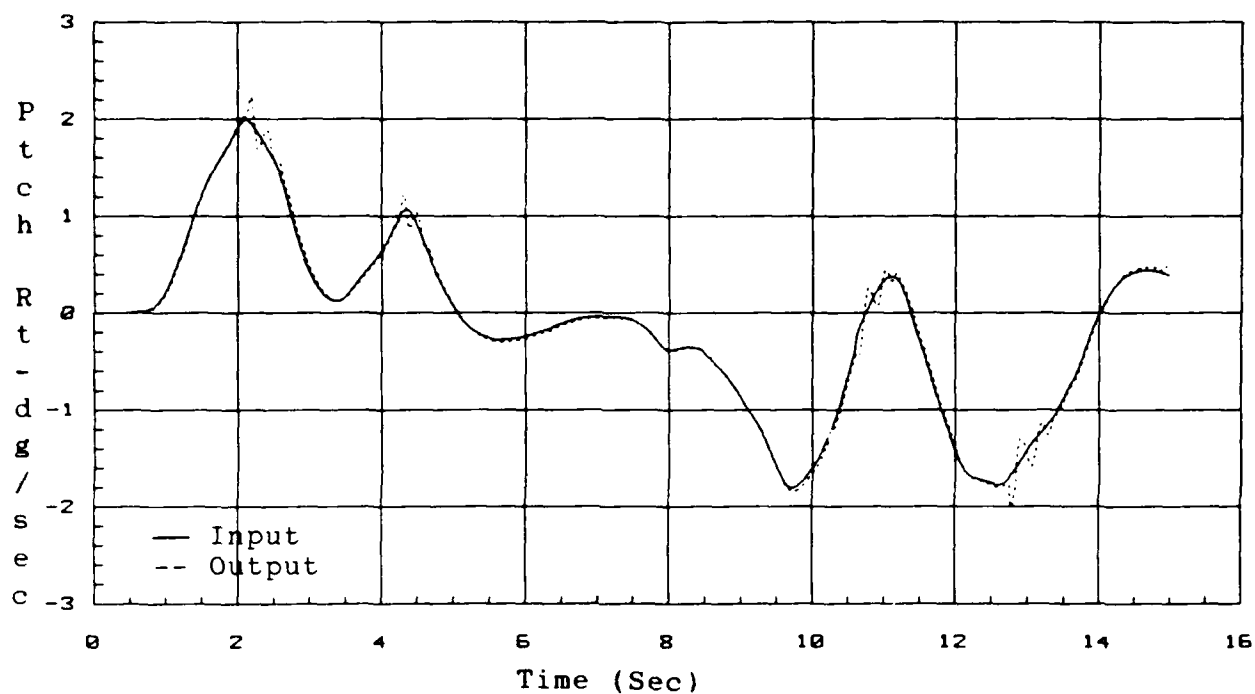
Figure 6-67. Pitch Rate Response
Nominal Model: 22K 0.65M/Operating Point: 22K 0.65M
SIG1=0.8 SIG2=0.7 RHO=0.8

$$1/t \int_{.01}^{t} .1 \; |\dot{\theta}_I| \; dt$$

$$1/t \int_{.01}^{t} |(\dot{\theta}_I - \dot{\theta}_O)| \; dt$$
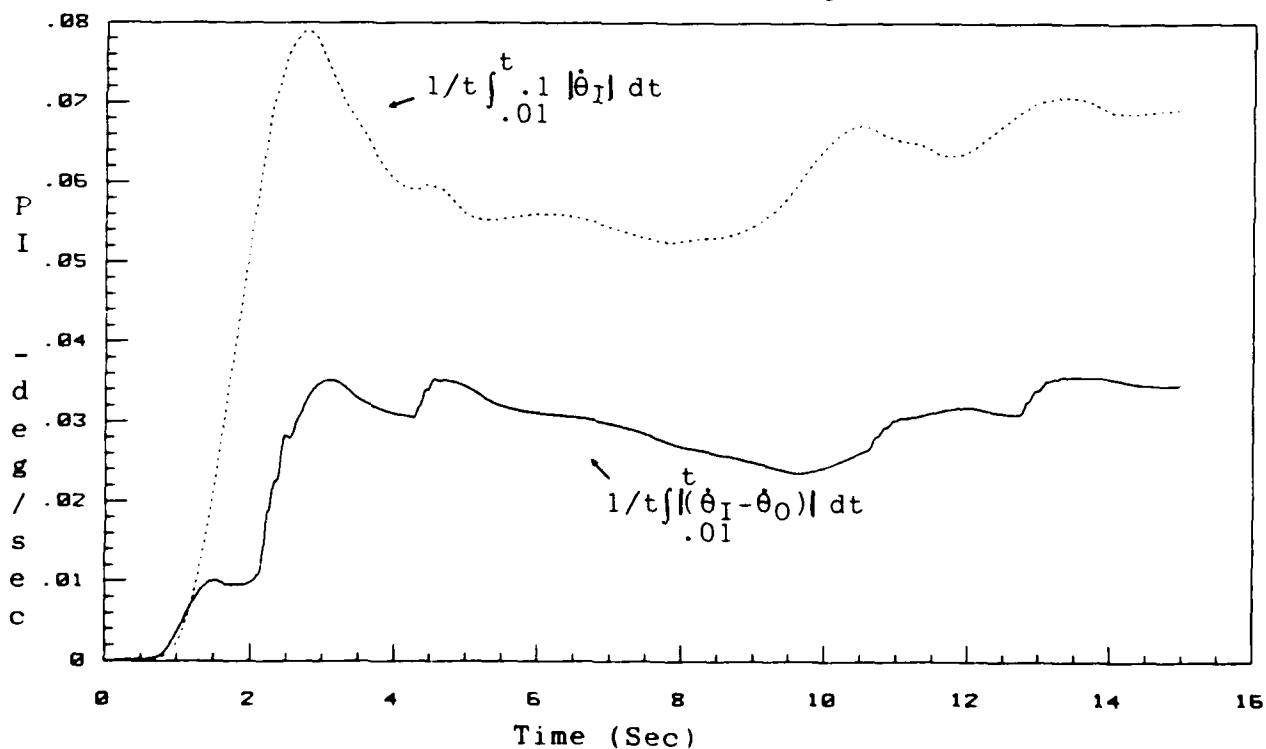
Figure 6-68. Pitch Rate Performance Criterion
Nominal Model: 22K 0.65M/Operating Point: 22K 0.65M
SIG1=0.8 SIG2=0.7 RHO=0.8

161
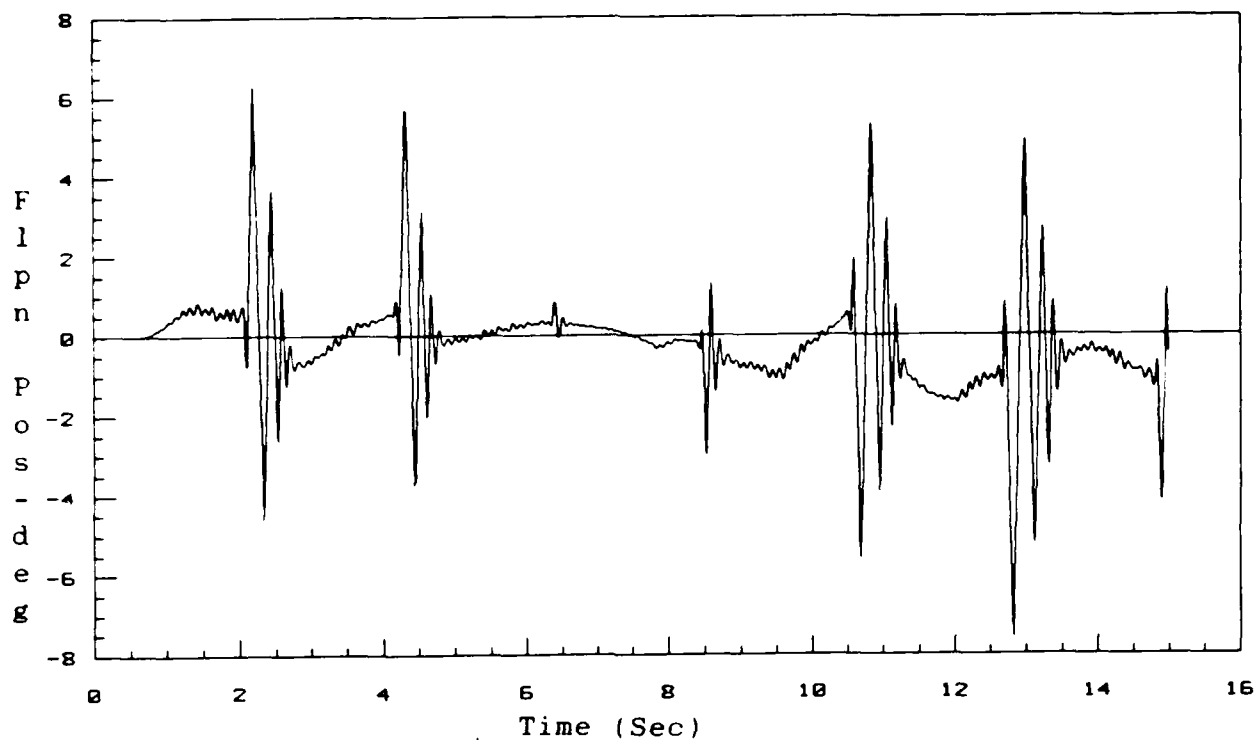
Figure 6-69.   Flaperon Position
Nominal Model: 22K 0.65M/Operating Point: 22K 0.65M
SIG1=0.8 SIG2=0.7 RHO=0.8
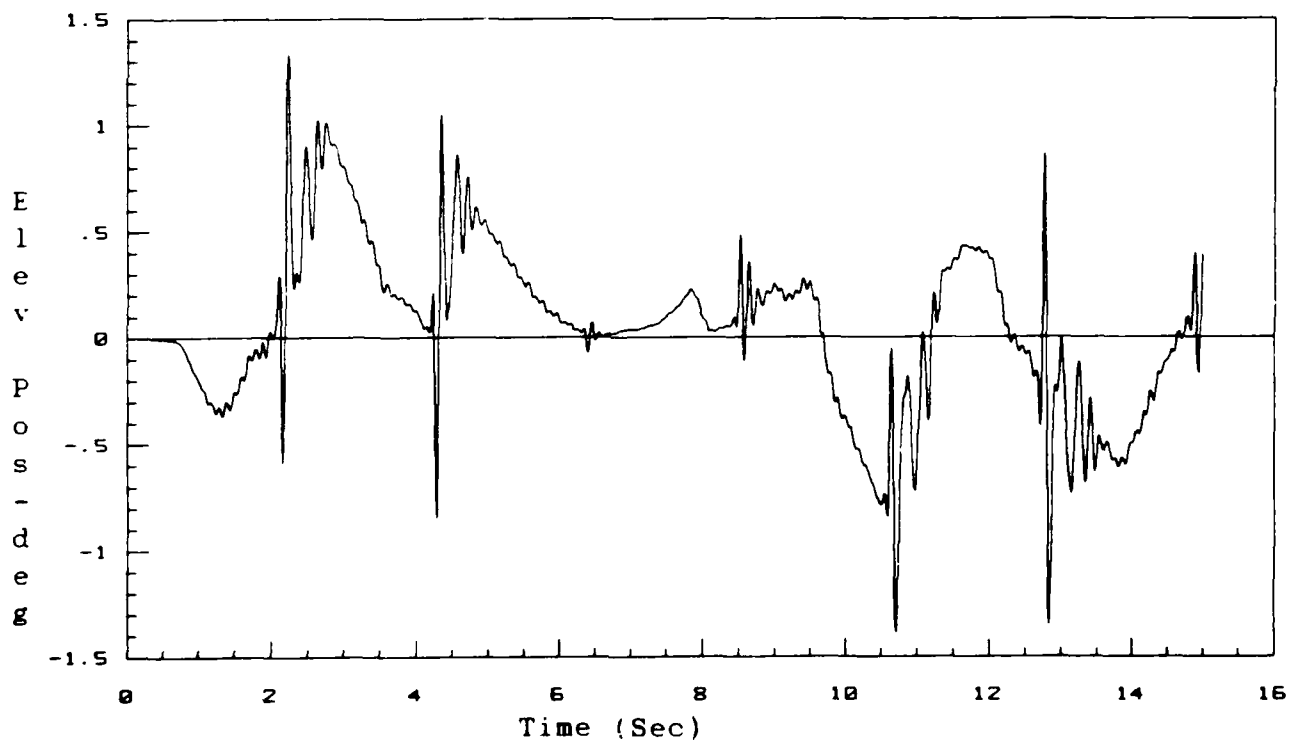
Figure 6-70.   Elevator Position
Nominal Model: 22K 0.65M/Operating Point: 22K 0.65M
SIG1=0.8 SIG2=0.7 RHO=0.8

162
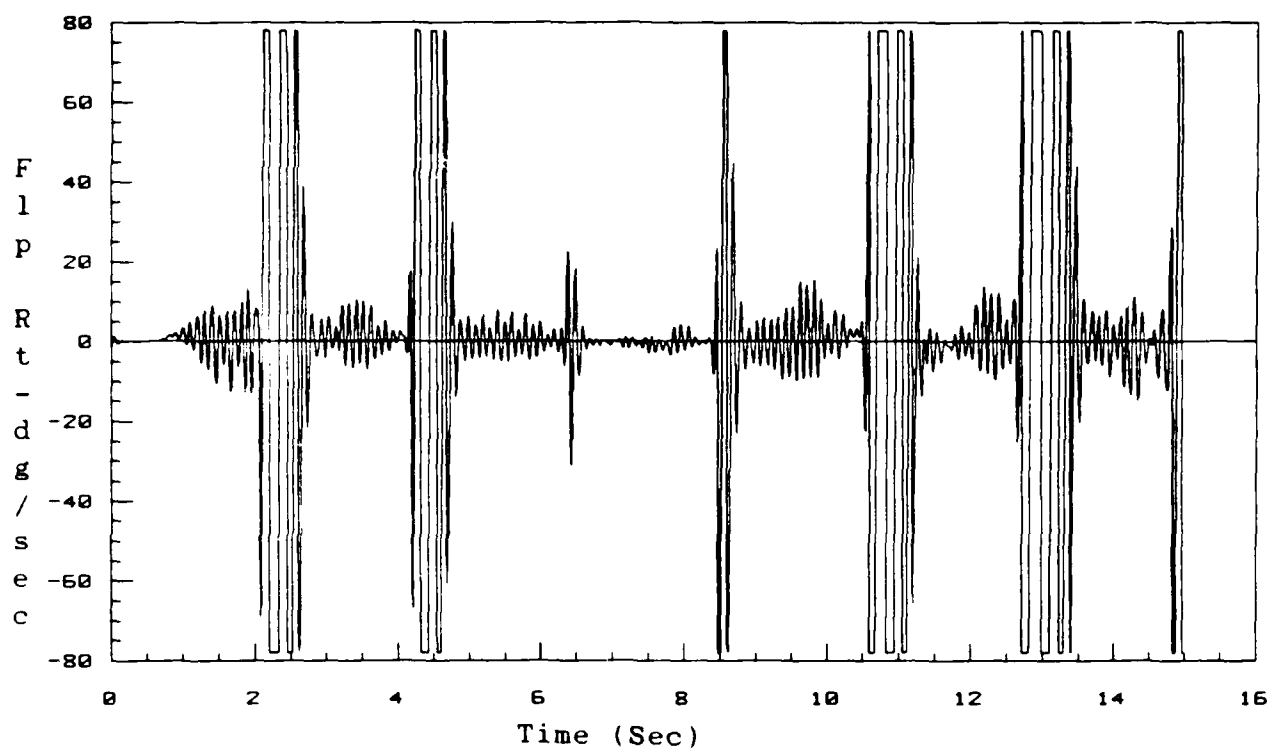
Figure 6-71.   Flaperon Rate
Nominal Model: 22K 0.65M/Operating Point: 22K 0.65M
SIG1=0.8 SIG2=0.7 RHO=0.8
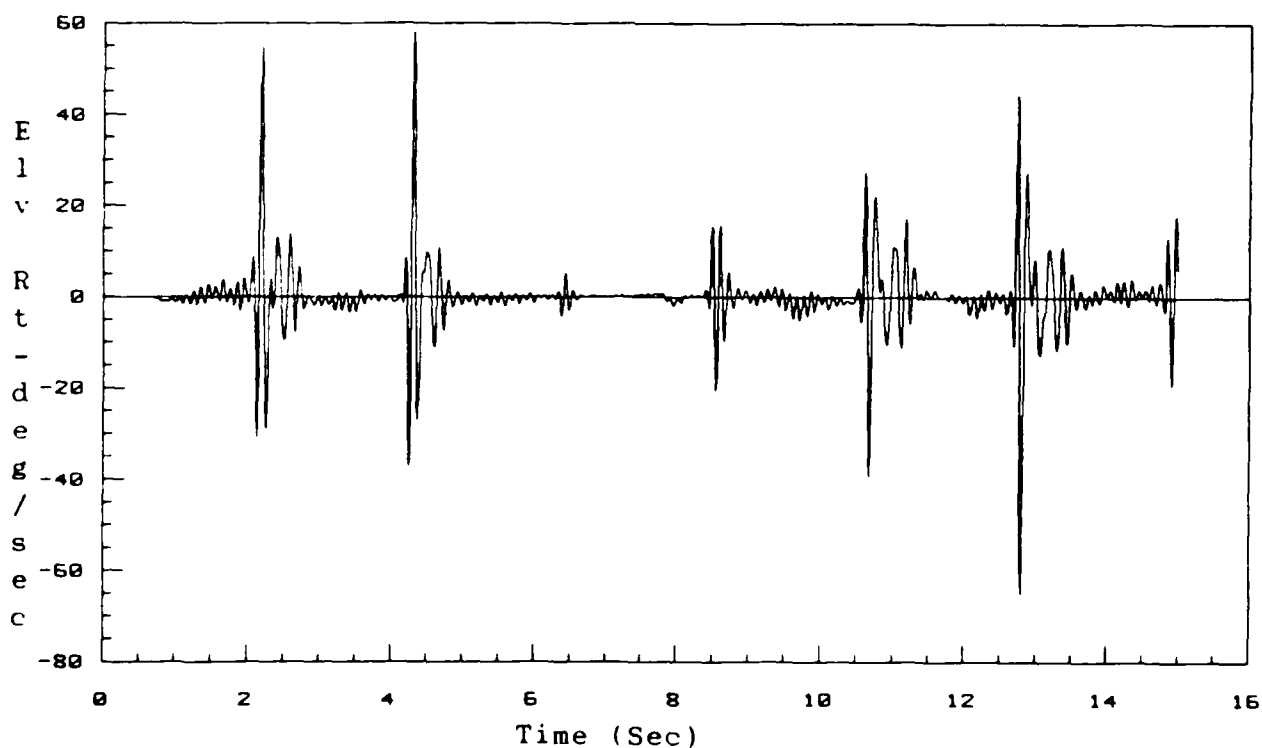
Figure 6-72.   Elevator Rate
Nominal Model: 22K 0.65M/Operating Point: 22K 0.65M
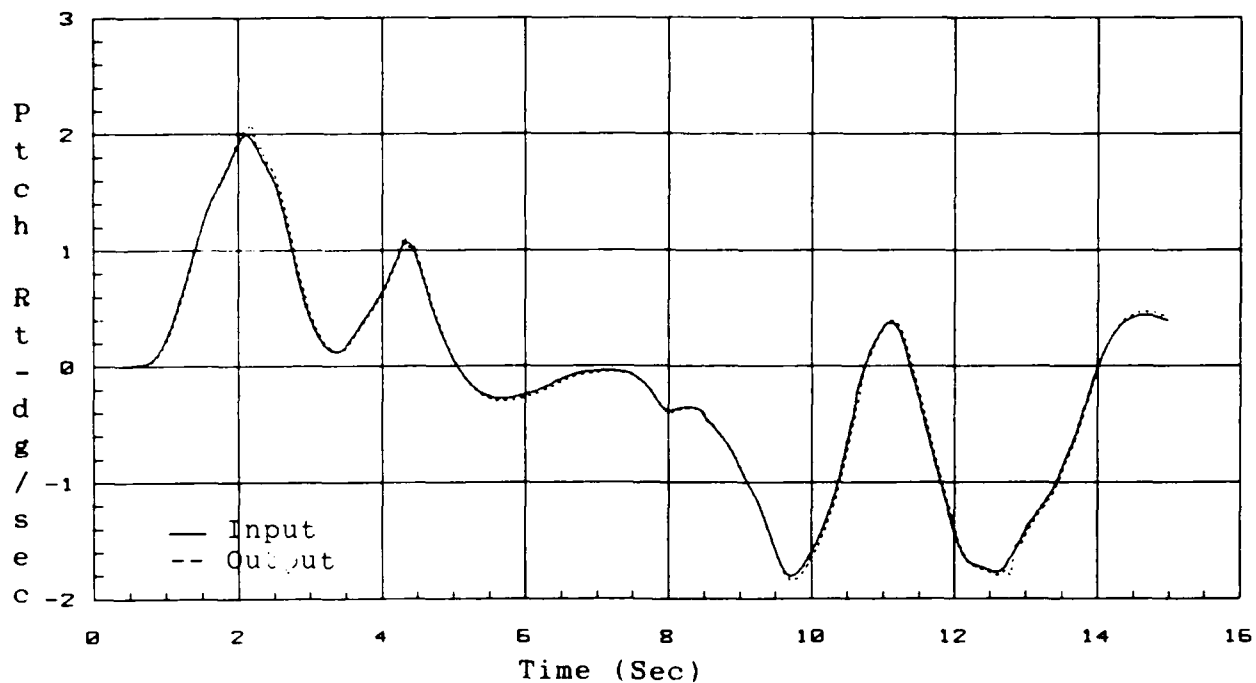SIG1=0.8 SIG2=0.7 RHO=0.8
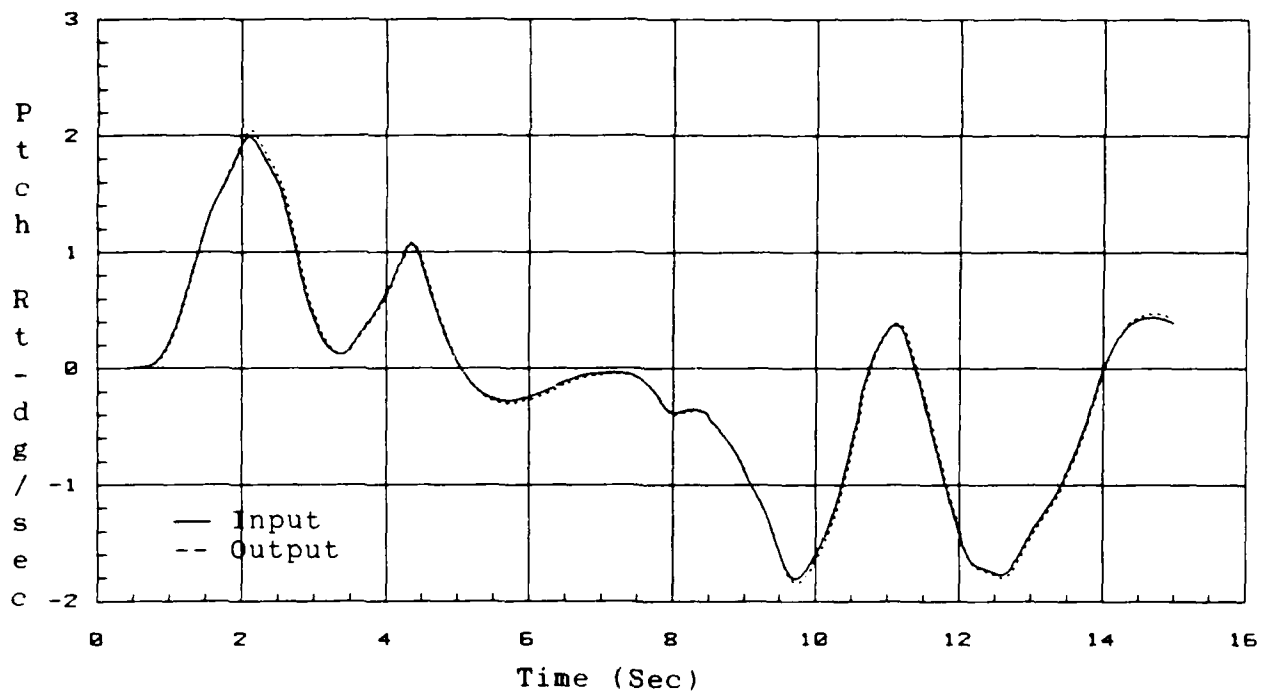
Figure 6-73.   Pitch Rate Response
Nominal Model: 22K 0.65M/Operating Point: 22K 0.65M
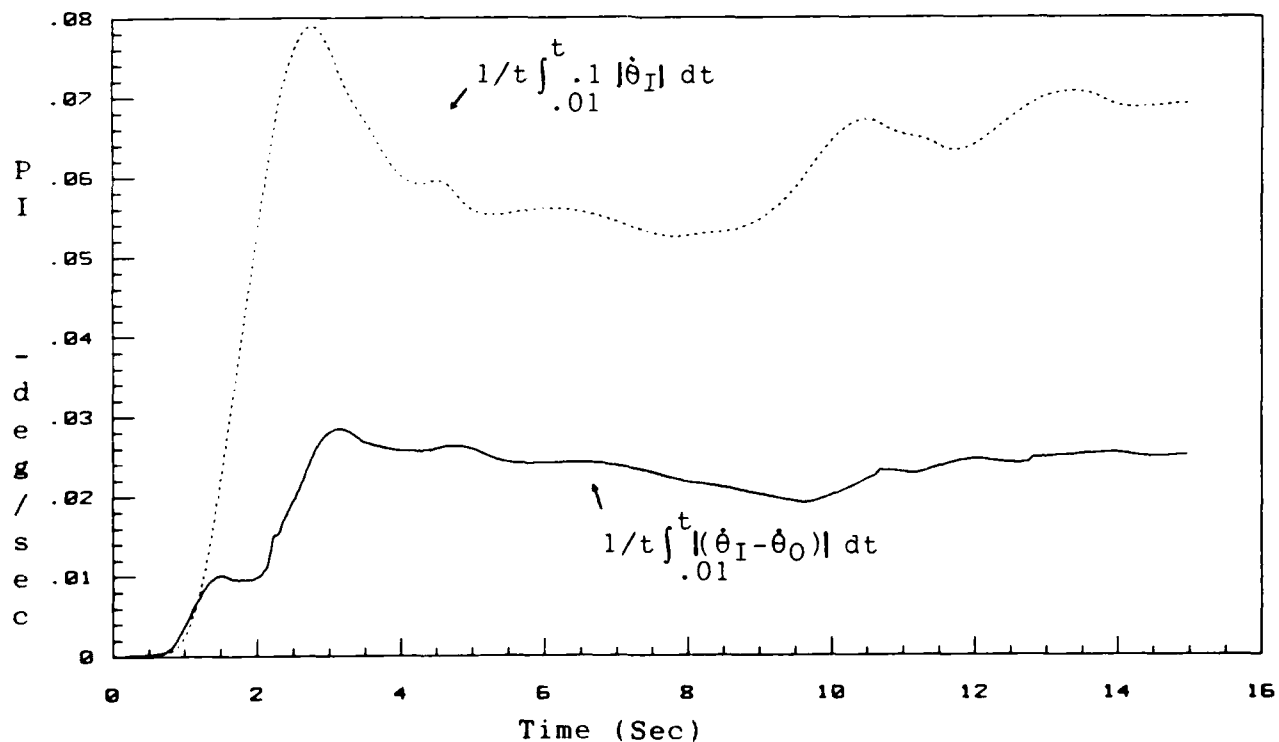SIG1=0.1 SIG2=0.7 RHO=0.8
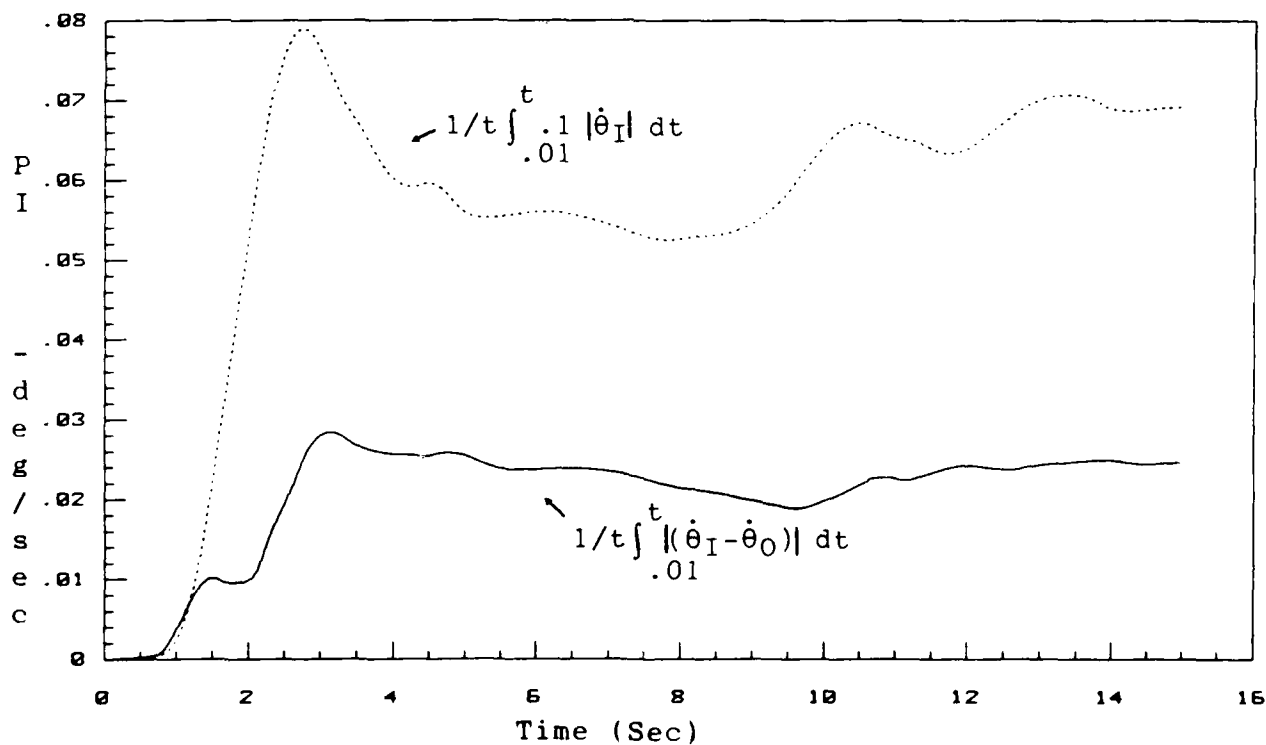
Figure 6-74.   Pitch Rate Performance Criterion
Nominal Model: 22K 0.65M/Operating Point: 22K 0.65M
SIG1=0.1 SIG2=0.7 RHO=0.8

164
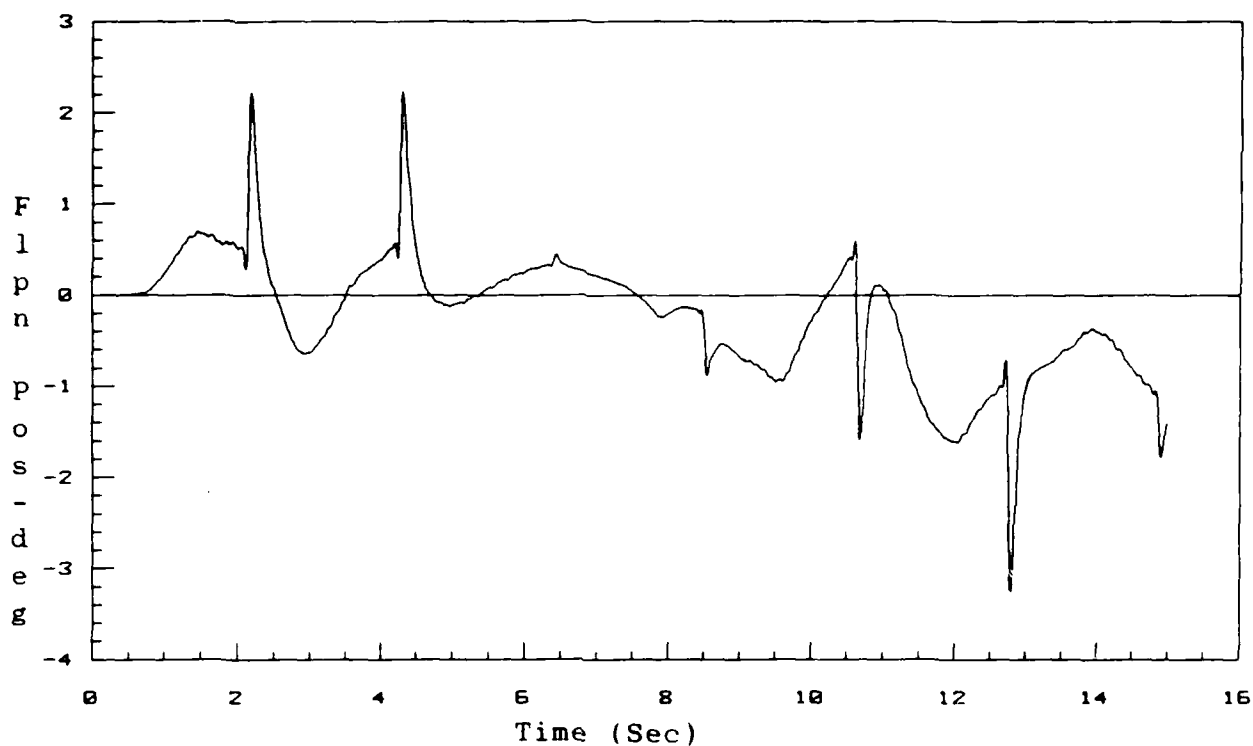
Figure 6-75.   Flaperon Position
Nominal Model: 22K 0.65M/Operating Point: 22K 0.65M
SIG1=0.1 SIG2=0.7 RHO=0.8
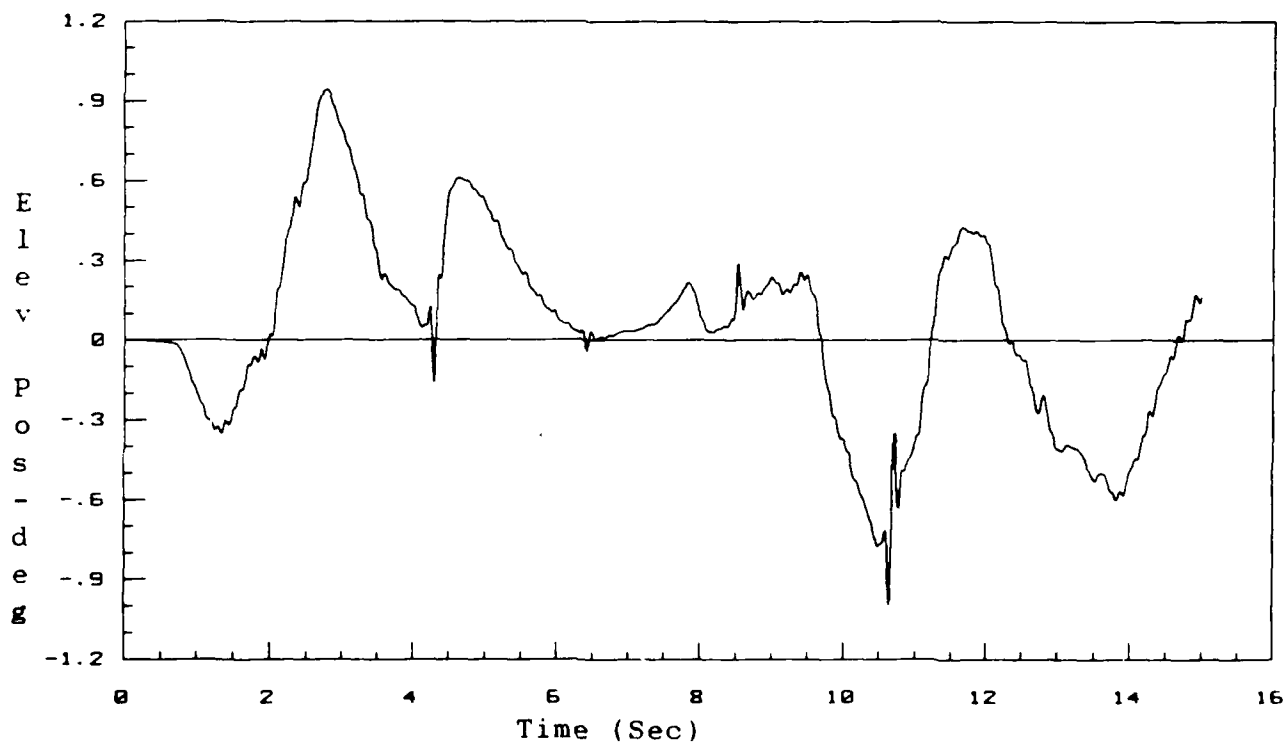
Figure 6-76.   Elevator Position
Nominal Model: 22K 0.65M/Operating Point: 22K 0.65M
SIG1=0.1 SIG2=0.7 RHO=0.8

165
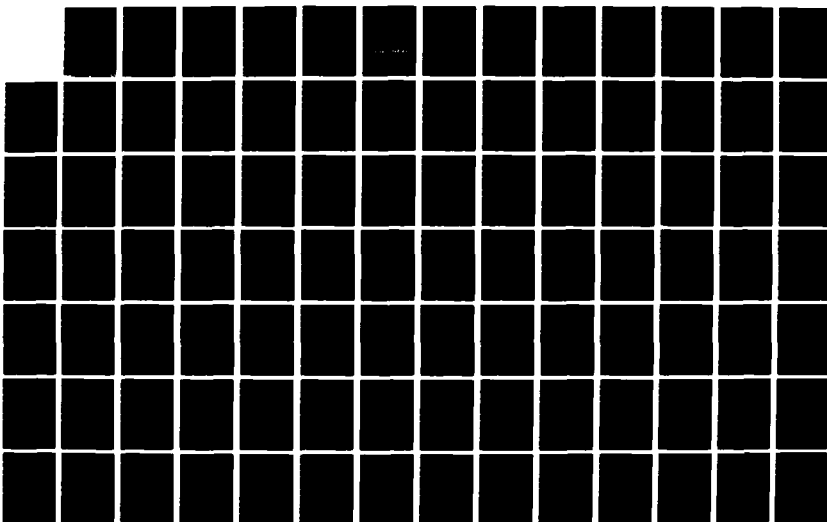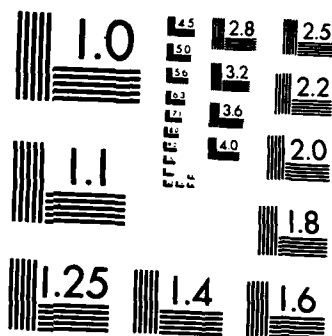
MICROCOPY RESOLUTION TEST CHART
NATIONAL BUREAU OF STANDARDS-1963-A
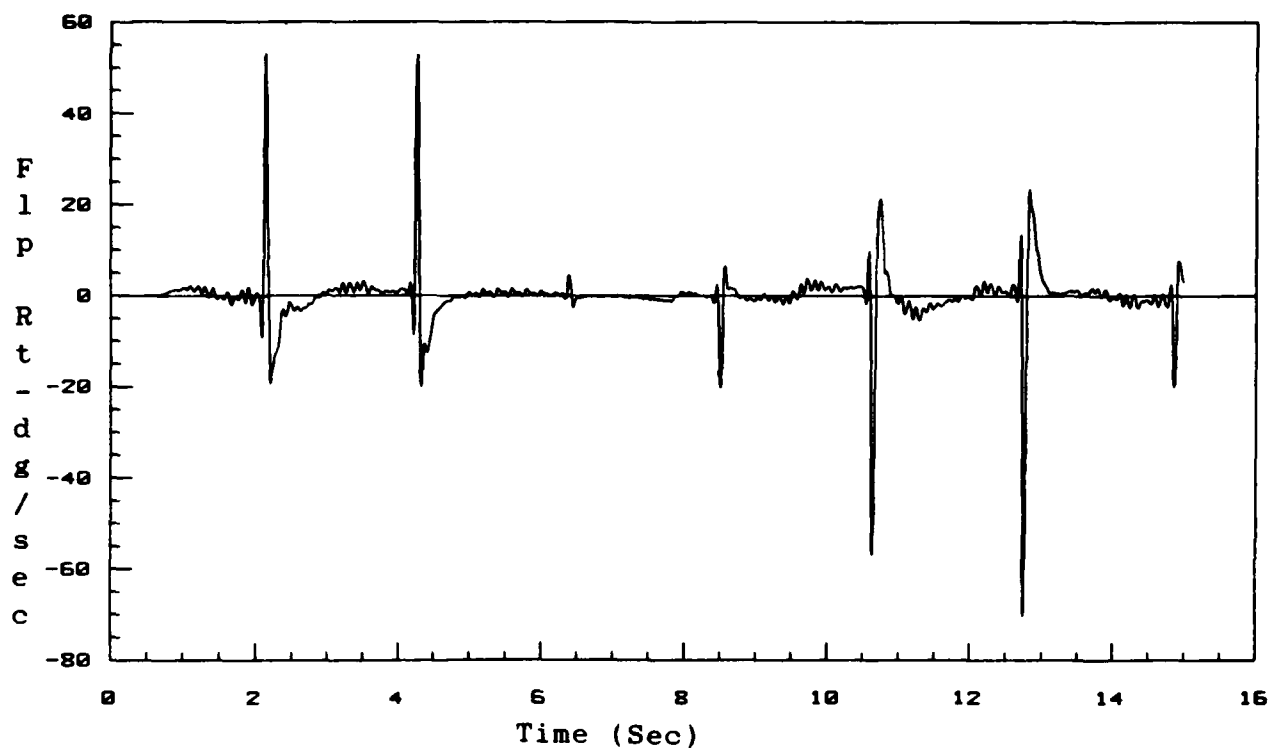
Figure 6-77. Flaperon Rate
Nominal Model: 22K 0.65M/Operating Point: 22K 0.65M
SIG1=0.1 SIG2=0.7 RHO=0.8
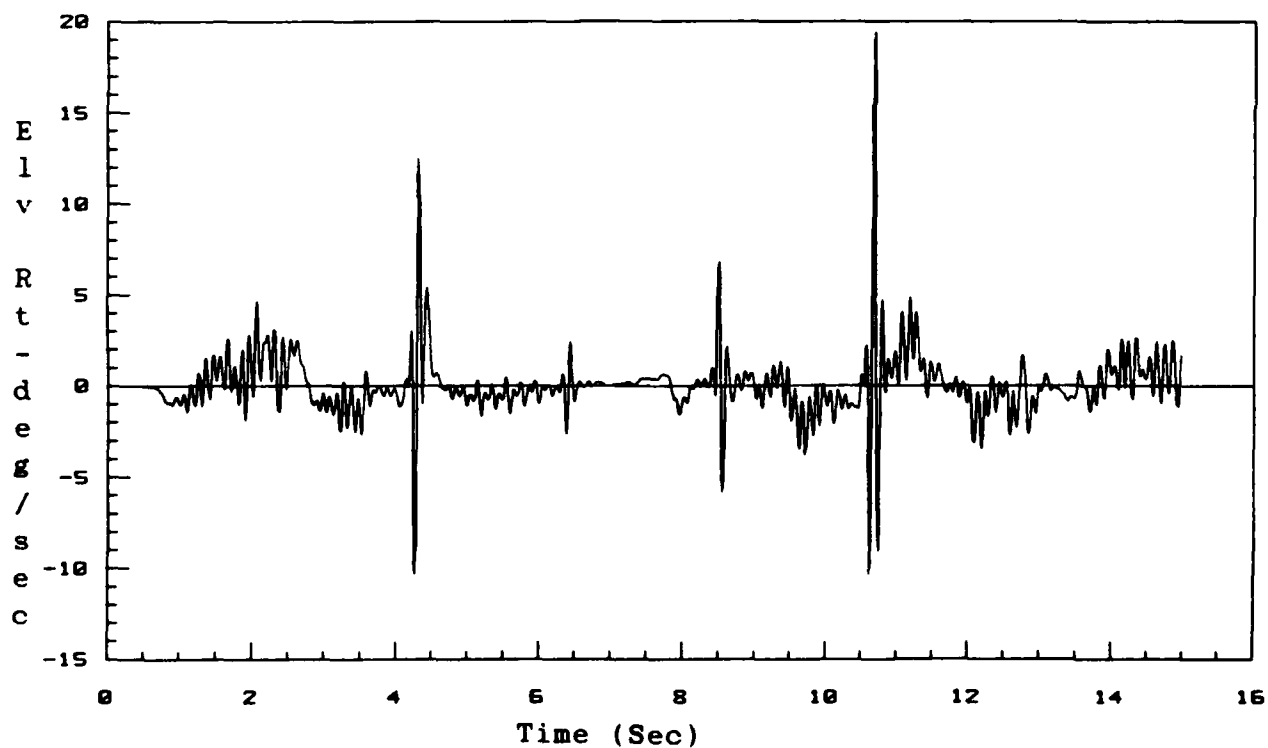
Figure 6-78. Elevator Rate
Nominal Model: 22K 0.65M/Operating Point: 22K 0.65M
SIG1=0.1 SIG2=0.7 RHO=0.8

166

case. However, the elevator and flaperon rates were much improved. The flaperon rates never reached rate limit for the entire simulation. The important point here is that, although the performance index was not affected significantly, decreasing Sigma 1 resulted in improved control surface activity.

Increasing Sigma 2 resulted in less error as shown on Figures 6-79 through 6-84 for simulation 7, but the control surfaces were more active, as can be seen on the elevator and flaperon positions and rates. Decreasing Sigma 2 had the effect of increasing the error as measured by the performance criteria. This is shown on Figures 6-85 through 6-90 which are simulations for simulation 9 on Table 6-14. Reducing Sigma 2 did not have much effect on the control surface rates, although Figure 6-89 shows that the amount of flaperon required to follow the input increased. The data showed that the ability of the output to tightly track the input was affected significantly by Sigma 2.

Following the determination of the effects of varying the control law design parameters, Sigma 1 was set equal to 0.1 to improve the control surface responses. With Sigma 1 equal to 0.1, simulations were run to determine the perfor-
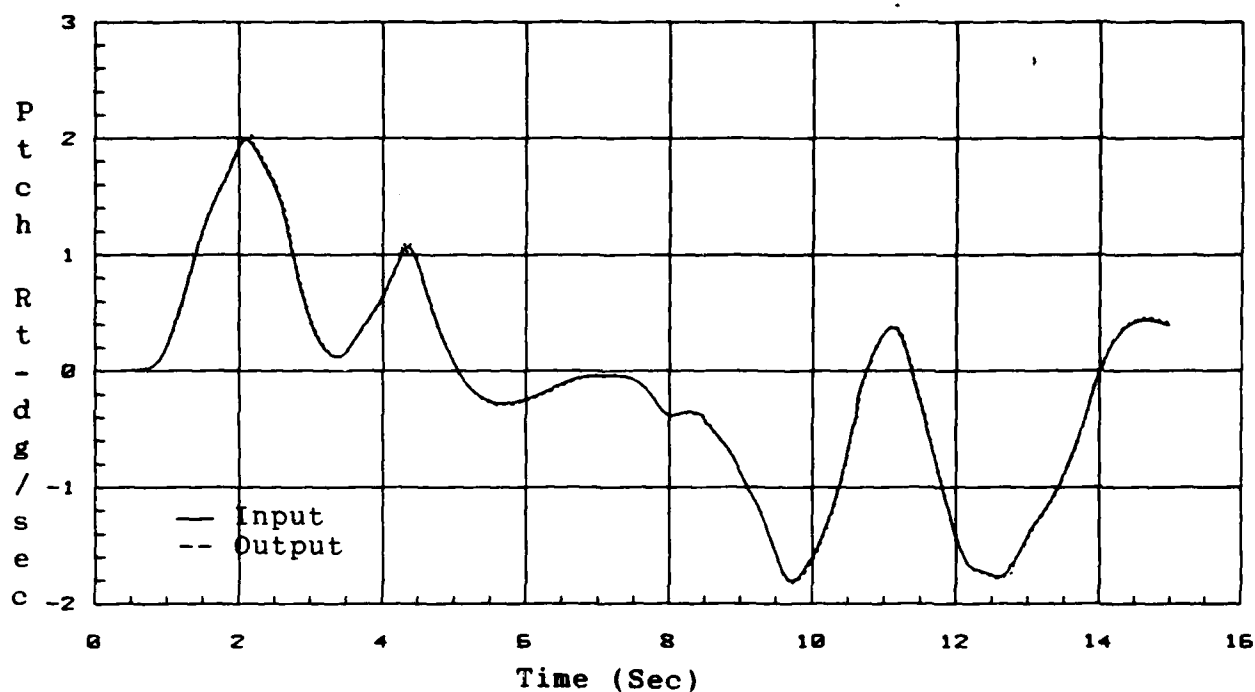
Figure 6-79. Pitch Rate Response
Nominal Model: 22K 0.65M/Operating Point: 22K 0.65M
SIG1=0.4 SIG2=1.5 RHO=0.8
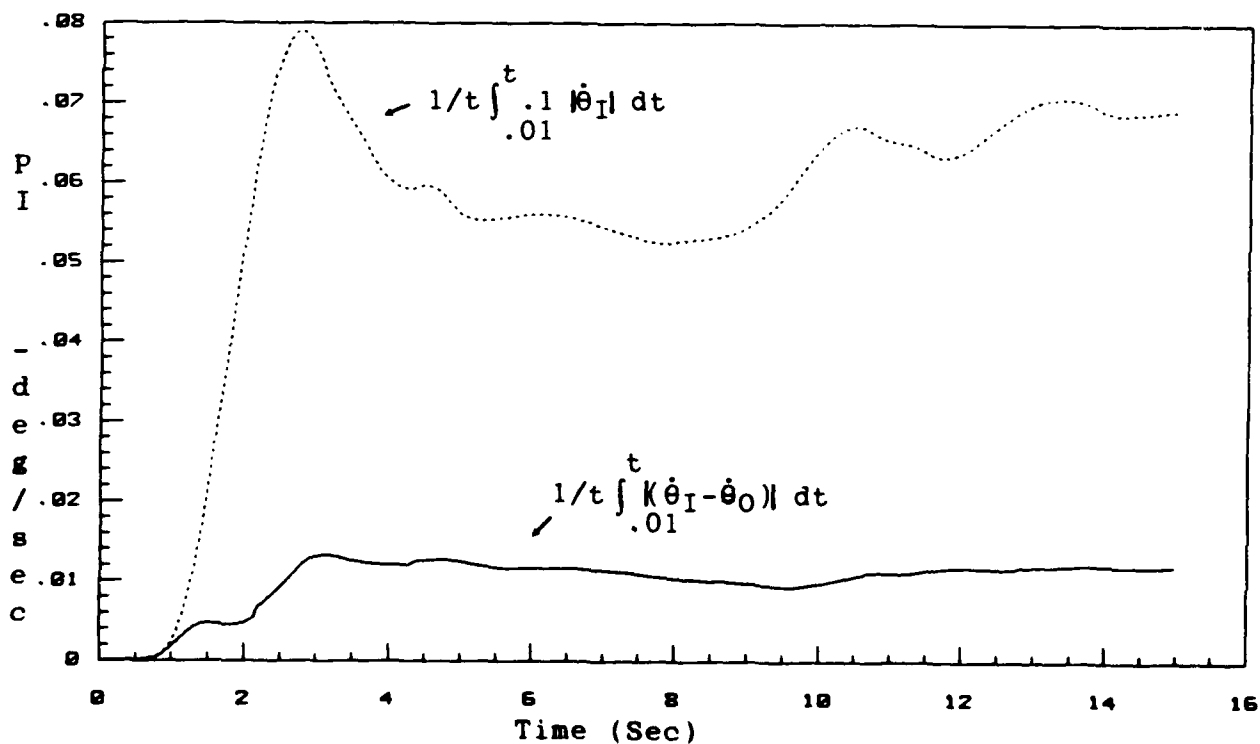
Figure 6-80. Pitch Rate Performance Criterion
Nominal Model: 22K 0.65M/Operating Point: 22K 0.65M
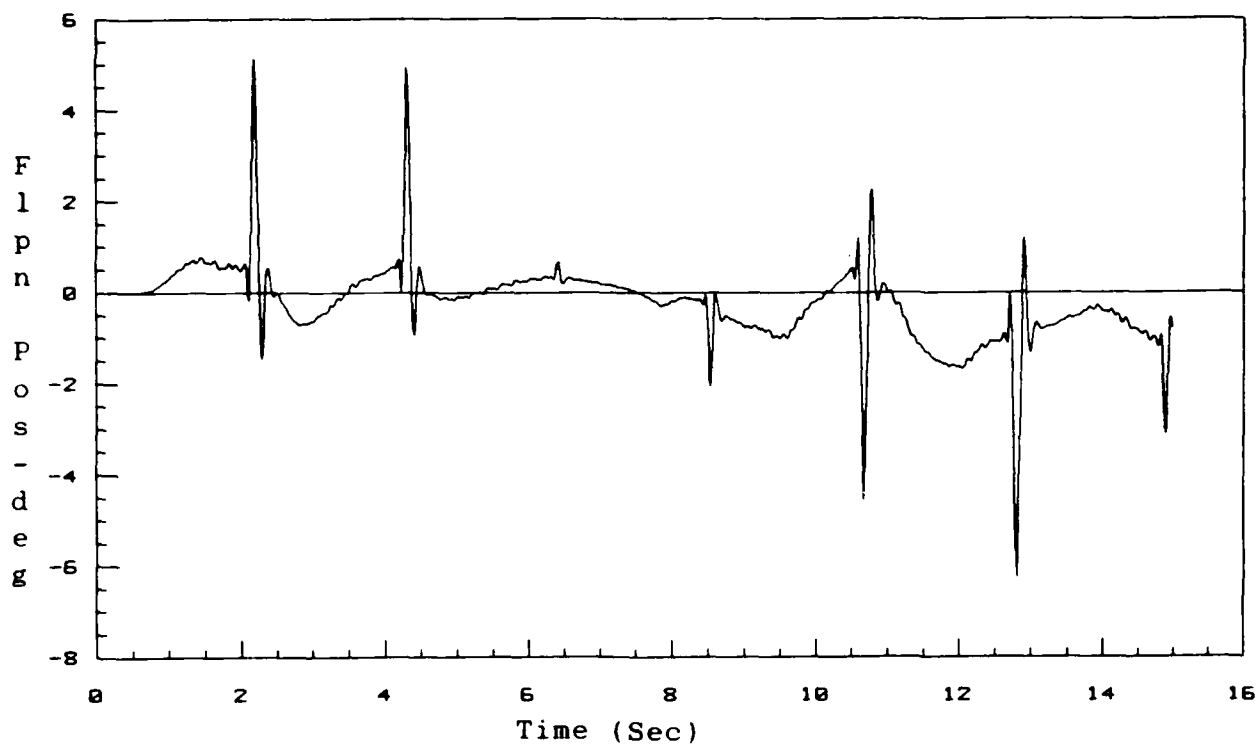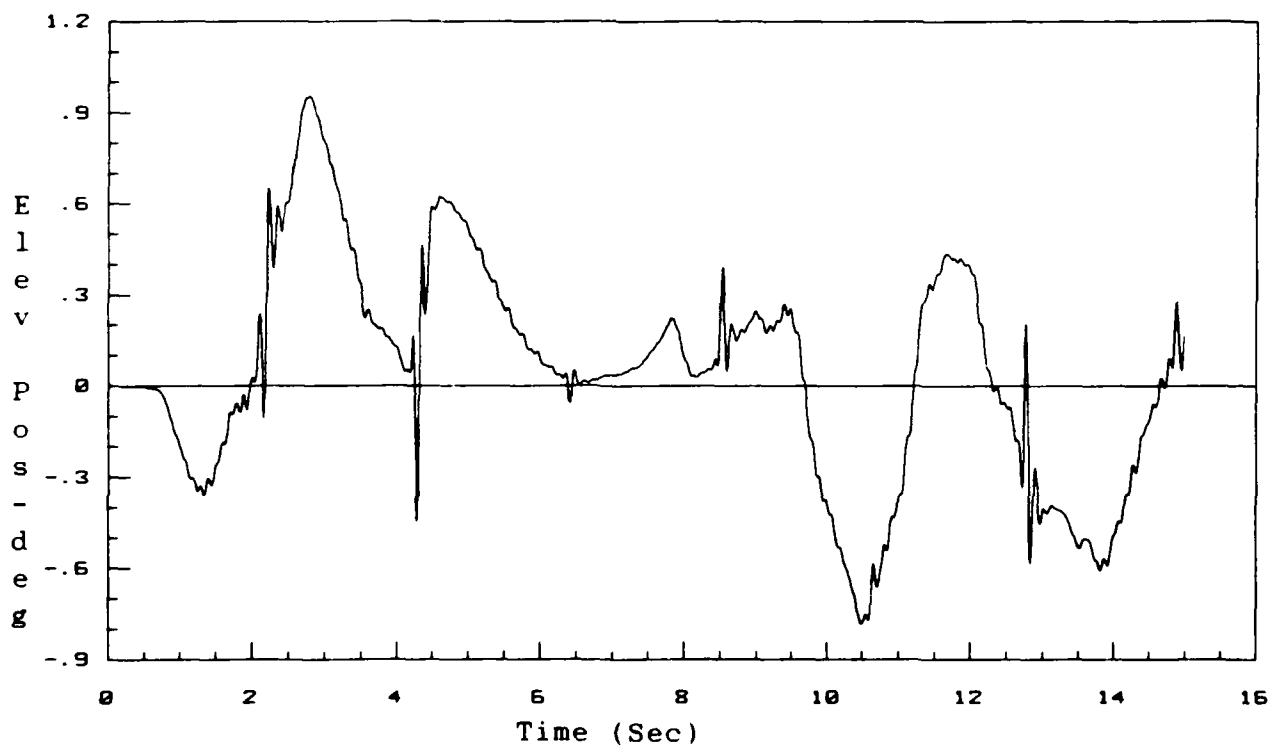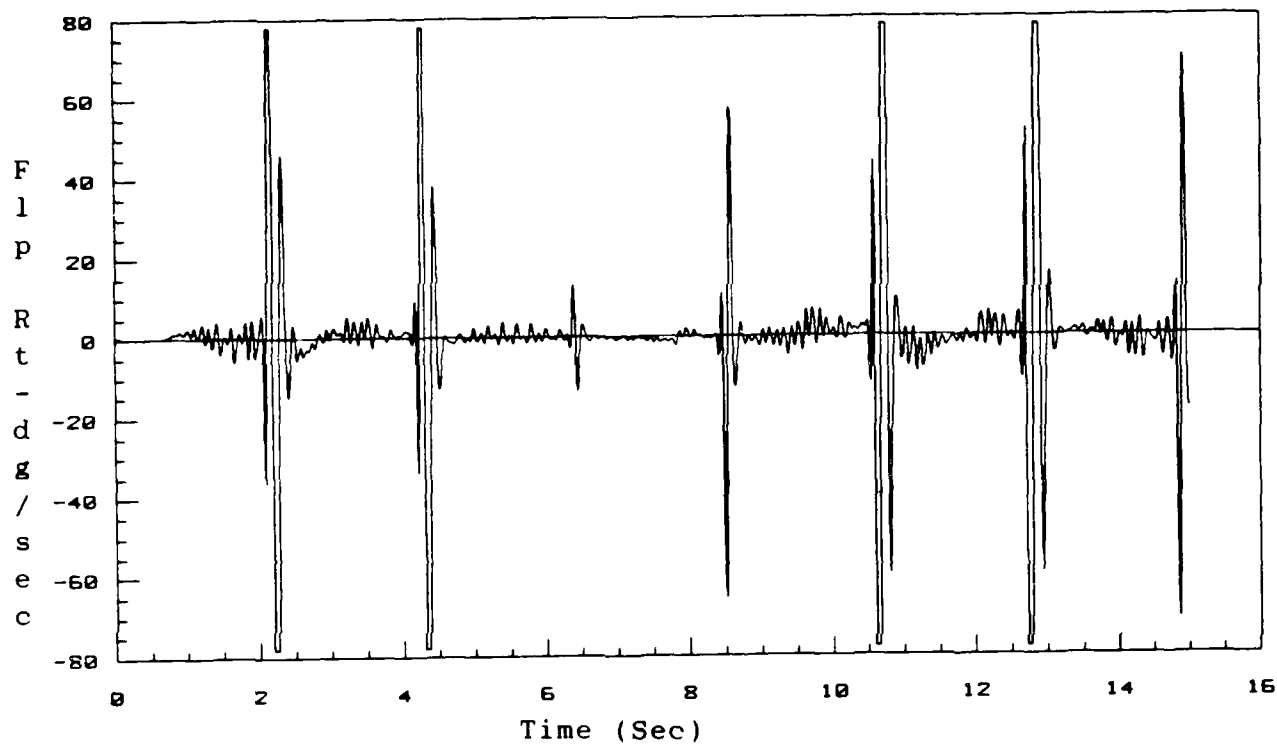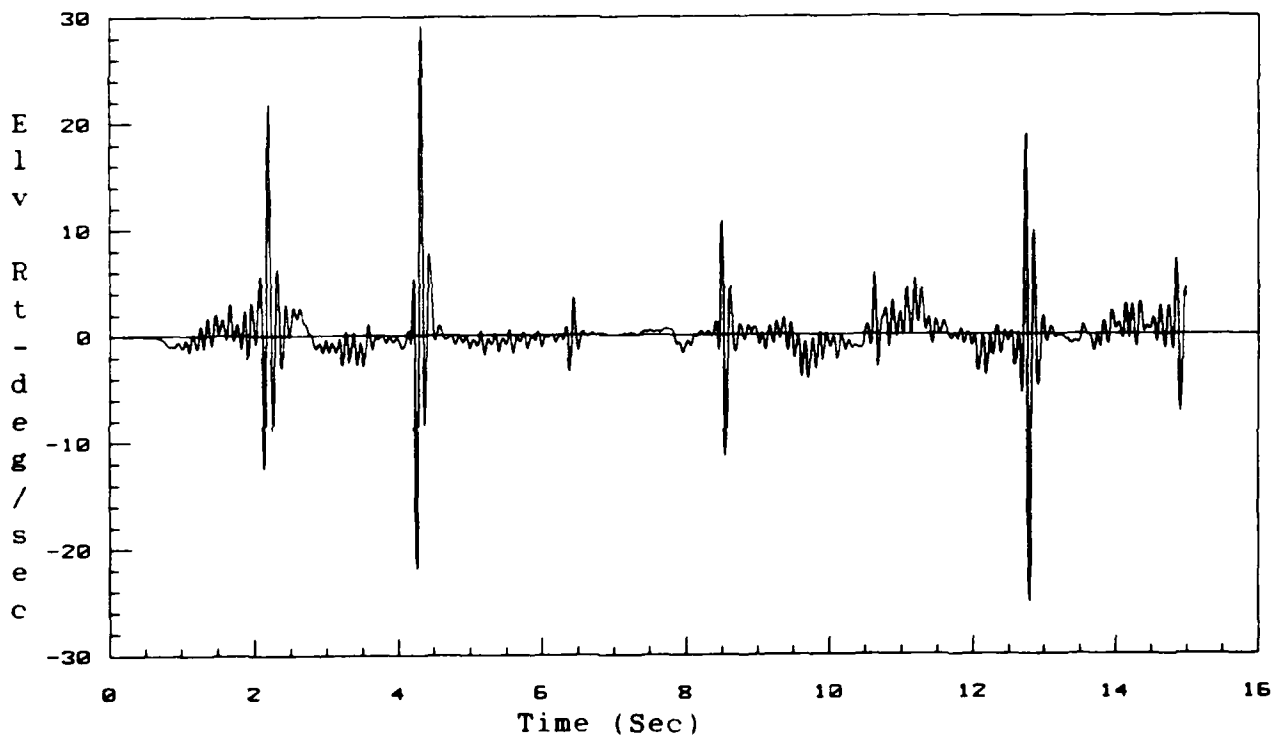SIG1=0.4 SIG2=1.5 RHO=0.8

168
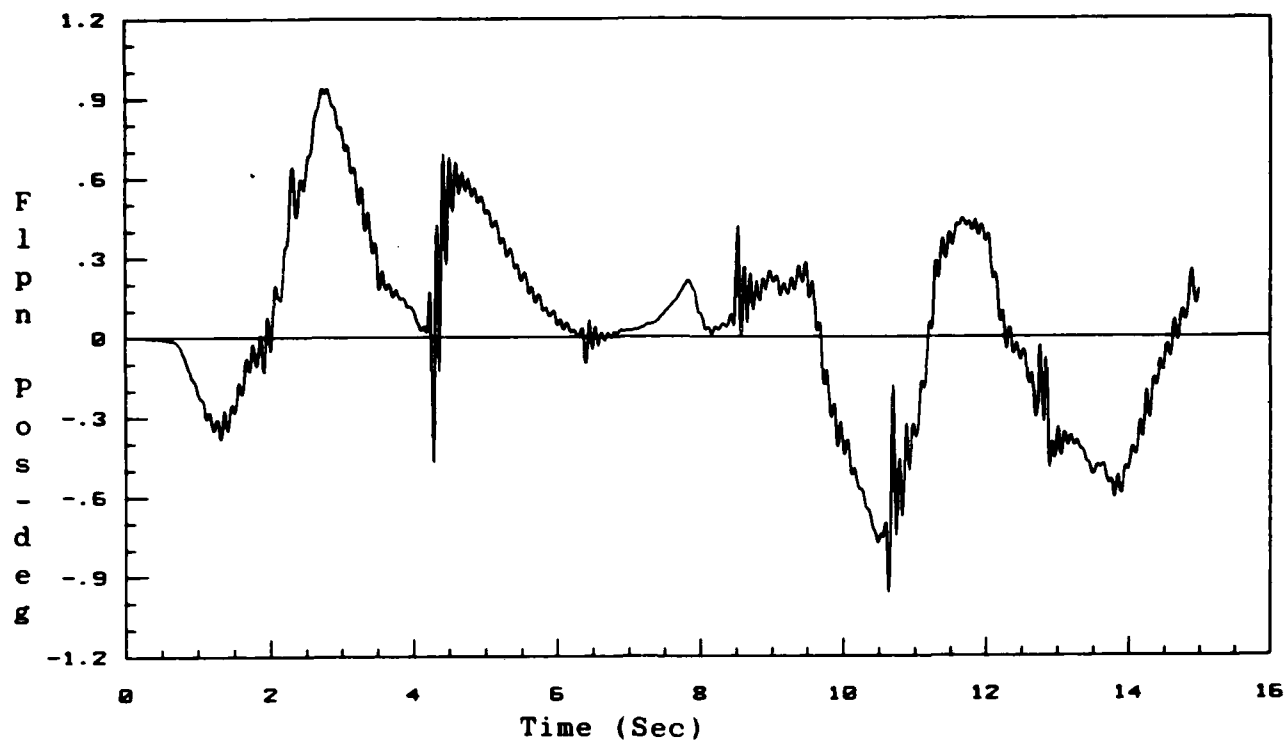
Figure 6-81. Flaperon Position
Nominal Model: 22K 0.65M/Operating Point: 22K 0.65M
SIG1=0.4 SIG2=1.5 RHO=0.8
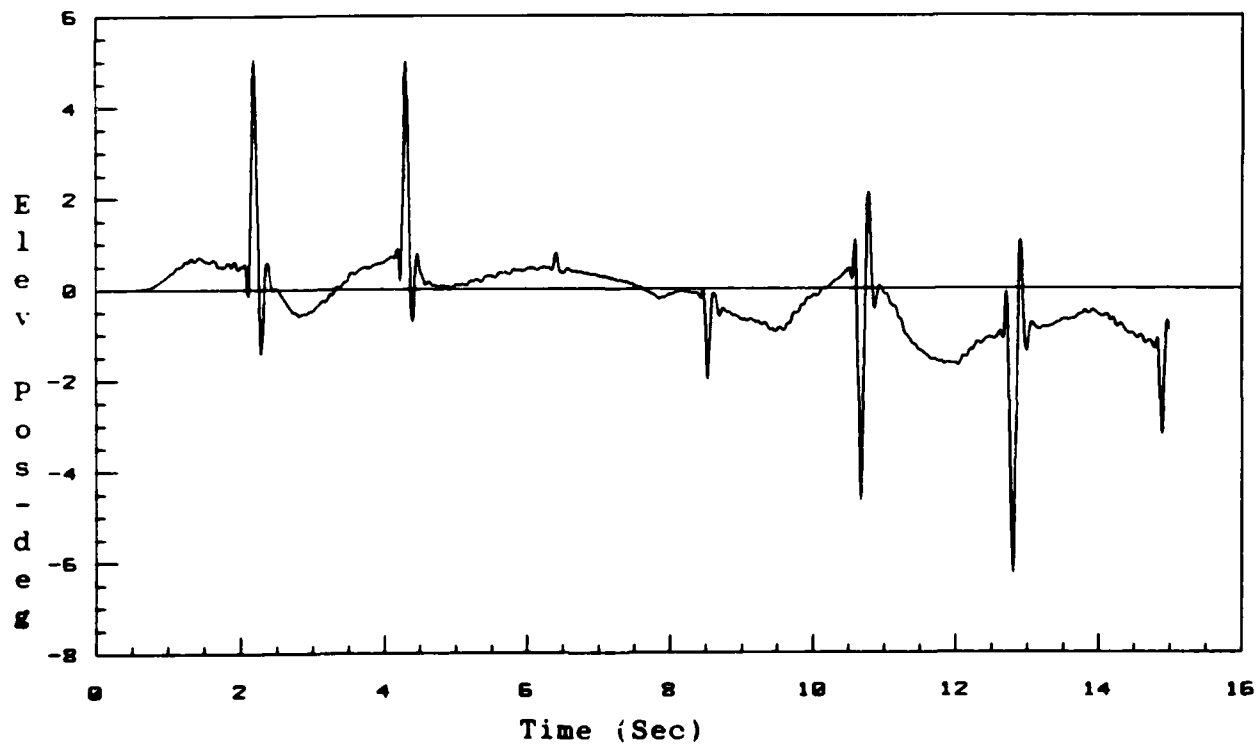
Figure 6-82. Elevator Position
Nominal Model: 22K 0.65M/Operating Point: 22K 0.65M
SIG1=0.4 SIG2=1.5 RHO=0.8

169
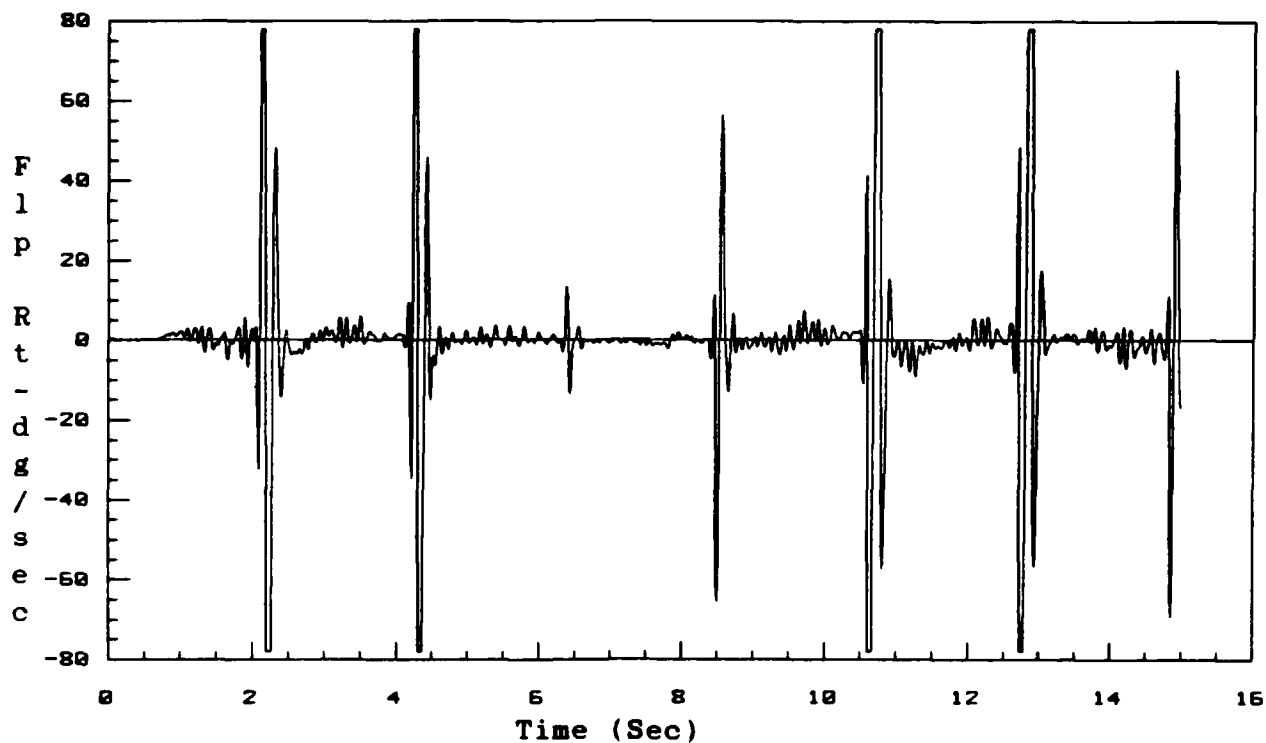
Figure 6-83. Flaperon Rate
Nominal Model: 22K 0.65M/Operating Point: 22K 0.65M
SIG1=0.4 SUG2=1.5 RHO=0.8
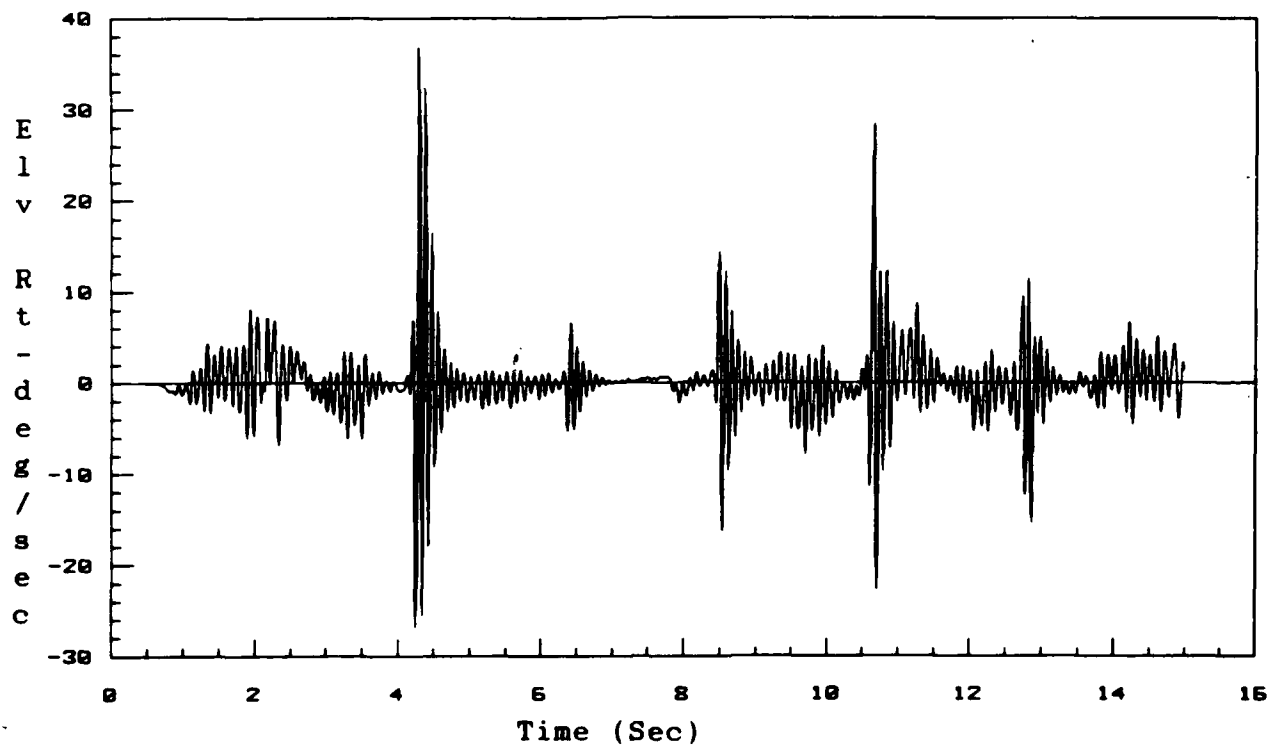
Figure 6-84. Elevator Rate
Nominal Model: 22K 0.65M/Operating Point: 22K 0.65M
SIG1=0.4 SIG2=1.5 RHO=0.8

170
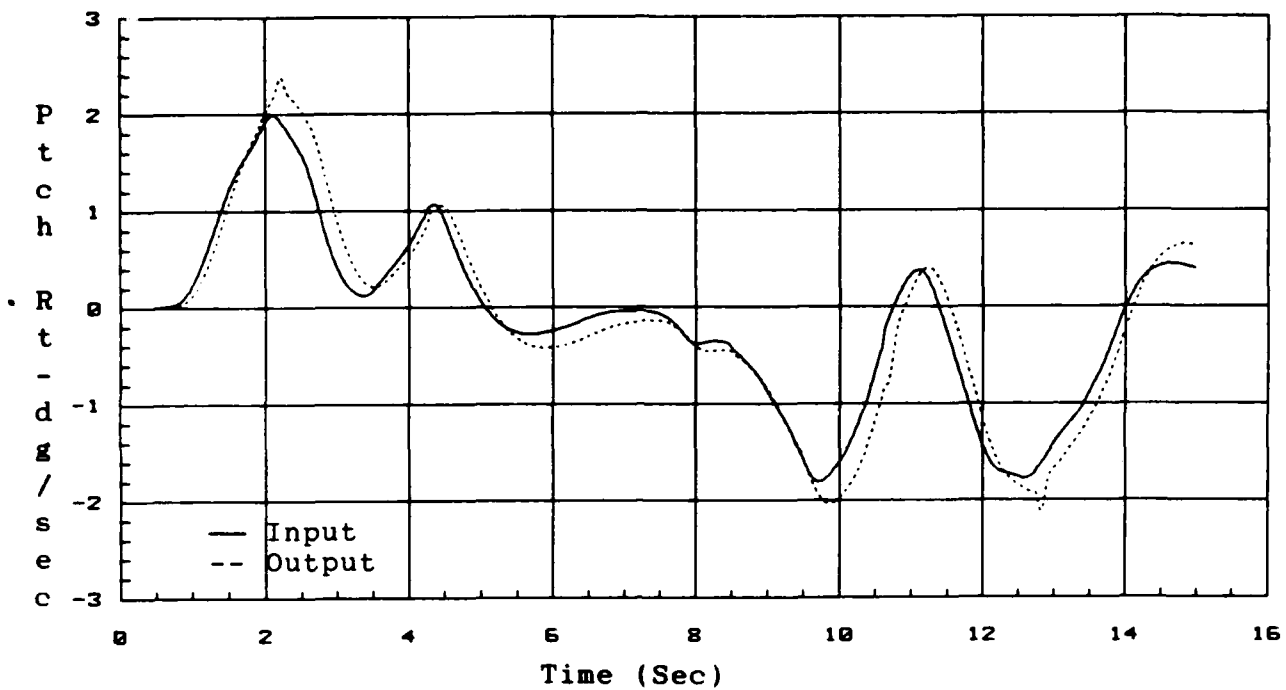
Figure 6-85.   Pitch Rate Response
Nominal Model: 22K 0.65M/Operating Point: 22K 0.65M
SIG1=0.4 SIG2=0.1 RHO=0.8
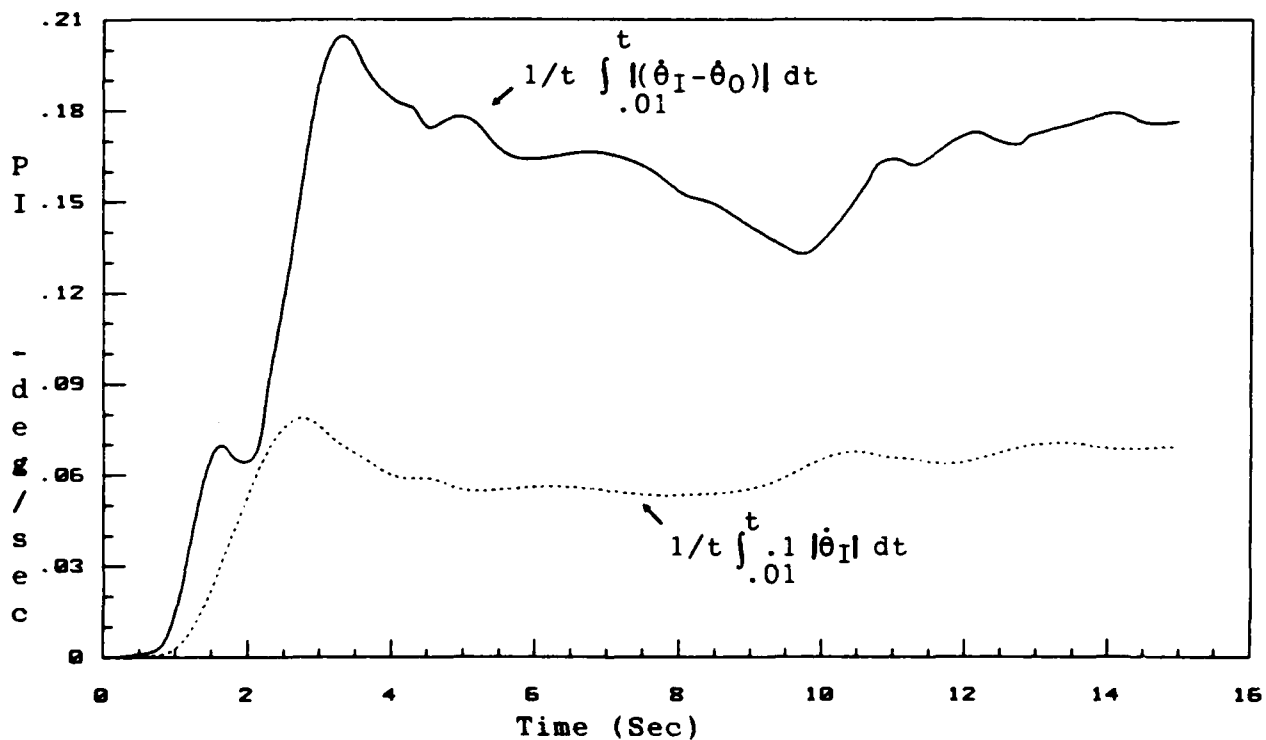
Figure 6-86.   Pitch Rate Performance Criterion
Nominal Model: 22K 0.65M/Operating Point: 22K 0.65M
SIG1=0.4 SIG2=0.1 RHO=0.8

171
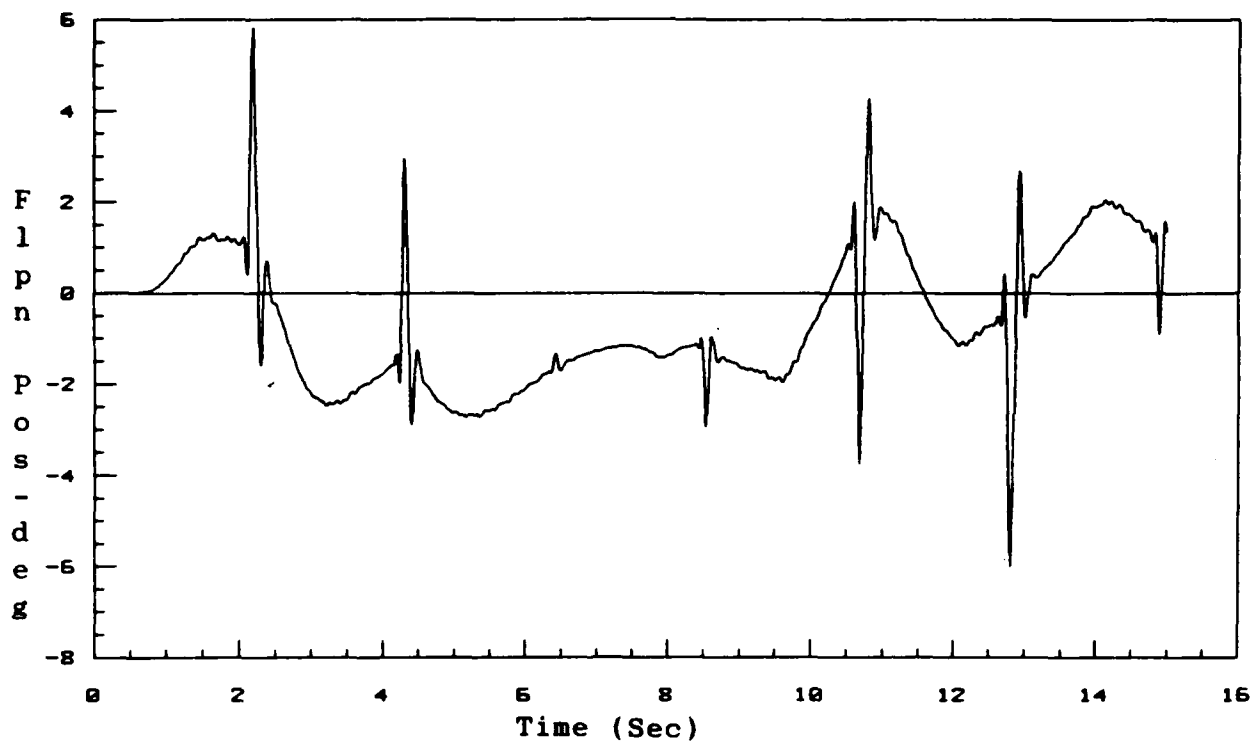
Figure 6-87. Flaperon Position
Nominal Model: 22K 0.65M/Operating Point: 22K 0.65M
SIG1=0.4 SIG2=0.1 RHO=0.8
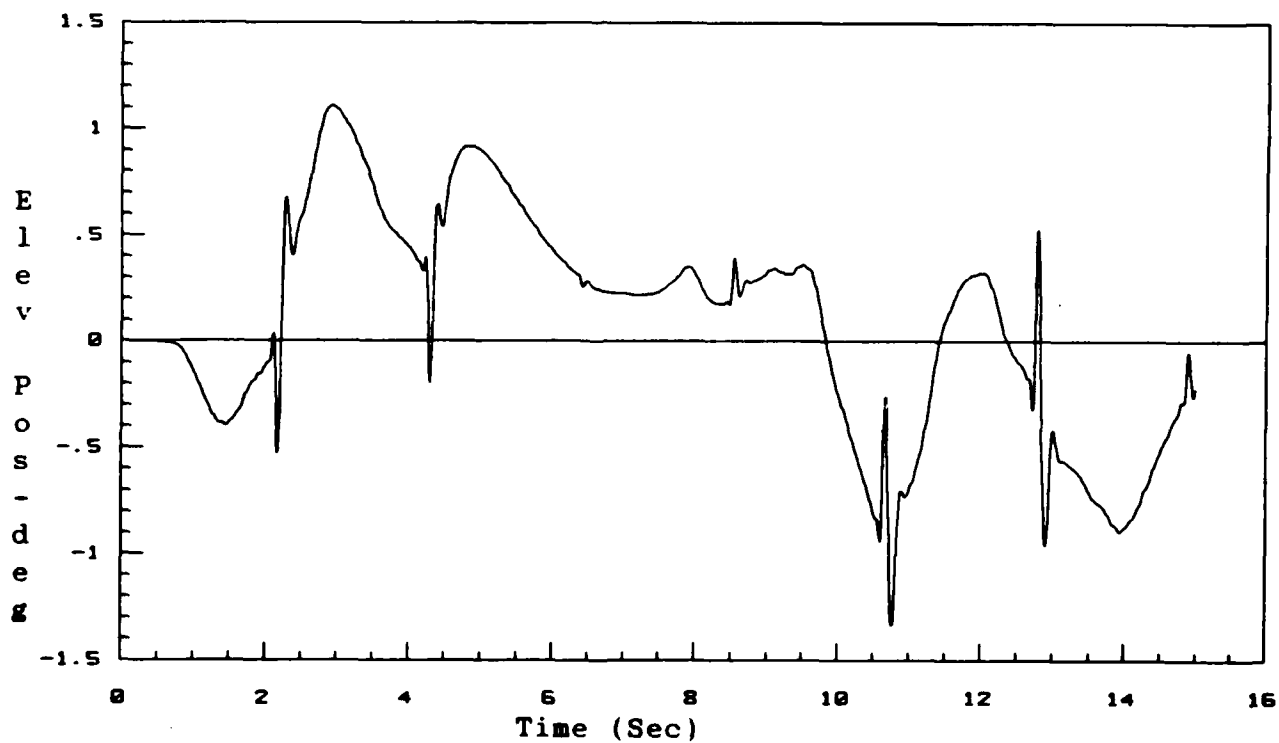
Figure 6-88. Elevator Position
Nominal Model: 22K 0.65M/Operating Point: 22K 0.65M
SIG1=0.4 SIG2=0.1 RHO=0.8

172
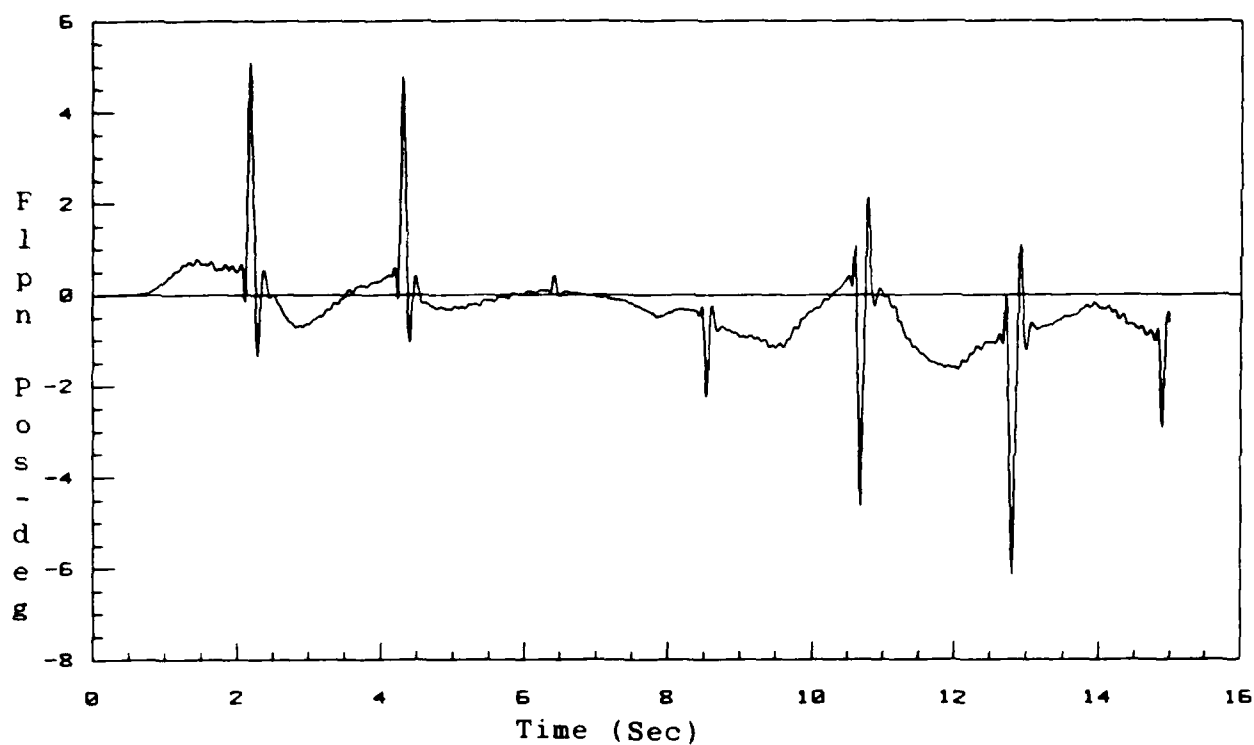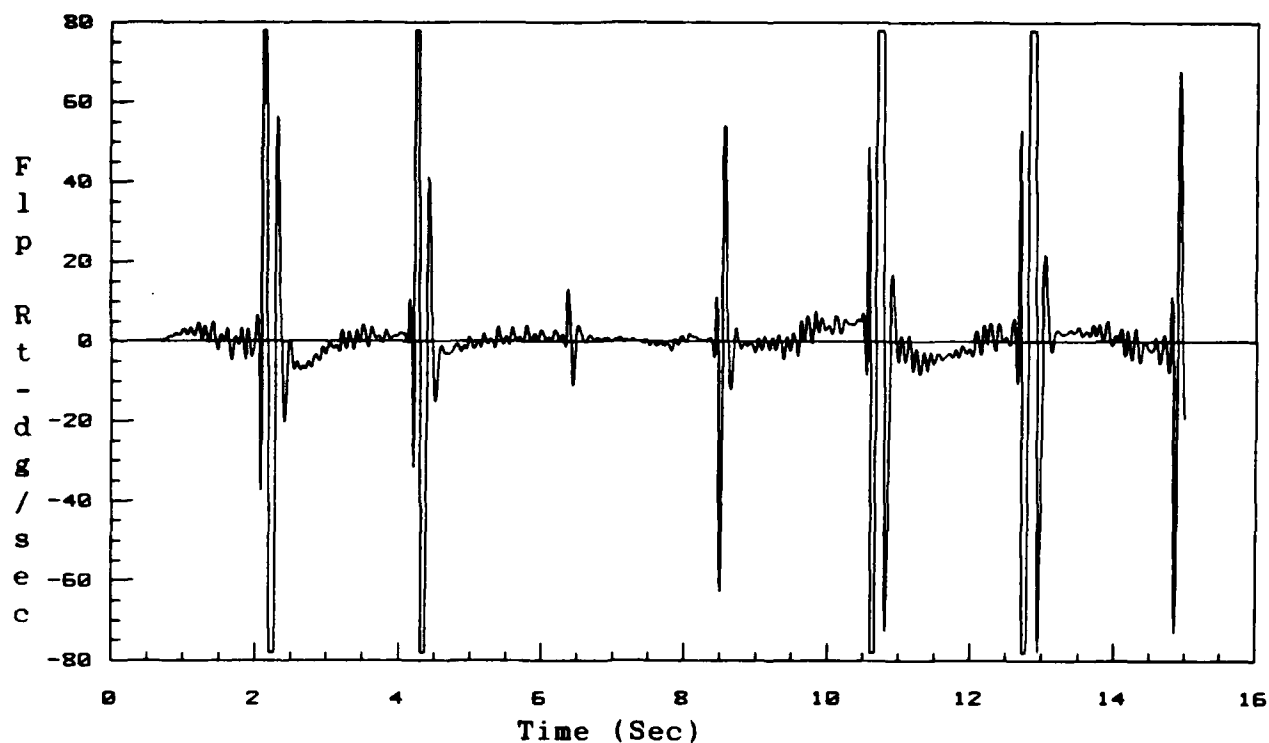
Figure 6-89.   Flaperon Rate
Nominal Model: 22K 0.65M/Operating Point: 22K 0.65M
SIG1=0.4 SIG2=0.1 RHO=0.8
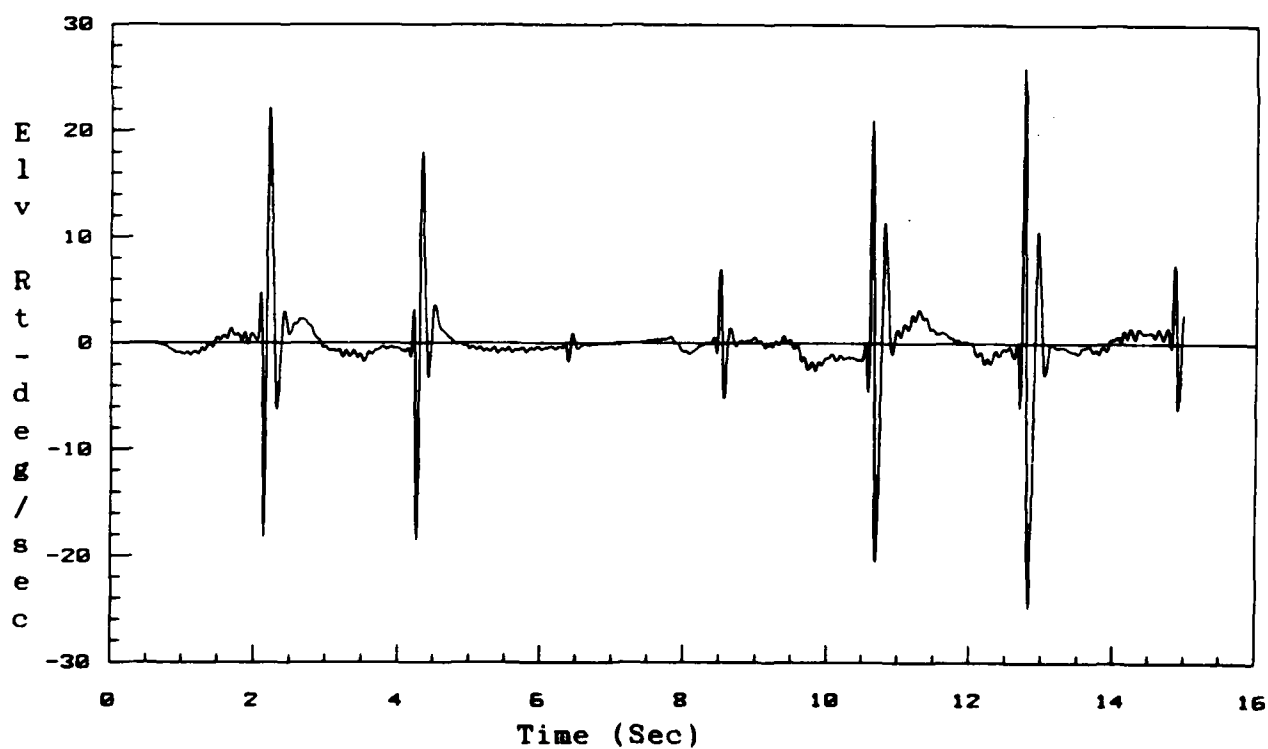
Figure 6-90.   Elevator Rate
Nominal Model: 22K 0.65M/Operating Point: 22K 0.65M
SIG1=0.4 SIG2=0.1 RHO=0.8

173

mance boundary for the nominal flight condition of 22,000 ft, 0.65 Mach. The data obtained from these simulations showed that the performance boundary was not affected by the reduction of the value of Sigma 1. The performance boundary for the decreased Sigma 1 case was the same as that shown on Figure 6-48. Figure 6-48 shows the performance boundary for the 22,000 ft, 0.65 Mach flight condition with the control law design parameters as given in Equations (6-14) and (6-15). Performance boundaries for nominal flight conditions of 18,000 ft, 0.45 Mach and 38,000 ft, 0.7 Mach were also determined with Sigma 1 set equal to 0.1. As was the case earlier, the performance boundaries with Sigma 1 equal to 0.1 were the same as those determined previously.

Due to the fact that the performance boundaries remained the same when decreasing the value of Sigma 1, the three-model configuration, configuration 8, had performance boundaries that covered the flight envelope of interest as before (see Figure 6-49). By using configuration 8 as the models in the parallel bank of secondary estimators for the multiple model algorithm (with Sigma 1=0.1), satisfactory tracking performance over the flight envelope of interest (from a performance criteria standpoint) was achieved as

before. However, the control surface responses were much
improved with the value of Sigma 1 set equal to 0.1. In
contrast to the simulations for configuration 8 with the
gains of Equations (6-14) and (6-15), the rate limits were
never encountered when Sigma 1 was set equal to 0.1. Fig-
ures 6-91 through 6-102 present simulation data for config-
uration 8 with Sigma 1 equal to 0.1. Note the responses of
the control surfaces and the fact that they do not reach the
rate limits for either the elevators or flaperons.

6.2.5 Sensor Noise Effects

To determine the effects of sensor noise on the perfor-
mance on the multiple model algorithm as the means of para-
meter identification, simulations were run where independent
white, gaussian noise was injected into each of the quanti-
ties of interest. The noise levels used in this thesis are
realistic noise levels for a comparable aircraft (Grumman
F-14 Tomcat) and are presented in Table 6-15.

To gain some insight into the effects of noise on the
multiple model algorithms performance, the two-model con-
figuration shown in Table 6-16 was considered. For the
configuration in Table 6-16, an operating point of 10,000
ft, 0.35 Mach was selected which was one of the models in

175
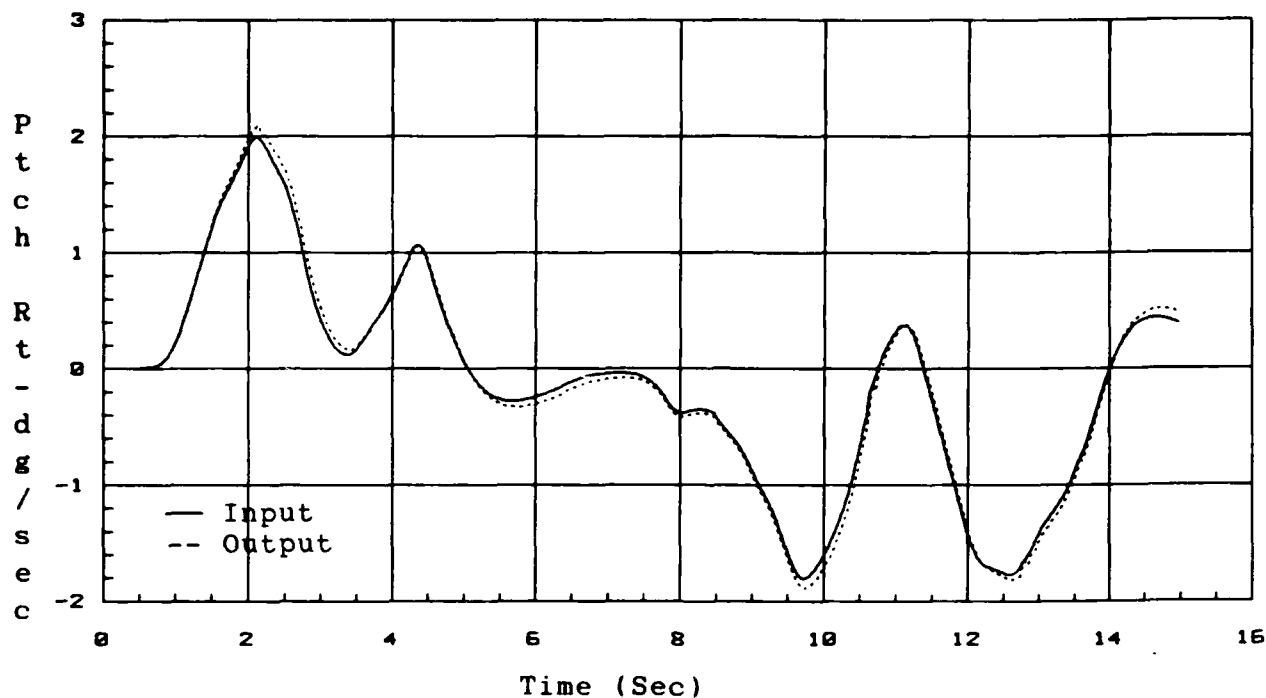
Figure 6-91.   Pitch Rate Response
Configuration 8/Operating Point: 10K 0.9M
SIG1=0.1 SIG2=0.7 RHO=0.8
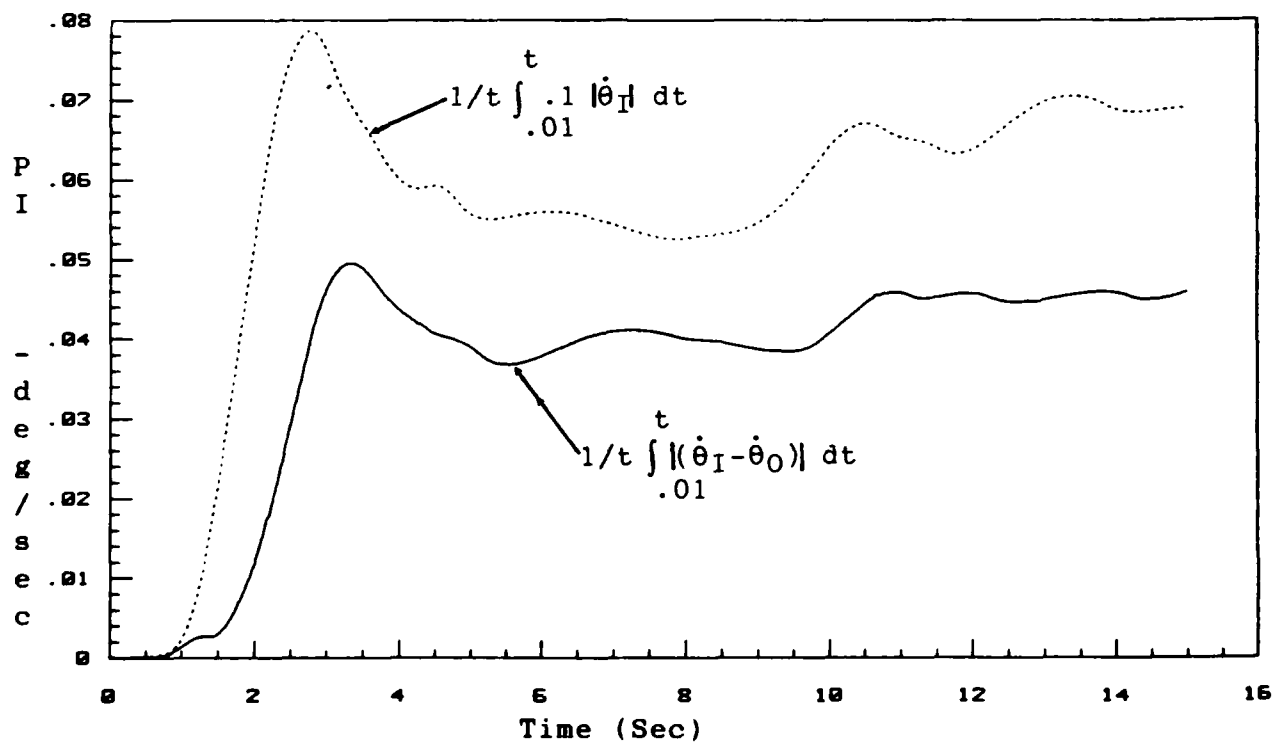
Figure 6-92.   Pitch Rate Performance Criterion
Configuration 8/Operating Point: 10K 0.9M
SIG1=0.1 SIG2=0.7 RHO=0.8

176
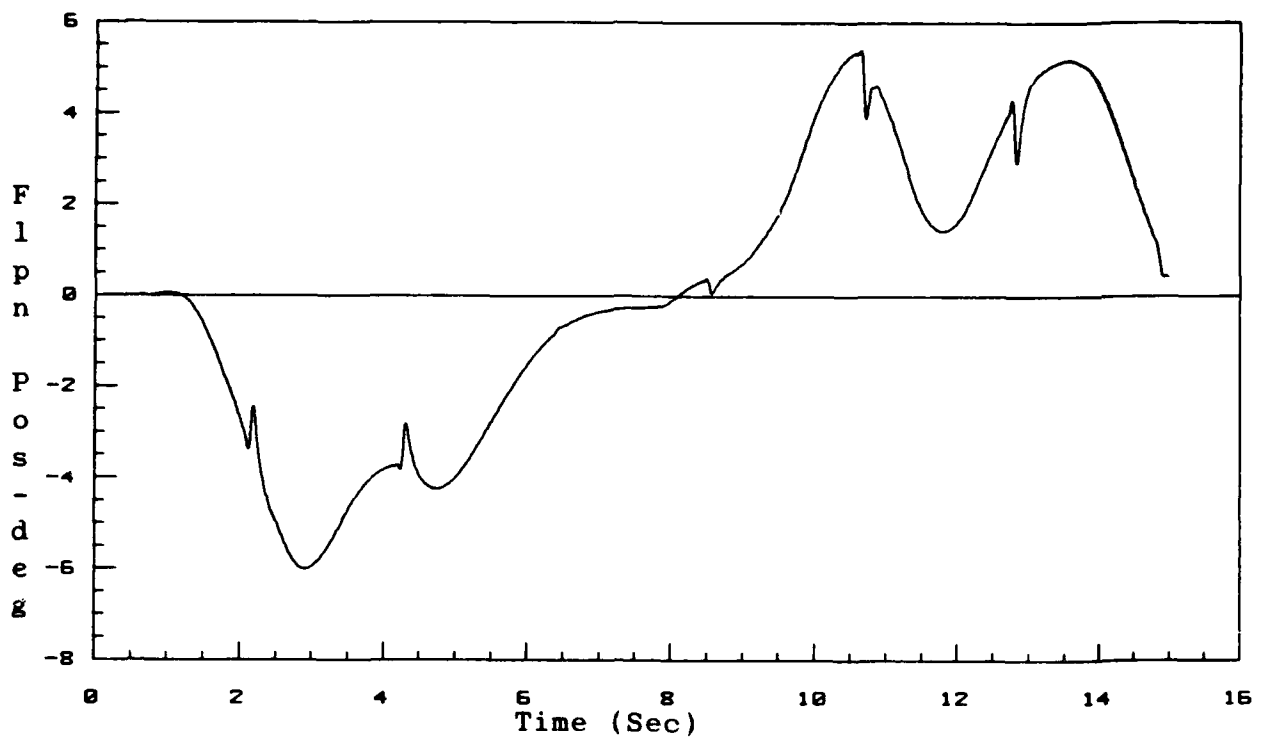
Figure 6-93.   Flaperon Position
Configuration 8/Operating Point: 10K 0.9M
SIG1=0.1 SIG2=0.7 RHO=0.8
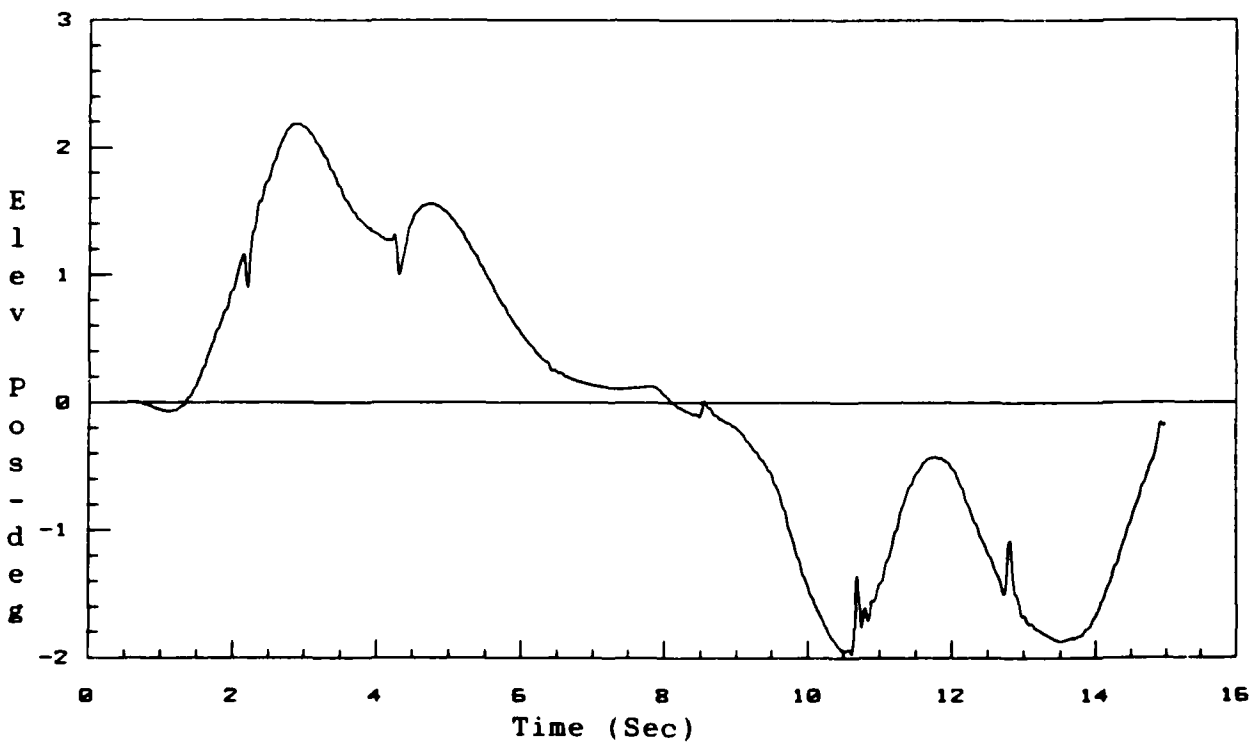
Figure 6-94.   Elevator Position
Configuration 8/Operating Point: 10K 0.9M
SIG1=0.1 SIG2=0.7 RHO=0.8
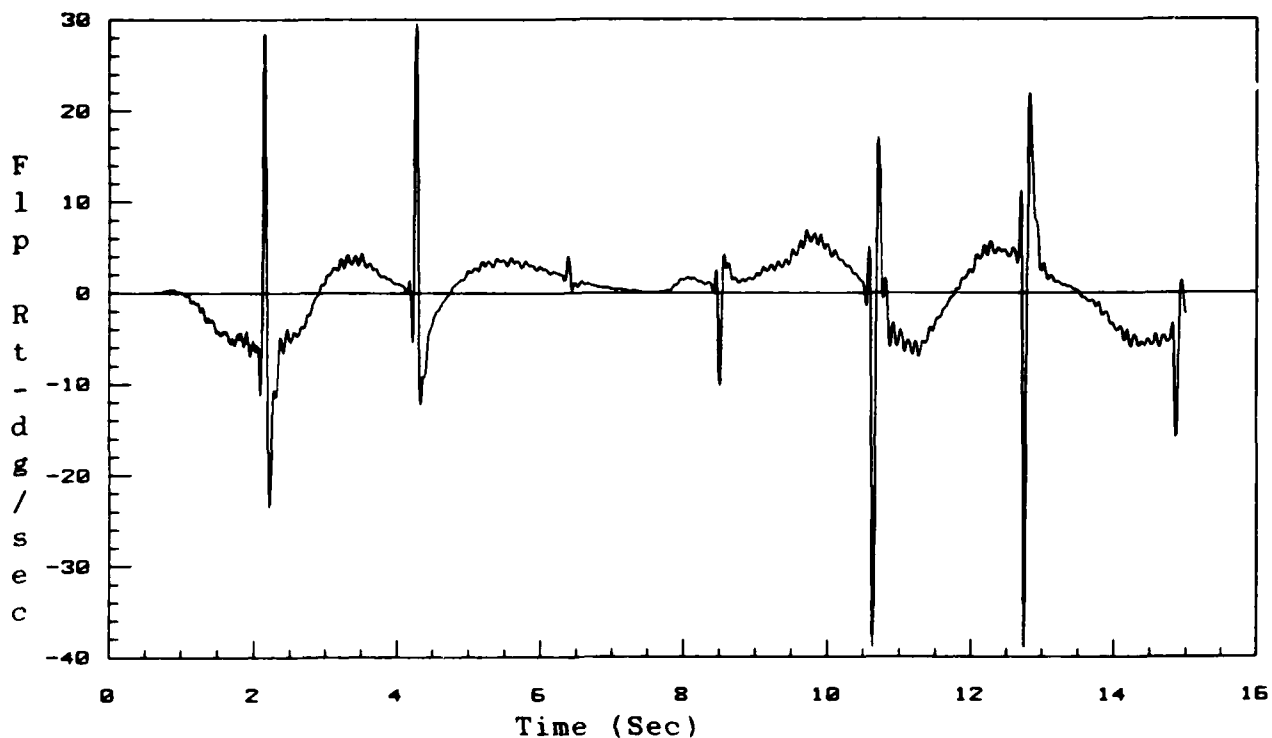
Figure 6-95. Flaperon Rate
Configuration 8/Operating Point: 10K 0.9M
SIG1=0.1 SIG2=0.7 RHO=0.8
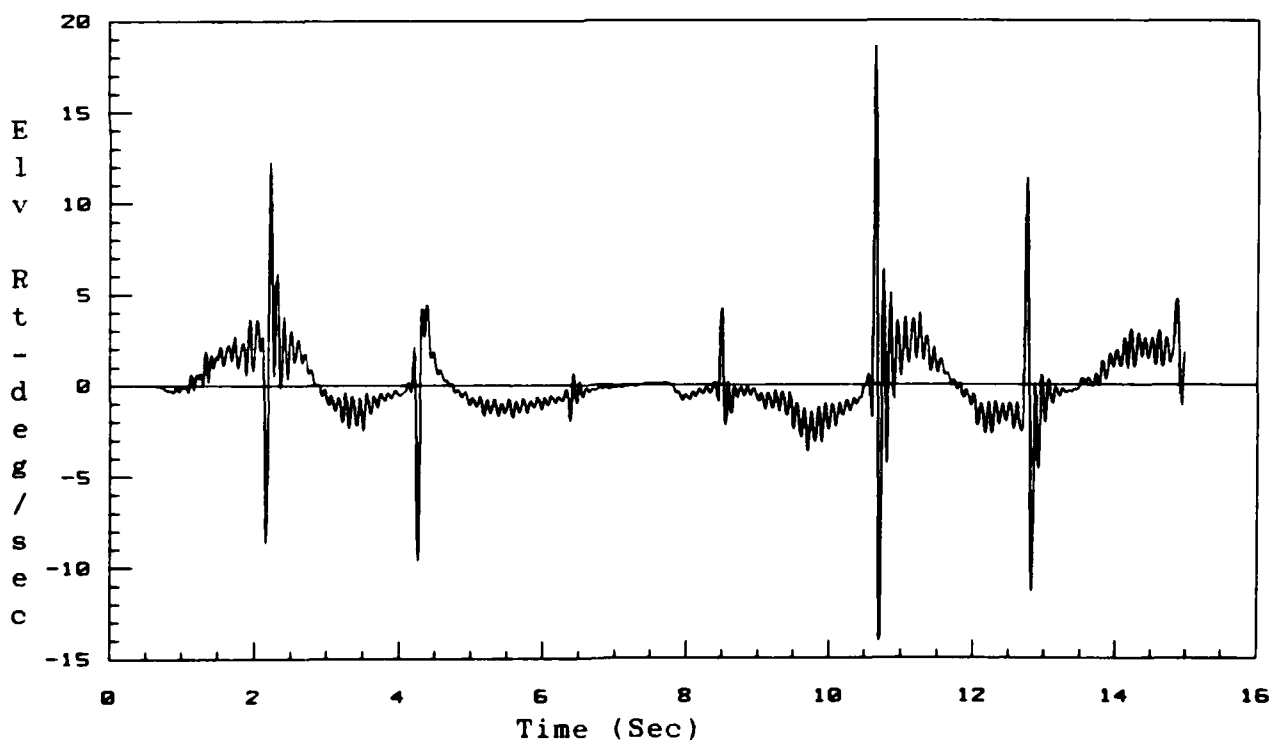
Figure 6-96. Elevator Rate
Configuration 8/Operating Point: 10K 0.9M
SIG1=0.1 SIG2=0.7 RHO=0.8

178
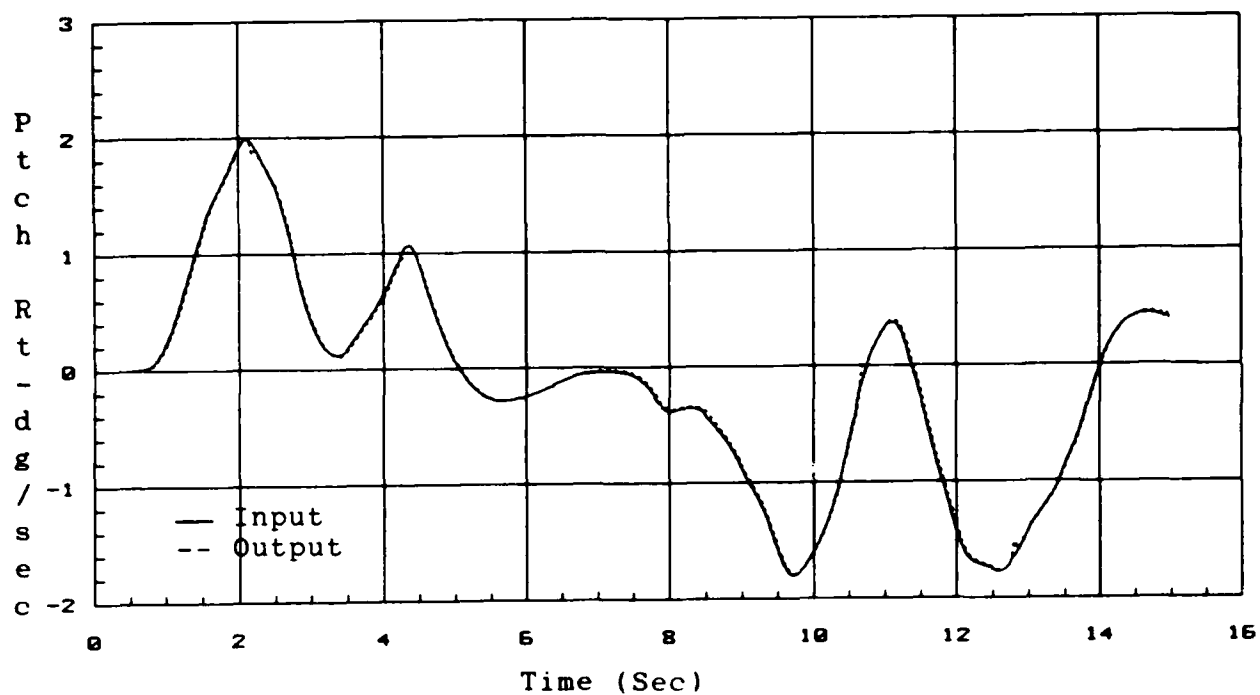
Figure 6-97.   Pitch Rate Response
Configuration 8/Operating Point: 38K 0.9M
SIG1=0.1 SIG2=0.7 RHO=0.7
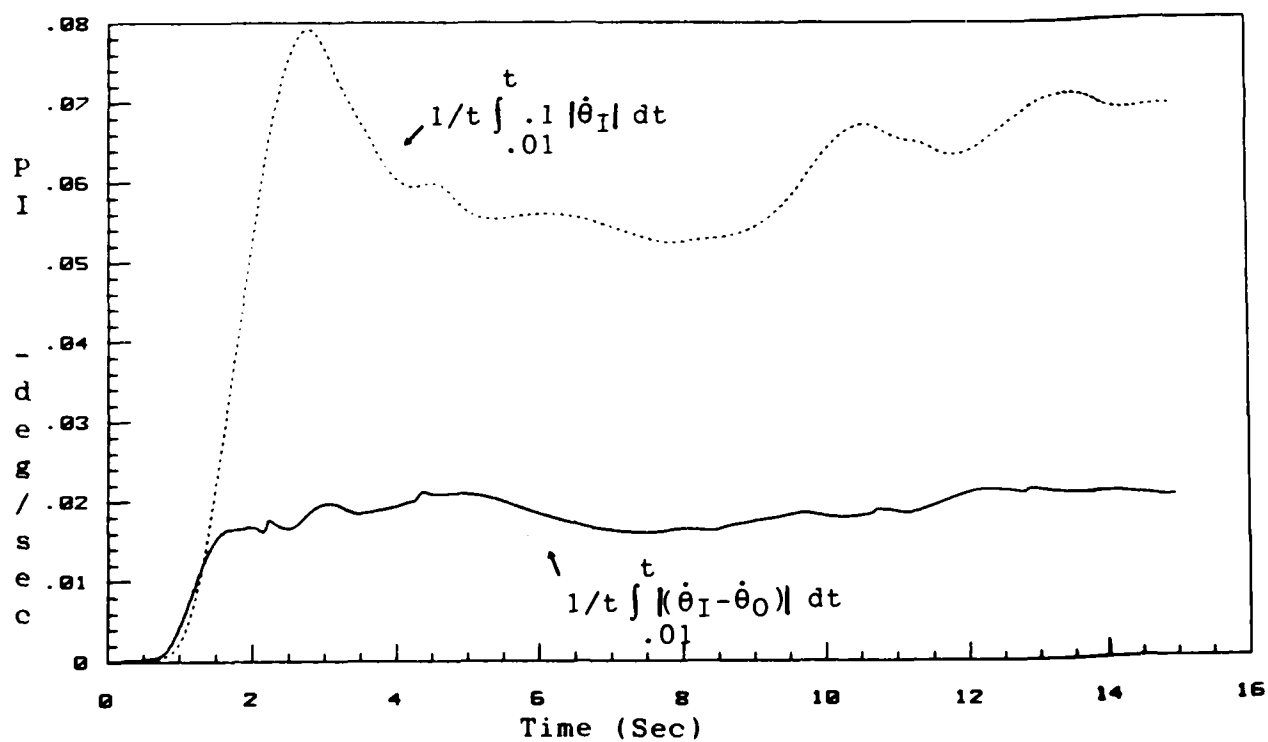
Figure 6-98.   Pitch Rate Performance Criterion
Configuration 8/Operating Point: 38K 0.9M
SIG1=0.1 SIG2=0.7 RHO=0.8

179
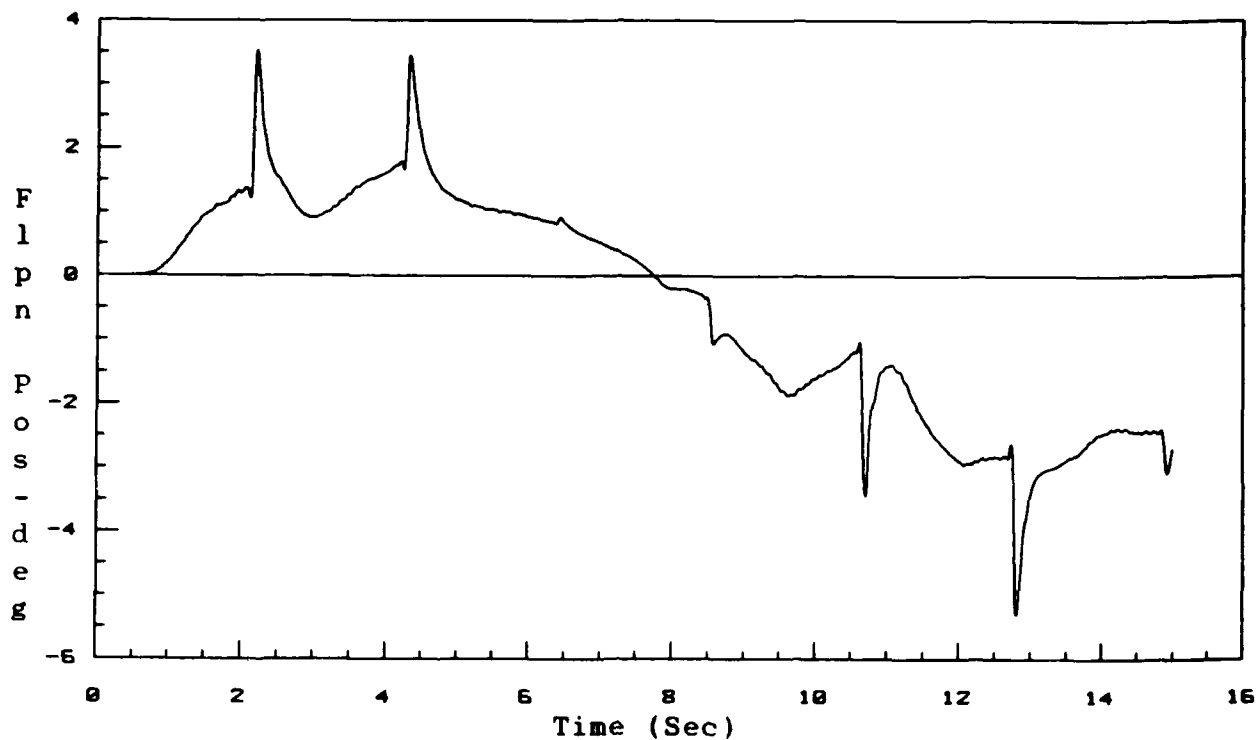
Figure 6-99. Flaperon Position
Configuration 8/Operating Point: 38K 0.9M
SIG1=0.1 SIG2=0.7 RHO=0.8
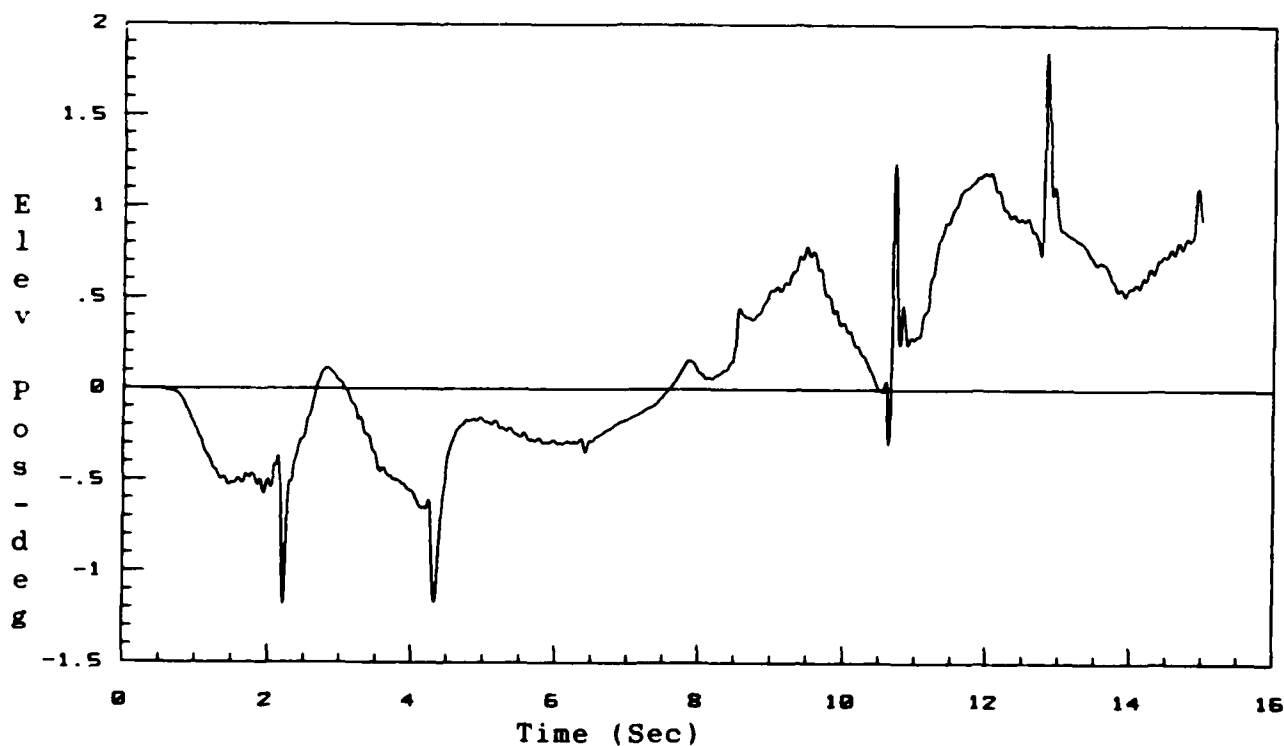
Figure 6-100. Elevator Position
Configuration 8/Operating Point: 38K 0.9M
SIG1=0.1 SIG2=0.7 RHO=0.8
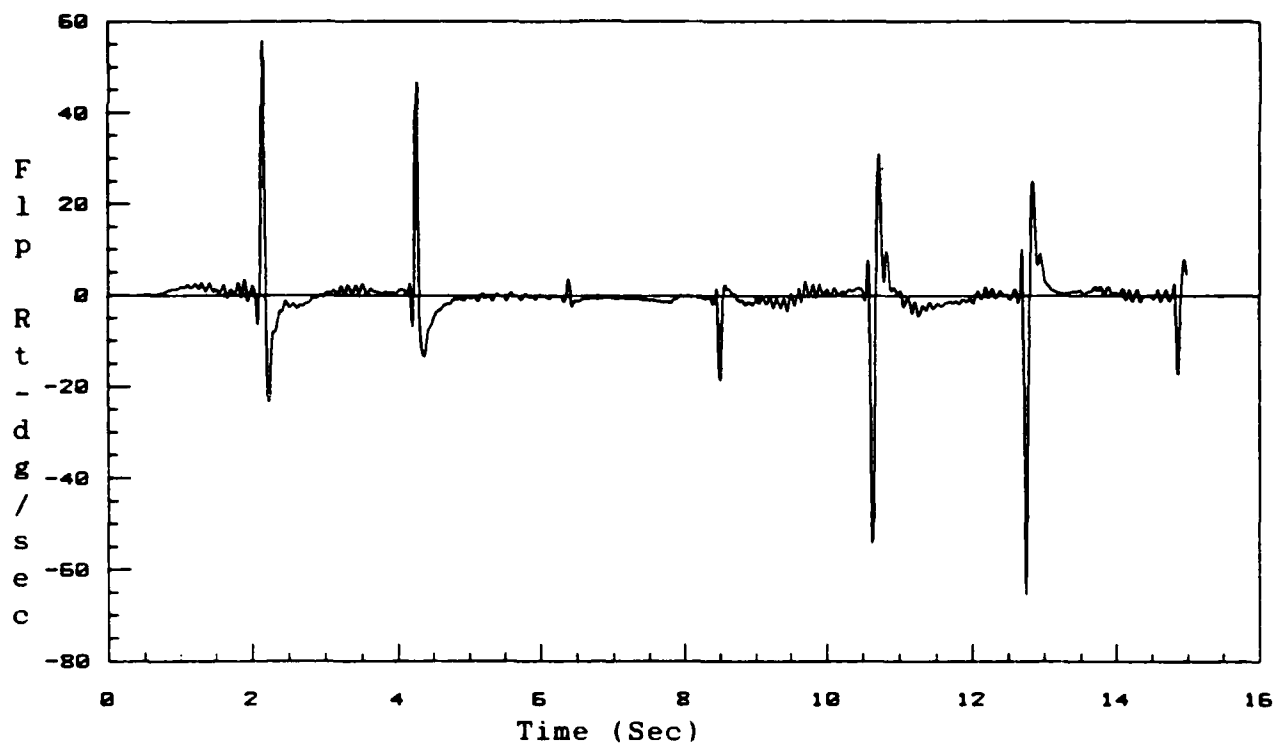
Figure 6-101.   Flaperon Rate
Configuration 8/Operating Point: 38K 0.9M
SIG1=0.1 SIG2=0.7 RHO=0.8
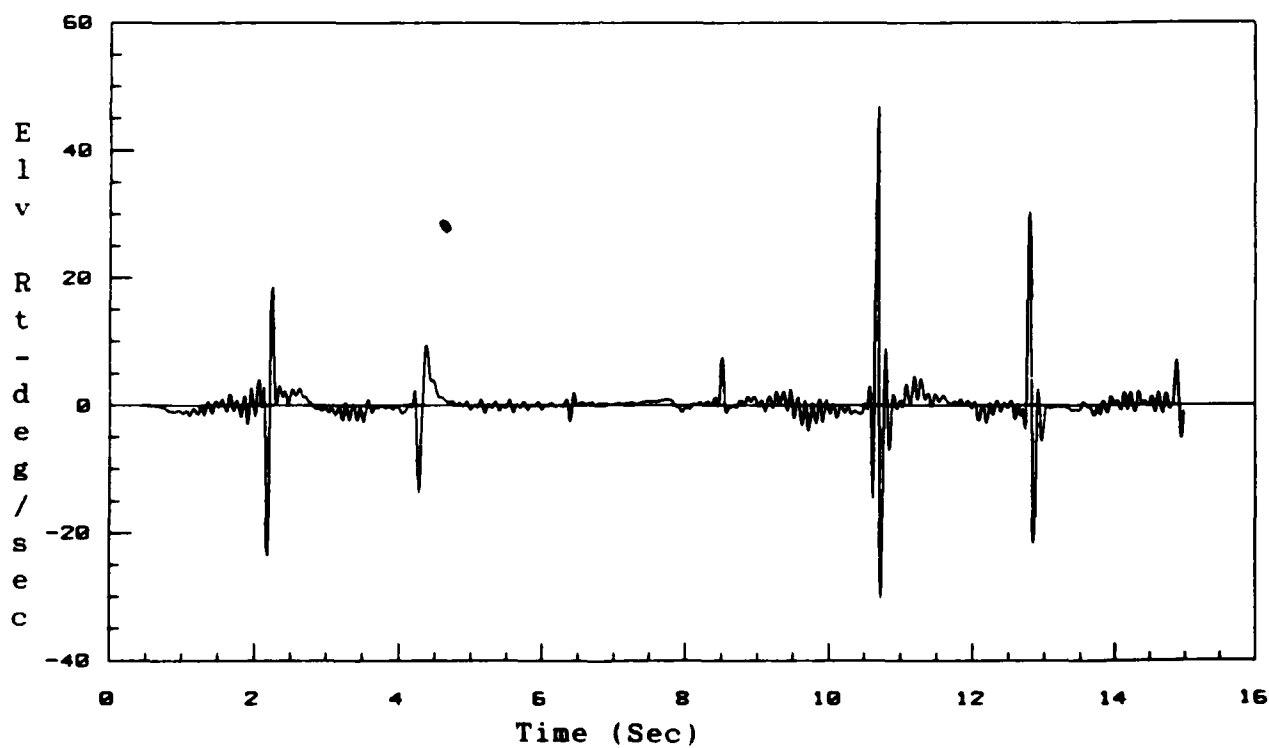
Figure 6-102.   Elevator Rate
Configuration 8/Operating Point: 38K 0.9M
SIG1=0.1 SIG2=0.7 RHO=0.8

Table 6-15

Sensor Noise Data
(units are degrees)

Measured Quantity	Noise Mean	Variance
q	0.0	7.438E-8
Θ	0.0	4.886E-7
α	0.0	3.404E-6

the bank of secondary estimators. As a baseline, a simulation without sensor noise was run. The weights associated with each candidate model as well as the prediction error variances are shown in Figures 6-103 through 6-107. From Figure 6-103, it can be seen that the probabilty of the model associated with the 10,000 ft, 0.35 Mach flight con-

Table 6-16

Two-Model Configuration for Noise Consideration

Model	Flight Condition
1	10,000 ft 0.35 Mach
2	10,000 ft 0.50 Mach
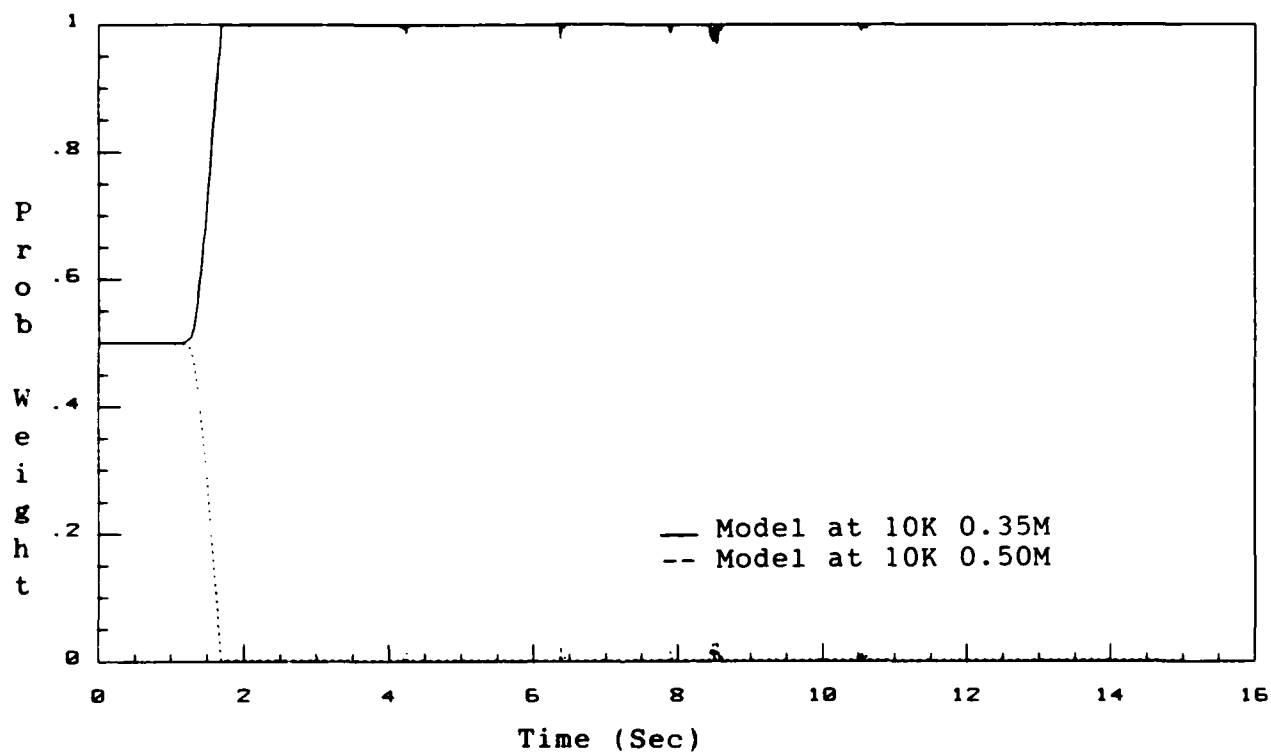
Figure 6-103.   Model Probability Weightings
Operating Point: 10K .35M

183
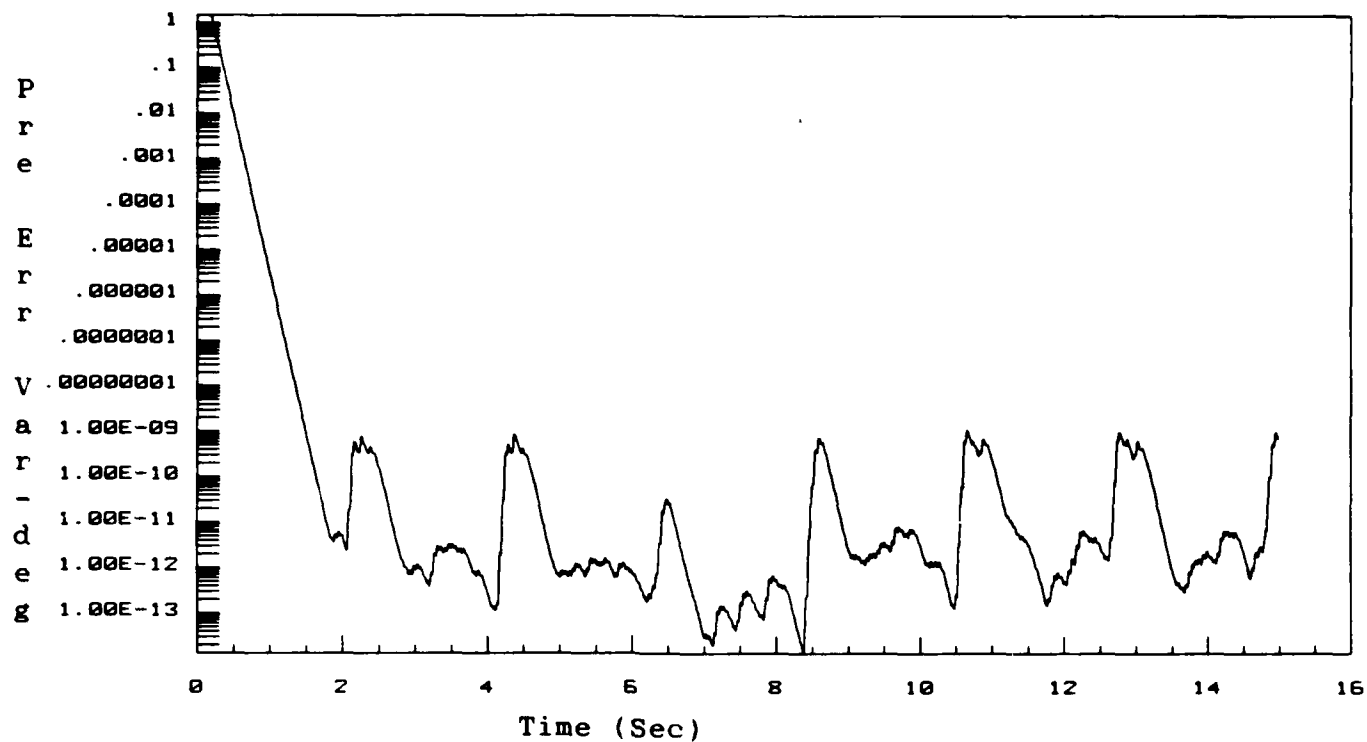
Figure 6-104.   Prediction Error Variance (1,1) for Model 1
Operating Point: 10K 0.35M
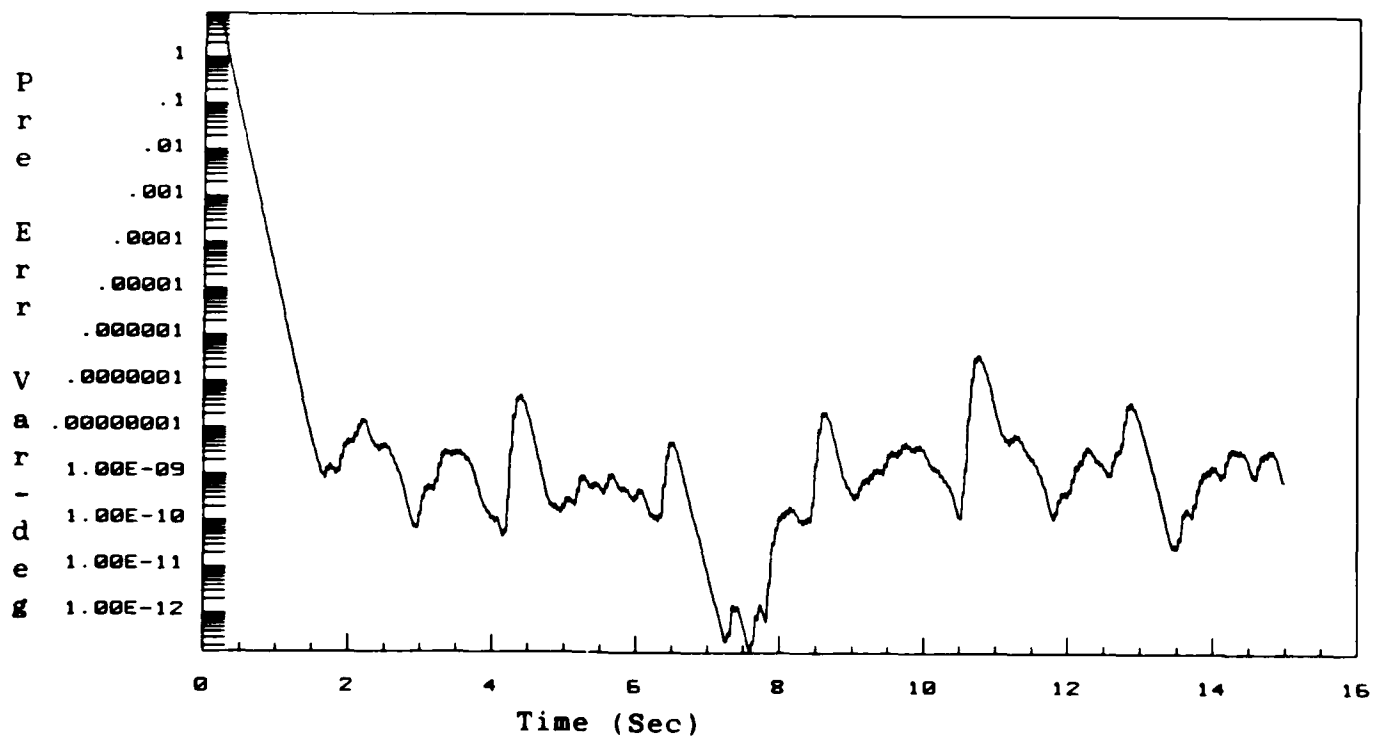
Figure 6-105.   Prediction Error Variance (2,2) for Model 1
Operating Point: 10K 0.35M

184
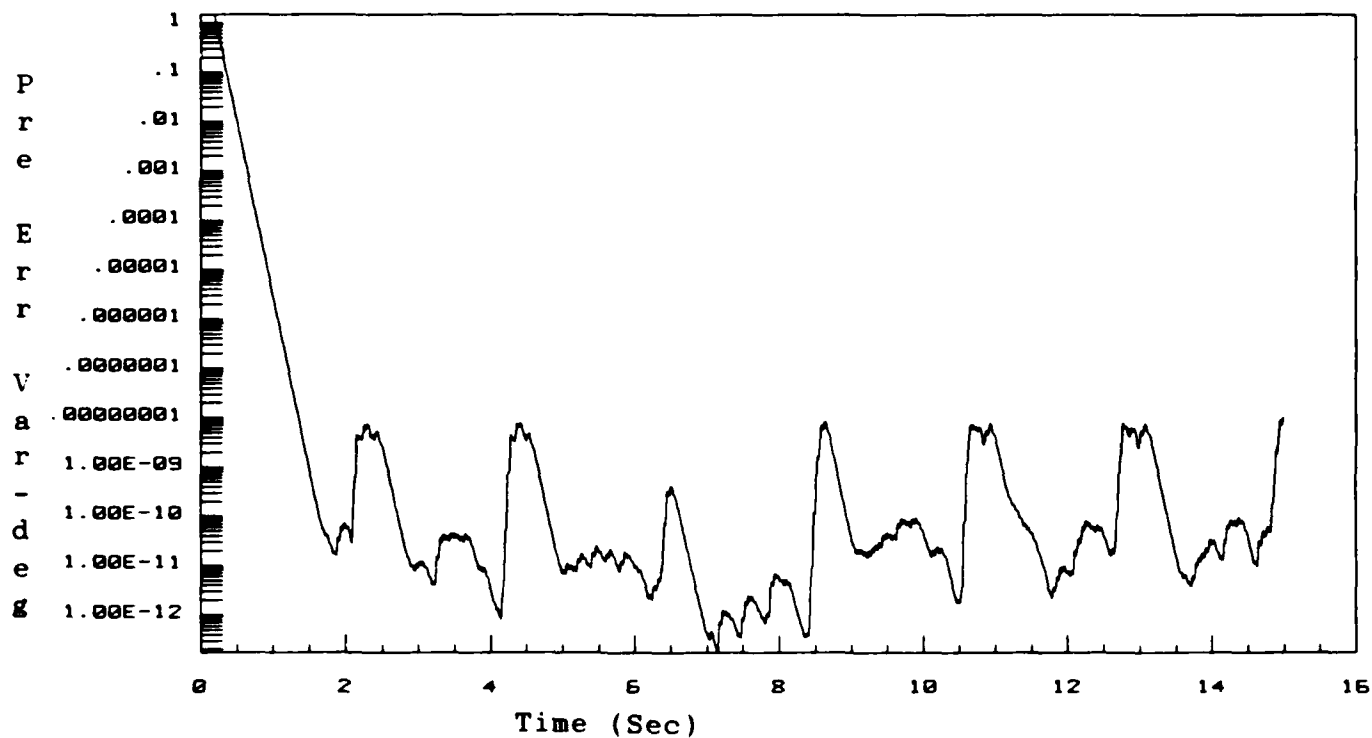
Figure 6-106.   Prediction Error Variance (1,1) for Model 2
              Operating Point: 10K 0.35M
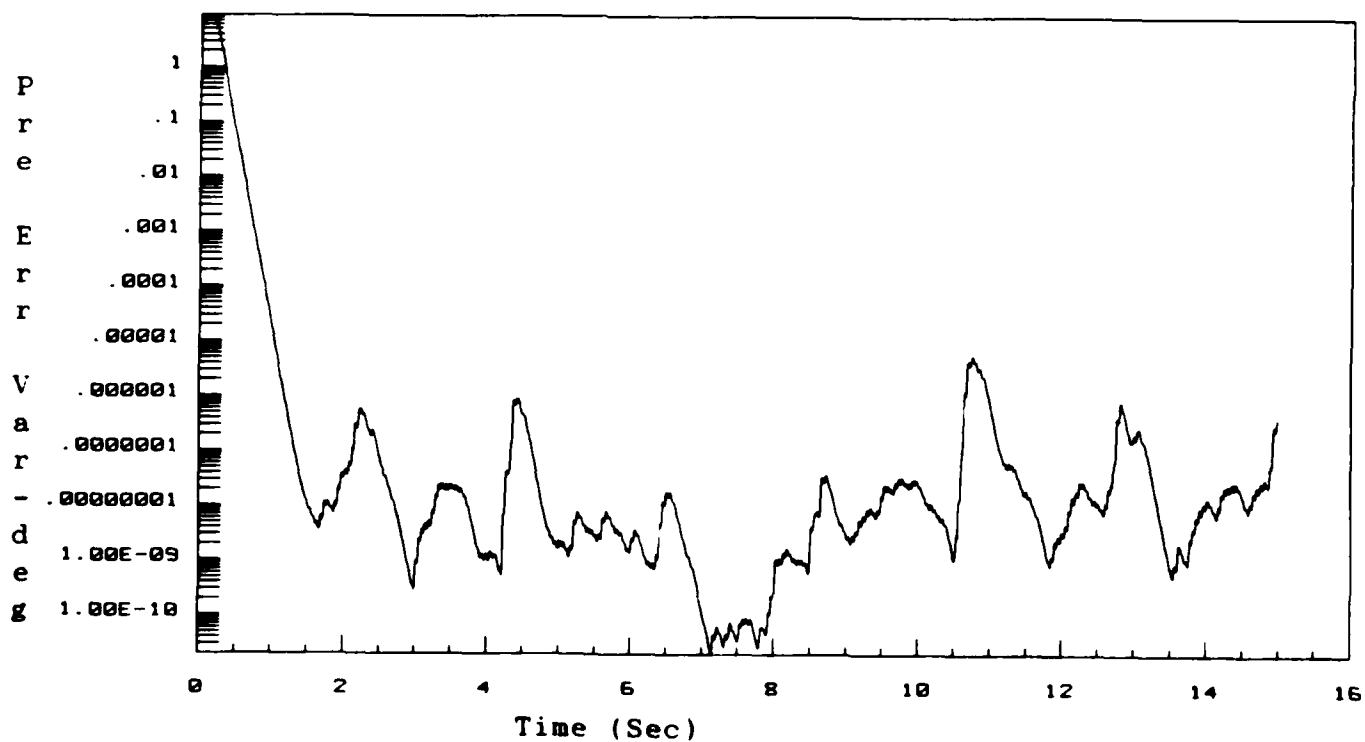
Figure 6-107.   Prediction Error Variance (2,2) for Model 2
              Operating Point: 10K 0.35M

185

figuration is very high. In comparing the prediction error variances for model 1 and model 2, Figures 6-104 through 6-107 show that the variances associated with model 1 are smaller, indicating that it is the better of the two models.

Adding the sensor noise levels as given in Table 6-15 and running a simulation for the configuration in Table 6-16 resulted in the data presented on Figures 6-108 through 6-112. The performance of the multiple model algorithm as shown on the probability curve of Figure 6-108 is very similar to that of Figure 6-103 (same conditions with no noise). The prediction error variances on Figures 6-109 through 6-112 have responses that are very similar to the no noise case, but are of increased magnitude. Figures 6-113 through 6-117 show a simulation that was performed with the sensor noise figures set at one-hundred times those shown in Table 6-15. The probability weighting curve shown on Figure 6-113 shows the effect of adding too much sensor noise on the performance of the multiple model algorithm. Instead of model 1 being selected as the correct model with a probability of almost one, a substantial contribution of model 2 is now present. The reason for this can be seen by comparing the prediction error variances as shown in Figures 6-114

186
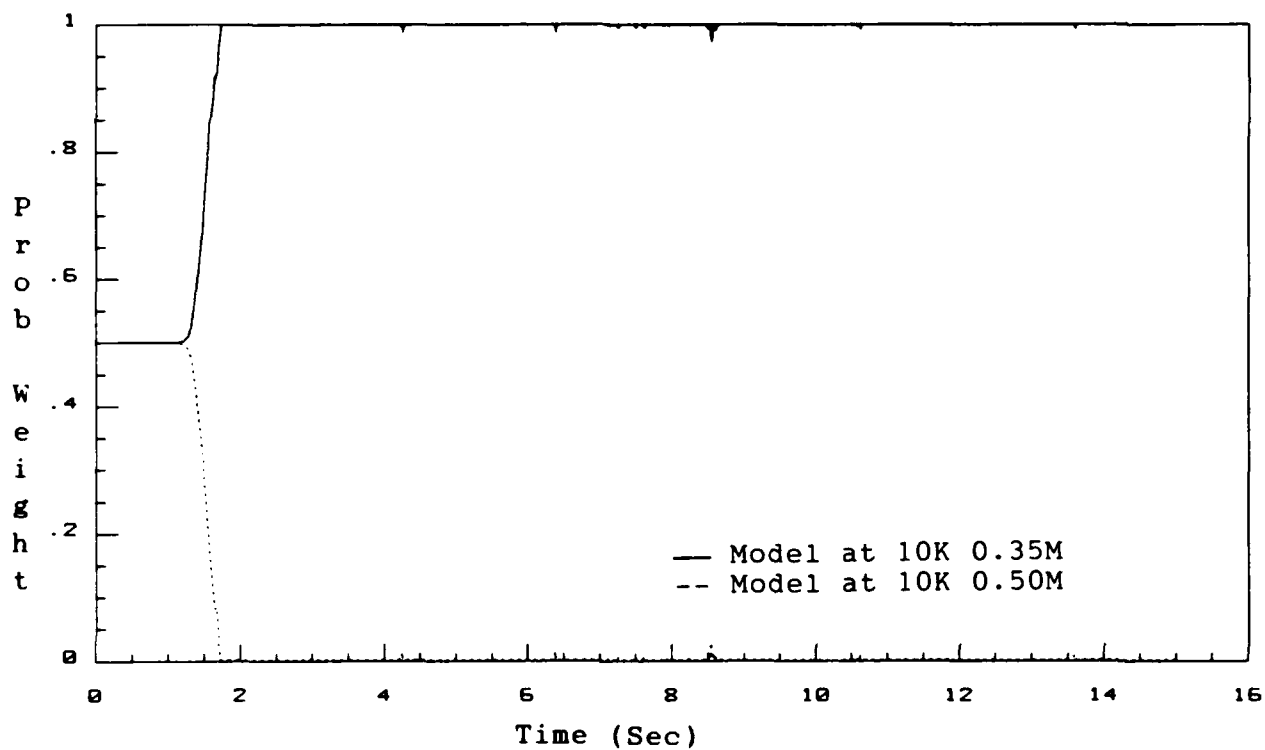
Figure 6-108. Model Probability Weightings
Sensor Noise/Operating Point: 10K 0.35M

187
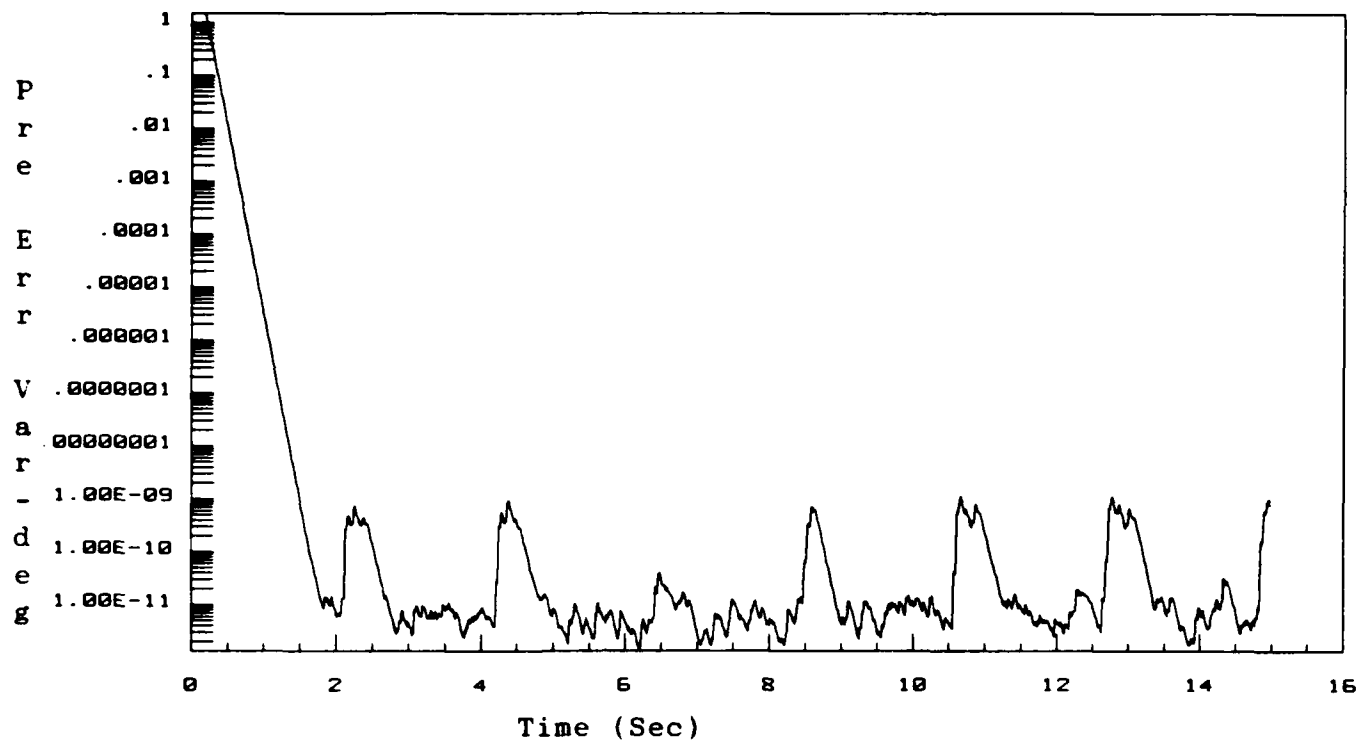
Figure 6-109. Prediction Error Variance (1,1) for Model 1
Sensor Noise/Operating Point: 10K 0.35M
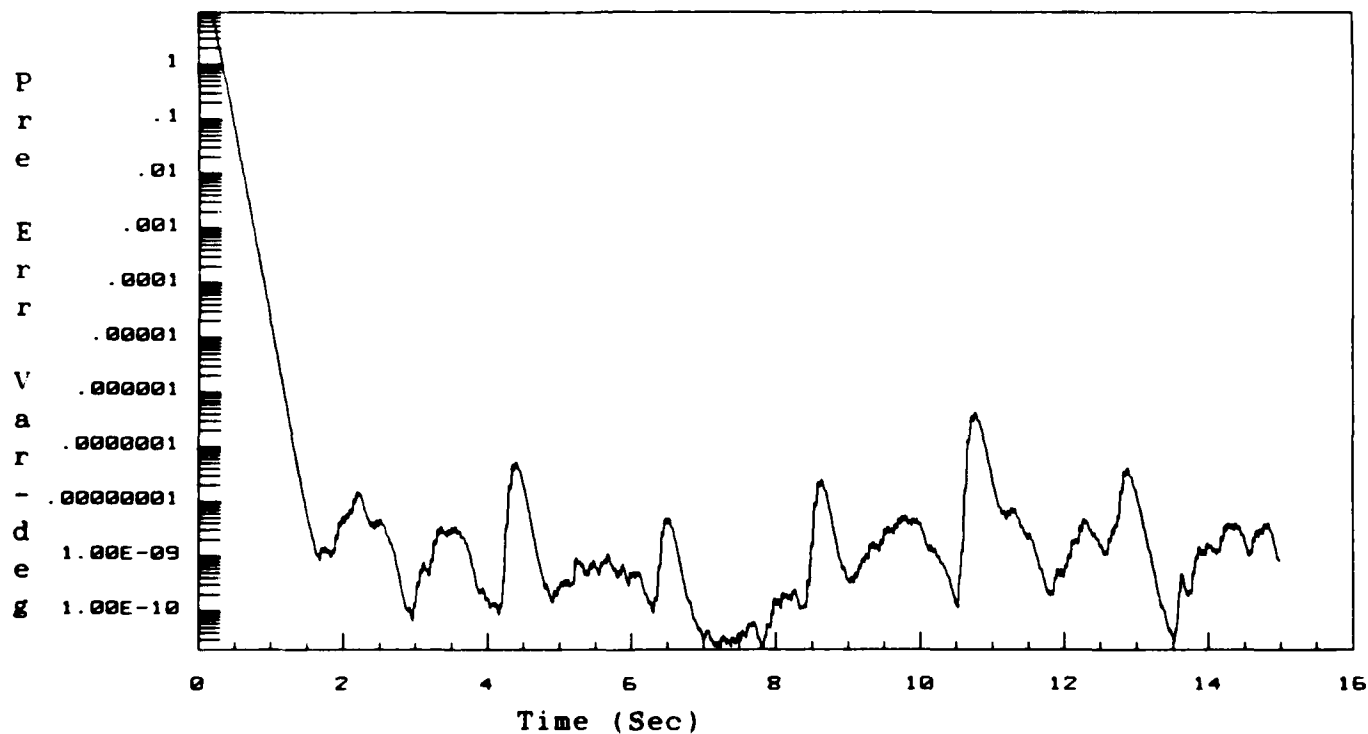
Figure 6-110.   Prediction Error Variance (2,2) for Model 1
Sensor Noise/Operating Ponit: 10K 0.35M

188
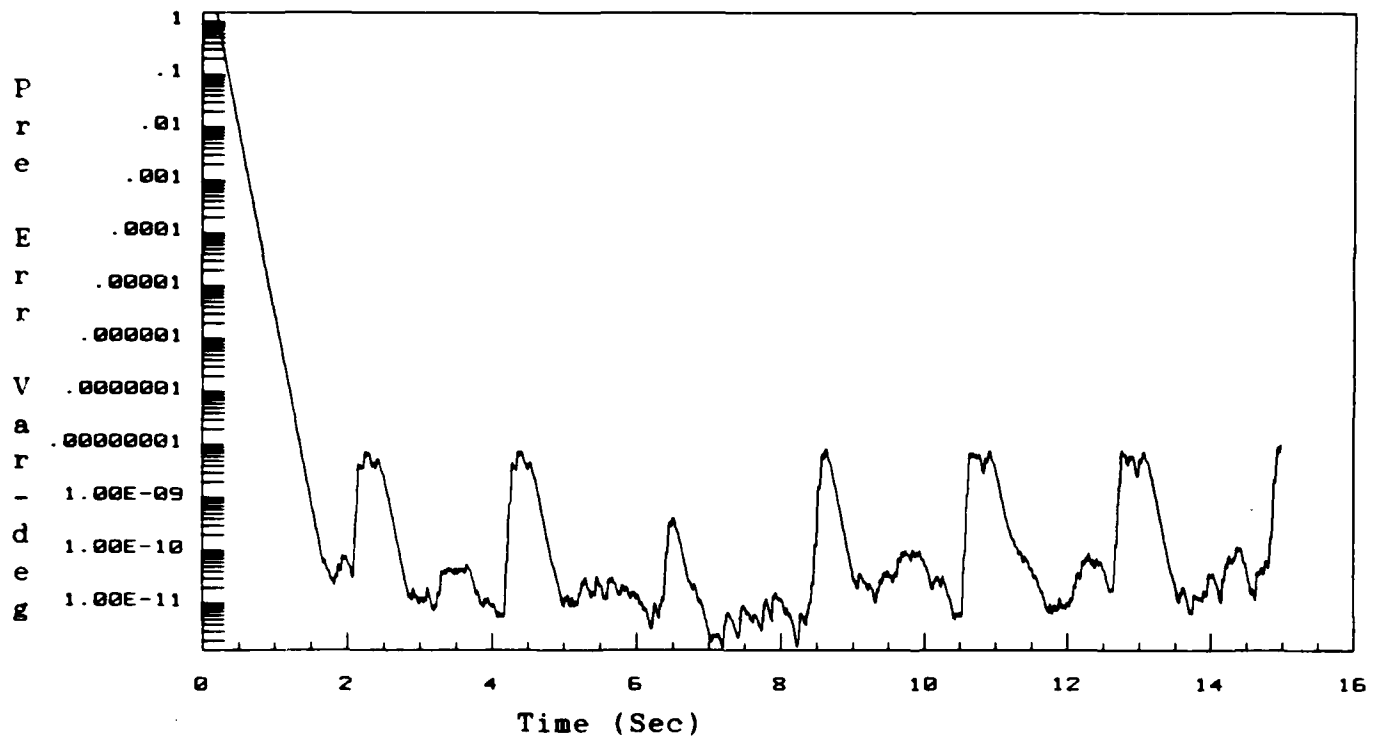
Figure 6-111.   Prediction Error Variance (1,1) for Model
Sensor Noise/Operating Point: 10K 0.35M
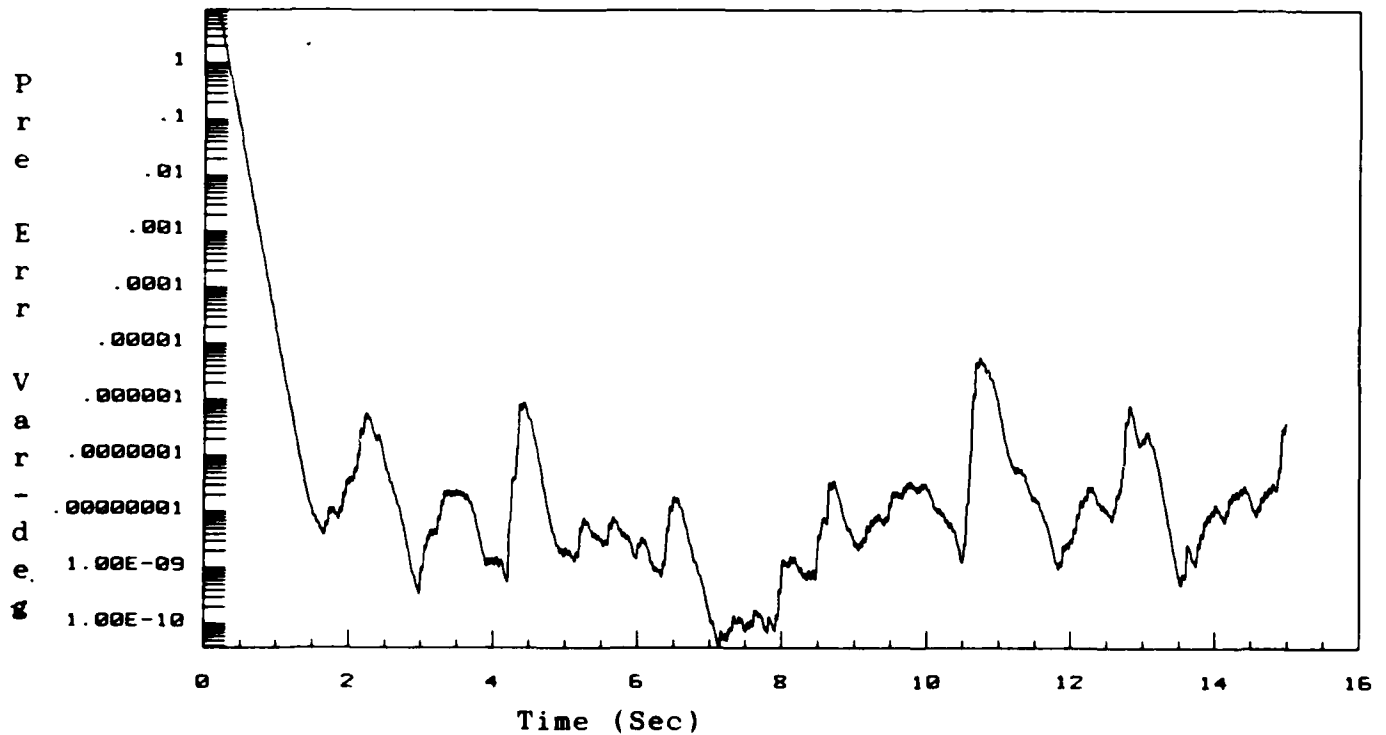
Figure 6-112.   Prediction Error Variance (2,2) for Model 2
Sensor Noise/Operating Point: 10K 0.35M

189
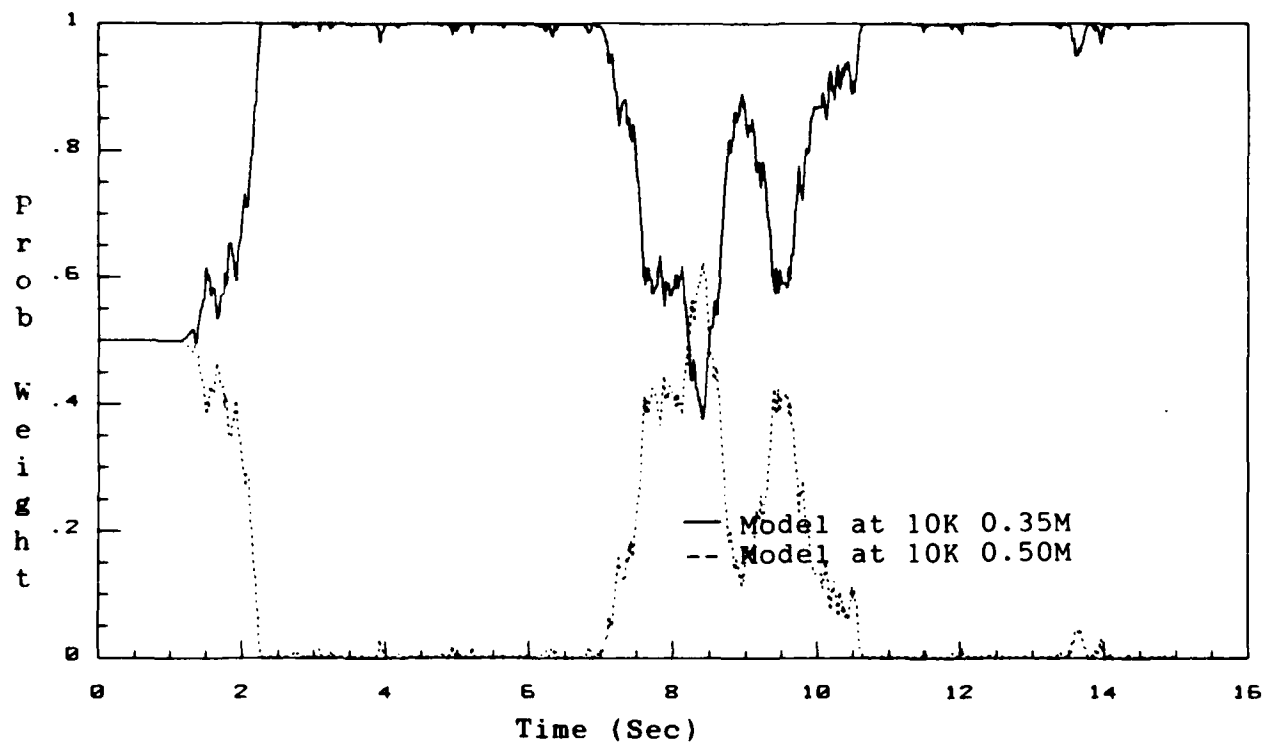
Figure 6-113.   Model Probability Weightings
Sensor Noise(*100)/Operating Point: 10K 0.35M
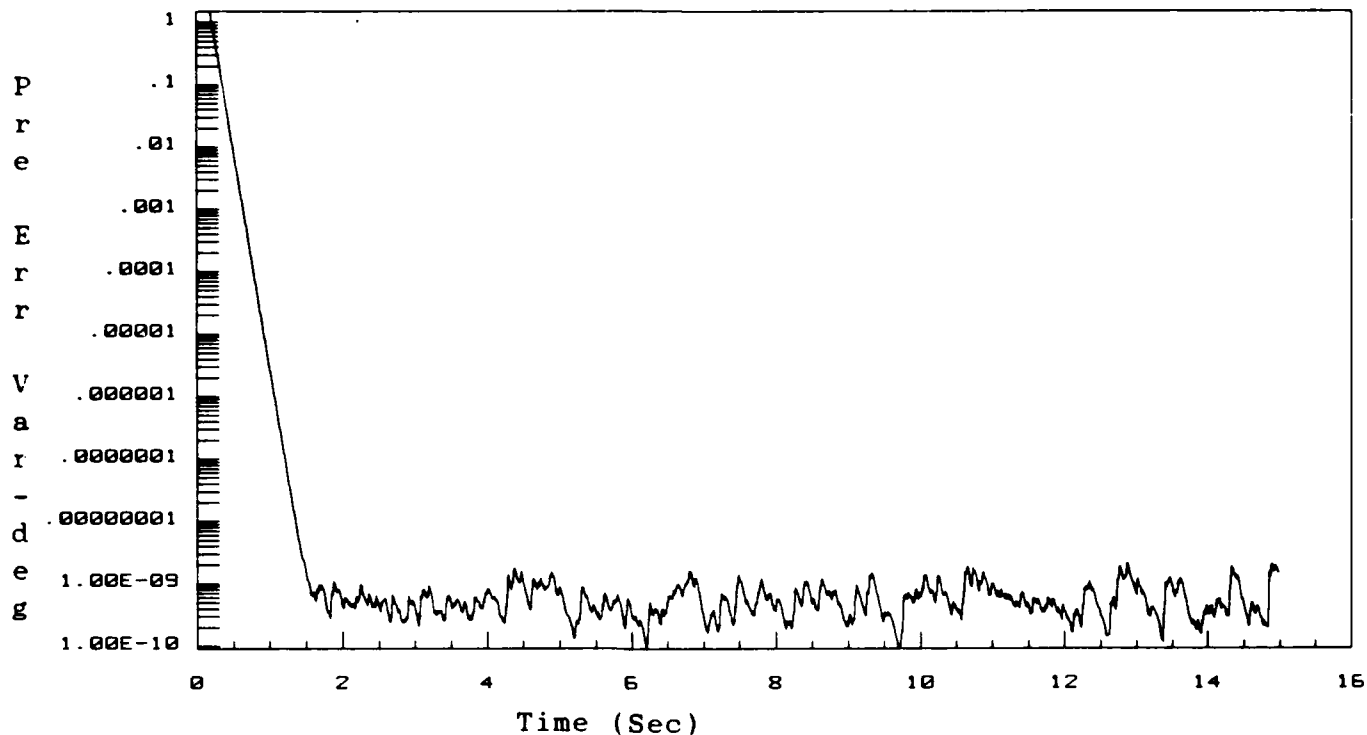
Figure 6-114. Prediction Error Variance (1,1) for Model 1
Sensor Noise(*100)/Operating Point: 10K 0.35M
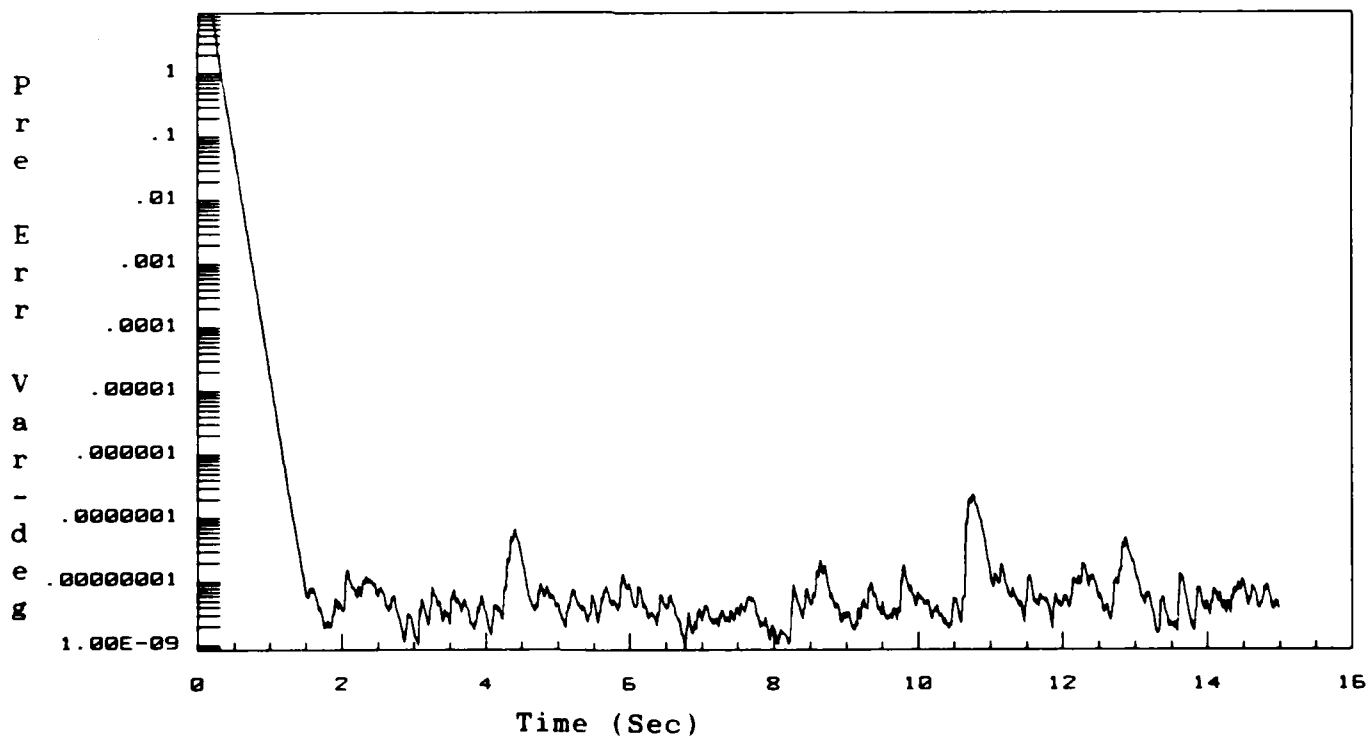
Figure 6-115. Prediction Error Variance (2,2) for Model 1
Sensor Noise(*100)/Operating Point: 10K 0.35M

191
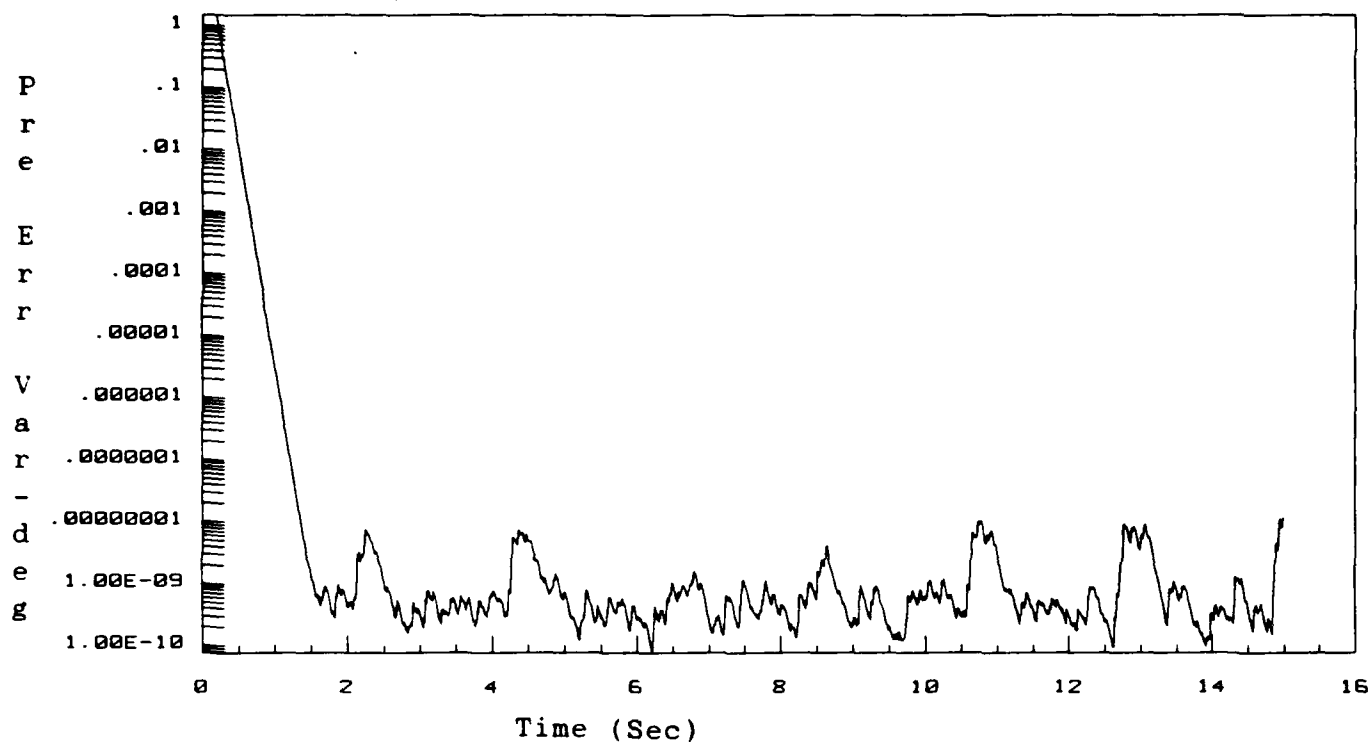
Figure 6-116.   Prediction Error Variance (1,1) for Model 2
              Sensor Noise(*100)/Operating Point: 10K 0.35M
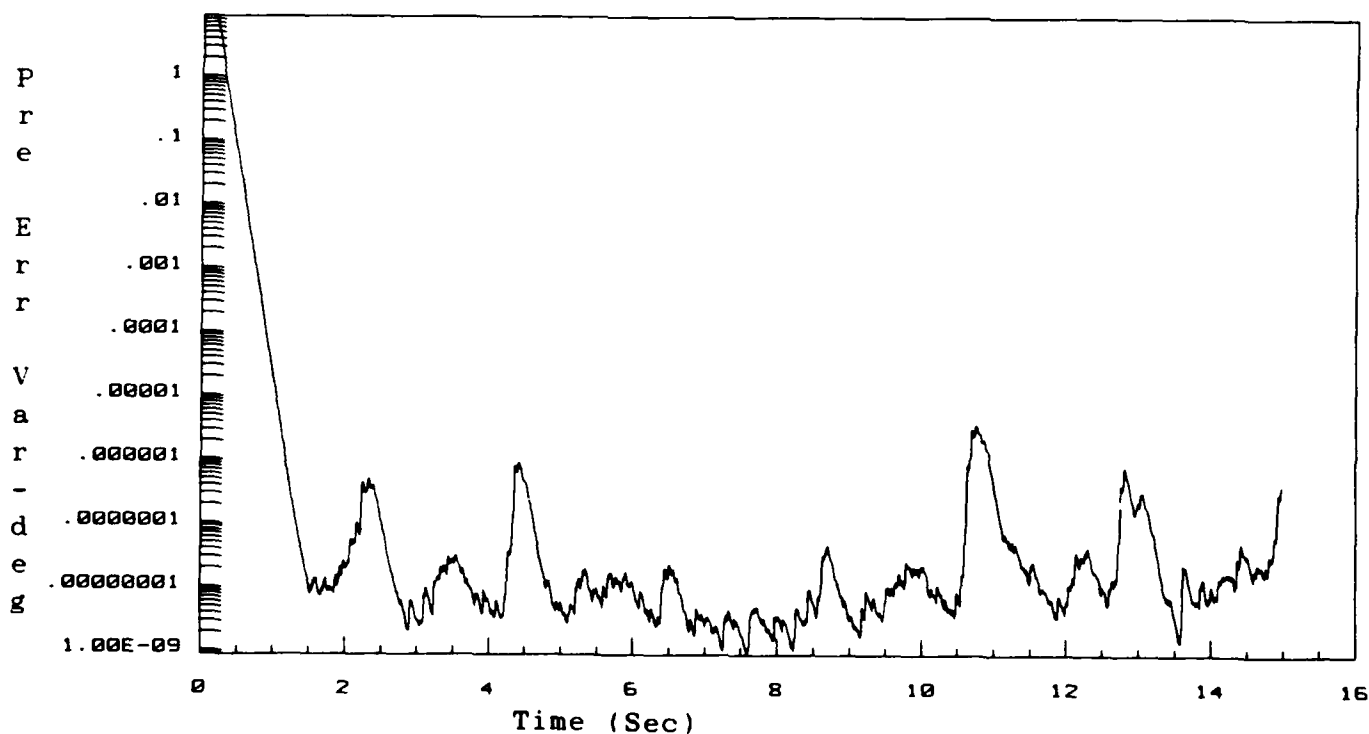
Figure 6-117.   Prediction Error Variance (2,2) for Model 2
              Sensor Noise(*100)/Operating Point: 10K 0.35M

192

through 6-117. By comparing Figures 6-114 and 6-116 (pre-diction error variance for pitch rate for models 1 and 2 respectively), one can see that the variances are very similar for the time of 7 through 10 seconds. Comparing Figure 6-115 to 6-117 (prediction error variance for flight path for models 1 and 2, respectively), reveals the same effect. This effect can be attributed to the sensor noise being added to the system. The noise is actually masking the residuals, thereby leading to a similarity in prediction error variances and hence to degraded multiple model algorithm performance. Comparison of the prediction error variances of the no-noise case of Figures 6-104 through 6-107 with those of Figures 6-114 through 6-117 shows clearly that the addition of sensor noise can mask the residuals, and if sufficiently high noise is added, the prediction error variances will all have the same relative responses. This similarity of response will result in degraded performance by the multiple model algorithm in assigning the weighting factors to the proper models.

The second two-model configuration evaluated is shown in Table 6-17. The two models were spaced farther apart than those of the two-model configuration presented in Table

Table 6-17

Two Model Configuration for Noise Consideration

Model	Flight Condition
1	10,000 ft 0.35 Mach
2	10,000 ft 0.75 Mach

6-16 to ascertain the effects of model spacing in relation to noise resistance. Figures 6-118 through 6-122 present simulation data for the two-model configuration with the actual flight condition set at 10,000 ft, 0.35 Mach. Figure 6-118 shows a very high probability associated with model 1, which is the model associated with the 10,000 ft, 0.35 Mach flight condition. Allowing the sensor noise to take on values one-hundred times those presented in Table 6-15 and running a simulation resulted in the data presented on Figures 6-123 through 6-127. The data shows that the probability weighting curve (Figure 6-123) indicates that model 1 is the correct model, as was the case with no noise. A comparison of the prediction error variances for models 1 and 2 (Figures 6-124 through 6-127) shows that the variances associated with model 1 are smaller than those of model 2.

194
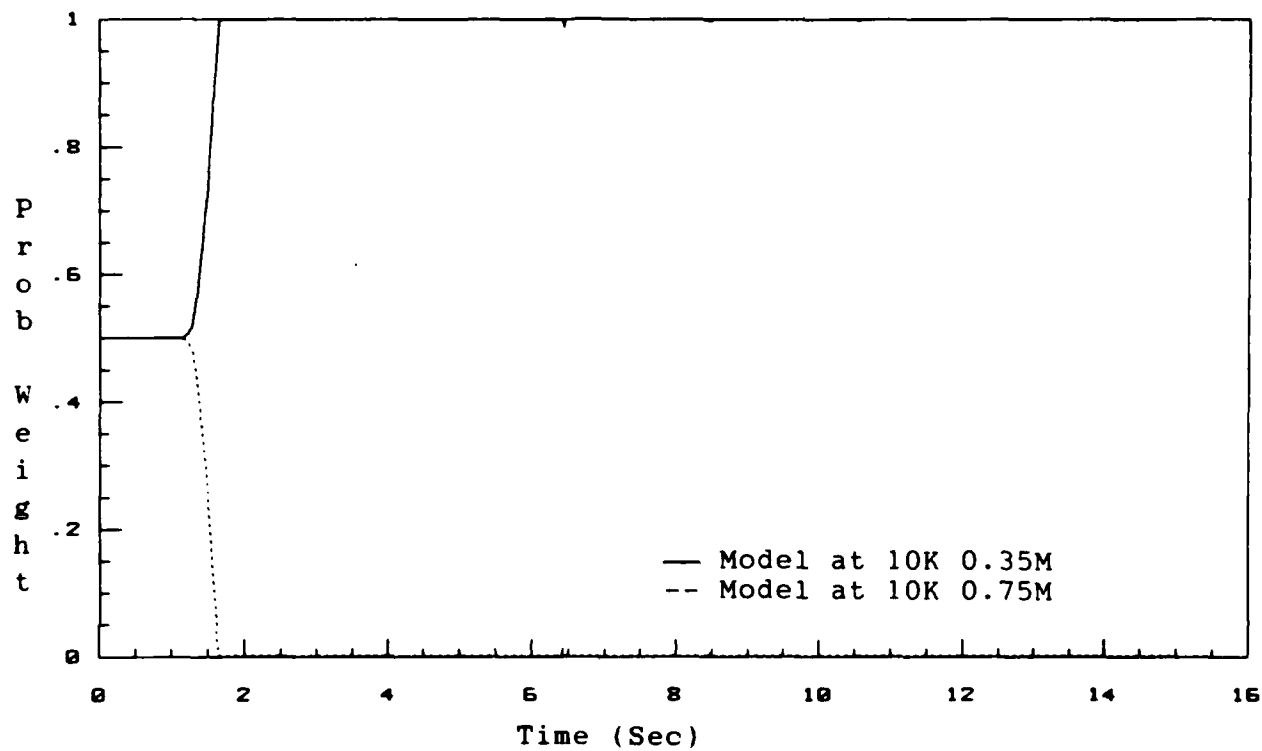
Figure 6-118.   Model Probability Weightings
Operating Point: 10K 0.35M

195
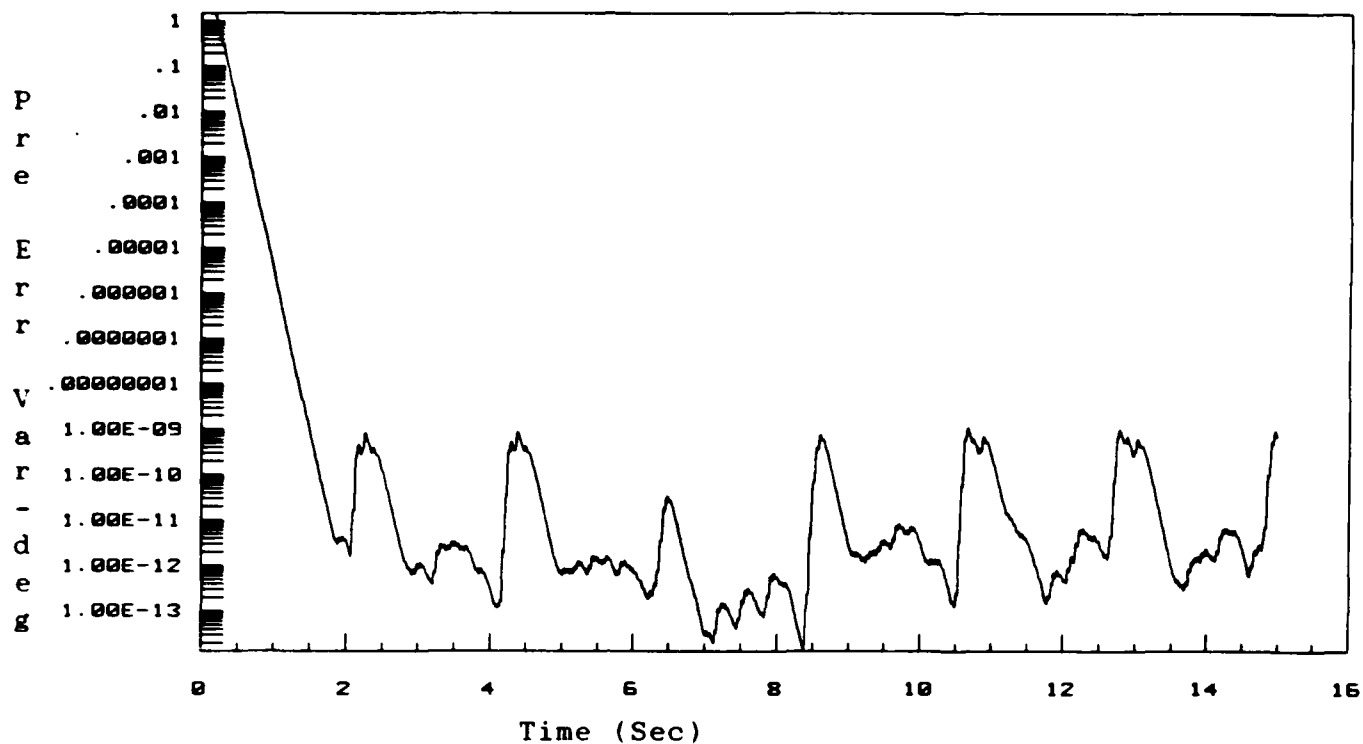
Figure 6-119. Prediction Error Variance (1,1) for Model 1
Operating Point: 10K 0.35M
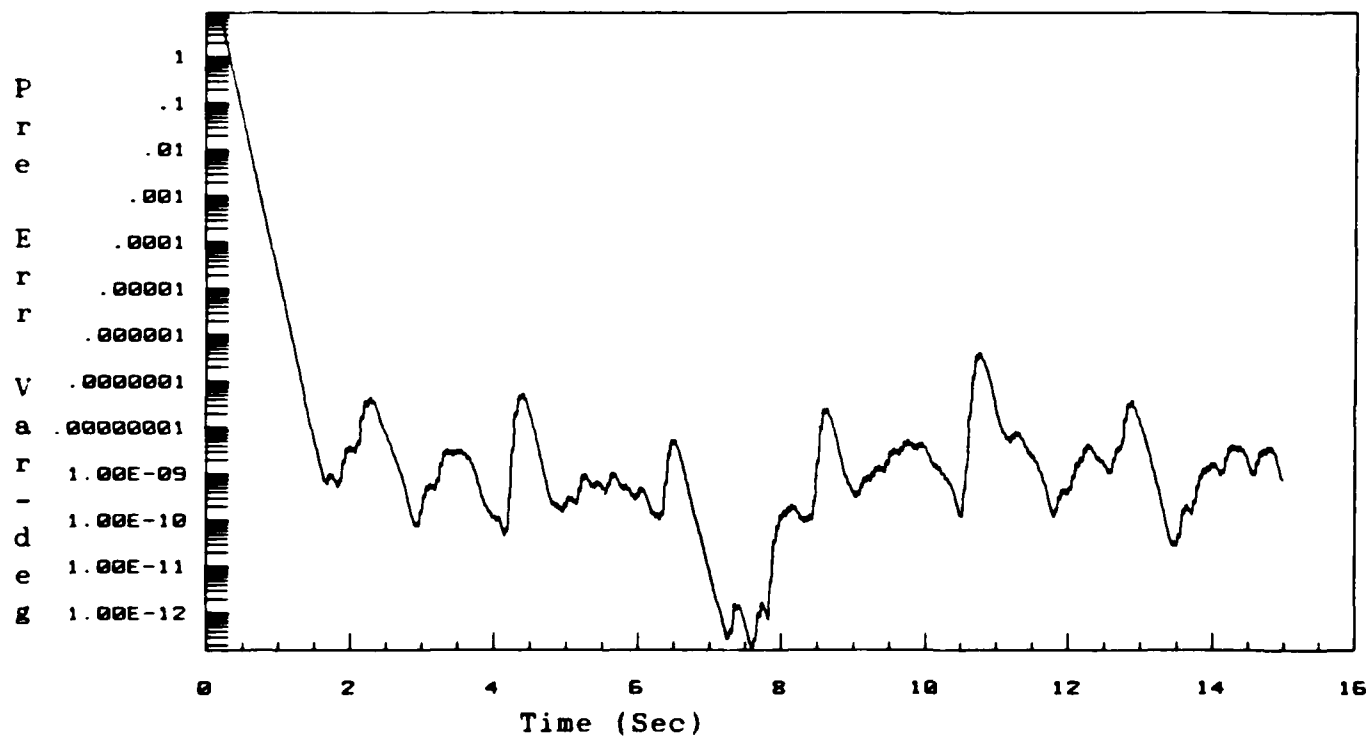
Figure 6-120. Prediction Error Variance (2,2) for Model 1
Operating Point: 10K 0.35M

196
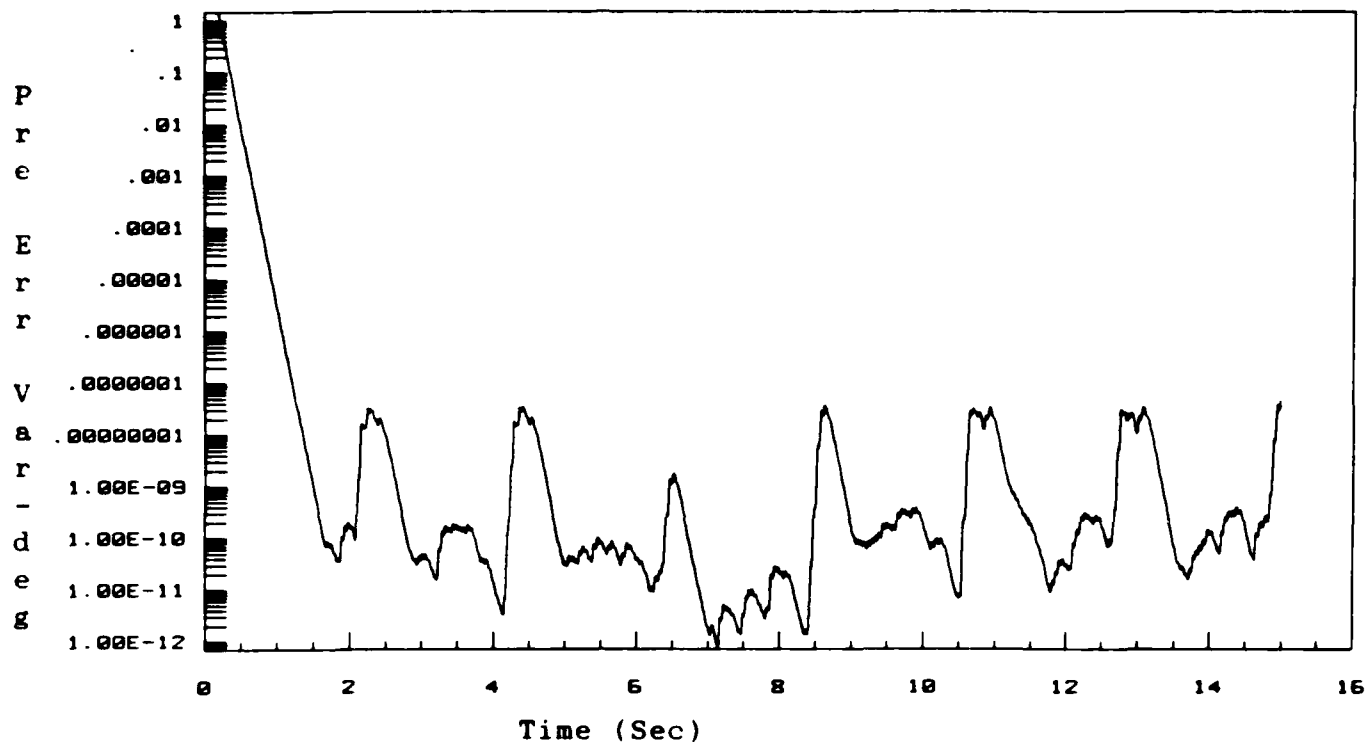
Figure 6-121.   Prediction Error Variance (1,1) for Model 2
Operating Point: 10K 0.35M
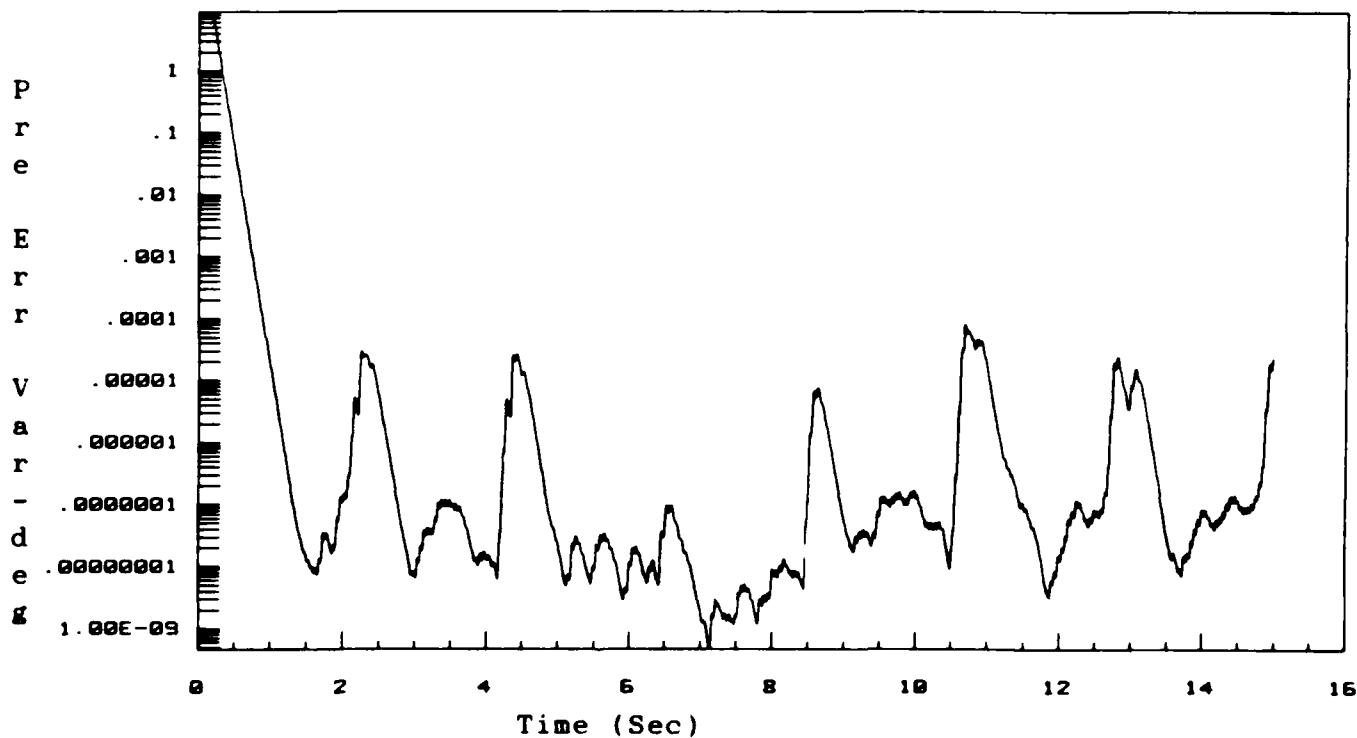
Figure 6-122.   Prediction Error Variance (2,2) for Model 2
Operating Point: 10K 0.35M

197
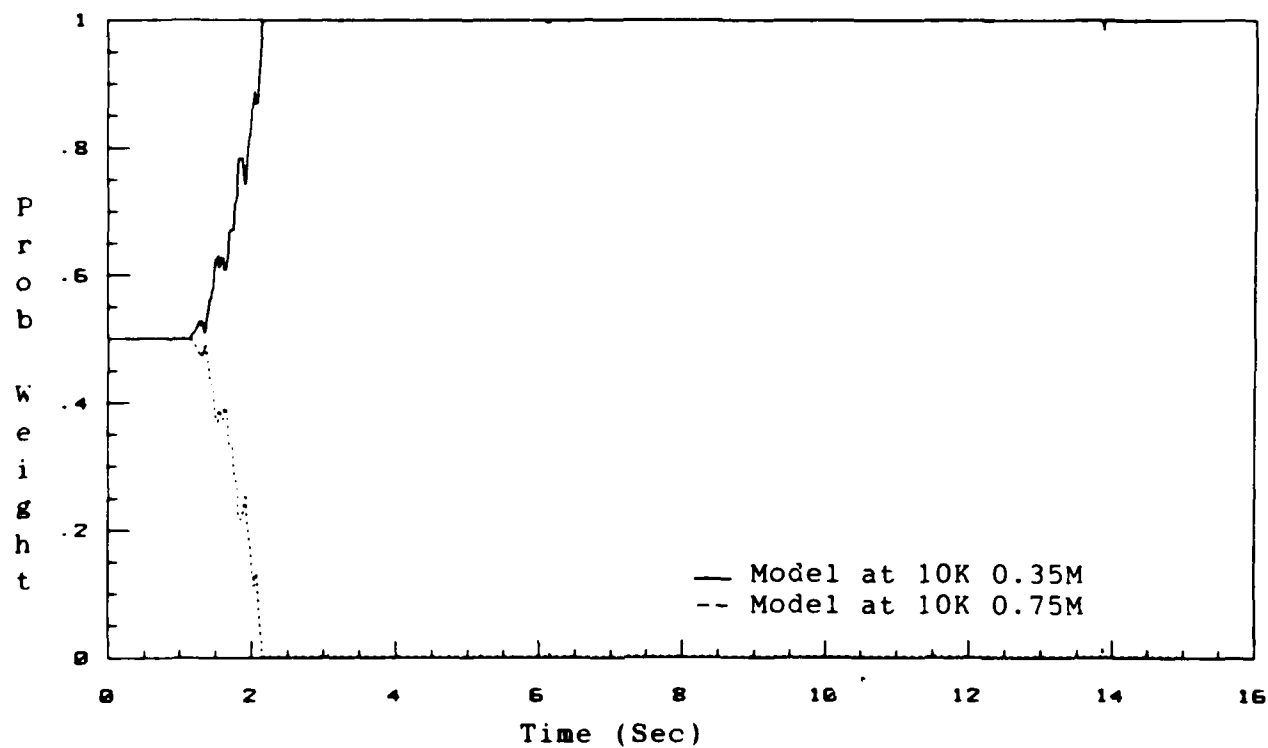
Figure 6-123.   Model Probability Weightings
Sensor Noise(*100)/Operating Point: 10K 0.35M

198
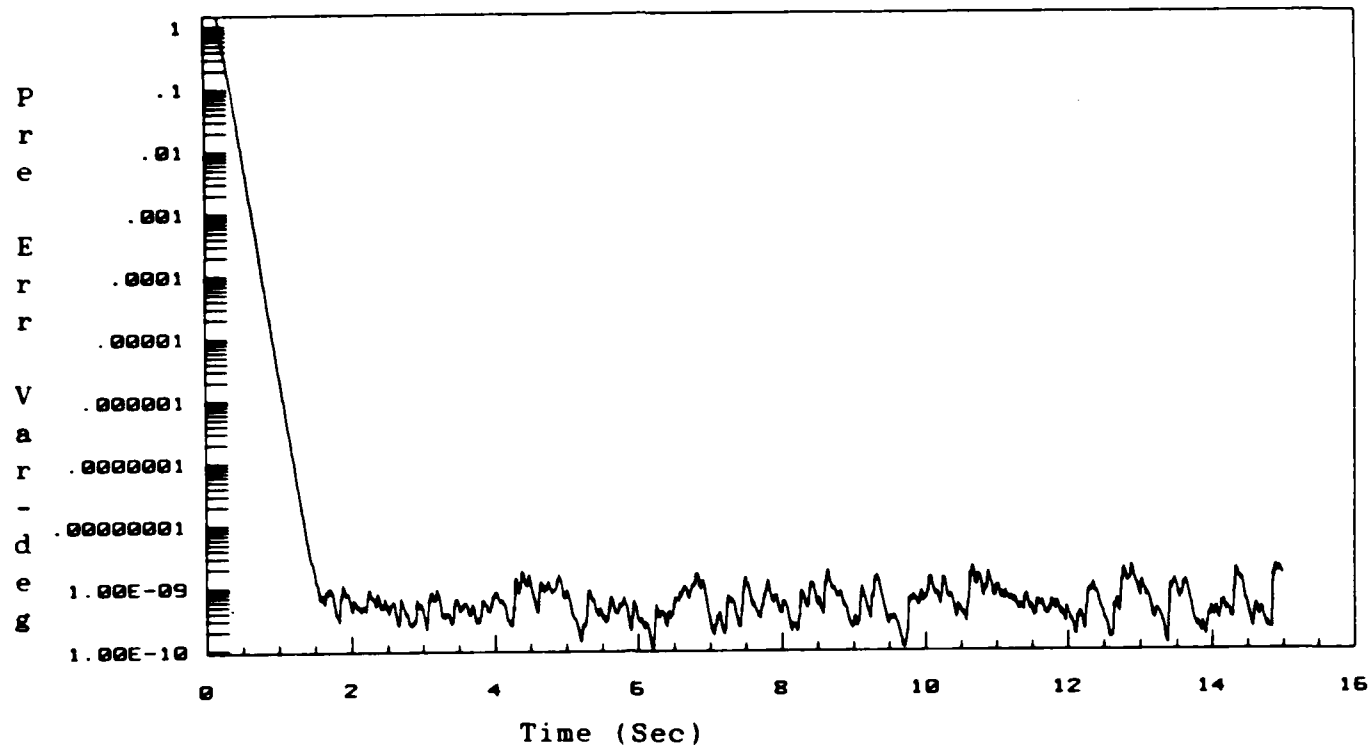
Figure 6-124. Prediction Error Variance (1,1) for Model 1
Sensor Noise(*100)/Operating Point: 10K 0.35M
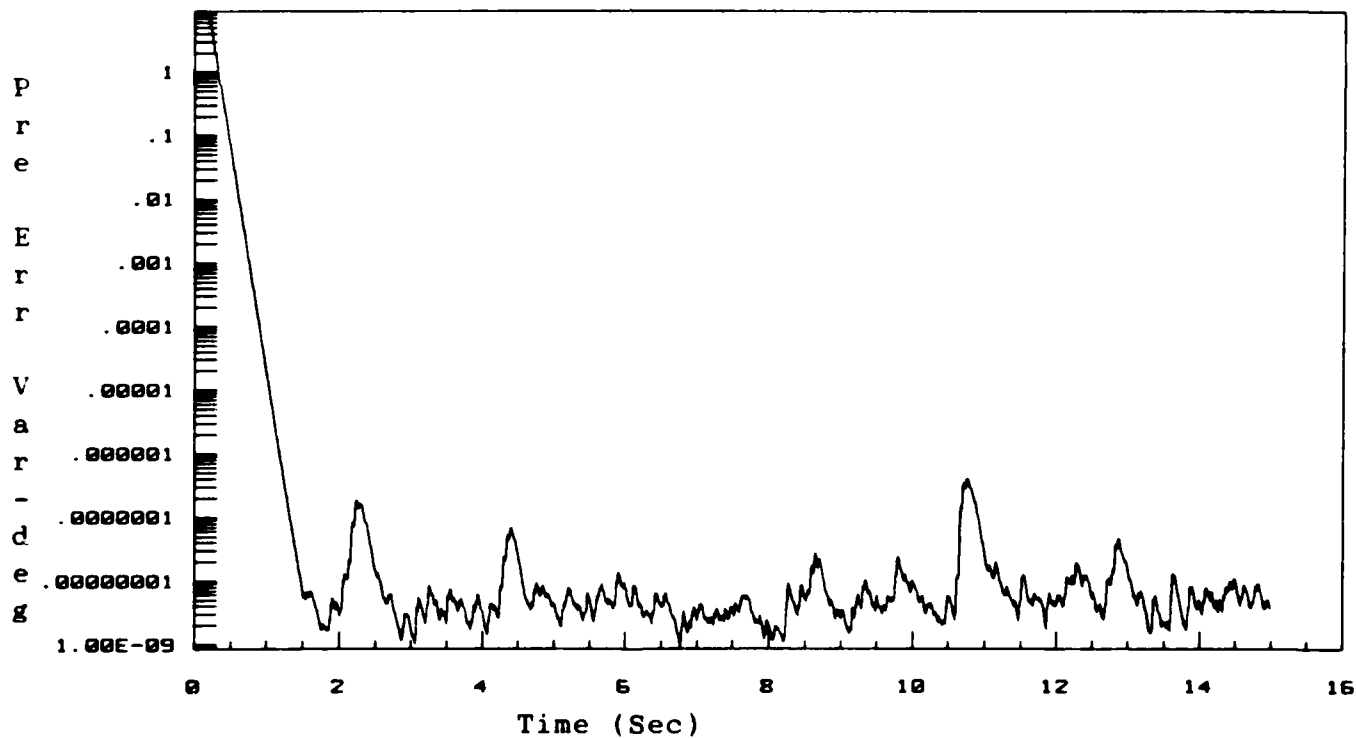
Figure 6-125. Prediction Error Variance (2,2) for Model 1
Sensor Noise(*100)/Operating Point: 10K 0.35M

199
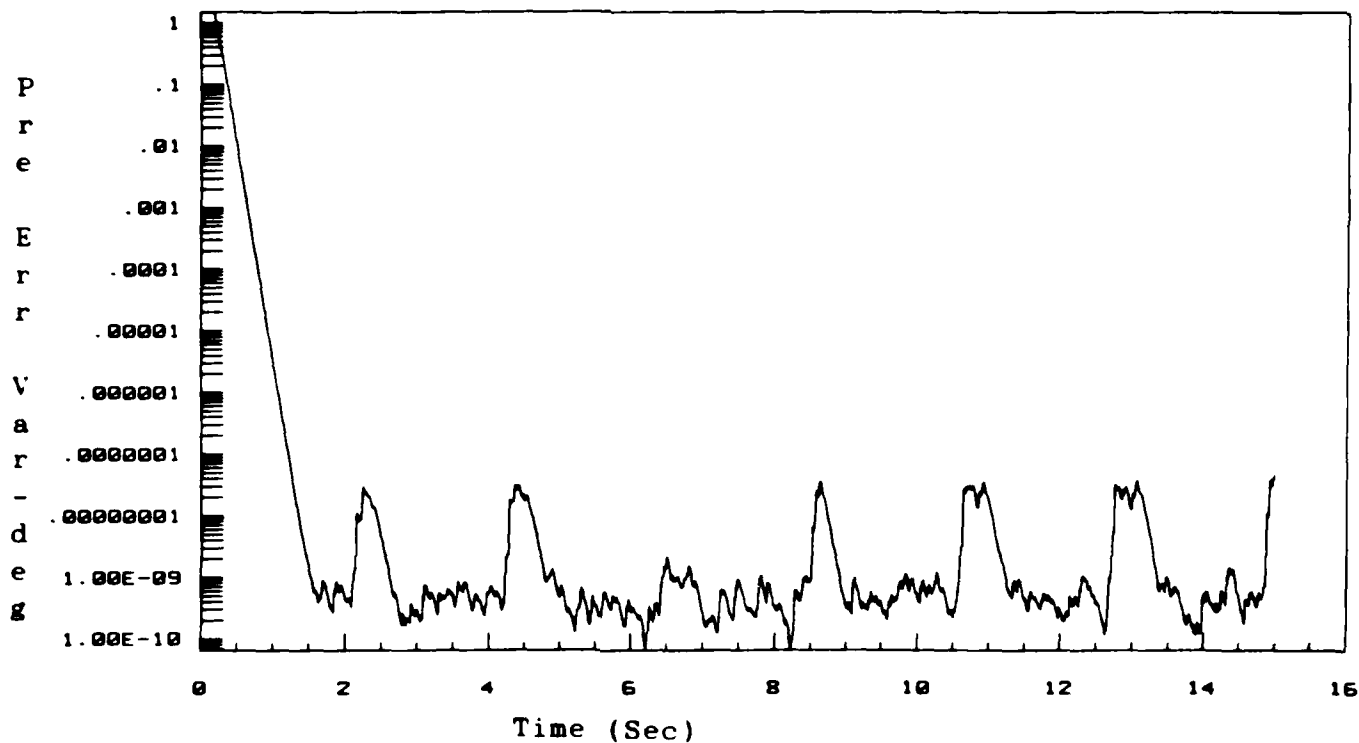
Figure 6-126. Prediction Error Variance (1,1) for Model 2
Sensor Noise(*100)/Operating Point: 10K 0.35M
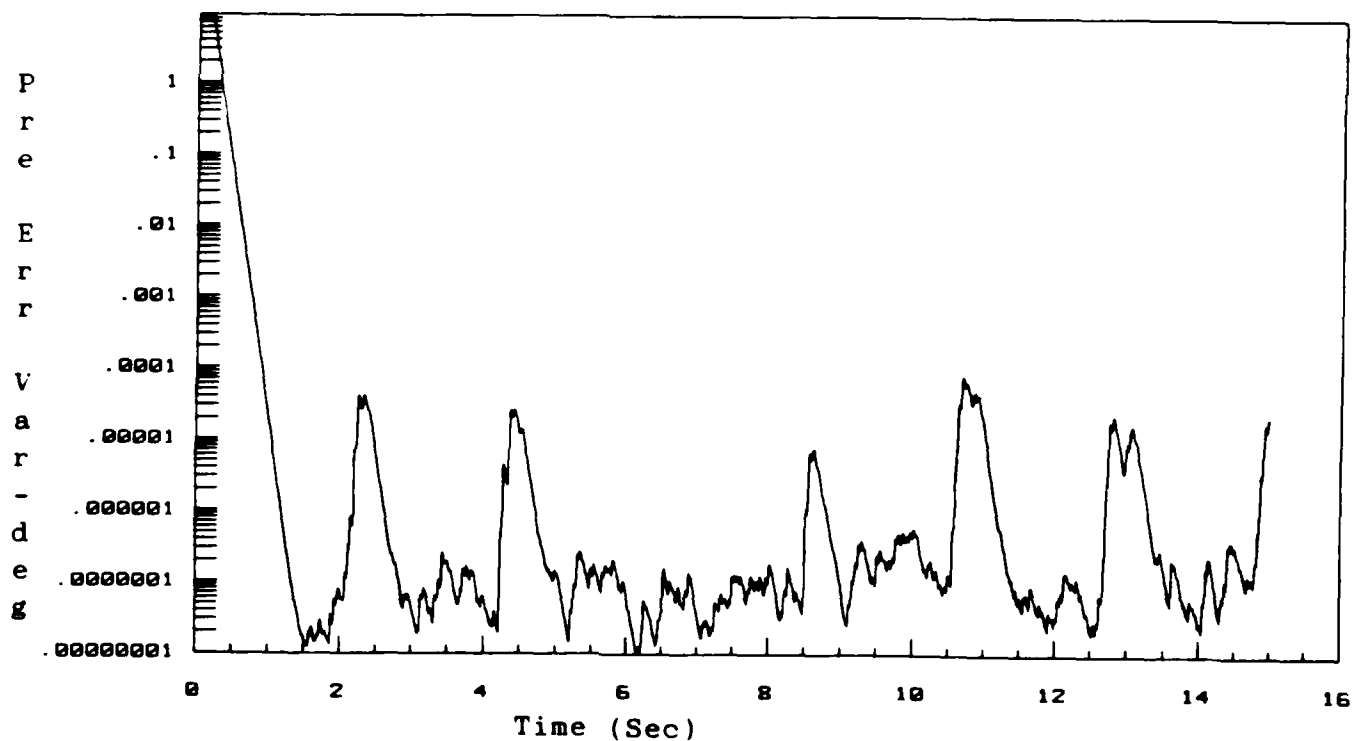
Figure 6-127. Prediction Error Variance (2,2) for Model 2
Sensor Noise(*100)/Operating Point: 10K 0.35M

200

Even with the sensor noise figures increased by a factor of one-hundred, the multiple model algorithm's performance has not been severely degraded, and the correct model has been selected. This is in contrast to the results obtained for the two-model configuration of Table 6-16. For the config- uration of Table 6-16, an increase in the sensor noise figures of one-hundred times resulted in degraded multiple model algorithm performance. The reason for the performance difference between the two-model configurations of Tables 6- 16 and 6-17 is due to the spacing of the models. The models of Table 6-13 are spaced farther apart (in dynamic pressure) than those of Table 6-16 and therefore the difference of the two models as seen in the residuals is more significant. Therefore, the error variance term introduced by a model not being the best fitting model (see Equation (5-9)) is still the dominant term and a difference in the prediction error variance responses is the result. This clearly points out the fact that, the farther apart the models of the multiple model algorithm are placed (from a dynamic pressure stand- point), the more noise resistance is possible.

Following the simulations for the two-model configura- tions, simulations using configuration 8 (see Table 6-9)

201

were run. Recall that configuration 8 was the three-model
configuration that gave the best performance from a perfor-
mance criteria standpoint. The purpose of these simulations
was to see if the performance of three-model configuration
was severely degraded in the presence of realistic sensor
noise. Several flight conditions were selected as operating
points, the first of which was 26,000 ft, and 0.9 Mach. The
data presented on Figures 6-128 through 6-134 are for the
case where no sensor noise was added. The probability
weighting curve (see Figure 6-128) shows that models 2 and 3
contribute significantly to the solution of finding the
correct model. Figures 6-129 through 6-134 show the predic-
tion error variances for the respective models. Figure 6-
135 shows the probability weighting curve for the sensor
noise values presented in Table 6-15. From this figure, it
can be seen that although models 2 and 3 are still the most
heavily weighted models, model 3 has more weight than it did
in the simulation without noise. Further increasing the
sensor noise to one-hundred times the values in Table 6-15
results in the data on Figures 6-136 through 6-142. The
probability weighting curve (see Figure 6-136) is now dras-
tically different from the case with no noise, and model 3
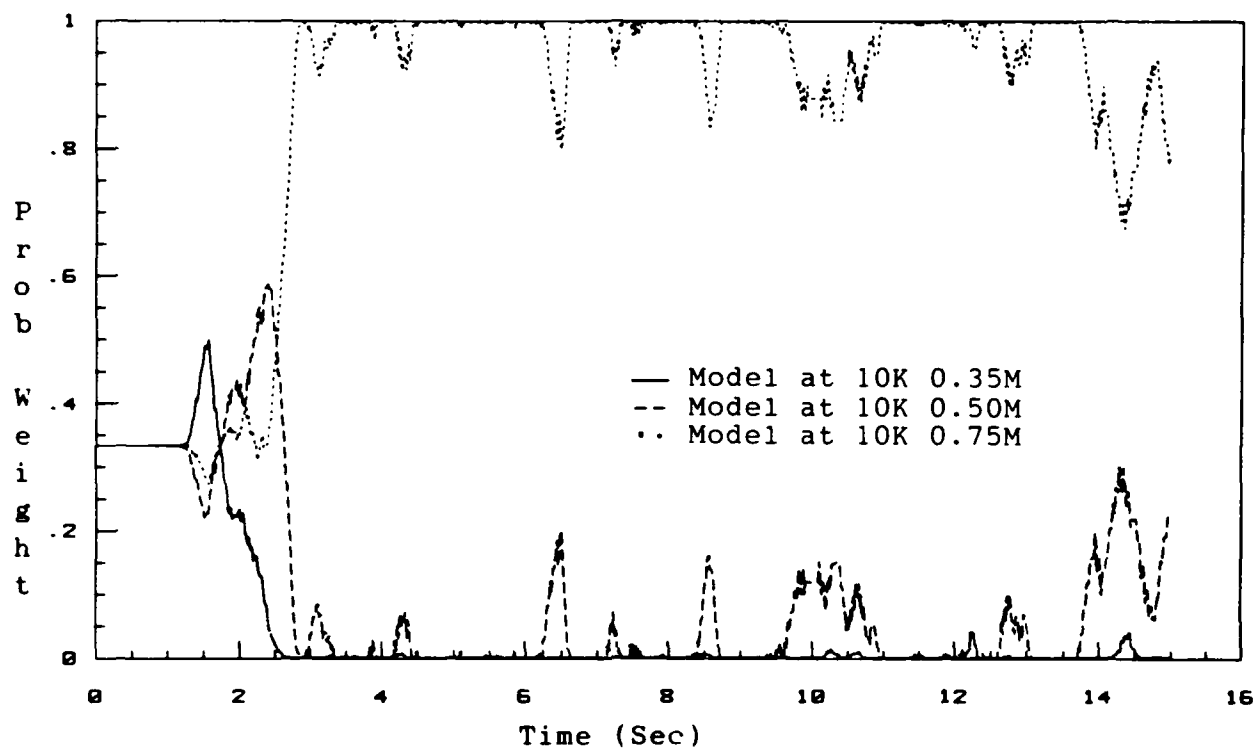
Figure 6-128.   Model Probability Weightings
Configuration 8/Operating Point: 26K 0.9M

203
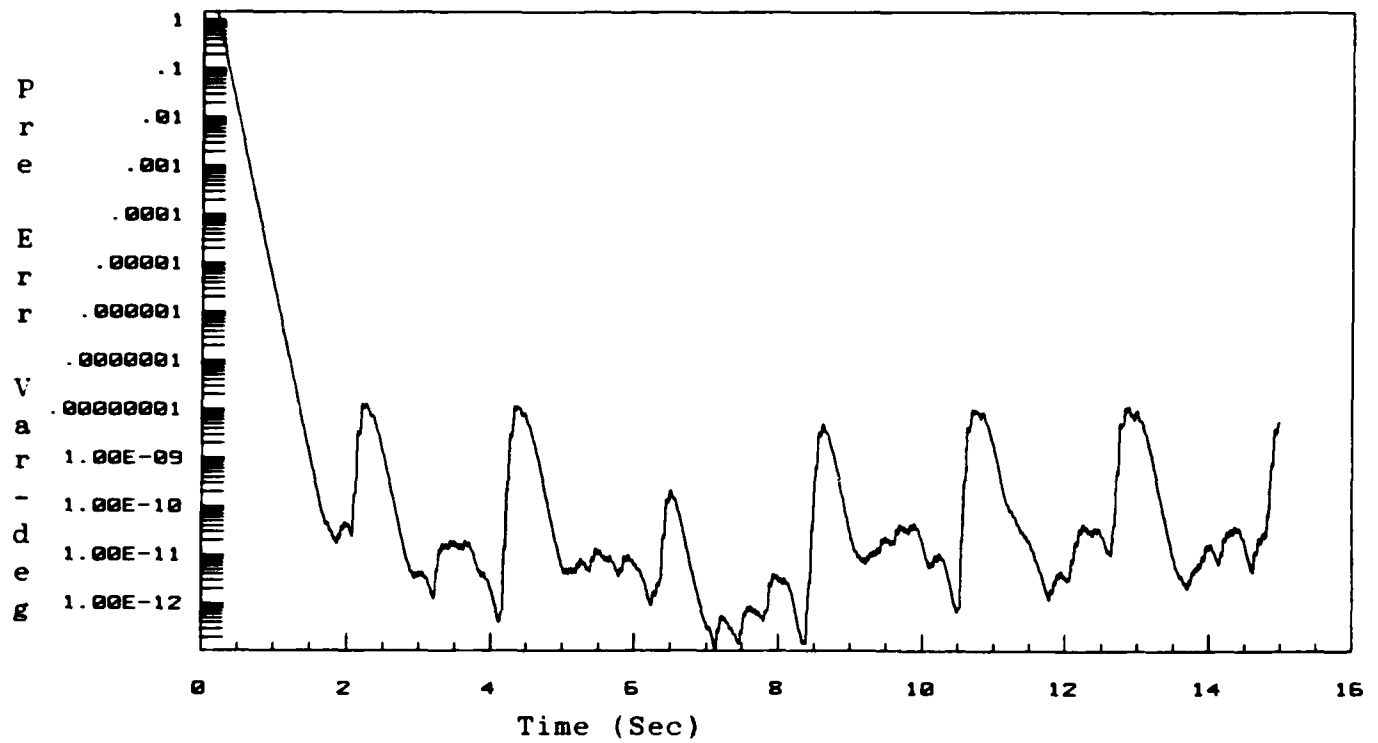
Figure 6-129.   Prediction Error Variance (1,1) for Model 1
Configuration 8/Operating Point: 26K 0.9M
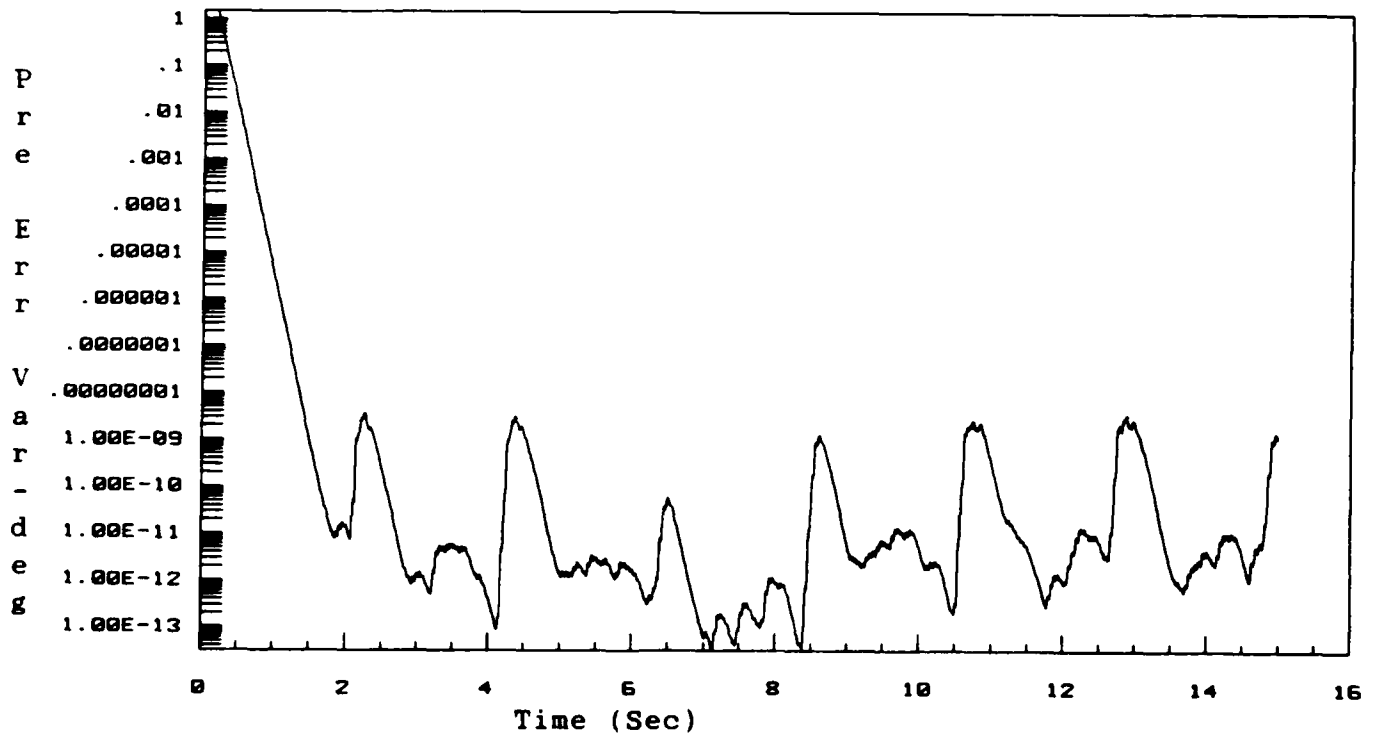
Figure 6-130.   Prediction Error Variance (2,2) for Model 1
Configuration 8/Operating Point: 26K 0.9M
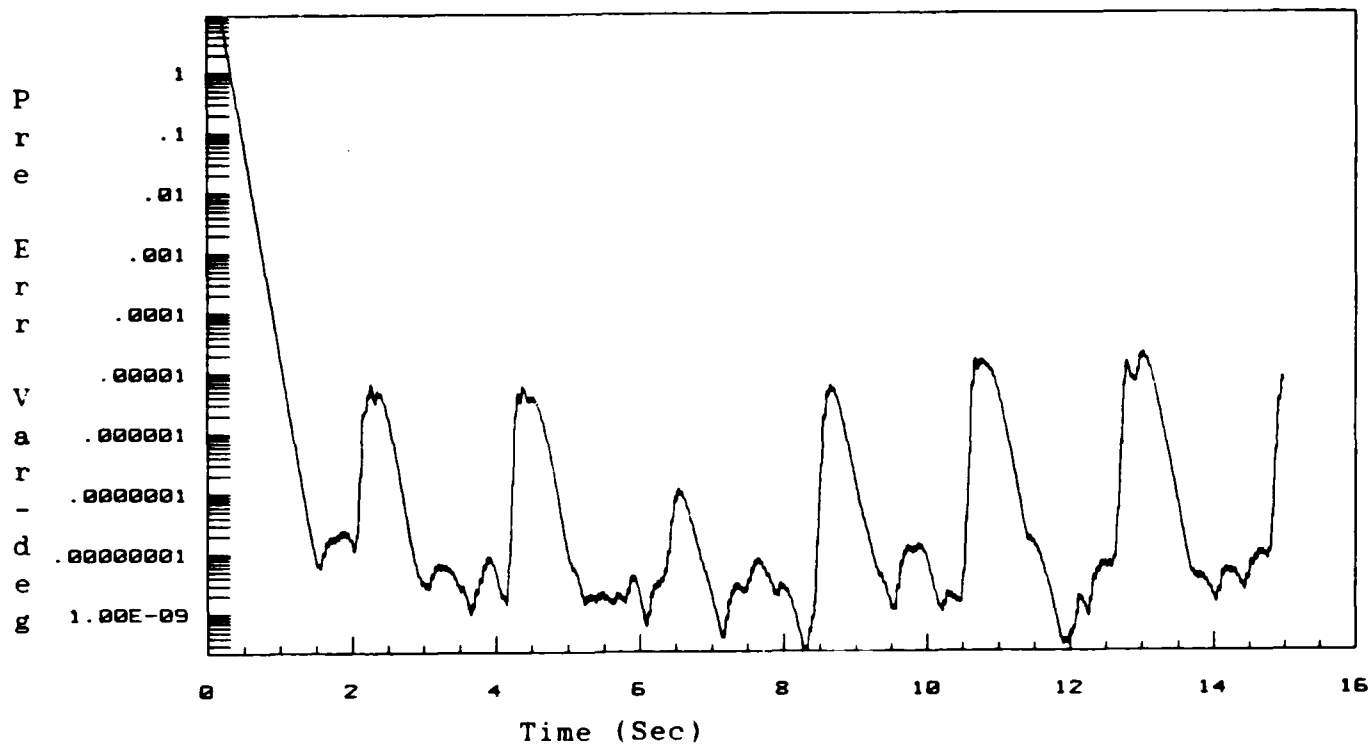
Figure 6-131.   Prediction Error Variance (1,1) for Model 2
Configuration 8/Operating Point: 26K 0.9M
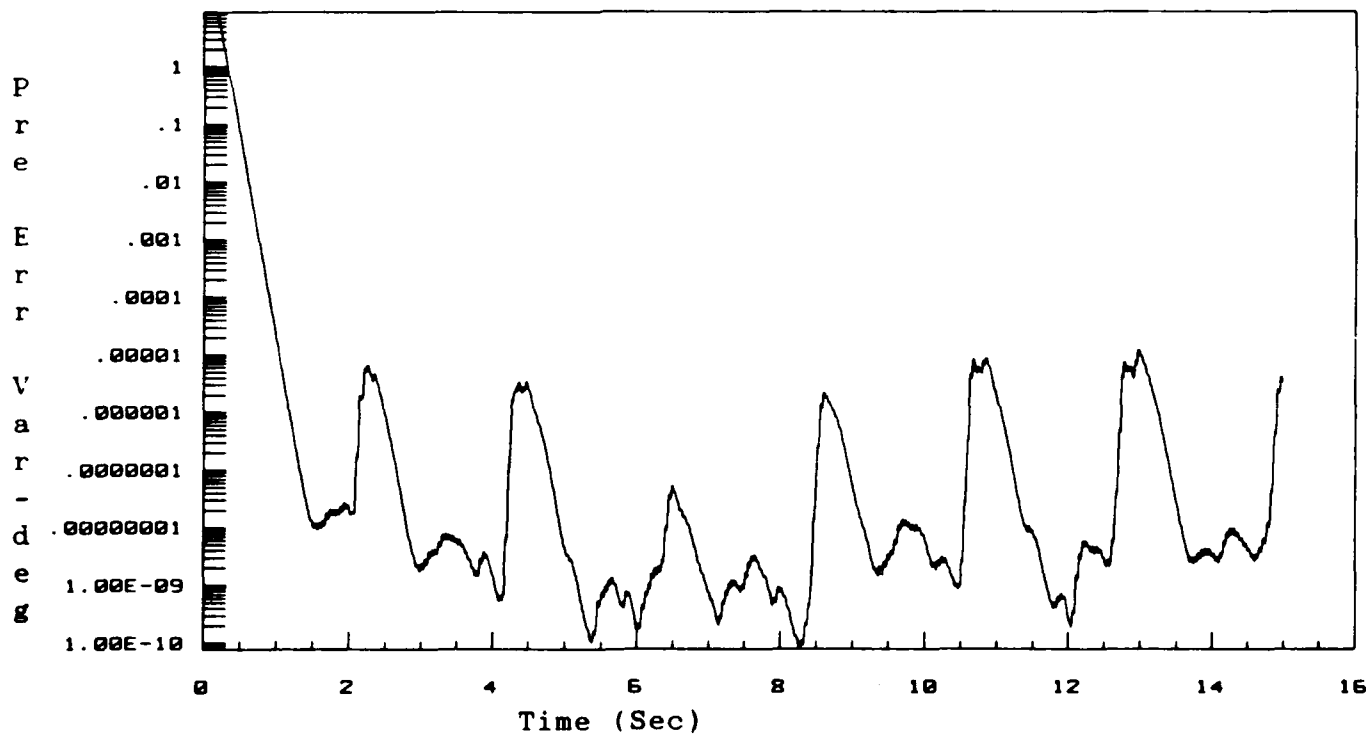
Figure 6-132.   Prediction Error Variance (2,2) for Model 2
Configuration 8/Operating Point: 26K 0.9M

205
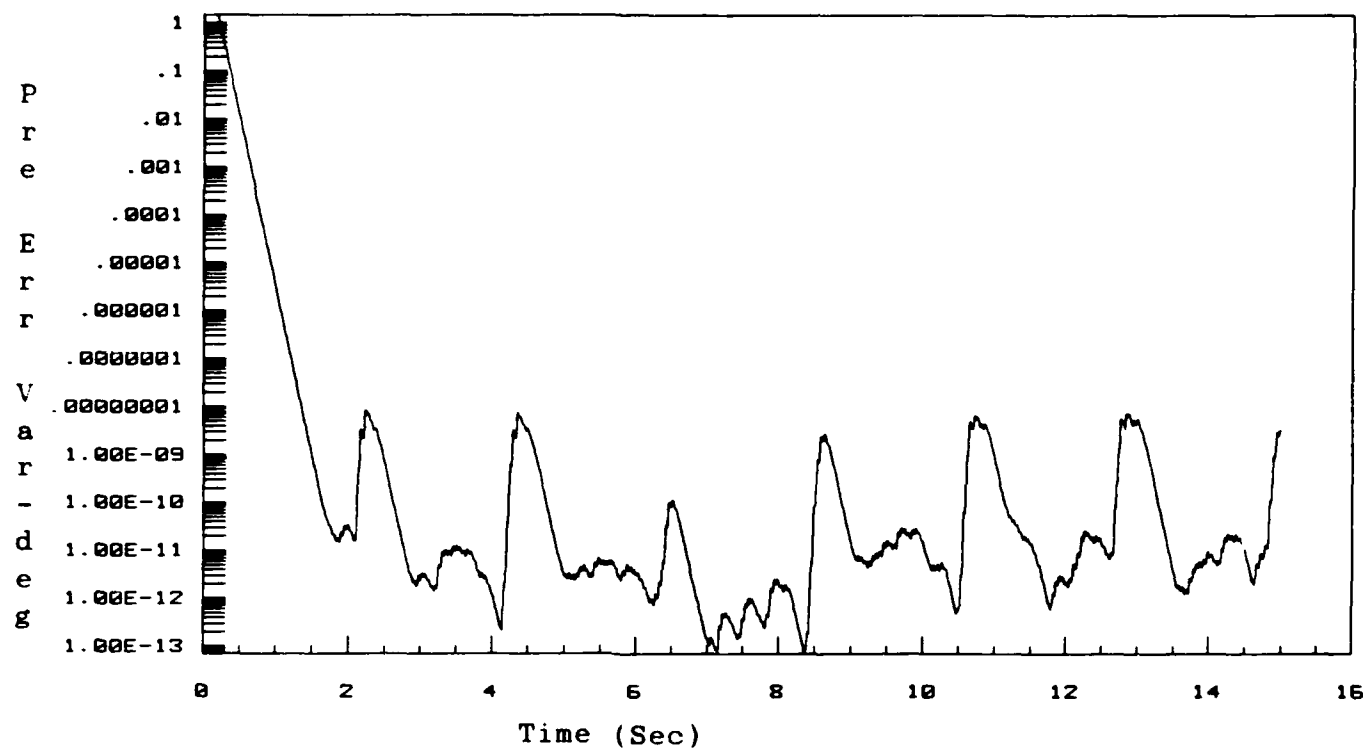
Figure 6-133.   Prediction Error Variance (1,1) for Model 3
Configuration 8/Operating Point: 26K 0.9M
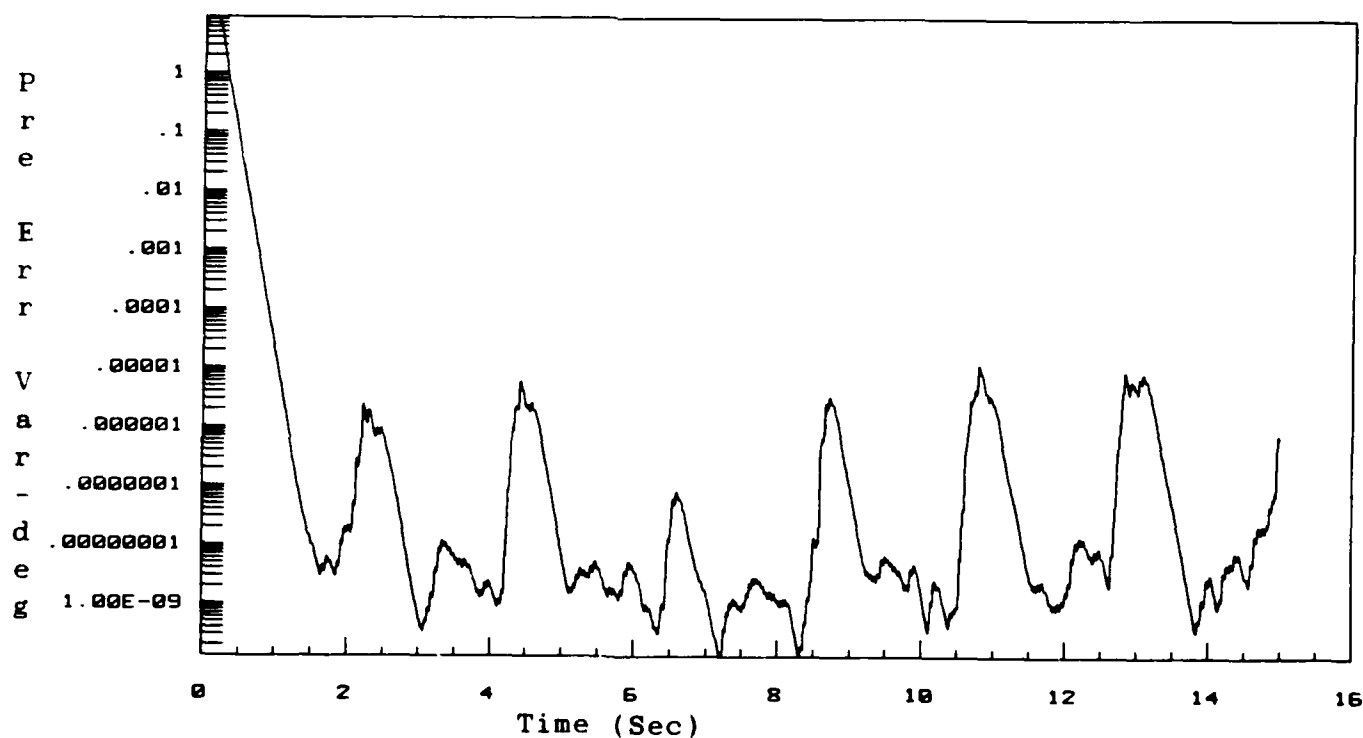
Figure 6-134.   Prediction Error Variance (2,2) for Model 3
Configuration 8/Operating Point: 26K 0.9M

206
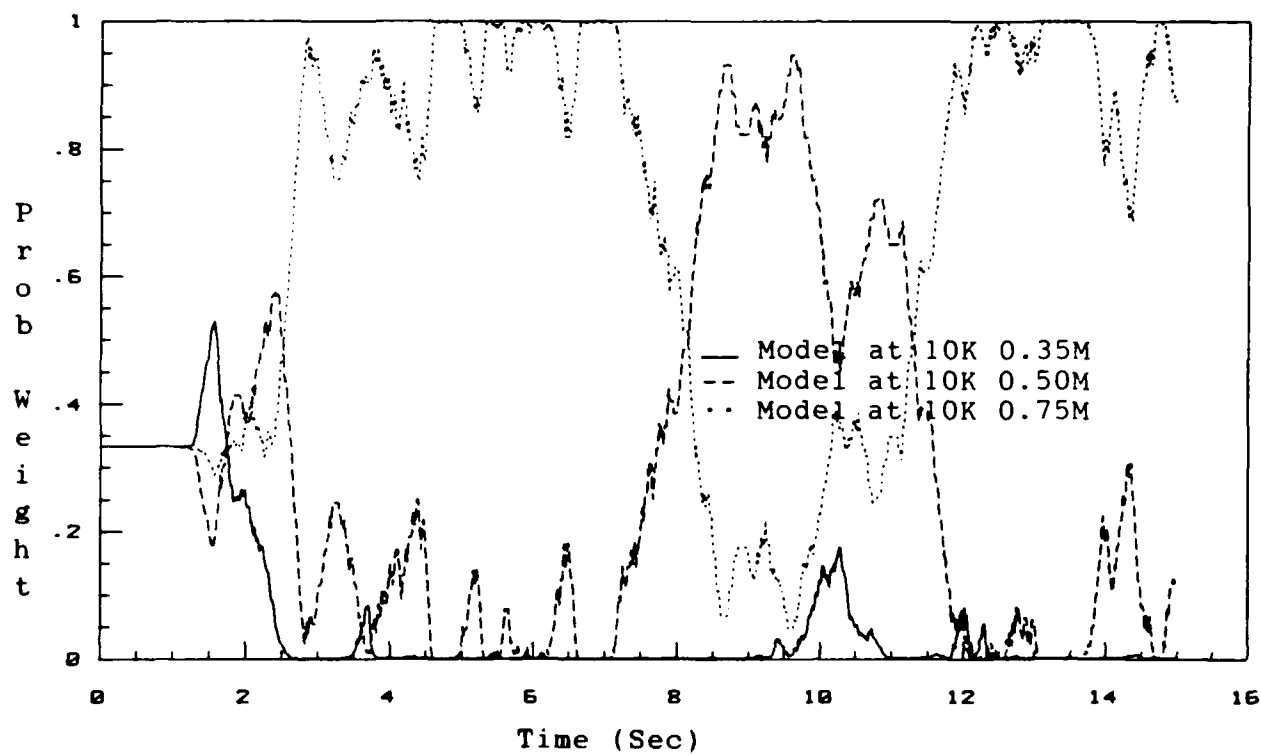
Figure 6-135.   Model Probability Weightings
Configuration 8/Sensor Noise/Operating Point: 26K 0.9M
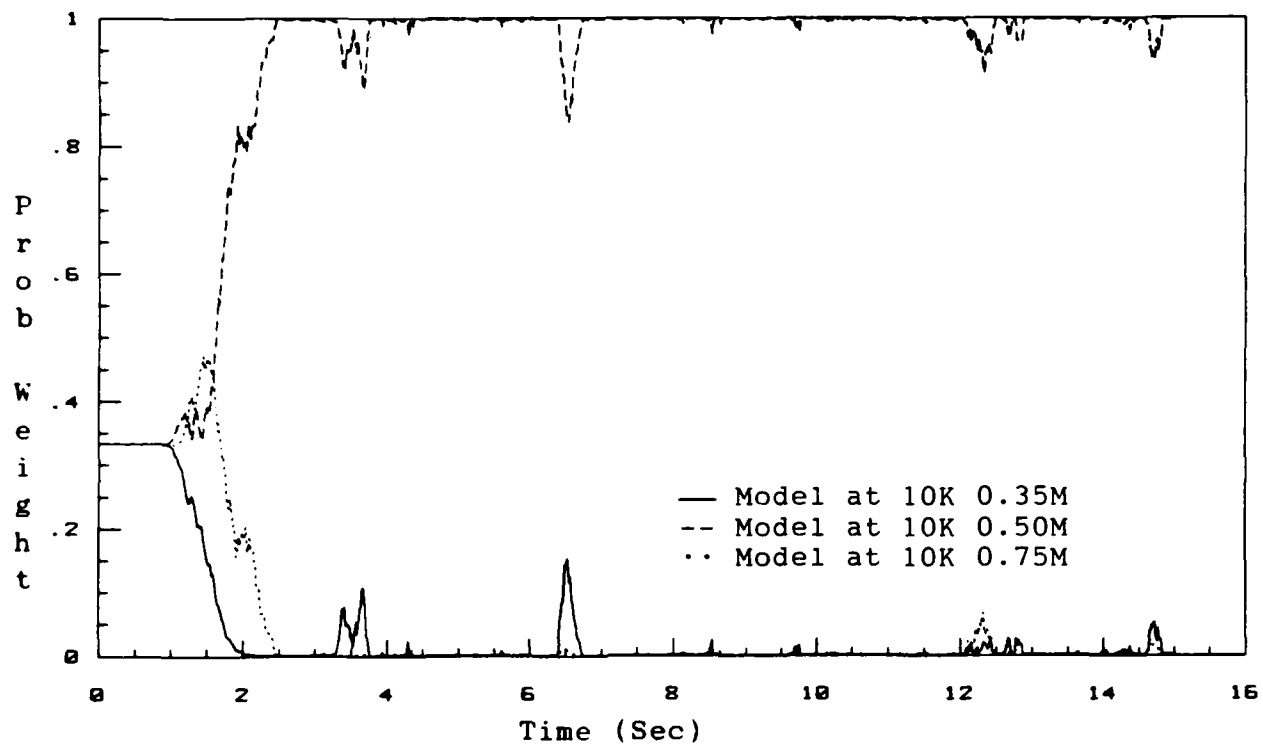
Figure 6-136.   Model Probability Weightings
Configuration 8/Sensor Noise(*100)/Operating Point: 26K 0.9M
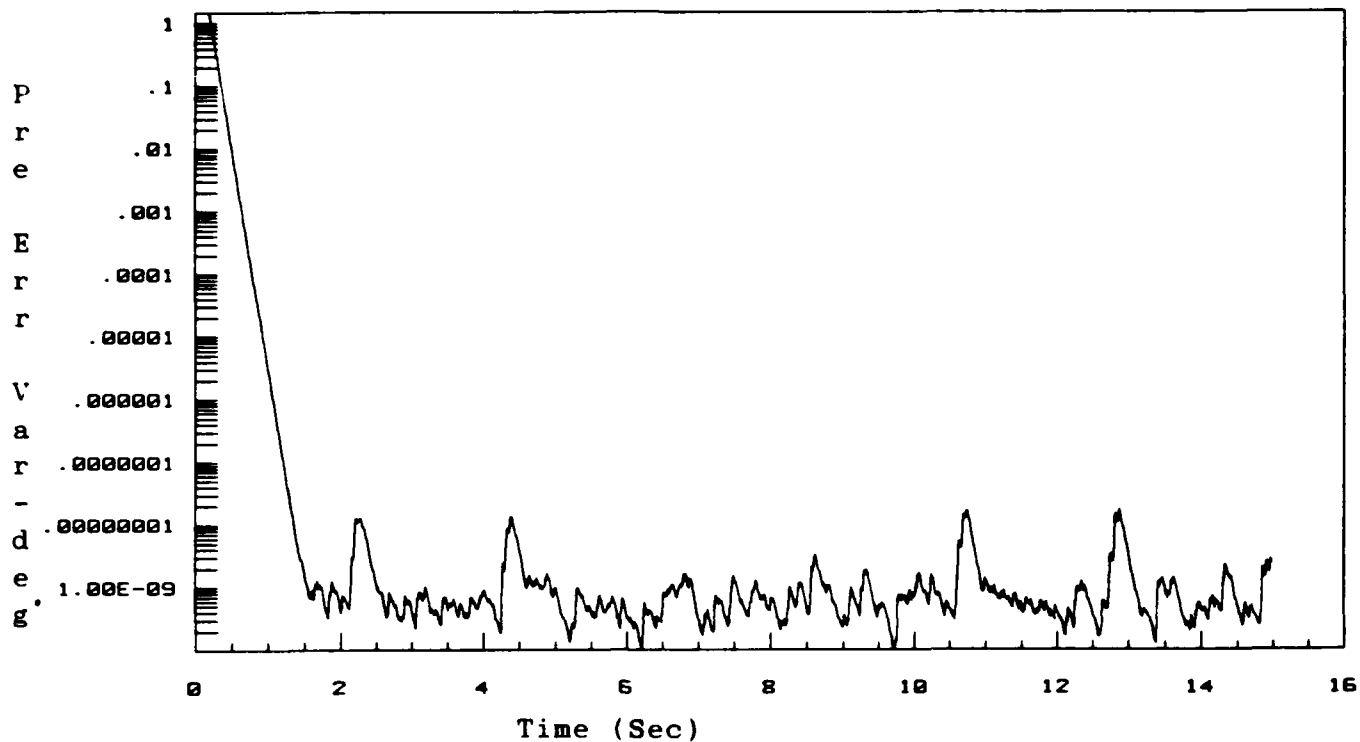
Figure 6-137. Prediction Error Variance (1,1) for Model 1
Configuration 8/Sensor Noise(*100)/Operating Point: 26K 0.9M
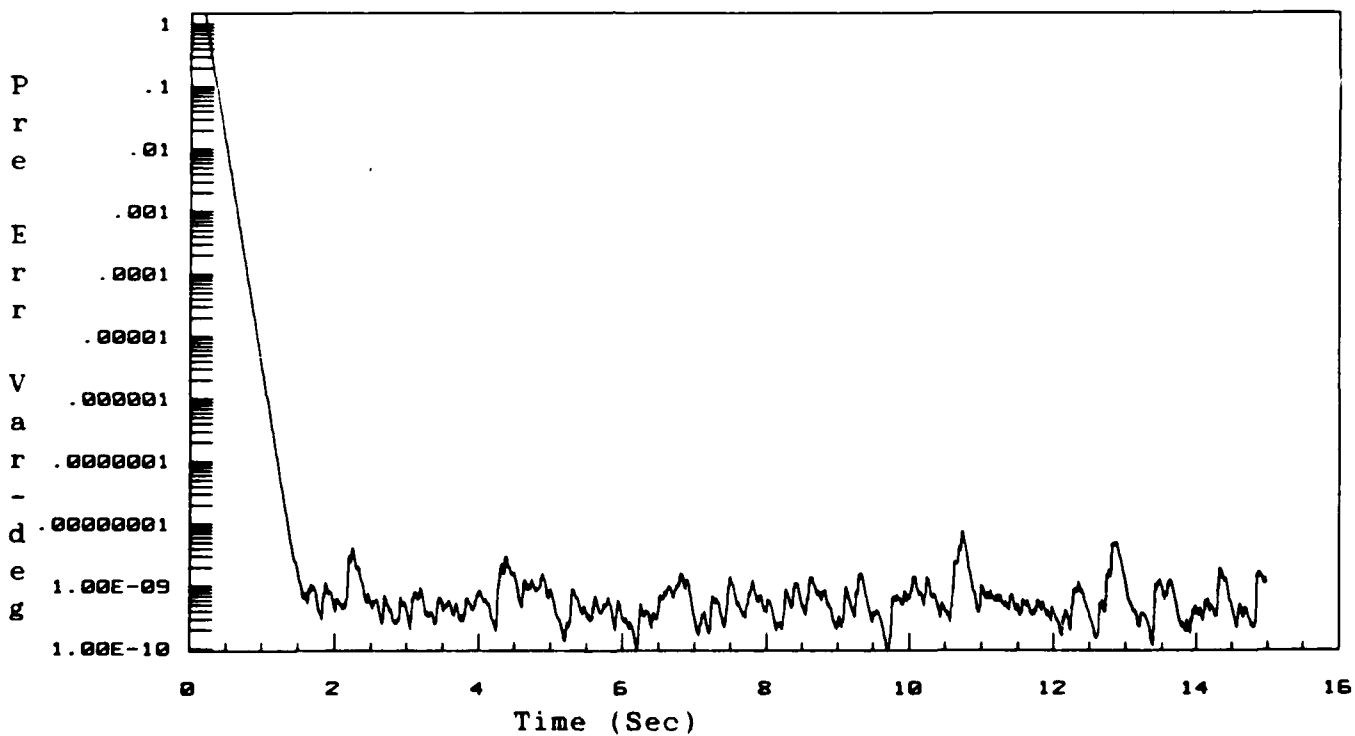
Figure 6-138. Prediction Error Variance (2,2) for Model 1
Configuration 8/Sensor Noise(*100)/Operating Point: 26K 0.9M

209
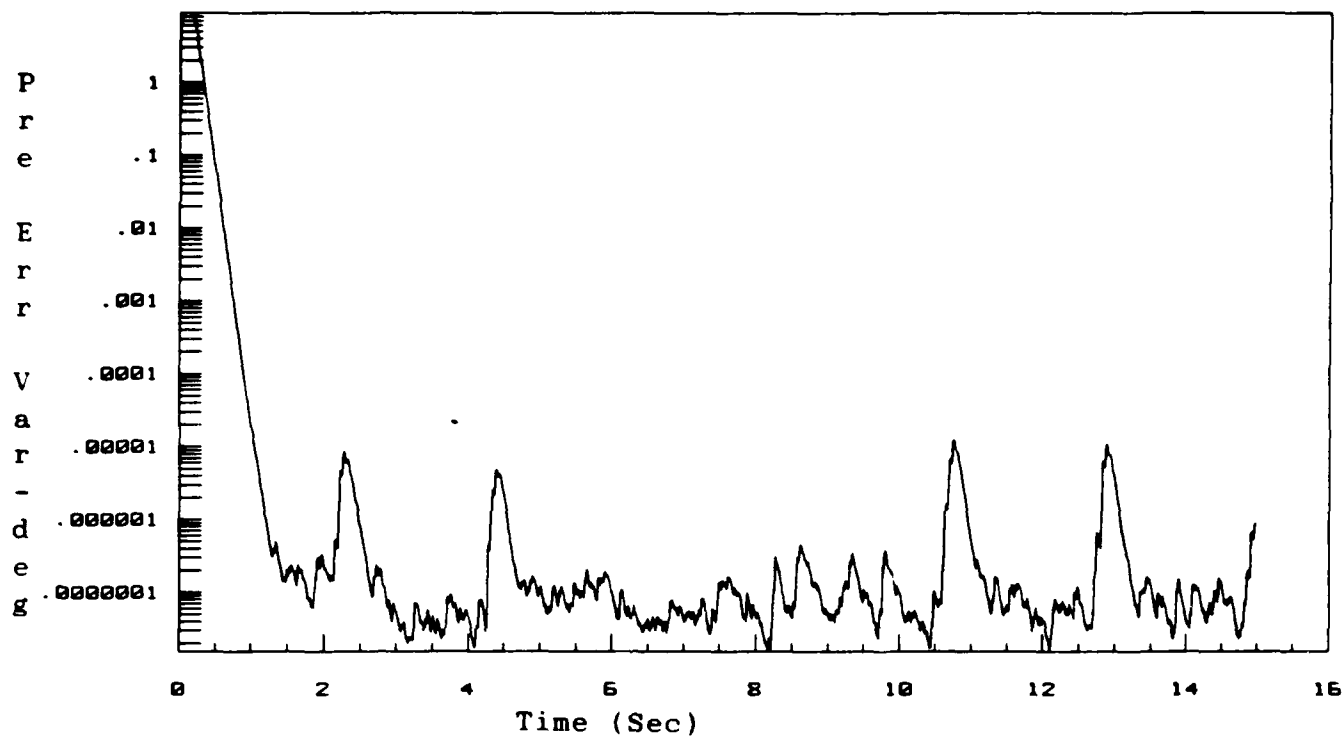
Figure 6-139.   Prediction Error Variance (1,1) for Model 2
Configuration 8/Sensor Noise(*100)/Operating Point: 26K 0.9M
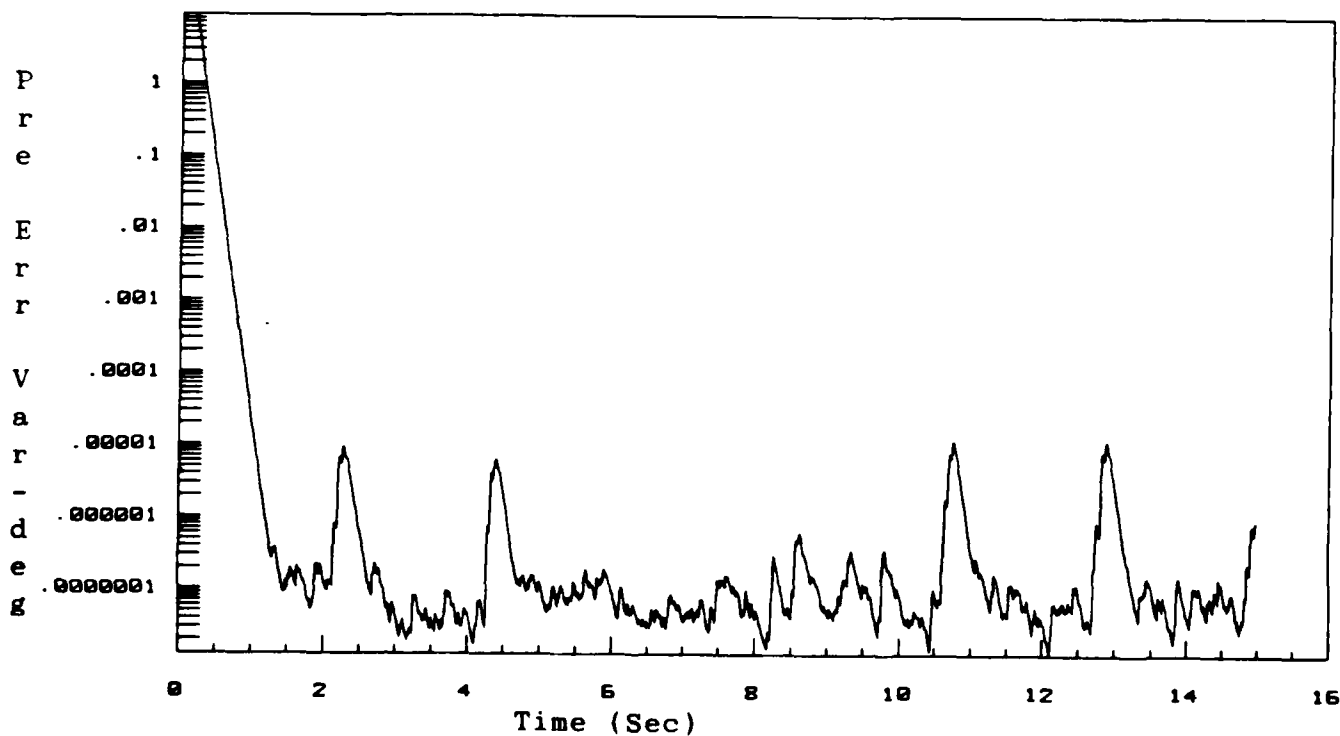
Figure 6-140.   Prediction Error Variance (2,2) for Model 2
Configuration 8/Sensor Noise(*100)/Operating Point: 26K 0.9M

210
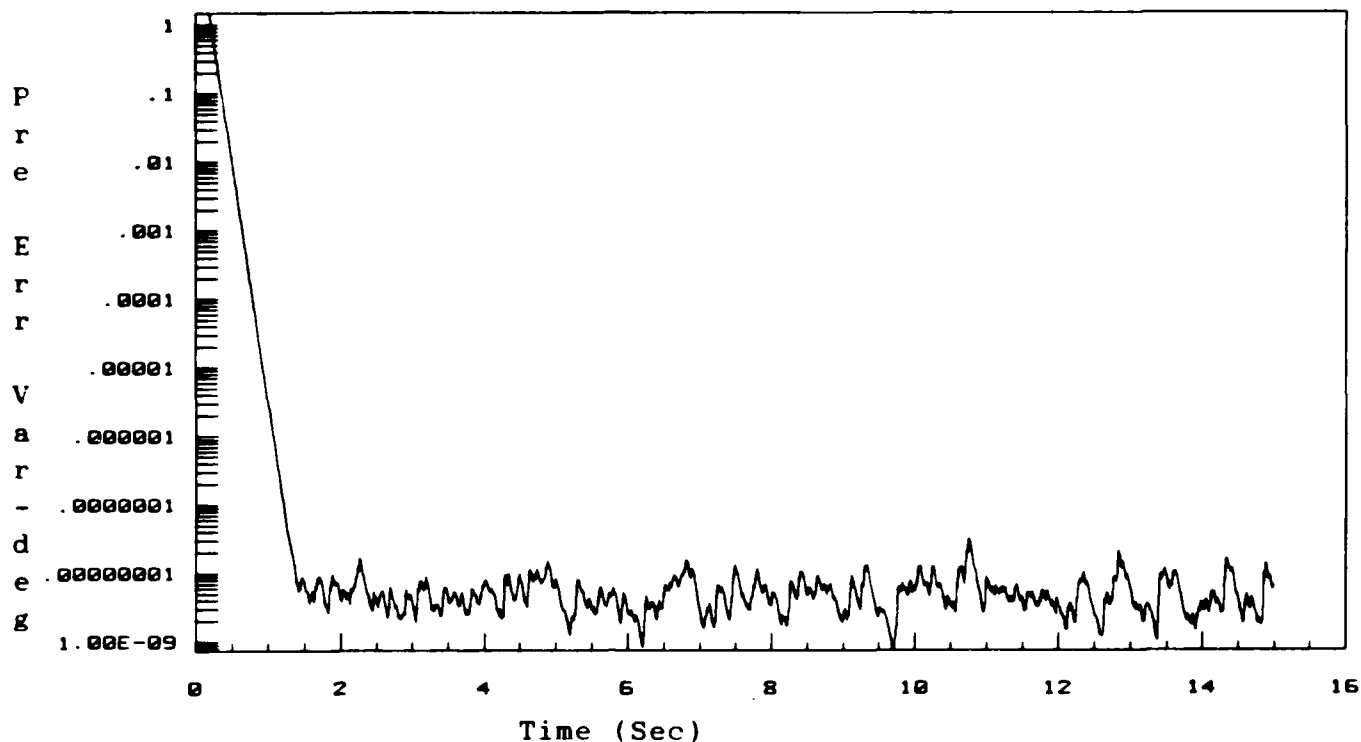
Figure 6-141.   Prediction Error Variance (1,1) for Model 3
Configuration 8/Sensor Noise(*100)/Operating Point: 26K 0.9M
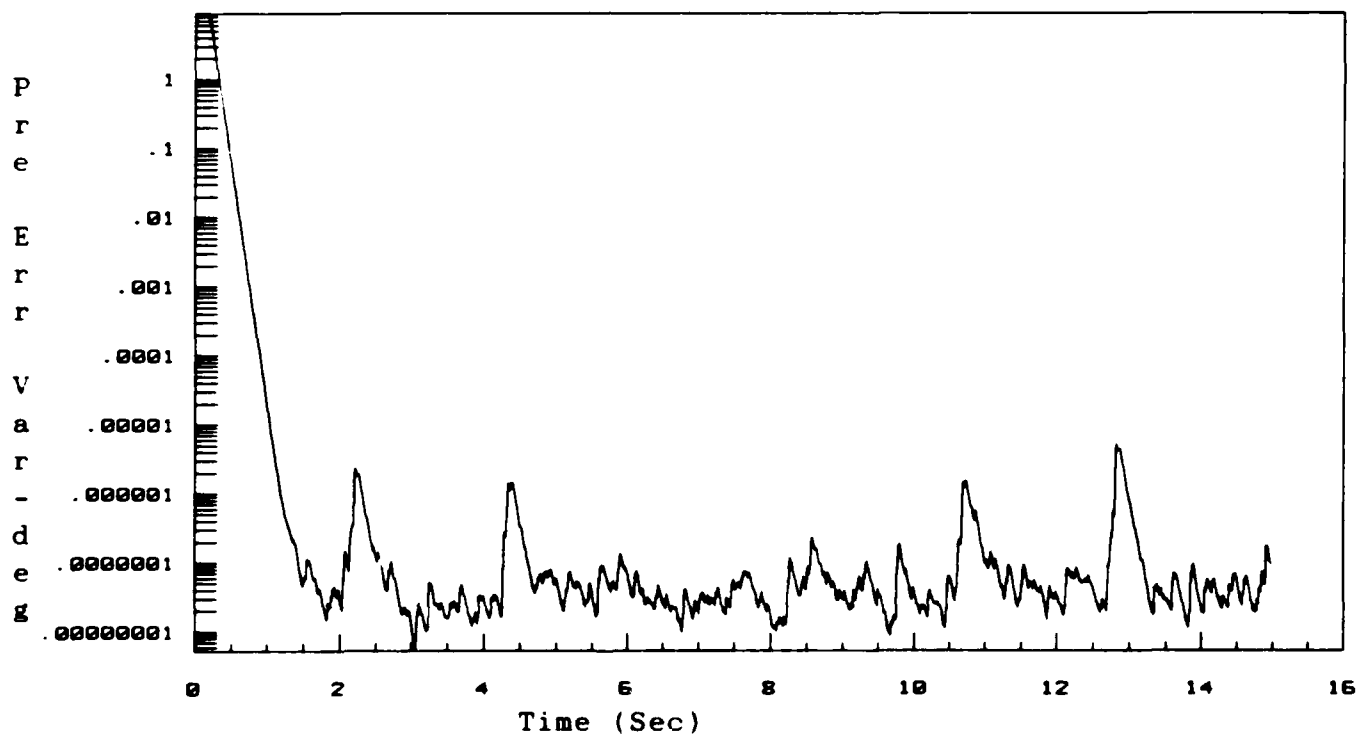
Figure 6-142.   Prediction Error Variance (2,2) for Model 3
Configuration 8/Sensor Noise(*100)/Operating Point: 26K 0.9M

211

has been selected as the most correct model. The prediction

error variances as shown in Figures 6-136 through 6-142 also

have much different responses from those that were obtained

from the simulations without noise. Several other simula-

tions were run with the same general results. Figures 6-143

through 6-146 present the probability weighting curves for

increasing values of sensor noise for the case where the

actual flight condition was at 38,000 ft, 0.6 Mach. As can

be seen from the weighting curves of Figures 6-143 through

6-146, increasing the level of sensor noise results in

increasing degradation of the multiple model algorithm's

performance. From the numerous simulations accomplished, it

was determined that the multiple model algorithm was more

sensitive to sensor noise when the probability weighting

curves for no noise had two models with significant influ-

ence on determining the correct model. In contrast, the

multiple model algorithm is less sensitive to sensor noise

when the actual flight condition is such that the probabili-

ty weighting calculation for no noise yields a single model

with a probability near one. The simulation results for

configuration 8 showed that the multiple model algorithm

yielded satisfactory results for the sensor noise levels
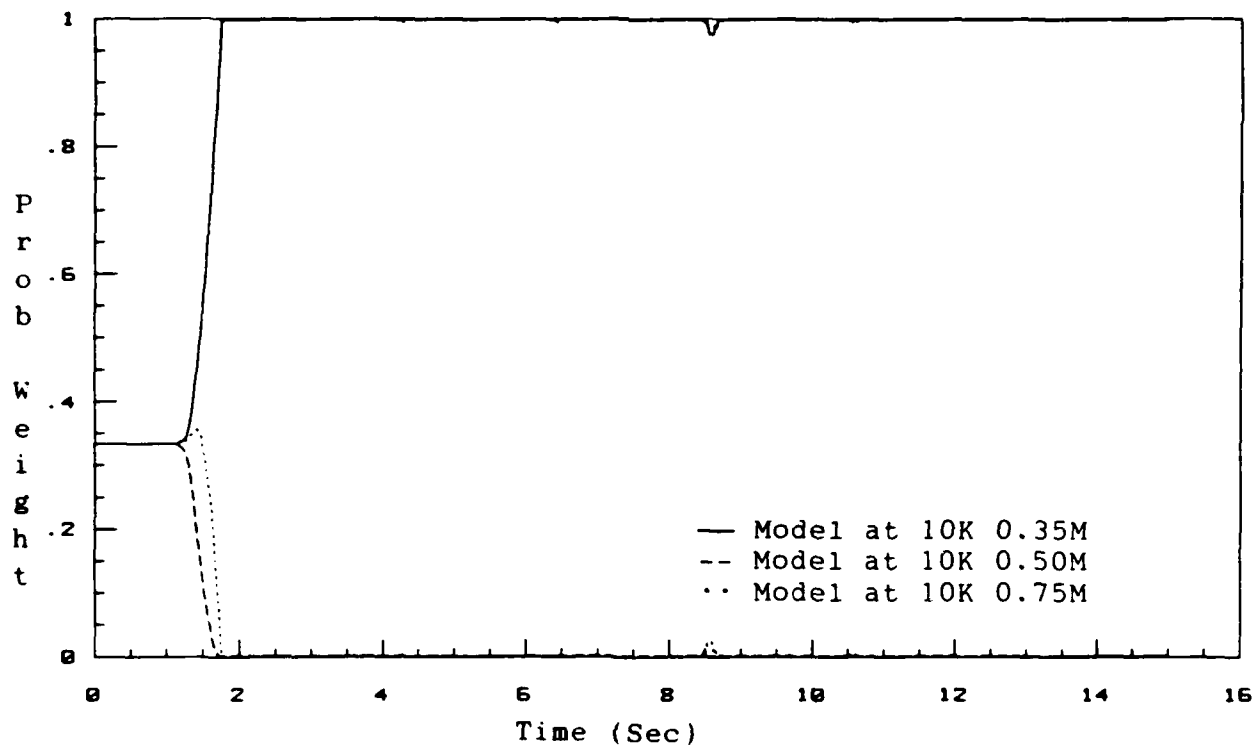
Figure 6-143.   Model Probability Weightings
Configuration 8/Operating Point: 38K 0.6M
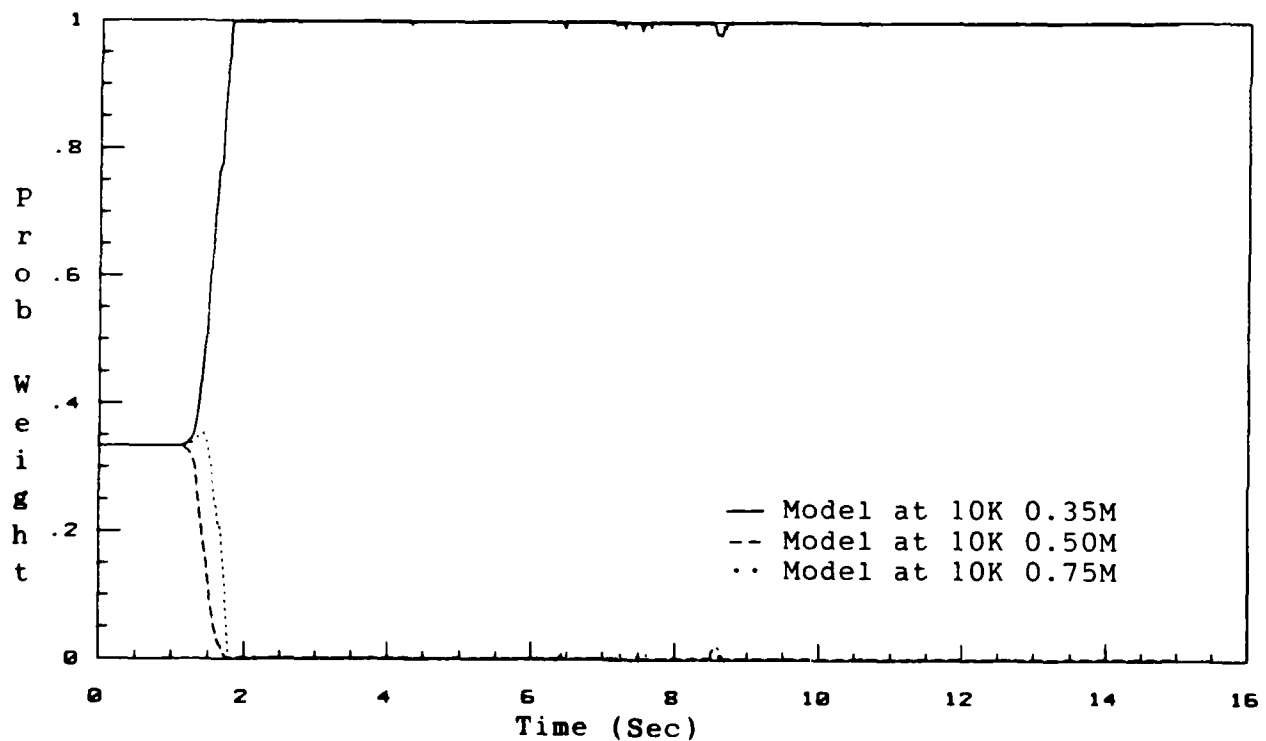
Figure 6-144.   Model Probability Weightings
Configuration 8/Sensor Noise/Operating Point: 38K 0.6M

213
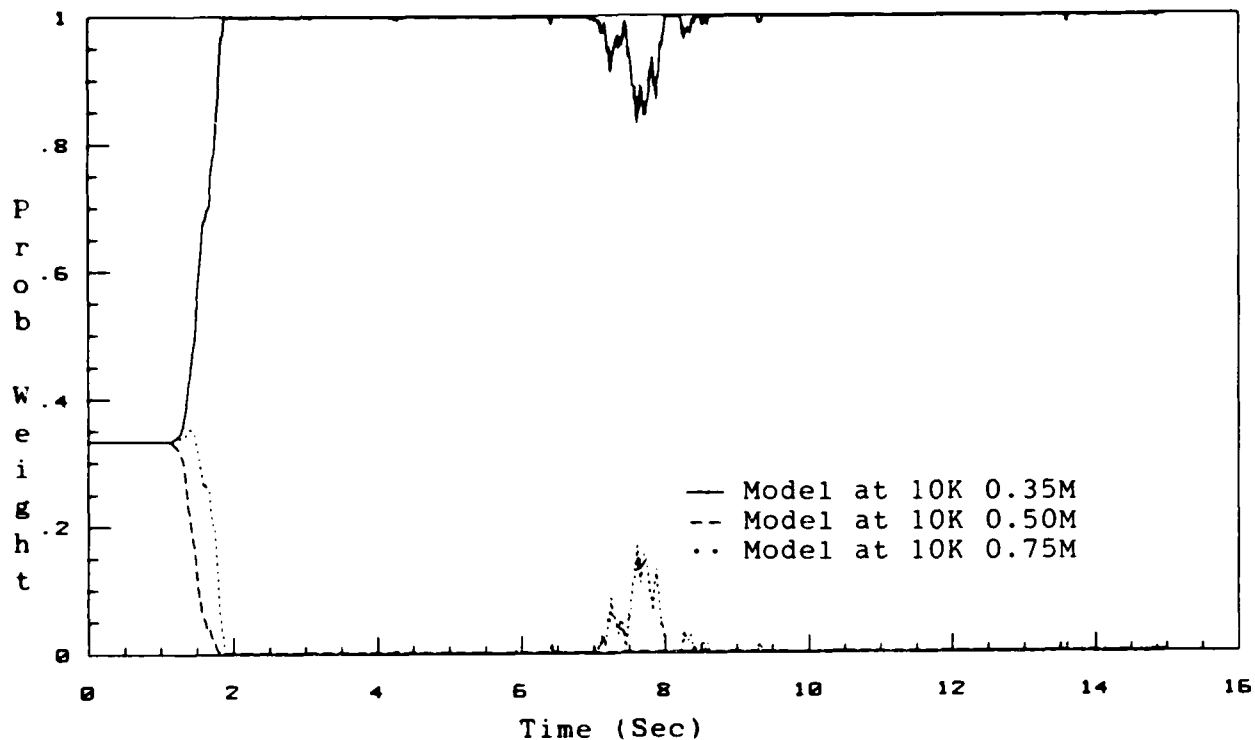
Figure 6-145.   Model Probability Weightings
Configuration 8/Sensor Noise (*10)/Operating Point: 38K 0.6M
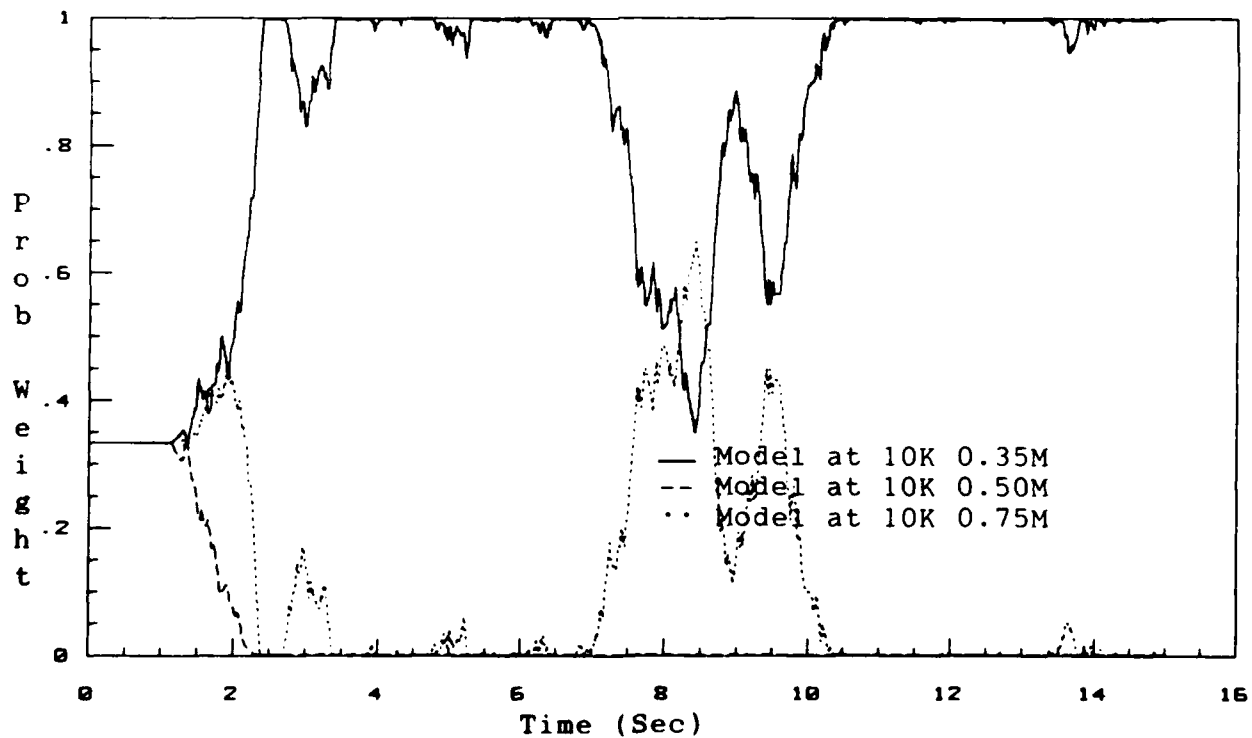
Figure 6-146.   Model Probability Weightings
Configuration 8/Sensor Noise(*100)/Operating Point: 38K 0.6M

given in Table 6-15.   However, increasing the noise levels

beyond those in Table 6-15 resulted in serious performance

degradation of the multiple model algorithm.

6.3 Summary

     This chapter presents the results that were obtained

during the accomplishment of this research effort.   Using

several nominal models as data points, performance bound-

aries are generated in an effort to determine regions of

robustness for the given models, and observations about the

primary factor in determining model equivalence are made.

The effects of varying the flight condition on the control

surface performance is also evaluated.   Next, simulations

with the multiple model algorithm are accomplished.   At

first, two models are placed in the secondary estimator

bank, to determine the required amount of overlap of the

performance boundaries of the elemental models to achieve

the desired tracking performance.   Following the evaluation

of the two-model configurations, several three-model config-

urations are evaluated and are found to to yield satisfacto-

ry tracking performance over the desired flight envelope.

In an effort to minimize the amount of time the control

surfaces reached the rate limits, the design parameters of the controller are adjusted. Finally, the effects of sensor noise on the performance of the multiple model algorithm are evaluated. The next chapter of this thesis presents the conclusions drawn from the results detailed in this chapter. Recommendations for further study are also presented.

7. Conclusions and Recommendations

7.1 Introduction

As mentioned several times throughout this thesis, the primary objective of this research is to determine the effects of model placement on the performance of the multiple model algorithm within an adaptive control law. Several hundred simulations were run which are the basis for the results presented in Chapter 6. The following list of conclusions presents the highlights of the results in Chapter 6. The recommendations outline further areas of study in this area of research.

7.2 Conclusions

The following is a list of the highlights of the results obtained in the course of this research effort.

1. Performance criteria must be selected prior to determining the performance robustness of a nominal aircraft model. The performance criteria dictate the degree to which the plant parameters can vary before unacceptable performance is reached and therefore influence the performance boundaries for a given nominal model.

2. In determining the performance boundaries for sev-

217

eral different nominal models, it has been learned that the

quantity model equivalence is most dependent on is dynamic

pressure. By taking several different models on approxi-

mately the same dynamic pressure line, it is shown that the

performance boundaries are the same.

3. Although the performance boundaries for nominal

models on the same dynamic pressure line are the same, the

control surface responses may be different. It is shown

that the reason for this is the different trim values of

angle-of-attack. It is also shown that control surface

performance is influenced by the aerodynamic gains as-

sociated with the actual flight condition. By decreasing

altitude and/or increasing Mach number, the aerodynamic gain

increases, causing the control surfaces to respond faster.

This information is useful when tuning the controller. Af-

ter selection of the models for the multiple model al-

gorithm, the controller can be tuned at the flight condition

with the worst case aerodynamic gains.

4. When trying to achieve satisfactory tracking per-

formance over the flight envelope of interest with two

models in the multiple model algorithm's secondary bank, it

is seen that the amount of overlap of the performance bound-

aries is very important. Due to the fact that the multiple model adaptive estimator arrives at a parameter estimate by weighting the "correctness" of the models in the bank, the final parameter estimate is a blend of those models' parameters. Because of the weighted blending of parameters of each of the models in the bank, a significant amount of overlap of the performance boundaries is required to yield satisfactory tracking performance. However, it is also shown that the lower bound on the computed probabilities affects the amount of overlap required of the performance boundaries. The amount of overlap increases as the value of the lower bound becomes larger. This performance boundary overlap requirement leads to the use of three models as secondary parameter estimators in lieu of two.

5. Due to the robustness of the controller to variations in the plant parameters, the flight envelope of interest can be modelled with three nominal models in the bank of secondary estimators in the multiple model algorithm. The robustness of the control law allows a large parameter space to be modelled by a relatively small number of discrete models while yielding excellent tracking performance.

6. In the analysis of the three-model configurations,

it is shown that, regardless of the altitudes or Mach numbers of the nominal models in the secondary estimator bank of the multiple model algorithm, the model assigned the highest weighting is the model with a value of dynamic pressure closest to that of the actual flight condition.

7. The limitation on how close the candidate models can be placed is shown to be dependent on the amount of sensor noise added to the longitudinal states. Sensor noise tends to mask the residuals generated for each of the models in the secondary estimator bank and hence degrades the multiple model algorithm's performance. It is shown that with greater separation between dynamic pressure parameterization the susceptability of the multiple model algorithm to the sensor noise is decreased.

From the above list of conclusions, it can be seen that model placement for the multiple model algorithm is dependent on many factors. First of all, performance criteria must be selected, which in turn determine the region of performance robustness of a given nominal model. The performance criteria also have a large effect on the number of models (for the multiple model algorithm's secondary estimation bank) that are necessary to achieve the desired track-

ing performance over the specified flight envelope. Less demanding performance criteria would result in larger regions of performance robustness and hence fewer models would be required to model the desired parameter space.

The amount of overlap of the performance boundaries is shown to require a tradeoff of conflicting requirements. These conflicting requirements are the result of wanting a large amount of overlap for enhanced tracking performance, yet desiring minimal overlap for sensor noise resistance. The results show that the minimum amount of overlap that is acceptable is that which yields satisfactory tracking performance over the flight envelope of interest. The maximum amount of overlap is dictated by the expected levels of sensor noise. Therefore, once performance criteria have been established and sensor noise figures determined, an analysis as to how far apart in dynamic pressure the secondary estimator models need to be can be accomplished.

7.3 Recommendations for Further Study

This thesis presents an initial evaluation of the factors that are important in the selection of models for the multiple model algorithm. The following list presents areas

221

of interest that could be investigated to further this effort.

1. The flight envelope of interest should be expanded to include transonic and supersonic flight conditions. The purpose of investigating this expanded flight envelope would be to verify if model equivalence is based primarily on dynamic pressure or on some other criteria. Model selection in this portion of the flight envelope might have different characteristics from those addressed in this thesis.

2. The multiple model algorithm could be tailored so that the gains implemented in the controller would not be a weighted gain matrix of the models in the bank, but would be the set of gains associated with the model with the highest probability. This would seem to have the effect of not requiring much overlap of the performance boundaries and therefore would provide greater sensor noise resistance.

3. Although the general effects of sensor noise on model selection is addressed in this effort, further re-search in this area needs to be accomplished to include an extensive Monte Carlo analysis.

Appendix A

This appendix presents the A and B matrices of the state space models for each of the flight conditions that are considered in the flight envelope of interest. In addition, the aircraft parameters that are constant for each flight condition are presented. This data was obtained from the Flight Dynamics Laboratory at Wright-Patterson AFB, OH.

Constant Aircraft Parameters

S (wing reference area - ft^2) = 300.00

c (wing mean aerodynamic chord - ft) = 11.32

ACGW (aircraft gross weight - lbs) = 21505.00

LOADFAC (load factor - g) = 1.0

b (wing span - ft) = 30.00

Inertias:

  Ixx (slug - ft^2) = 14224.04

  Iyy (slug - ft^2) = 61352.40

  Izz (slug - ft^2) = 72651.75

Flight Condition: 10,000 ft, 0.9 Mach

```
        0.0000    0.0000    0.0000    1.0000        0.0000    0.0000
A = -32.1640   -0.0154   43.4875  -24.0510  B = -0.9568   19.0164
       -0.0008    0.0000   -2.0397    0.9999       -0.2063   -0.3610
        0.0003   -0.0005    6.9843   -0.9769      -30.8710   -9.4022
```

Flight Condition: 10,000 ft, 0.85 Mach

```
        0.0000    0.0000    0.0000    1.0000        0.0000    0.0000
A = -32.1625   -0.0156   39.7461  -24.4587  B = -0.4927   15.6819
       -0.0009    0.0000   -1.8507    1.0000       -0.3380   -0.1833
        0.0003   -0.0010    7.1505   -0.9116      -26.8660   -7.5573
```

Flight Condition: 10,000 ft, 0.8 Mach

```
        0.0000    0.0000    0.0000    1.0000        0.0000    0.0000
A = -32.1603   -0.0149   35.8901  -25.1231  B = -0.2750   12.8572
       -0.0011   -0.0001   -1.6730    1.0000       -0.1833   -0.3151
        0.0003   -0.0010    7.1562   -0.8477      -23.1933   -5.9530
```

Flight Condition: 10,000 ft, 0.75 Mach

```
        0.0000    0.0000    0.0000    1.0000        0.0000    0.0000
A = -32.1584   -0.0138   33.9936  -25.1510  B =  0.6016   10.4851
       -0.0012   -0.0001   -1.5069    1.0000       -0.1662   -0.2979
        0.0003   -0.0010    6.8526   -0.7854      -19.8129   -4.6123
```

Flight Condition: 10.000 ft, 0.7 Mach

```
        0.0000    0.0000    0.0000    1.0000        0.0000    0.0000
A = -32.1575   -0.0118   30.9741  -24.1602  B =  2.2460    3.8331
       -0.0014   -0.0001   -1.3407    1.0000       -0.1547   -0.2636
        0.0003   -0.0010    6.5776   -0.7244      -16.7132   -3.1283
```

Flight Condition: 10,000 ft, 0.65 Mach

```
        0.0000    0.0000    0.0000    1.0000        0.0000    0.0000
A = -32.1550   -0.0112   30.6762  -24.0485  B =  3.5408   -5.0936
       -0.0016   -0.0001   -1.1975    1.0000       -0.1432   -0.2406
        0.0003   -0.0010    6.1077   -0.6648      -13.9687   -1.6329
```

Flight Condition: 10,000 ft, 0.6 Mach

```
        0.0000    0.0000    0.0000    1.0000        0.0000    0.0000
A = -32.1506   -0.0108   32.2231  -24.6667  B =     4.3316   -6.2338
       -0.0019   -0.0001   -1.0657    1.0000       -0.1317   -0.2349
        0.0003   -0.0004    5.4030   -0.6067      -11.6081   -0.9454
```

Flight Condition: 10,000 ft, 0.55 Mach

```
        0.0000    0.0000    0.0000    1.0000        0.0000    0.0000
A = -32.1429   -0.0099   32.7156  -26.0481  B =     4.4748   -5.0133
       -0.0024   -0.0001   -0.9855    1.0000       -0.1261   -0.2120
        0.0003    0.0002    4.3259   -0.5577       -9.7689   -0.7850
```

Flight Condition: 10,000 ft, 0.5 Mach

```
        0.0000    0.0000    0.0000    1.0000        0.0000    0.0000
A = -32.1305   -0.0102   32.2804  -28.0069  B =     4.3889   -4.1826
       -0.0031   -0.0001   -0.8995    1.0000       -0.1146   -0.1891
        0.0004    0.0002    3.5523   -0.5124       -8.0844   -0.5730
```

Flight Condition: 10,000 ft, 0.45 Mach

```
        0.0000    0.0000    0.0000    1.0000        0.0000    0.0000
A = -32.1092   -0.0100   31.8221  -30.7710  B =     3.7471   -3.3174
       -0.0042   -0.0001   -0.8079    1.0000       -0.1089   -0.1662
        0.0004    0.0001    3.0825   -0.4675       -6.5832   -0.3724
```

Flight Condition: 10,000 ft, 0.4 Mach

```
        0.0000    0.0000    0.0000    1.0000        0.0000    0.0000
A = -32.0708   -0.0102   27.0092  -34.5258  B =     2.6872   -2.1371
       -0.0060   -0.0002   -0.6933    1.0000       -0.0974   -0.1432
        0.0005    0.0001    2.7158   -0.4228       -5.1967   -0.1833
```

Flight Condition: 10,000 ft, 0.35 Mach

```
        0.0000    0.0000    0.0000    1.0000        0.0000    0.0000
A = -31.9931   -0.0109   19.7499  -40.0088  B =     1.9309   -3.3690
       -0.0090   -0.0002   -0.5672    1.0000       -0.0859   -0.1031
        0.0006    0.0001    2.0512   -0.3905       -3.9362    0.0344
```

Flight Condition: 10,000 ft, 0.3 Mach

```
        0.0000    0.0000    0.0000    1.0000         0.0000   0.0000
A =   -31.8063   -0.0127   19.4232  -48.9139   B =   1.6157  -3.3289
       -0.0150   -0.0003   -0.4526    1.0000        -0.0745  -0.0630
        0.0008    0.0001    1.8793   -0.3862        -2.9794   0.3724
```

Flight Condition: 10,000 ft, 0.25 Mach

```
        0.0000    0.0000    0.0000    1.0000         0.0000   0.0000
A =   -31.2389    0.0075   11.6253  -65.0974   B =  -0.2005  -2.1257
       -0.0286   -0.0004   -3.5626    1.0000        -0.0630  -0.0573
        0.0003    0.0001    0.6131   -0.4665        -2.0684   0.2349
```

Flight Condition: 14,000 ft, 0.9 Mach

```
        0.0000    0.0000    0.0000    1.0000         0.0000    0.0000
A =   -32.1621   -0.0129   37.7866  -25.9832   B =  -0.9397   16.5356
       -0.0009    0.0000   -1.7819    1.0000        -0.1776   -0.3266
        0.0003   -0.0005    5.6207   -0.8498       -26.6024   -8.1932
```

Flight Condition: 14,000 ft, 0.85 Mach

```
        0.0000    0.0000    0.0000    1.0000         0.0000    0.0000
A =   -32.1599   -0.0132   34.5150  -26.6752   B =  -0.6303   13.6708
       -0.0011   -0.0001   -1.6157    1.0000        -0.1662   -0.3037
        0.0003   -0.0009    5.8270   -0.7927       -23.1246   -6.5776
```

Flight Condition: 14,000 ft, 0.8 Mach

```
        0.0000    0.0000    0.0000    1.0000         0.0000    0.0000
A =   -32.1569   -0.0126   34.6410  -27.6587   B =  -0.5386   11.2529
       -0.0012   -0.0001   -1.4610    1.0000        -0.1604   -0.2807
        0.0003   -0.0009    5.7353   -0.7369       -19.9447   -5.1738
```

Flight Condition: 14,000 ft, 0.75 Mach

```
        0.0000    0.0000    0.0000    1.0000         0.0000    0.0000
A =   -32.1549   -0.0115   32.4638  -27.4111   B =   6.4171    9.2246
       -0.0014   -0.0001   -1.3178    1.0000        -0.1489   -0.2636
        0.0003   -0.0009    5.4947   -0.6826       -16.9997   -4.0164
```

Flight Condition: 14,000 ft, 0.7 Mach

```
        0.0000    0.0000    0.0000    1.0000          0.0000   0.0000
A =   -32.1532   -0.0099   29.7479  -26.7275   B =    1.9881   0.7391
       -0.0016   -0.0001   -1.1745    1.0000         -0.1375  -0.2291
        0.0003    0.0010    5.2196   -0.6294        -14.3182  -2.4981
```

Flight Condition: 14,000 ft, 0.65 Mach

```
        0.0000    0.0000    0.0000    1.0000          0.0000   0.0000
A =   -32.1490   -0.0102   30.6876  -27.1841   B =    3.2771  -6.7577
       -0.0018   -0.0001   -1.0509    1.0000         -0.1255  -0.2087
        0.0003   -0.0010    4.8210   -0.5777        -11.9849  -1.2483
```

Flight Condition: 14,000 ft, 0.6 Mach

```
        0.0000    0.0000    0.0000    1.0000          0.0000   0.0000
A =   -32.1426   -0.0098   31.8444  -28.1420   B =    3.8231  -4.9670
       -0.0022   -0.0001   -0.9408    1.0000         -0.1164  -0.2058
        0.0003   -0.0004    4.2991   -0.5277         -9.9623  -0.8613
```

Flight Condition: 14,000 ft, 0.55 Mach

```
        0.0000    0.0000    0.0000    1.0000          0.0000   0.0000
A =   -32.1322   -0.0087   31.8936  -29.7446   B =    3.9308  -4.2254
       -0.0028   -0.0001   -0.8662    1.0000         -0.1089  -0.1853
        0.0003    0.0002    3.5602   -0.4883         -8.3808  -0.6284
```

Flight Condition: 14,000 ft, 0.5 Mach

```
        0.0000    0.0000    0.0000    1.0000          0.0000   0.0000
A =   -32.1151   -0.0088   31.5910  -32.1056   B =    3.8867  -3.4343
       -0.0037   -0.0001   -0.7893    1.0000         -0.1007  -0.1649
        0.0004    0.0001    3.0968   -0.4492         -6.9347  -0.4166
```

Flight Condition: 14,000 ft, 0.45 Mach

```
        0.0000    0.0000    0.0000    1.0000          0.0000   0.0000
A =   -32.0859   -0.0085   28.8189  -35.3574   B =    3.2049  -2.1644
       -0.0050   -0.0002   -0.6937    1.0000         -0.0926  -0.1440
        0.0004    0.0001    2.8036   -0.4105         -5.6439  -0.1982
```

Flight Condition: 14,000 ft, 0.4 Mach

```
        0.0000    0.0000    0.0000    1.0000         0.0000   0.0000
A =   -32.0320   -0.0090   22.3943  -39.8968   B =   2.2655  -1.8722
       -0.0071   -0.0002   -0.5802    1.0000        -0.0834  -0.1248
        0.0005    0.0001    2.3182   -0.3763        -4.4398  -0.1450
```

Flight Condition: 14,000 ft, 0.35 Mach

```
        0.0000    0.0000    0.0000    1.0000         0.0000   0.0000
A =   -31.9175   -0.0104   17.6824  -46.9432   B =   1.9270  -4.4673
       -0.0109   -0.0002   -0.4728    1.0000        -0.0730  -0.0672
        0.0006    0.0001    1.8844   -0.3560        -3.4005   0.2782
```

Flight Condition: 14,000 ft, 0.3 Mach

```
        0.0000    0.0000    0.0000    1.0000         0.0000   0.0000
A =   -31.6421   -0.0061   17.8659  -57.9781   B =   0.6524  -2.4686
       -0.0183   -0.0003   -0.3965    1.0000        -0.0632  -0.0569
        0.0007    0.0001    1.3232   -0.3805        -2.5582   0.3444
```

Flight Condition: 14,000 ft, 0.25 Mach

```
        0.0000    0.0000    0.0000    1.0000         0.0000   0.0000
A =   -30.8164    0.0196    8.2127  -77.3577   B =  -0.9529  -1.4814
       -0.0349   -0.0004   -0.3112    1.0000        -0.0558  -0.0425
       -0.0004    0.0000    0.1568   -0.4605        -1.7615   0.1750
```

Flight Condition: 18,000 ft, 0.9 Mach

```
        0.0000    0.0000    0.0000    1.0000         0.0000   0.0000
A =   -32.1594   -0.0107   33.1373  -28.3554   B =  -0.9453  14.3090
       -0.0010    0.0000   -1.5498    1.0000        -0.1563  -0.2896
        0.0003   -0.0004    4.4287   -0.7359       -22.8082  -7.1031
```

Flight Condition: 18,000 ft, 0.85 Mach

```
        0.0000    0.0000    0.0000    1.0000         0.0000   0.0000
A =   -32.1564   -0.0110   33.7813  -29.3747   B =  -0.7707  11.8716
       -0.0012   -0.0001   -1.4085    1.0000        -0.1469  -0.2698
        0.0003   -0.0009    4.6260   -0.6862       -19.8074  -5.7001
```

229

Flight Condition: 18,000 ft, 0.8 Mach

```
        0.0000    0.0000    0.0000    1.0000        0.0000    0.0000
A =   -32.1523   -0.0106   33.8536  -30.7268   B = -0.7800    9.8209
       -0.0014   -0.0001   -1.2760    1.0000       -0.1376   -0.2503
        0.0003   -0.0008    4.5196   -0.6377      -17.0651   -4.4756
```

Flight Condition: 18,000 ft, 0.75 Mach

```
        0.0000    0.0000    0.0000    1.0000        0.0000    0.0000
A =   -32.1502   -0.0095   31.0658  -30.1219   B =  0.6827    8.0728
       -0.0016   -0.0001   -1.1479    1.0000       -0.1269   -0.2323
        0.0003   -0.0009    4.3139   -0.5906      -14.5146   -3.4819
```

Flight Condition: 18,000 ft, 0.7 Mach

```
        0.0000    0.0000    0.0000    1.0000        0.0000    0.0000
A =   -32.1471   -0.0085   29.1475  -29.9090   B =  1.8901   -2.0696
       -0.0018   -0.0001   -1.0273    1.0000       -0.1168   -0.1970
        0.0003   -0.0010    4.0470   -0.5446      -12.2165   -1.9520
```

Flight Condition: 18,000 ft, 0.65 Mach

```
        0.0000    0.0000    0.0000    1.0000        0.0000    0.0000
A =   -32.1408   -0.0093   30.5283  -30.8667   B =  3.0186   -5.9469
       -0.0022   -0.0001   -0.9214    1.0000       -0.1091   -0.1829
        0.0003   -0.0010    3.7710   -0.5006      -10.2335   -1.0895
```

Flight Condition: 18,000 ft, 0.6 Mach

```
        0.0000    0.0000    0.0000    1.0000        0.0000    0.0000
A =   -32.1318   -0.0088   31.2822  -32.1163   B =  3.3522   -4.1756
       -0.0026   -0.0001   -0.8267    1.0000       -0.1011   -0.1787
        0.0003   -0.0004    3.4283   -0.4603       -8.5088   -0.6662
```

Flight Condition: 18,000 ft, 0.55 Mach

```
        0.0000    0.0000    0.0000    1.0000        0.0000    0.0000
A =   -32.1173   -0.0075   31.1300  -34.1163   B =  3.4816   -3.4524
       -0.0033   -0.0001   -0.7600    1.0000       -0.0945   -0.1602
        0.0003    0.0001    2.9861   -0.4264       -7.1575   -0.4477
```

Flight Condition: 18,000 ft, 0.5 Mach

```
         0.0000    0.0000    0.0000    1.0000       0.0000   0.0000
A = -32.0936   -0.0075   29.8492  -36.9519   B = -3.4330  -2.4262
        -0.0044   -0.0001   -0.6817    1.0000      -0.0874  -0.1415
         0.0004    0.0001    2.7699   -0.3929      -5.9225  -0.2430
```

Flight Condition: 18,000 ft, 0.45 Mach

```
         0.0000    0.0000    0.0000    1.0000       0.0000   0.0000
A = -32.0531   -0.0073   24.1220  -40.7828   B =  2.6617  -1.8464
        -0.0059   -0.0002   -0.5797    1.0000      -0.0803  -0.1238
         0.0004    0.0001    2.4959   -0.3597      -4.8122  -0.1299
```

Flight Condition: 18,000 ft, 0.4 Mach

```
         0.0000    0.0000    0.0000    1.0000       0.0000   0.0000
A = -31.9747   -0.0082   18.7640  -46.5509   B =  1.9813  -3.1842
        -0.0086   -0.0002   -0.4866    1.0000      -0.0720  -0.0895
         0.0005    0.0001    1.8995   -0.3399      -3.7773   0.0107
```

Flight Condition: 18,000 ft, 0.35 Mach

```
         0.0000    0.0000    0.0000    1.0000       0.0000   0.0000
A = -31.8054   -0.0099   19.3550  -55.4223   B =  1.5535  -3.0116
        -0.0133   -0.0002   -0.3987    1.0000      -0.0632  -0.0564
         0.0006    0.0000    1.9253d  -0.3394      -2.9367   0.3274
```

Flight Condition: 18,000 ft, 0.3 Mach

```
         0.0000    0.0000    0.0000    1.0000       0.0000   0.0000
A = -31.3589    0.0030   10.9466  -70.7275   B = -0.1042  -2.2708
        -0.0230   -0.0003   -0.3144    1.0000      -0.0552  -0.0518
         0.0004    0.0001    0.7266   -0.3968      -2.1851   0.2266
```

Flight Condition: 22,000 ft, 0.9 Mach

```
         0.0000    0.0000    0.0000    1.0000       0.0000   0.0000
A = -32.1556   -0.0089   32.7182  -31.2667   B = -0.9673  12.3245
        -0.0012    0.0000   -1.3438    1.0000      -0.1355  -0.2575
         0.0003   -0.0004    3.4854   -0.6342     -19.4559  -6.1317
```

231

Flight Condition: 22,000 ft, 0.85 Mach

```
        0.0000    0.0000    0.0000    1.0000        0.0000    0.0000
A = -32.1516   -0.0092   33.1820  -32.6659   B = -0.9029   10.2662
     -0.0014   -0.0001   -1.2226    1.0000       -0.1272   -0.2392
      0.0003   -0.0008    3.6189   -0.5912      -16.8790   -4.9160
```

Flight Condition: 22,000 ft, 0.8 Mach

```
        0.0000    0.0000    0.0000    1.0000        0.0000    0.0000
A = -32.1465   -0.0088   32.6936  -34.0209   B = -0.7153    8.5536
     -0.0016   -0.0001   -1.1084    1.0000       -0.1188   -0.2213
      0.0003   -0.0008    3.4979   -0.5493      -14.5178   -3.8630
```

Flight Condition: 22,000 ft, 0.75 Mach

```
        0.0000    0.0000    0.0000    1.0000        0.0000    0.0000
A = -32.1439   -0.0079   29.7815  -33.3828   B =  0.7297    3.9226
     -0.0018   -0.0001   -0.9977    1.0000       -0.1091   -0.1963
      0.0003   -0.0009    3.2901   -0.5087      -12.3246   -2.7491
```

Flight Condition: 22,000 ft, 0.7 Mach

```
        0.0000    0.0000    0.0000    1.0000        0.0000    0.0000
A = -32.1385   -0.0079   29.2537  -33.8576   B =  1.9675   -5.0544
     -0.0021   -0.0001   -0.8954    1.0000       -0.1012   -0.1655
      0.0003   -0.0009    3.1065   -0.4698      -10.3758   -1.4094
```

Flight Condition: 22,000 ft, 0.65 Mach

```
        0.0000    0.0000    0.0000    1.0000        0.0000    0.0000
A = -32.1295   -0.0085   30.1848  -35.1522   B =  2.8210   -5.1979
     -0.0025   -0.0001   -0.8049    1.0000       -0.0944   -0.1580
      0.0003   -0.0009    2.9456   -0.4336       -8.6946   -0.8203
```

Flight Condition: 22,000 ft, 0.6 Mach

```
        0.0000    0.0000    0.0000    1.0000        0.0000    0.0000
A = -32.1167   -0.0077   30.6728  -36.8395   B =  2.9755   -3.3906
     -0.0031   -0.0001   -0.7235    1.0000       -0.0875   -0.1537
      0.0003   -0.0004    2.7733   -0.4003       -7.2322   -0.4626
```

Flight Condition: 22,000 ft, 0.55 Mach

```
         0.0000    0.0000    0.0000    1.0000        0.0000   0.0000
A = -32.0964   -0.0064   29.8824  -39.3114   B =  3.0743  -2.6019
       -0.0039   -0.0001   -0.6564    1.0000       -0.0817  -0.1371
        0.0003    0.0001    2.6459   -0.3714       -6.0831  -0.2751
```

Flight Condition: 22,000 ft, 0.5 Mach

```
         0.0000    0.0000    0.0000    1.0000        0.0000   0.0000
A = -32.0631   -0.0063   25.0218  -42.7143   B =  2.9967  -1.7863
       -0.0052   -0.0001   -0.5651    1.0000       -0.0756  -0.1206
        0.0004    0.0001    2.5765   -0.3428       -5.0334  -0.1229
```

Flight Condition: 22,000 ft, 0.45 Mach

```
         0.0000    0.0000    0.0000    1.0000        0.0000   0.0000
A = -32.0028   -0.0067   19.2694  -47.7705   B =  2.3106  -1.6663
       -0.0072   -0.0002   -0.4761    1.0000       -0.0692  -0.1055
        0.0004    0.0001    2.0689   -0.3229       -4.0799  -0.1306
```

Flight Condition: 22,000 ft, 0.4 Mach

```
         0.0000    0.0000    0.0000    1.0000        0.0000   0.0000
A = -31.8847   -0.0080   16.6361  -55.2176   B =  1.9790  -4.2280
       -0.0105   -0.0002   -0.3987    1.0000       -0.0618  -0.0573
        0.0005    0.0000    1.8429   -0.3112       -3.2305   0.2286
```

Flight Condition: 22,000 ft, 0.35 Mach

```
         0.0000    0.0000    0.0000    1.0000        0.0000   0.0000
A = -31.6324   -0.0055   16.7535  -66.1551   B =  0.6164  -2.4477
       -0.0163   -0.0003   -0.3430    1.0000       -0.0544  -0.0507
        0.0005    0.0001    1.2263   -0.3337       -2.4932   0.2732
```

Flight Condition: 22,000 ft, 0.3 Mach

```
         0.0000    0.0000    0.0000    1.0000        0.0000   0.0000
A = -30.9268    0.0149    9.3812  -86.2052   B = -0.8816  -1.3931
       -0.0287   -0.0003   -0.2812    1.0000       -0.0489  -0.0387
       -0.0001    0.0000    0.2887   -0.4023       -1.8403   0.1853
```

Flight Condition: 26,000 ft, 0.9 Mach

```
        0.0000    0.0000    0.0000    1.0000          0.0000    0.0000
A =   -32.1504   -0.0074   32.3066  -34.8809   B =   -1.0182   10.5448
       -0.0014    0.0000   -1.1604    1.0000          -0.1167   -0.2272
        0.0003   -0.0004    2.7299   -0.5435          -16.4857  -5.2653
```

Flight Condition: 26,000 ft, 0.85 Mach

```
        0.0000    0.0000    0.0000    1.0000          0.0000    0.0000
A =   -32.1447   -0.0077   32.6038  -36.7208   B =   -1.0436    8.8273
       -0.0016   -0.0001   -1.0571    1.0000          -0.1095   -0.2104
        0.0003   -0.0008    2.7933   -0.5065          -14.2904  -4.2162
```

Flight Condition: 26,000 ft, 0.8 Mach

```
        0.0000    0.0000    0.0000    1.0000          0.0000    0.0000
A =   -32.1395   -0.0074   31.1195  -37.4928   B =   -0.3898    6.8315
       -0.0018   -0.0001   -0.9584    1.0000          -0.1016   -0.1936
        0.0003   -0.0008    2.6541   -0.4705          -12.2624  -3.2875
```

Flight Condition: 26,000 ft, 0.75 Mach

```
        0.0000    0.0000    0.0000    1.0000          0.0000    0.0000
A =   -32.1353   -0.0064   28.4955  -37.2294   B =    0.7821   -0.1848
       -0.0021   -0.0001   -0.8636    1.0000          -0.0932   -0.1621
        0.0003   -0.0009    2.4161   -0.4362          -10.3980  -2.0645
```

Flight Condition: 26,000 ft, 0.7 Mach

```
        0.0000    0.0000    0.0000    1.0000          0.0000    0.0000
A =   -32.1264   -0.0071   29.1362  -38.5424   B =    2.0781   -5.9435
       -0.0025   -0.0001   -0.7770    1.0000          -0.0872   -0.1388
        0.0003   -0.0009    2.3830   -0.4040          -8.7604   -0.9883
```

Flight Condition: 26,000 ft, 0.65 Mach

```
        0.0000    0.0000    0.0000    1.0000          0.0000    0.0000
A =   -32.1136   -0.0077   29.7819  -40.3133   B =    2.6433   -4.2897
       -0.0030   -0.0001   -0.6998    1.0000          -0.0813   -0.1354
        0.0003   -0.0009    2.3370   -0.3742          -7.3461   -0.6062
```

Flight Condition: 26,000 ft, 0.6 Mach

```
        0.0000    0.0000    0.0000    1.0000        0.0000   0.0000
A = -32.0952   -0.0068   29.3384  -42.5014  B =   2.6237  -2.6088
     -0.0037   -0.0001   -0.6217    1.0000       -0.0753  -0.1308
      0.0003   -0.0004    2.7507   -0.3472       -6.1146  -0.2784
```

Flight Condition: 26,000 ft, 0.55 Mach

```
        0.0000    0.0000    0.0000    1.0000        0.0000   0.0000
A = -32.0663   -0.0054   24.8845  -45.5421  B =   2.6719  -1.6807
     -0.0047   -0.0001   -0.5397    1.0000       -0.0704  -0.1156
      0.0003    0.0001    2.5580   -0.3227       -5.1425  -0.1073
```

Flight Condition: 26,000 ft, 0.5 Mach

```
        0.0000    0.0000    0.0000    1.0000        0.0000   0.0000
A = -32.0164   -0.0057   19.6408  -50.0936  B =   2.5507  -1.6174
     -0.0063   -0.0001   -0.4608    1.0000       -0.0651  -0.1021
      0.0004    0.0001    2.1749   -0.3043       -4.2555  -0.1150
```

Flight Condition: 26,000 ft, 0.45 Mach

```
        0.0000    0.0000    0.0000    1.0000        0.0000   0.0000
A = -31.9272   -0.0064   16.5774  -56.4384  B =   2.0763  -3.6976
     -0.0087   -0.0002   -0.3935    1.0000       -0.0594  -0.0654
      0.0004    0.0001    1.8059   -0.2912       -3.4448   0.0732
```

Flight Condition: 26,000 ft, 0.4 Mach

```
        0.0000    0.0000    0.0000    1.0000        0.0000   0.0000
A = -31.7515   -0.0072   19.8437  -65.6687  B =   1.1662  -2.6180
     -0.0128   -0.0002   -0.3387    1.0000       -0.0528  -0.0485
      0.0005    0.0001    1.8617   -0.2993       -2.7267   0.2641
```

Flight Condition: 26,000 ft, 0.35 Mach

```
        0.0000    0.0000    0.0000    1.0000        0.0000   0.0000
A = -31.3002    0.0039    8.4819  -82.7277  B =  -0.1514  -2.5498
     -0.0210   -0.0002   -0.2573    1.0000       -0.0474  -0.0417
      0.0003    0.0000    0.6050   -0.3517       -2.1251   0.2159
```

Flight Condition: 26,000 ft, 0.3 Mach

```
        0.0000    0.0000    0.0000    1.0000        0.0000    0.0000
A = -30.2511      0.0360   -2.5161-105.4813  B =  -0.7843  -2.4663
       -0.0361   -0.0003   -0.1702    1.0000       -0.0449  -0.0252
       -0.0005    0.0000   -0.3671   -0.3849        1.5641    0.2375
```

Flight Condition: 30,000 ft, 0.9 Mach

```
        0.0000    0.0000    0.0000    1.0000        0.0000    0.0000
A = -32.1428     -0.0061   31.8627  -39.4235  B =  -1.1166    8.9296
       -0.0016   -0.0001   -0.9970    1.0000       -0.0997   -0.1976
        0.0003   -0.0004    2.1557   -0.4624      -13.8388   -4.4916
```

Flight Condition: 30,000 ft, 0.85 Mach

```
        0.0000    0.0000    0.0000    1.0000        0.0000    0.0000
A = -32.1351     -0.0064   31.9249  -41.5880  B =  -1.1622    6.8048
       -0.0019   -0.0001   -0.9095    1.0000       -0.0935   -0.1813
        0.0003   -0.0007    2.1452   -0.4300      -11.9926   -3.5649
```

Flight Condition: 30,000 ft, 0.8 Mach

```
        0.0000    0.0000    0.0000    1.0000        0.0000    0.0000
A = -32.1298     -0.0057   29.5791  -41.7366  B =  -0.0915    5.2296
       -0.0021   -0.0001   -0.8244    1.0000       -0.0862   -0.1654
        0.0003   -0.0007    1.9695   -0.4002      -10.2681   -2.7791
```

Flight Condition: 30,000 ft, 0.75 Mach

```
        0.0000    0.0000    0.0000    1.0000        0.0000    0.0000
A = -32.1221     -0.0056   28.2165  -42.3777  B =   1.1123   -3.6678
       -0.0024   -0.0001   -0.7437    1.0000       -0.0797   -0.1288
        0.0003   -0.0008    1.8191   -0.3719       -8.7032   -1.4175
```

Flight Condition: 30,000 ft, 0.7 Mach

```
        0.0000    0.0000    0.0000    1.0000        0.0000    0.0000
A = -32.1089     -0.0065   29.1151  -44.3135  B =   2.1226   -4.9686
       -0.0029   -0.0001   -0.6688    1.0000       -0.0748   -0.1178
        0.0003   -0.0008    1.8816   -0.3456       -7.3431   -0.7534
```

236

Flight Condition: 30,000 ft, 0.65 Mach

```
        0.0000    0.0000    0.0000    1.0000        0.0000   0.0000
A = -32.0904   -0.0071   27.4961  -46.6131  B =   2.4433  -3.3079
     -0.0036   -0.0001   -0.5917    1.0000       -0.0697  -0.1142
      0.0003   -0.0009    2.1986   -0.3217       -6.1665  -0.3962
```

Flight Condition: 30,000 ft, 0.6 Mach

```
        0.0000    0.0000    0.0000    1.0000        0.0000   0.0000
A = -32.0640   -0.0060   23.9335  -49.3741  B =   2.2557  -1.5574
     -0.0045   -0.0001   -0.5044    1.0000       -0.0646  -0.1090
      0.0003   -0.0004    2.5022   -0.3004       -5.1389  -0.0785
```

Flight Condition: 30,000 ft, 0.55 Mach

```
        0.0000    0.0000    0.0000    1.0000        0.0000   0.0000
A = -32.0197   -0.0049   19.1986  -53.6084  B =   2.2337  -1.5512
     -0.0058   -0.0001   -0.4346    1.0000       -0.0604  -0.0970
      0.0003    0.0001    2.2250   -0.2848       -4.3218  -0.0947
```

Flight Condition: 30,000 ft, 0.5 Mach

```
        0.0000    0.0000    0.0000    1.0000        0.0000   0.0000
A = -31.9453   -0.0055   16.3750  -59.3404  B =   2.1582  -2.3112
     -0.0077   -0.0001   -0.3781    1.0000       -0.0559  -0.0773
      0.0004    0.0001    1.7976   -0.2731       -3.5762  -0.0735
```

Flight Condition: 30,000 ft, 0.45 Mach

```
        0.0000    0.0000    0.0000    1.0000        0.0000   0.0000
A = -31.8042   -0.0063   18.5182  -67.9412  B =   1.3656  -2.8570
     -0.0109   -0.0002   -0.3214    1.0000       -0.0503  -0.0460
      0.0004    0.0000    2.0308   -0.2759       -2.8834   0.2386
```

Flight Condition: 30,000 ft, 0.4 Mach

```
        0.0000    0.0000    0.0000    1.0000        0.0000   0.0000
A = -31.5127   -0.0017   12.3981  -80.8201  B =   0.1373  -2.5923
     -0.0163   -0.0002   -0.2733    1.0000       -0.0448  -0.0431
      0.0004    0.0000    0.8712   -0.3038       -2.2822   0.1731
```

Flight Condition: 30,000 ft, 0.35 Mach

```
        0.0000    0.0000    0.0000    1.0000        0.0000    0.0000
A = -30.8031    0.0187    8.5235-102.0108   B = -0.8702  -1.7816
     -0.0267   -0.0002   -0.2365    1.0000       -0.0417   -0.0303
     -0.0002    0.0000    0.1110   -0.3536        1.7818    0.1746
```

Flight Condition: 34,000 ft, 0.9 Mach

```
        0.0000    0.0000    0.0000    1.0000        0.0000    0.0000
A = -32.1324   -0.0049   31.3064  -44.7614   B = -1.1430    6.7633
     -0.0019   -0.0001   -0.8530    1.0000       -0.0847   -0.1694
      0.0002   -0.0003    1.6794   -0.3892      -11.5448   -3.7862
```

Flight Condition: 34,000 ft, 0.85 Mach

```
        0.0000    0.0000    0.0000    1.0000        0.0000    0.0000
A = -32.1226   -0.0049   30.8306  -46.9536   B = -0.9896    5.6691
     -0.0022   -0.0001   -0.7789    1.0000       -0.0791   -0.1555
      0.0002   -0.0006    1.6010   -0.3626       -9.9930   -3.0202
```

Flight Condition: 34,000 ft, 0.8 Mach

```
        0.0000    0.0000    0.0000    1.0000        0.0000    0.0000
A = -32.1161   -0.0043   28.1732  -46.9351   B =  0.1797    0.7674
     -0.0025   -0.0001   -0.7061    1.0000       -0.0726   -0.1297
      0.0002   -0.0007    1.3805   -0.3383       -8.5408   -2.0317
```

Flight Condition: 34,000 ft, 0.75 Mach

```
        0.0000    0.0000    0.0000    1.0000        0.0000    0.0000
A = -32.1027   -0.0052   27.7174  -48.8071   B =  1.4527   -5.4077
     -0.0029   -0.0001   -0.6320    1.0000       -0.0681   -0.1018
      0.0002   -0.0008    1.5937   -0.3154       -7.2383   -0.9031
```

Flight Condition: 34,000 ft, 0.7 Mach

```
        0.0000    0.0000    0.0000    1.0000        0.0000    0.0000
A = -32.0835   -0.0060   25.3429  -51.3329   B =  2.1302   -3.6767
     -0.0035   -0.0001   -0.5556    1.0000       -0.0638   -0.0986
      0.0003   -0.0008    1.9931   -0.2944       -6.1176   -0.4988
```

Flight Condition: 34,000 ft, 0.65 Mach

```
        0.0000    0.0000    0.0000    1.0000        0.0000   0.0000
A = -32.0568   -0.0065   22.2663  -54.2504  B =   2.2139  -2.3546
       -0.0043   -0.0001   -0.4779    1.0000       -0.0595  -0.0951
        0.0003   -0.0009    2.2699   -0.2756       -5.1454  -0.2089
```

Flight Condition: 34,000 ft, 0.6 Mach

```
        0.0000    0.0000    0.0000    1.0000        0.0000   0.0000
A = -32.0148   -0.0057   17.9322  -58.3606  B =   1.8413  -1.4707
       -0.0054   -0.0001   -0.4001    1.0000       -0.0553  -0.0907
        0.0003   -0.0004    2.2327   -0.2647       -4.2934  -0.0763
```

Flight Condition: 34,000 ft, 0.55 Mach

```
        0.0000    0.0000    0.0000    1.0000        0.0000   0.0000
A = -31.9478   -0.0047   15.7087  -63.7817  B =   1.8574  -1.3914
       -0.0071   -0.0001   -0.3535    1.0000       -0.0517  -0.0810
        0.0003    0.0001    1.8135   -0.2546       -3.6097  -0.1241
```

Flight Condition: 34,000 ft, 0.5 Mach

```
        0.0000    0.0000    0.0000    1.0000        0.0000   0.0000
A = -31.8282   -0.0056   16.7474  -71.7205  B =   1.3982  -3.5083
       -0.0096   -0.0001   -0.3003    1.0000       -0.0472  -0.0436
        0.0004    0.0000    2.0240   -0.2551       -2.9656   0.1677
```

Flight Condition: 34,000 ft, 0.45 Mach

```
        0.0000    0.0000    0.0000    1.0000        0.0000   0.0000
A = -31.6185   -0.0046   14.3289  -81.8577  B =   0.5153  -2.5631
       -0.0135   -0.0002   -0.2700    1.0000       -0.0424  -0.0408
        0.0004    0.0000    1.0496   -0.2694       -2.3903   0.1522
```

Flight Condition: 34,000 ft, 0.4 Mach

```
        0.0000    0.0000    0.0000    1.0000        0.0000   0.0000
A = -31.0439    0.0105    8.0406 -103.9423  B =  -0.7184  -2.4958
       -0.0216   -0.0002   -0.2205    1.0000       -0.0393  -0.0297
        0.0000    0.0000    0.3937   -0.3236       -1.9481   0.2287
```

Flight Condition: 38,000 ft, 0.9 Mach

```
        0.0000    0.0000    0.0000    1.0000         0.0000    0.0000
A = -32.1172   -0.0038   30.8408  -51.7604   B = -1.1699    5.5244
       -0.0022   -0.0001   -0.7213    1.0000        -0.0709   -0.1430
        0.0002   -0.0003    1.2864   -0.3225        -9.5743   -3.1572
```

Flight Condition: 38,000 ft, 0.85 Mach

```
        0.0000    0.0000    0.0000    1.0000         0.0000    0.0000
A = -32.1070   -0.0037   28.9780  -53.1253   B = -0.4986    4.7349
       -0.0025   -0.0001   -0.6545    1.0000        -0.0657   -0.1320
        0.0002   -0.0006    1.2741   -0.3015        -8.2649   -2.5621
```

Flight Condition: 38,000 ft, 0.8 Mach

```
        0.0000    0.0000    0.0000    1.0000         0.0000    0.0000
A = -32.0951   -0.0037   26.2610  -54.2606   B =  0.6600   -3.3294
       -0.0029   -0.0001   -0.5870    1.0000        -0.0608   -0.0950
        0.0002   -0.0007    1.4028   -0.2820        -7.0516   -1.2971
```

Flight Condition: 38,000 ft, 0.75 Mach

```
        0.0000    0.0000    0.0000    1.0000         0.0000    0.0000
A = -32.0744   -0.0048   23.0363  -57.1571   B =  1.6924   -3.8681
       -0.0035   -0.0001   -0.5114    1.0000        -0.0574   -0.0835
        0.002    -0.0007    1.8436   -0.2638        -5.9839   -0.5967
```

Flight Condition: 38,000 ft, 0.7 Mach

```
        0.0000    0.0000    0.0000    1.0000         0.0000    0.0000
A = -32.0459   -0.0057   20.1578  -60.4982   B =  2.0538   -3.0343
       -0.0042   -0.0001   -0.4428    1.0000        -0.0538   -0.0816
        0.0002   -0.0008    2.0441   -0.2484        -5.0675   -0.3653
```

Flight Condition: 38,0000 ft, 0.65 Mach

```
        0.0000    0.0000    0.0000    1.0000         0.0000    0.0000
A = -32.0028   -0.0065   16.3861  -64.9370   B =  1.9161   -2.1631
       -0.0053   -0.0001   -0.3751    1.0000        -0.0503   -0.0788
        0.0003   -0.0009    1.9789   -0.2394        -4.2700   -0.2208
```

Flight Condition: 38,000 ft, 0.6 Mach

```
        0.0000    0.0000    0.0000    1.0000        0.0000    0.0000
A = -31.9389   -0.0057   14.5232  -70.2645  B =   1.4981   -1.3132
     -0.0067   -0.0001   -0.3194    1.0000       -0.0467   -0.0747
      0.0003   -0.0005    1.8149   -0.2341       -3.5656   -0.1188
```

Flight Condition: 38,000 ft, 0.55 Mach

```
        0.0000    0.0000    0.0000    1.0000        0.0000    0.0000
A = -31.8311   -0.0049   15.5895  -77.8026  B =   1.2700   -3.6987
     -0.0088   -0.0001   -0.2740    1.0000       -0.0433   -0.0398
      0.0003    0.0000    2.0114   -0.2346       -2.9784    0.1275
```

Flight Condition: 38,000 ft, 0.5 Mach

```
        0.0000    0.0000    0.0000    1.0000        0.0000    0.0000
A = -31.6553   -0.0048   14.8821  -87.0302  B =   0.5640   -2.5569
     -0.0119   -0.0001   -0.2523    1.0000       -0.0391   -0.0376
      0.0003    0.0000    1.2438   -0.2439       -2.4339    0.1274
```

Flight Condition: 38,000 ft, 0.45 Mach

```
        0.0000    0.0000    0.0000    1.0000        0.0000    0.0000
A = -31.1779    0.0064    6.1007 -108.6833  B =  -0.4276   -2.9478
     -0.0182   -0.0002   -0.1880    1.0000       -0.0365   -0.0273
      0.0001    0.0000    0.4764   -0.2895       -2.0557    0.2277
```

Appendix B

This appendix presents the mathematical development of
obtaining the Nth order autoregressive vector difference
equation that results in a set of parameters representing an
aircraft model at a given flight condition.   This appendix
was taken largely from material presented by Pineiro (1).

242

The difference equation model used in this thesis for the open-loop longitudinal dynamics of the host airplane is based on the discrete state and output relationships given in Equations (2-8) and (2-9) (Equations (2-8) and (2-9) repeated here for reading continuity):

$$\underline{x}[(k+1)T] = \underline{\Phi}\,\underline{x}(kT) + \underline{\Psi}\,\underline{u}(kT) \qquad (A-1)$$

$$\underline{y}(kT) = \underline{C}\,\underline{x}(kT) \qquad (A-2)$$

By taking the Z transform of Equations (A-1) and (A-2) and obtaining a transfer function model, the desired input-output relationship can be obtained.

$$\gamma\{\underline{x}(k+1)\} = z\underline{I}X(z) = \underline{\Phi}X(z) + \underline{\Psi}\,\underline{U}(z) \qquad (A-3)$$

$$\gamma\{\underline{y}(k)\} = \underline{y}(z) = \underline{C}X(z) \qquad (A-4)$$

Rearranging equation (A-3) yields

$$z\underline{I}X(z) - \underline{\Phi}\underline{x}(z) = \underline{\Psi}\,\underline{U}(z) \qquad (A-5)$$

Therefore,

$$[z\underline{I} - \underline{\Phi}]\underline{X}(z) = \underline{\Psi}\,\underline{U}(z) \qquad (A-6)$$

$$\underline{X}(z) = [z\underline{I} - \underline{\Phi}]^{-1}\underline{\Psi}\,\underline{U}(z) \qquad (A-7)$$

By substituting Equation (A-2) into Equation (A-7) and per-

243

forming some matrix manipulation the following expression

for $\underline{Y}(z)$ is obtained

$$\underline{Y}(z) = \underline{C}[z\underline{I} - \underline{\Phi}]^{-1}\underline{\Psi}\underline{U}(z) \qquad (A-8)$$

$$= \underline{G}(z)\underline{U}(z) \qquad (A-9)$$

The m x 1 vector $\underline{Y}(z)$, the m x m matrix $\underline{G}(z)$, and the m x 1

vector $\underline{U}(z)$ are given by

$$\underline{Y}(z) = \begin{bmatrix} Y_1(z) \\ Y_2(z) \\ \cdot \\ \cdot \\ Y_3(z) \end{bmatrix} \qquad (A-10)$$

$$\underline{G}(z) = \begin{bmatrix} G_{11}(z) & G_{12}(z) & \cdots & G_{1m}(z) \\ G_{21}(z) & G_{22}(z) & \cdots & G_{2m}(z) \\ \cdots & \cdots & \cdots & \cdots \\ G_{m1}(z) & G_{m2}(z) & \cdots & G_{mm}(z) \end{bmatrix} \qquad (A-11)$$

$$\underline{U}(z) = \begin{bmatrix} U_1(z) \\ U_2(z) \\ \cdot \\ \cdot \\ U_m(z) \end{bmatrix} \qquad (A-12)$$

The elements of $\underline{G}(z)$, denoted $G_{ij}(z)$, are the transfer

functions relating the output Y_i to the control input U_j

and are of the form

244

$$G_{ij}(z) = \frac{b_1 z^w + b_2 z^{w-1} + \ldots + b_w z + b_{w+1}}{z^n + a_1 z^{n-1} + \ldots + a_{n-1} z + a_n} \quad (w < n) \quad (A-13)$$

By dividing the numerator and denominator of each transfer function $\underline{G}(z)$ by z^n, the transfer function matrix is transformed into the delay operator form given by

$$G_{ij}(z) = \frac{b_1 z^{w-n} + b_2 z^{w-n-1} + \ldots + b_{w+1} z^{-n}}{1 + a_1 z^{-1} + \ldots + a_{n-1} z^{-n+1} + a_n z^{-n}} \quad (w < n) \quad (A-14)$$

By grouping the coefficients with the same amount of delay in every transfer function $G_{ij}(z)$ in $\underline{G}(z)$, and taking the inverse Z transform, the Nth order autoregressive difference equation of the open-loop plant is obtained

$$\underline{y}(kT) = \underline{B}_1 \underline{u}\{(k-1)T\} - \underline{A}_1 \underline{y}\{(k-1)T\} + \ldots$$

$$+ \underline{B}_n \underline{u}\{(k-N)T\} - \underline{A}_n \underline{y}\{(k-N)T\} + \underline{e}(kT) \quad (A-15)$$

or

$$\underline{y}(kT) = \Upsilon^T(kT) \underline{\theta} + \underline{e}(kT) \quad (A-16)$$

where $\underline{e}(kT)$ is an equation error term assumed to be a zero-mean Gaussian white noise vector added to account for modelling errors, $\underline{\Upsilon}^T(kT) \in R^{m \times l}$ is a matrix of past values of

245

$\{\underline{y}(kT)$ and $\underline{u}(kT)\}$, and the matrices $A_i \in R^{m \times m}$ $(i=1,2,\ldots,N)$, $B_i \in R^{m \times m}$ $(i=1,2,\ldots N)$ and the vector $\underline{\theta} \in R^l$ are the parameters of the Nth order difference equation.

Appendix C

This Appendix presents the position limits for the
elevators and flaperons for each flight condition. As dis-
cussed in Chapter 2, the reason for the different position
limits is due to the fact that the trim values for the
elevator and flaperon positions differ for each flight con-
dition.

| Flight Condition | | Elevator Position | Flaperon Position |
Alt (Kft)	Mach	Limits	Limits
10	.90	27.3171,-22.6829	22.0000,-21.0000
10	.85	27.1407,-22.8259	22.0000,-21.0000
10	.80	27.0100,-22.9900	22.0000,-21.0000
10	.75	26.9343,-23.0657	21.5916,-21.4084
10	.70	26.9769,-23.0231	20.5543,-22.4457
10	.65	26.9687,-23.0313	20.5019,-22.4981
10	.60	26.9011,-23.0988	18.4067,-24.5933
10	.55	27.0884,-22.9116	17.2362,-25.7638
10	.50	27.2365,-22.7635	15.9609,-27.0390
10	.45	27.3375,-22.6625	14.4776,-28.5224
10	.40	27.3085,-22.6915	12.6417,-30.3583
10	.35	27.1404,-22.8597	10.1102,-32.8898
10	.30	26.1426,-23.8574	6.0729,-36.9271
10	.25	25.1583,-24.8417	5.0000,-38.0000
14	.90	27.2899,-22.7100	22.0000,-21.0000
14	.85	27.1375,-22.8625	22.0000,-21.0000
14	.80	26.9598,-23.0402	22.0000,-21.0000
14	.75	26.9439,-23.0561	21.3222,-21.6778
14	.70	26.9699,-23.0301	20.2337,-22.7664
14	.65	26.9715,-23.0285	19.0859,-23.0141
14	.60	26.8681,-23.1319	17.9156,-25.0844
14	.55	27.0560,-22.9440	16.6666,-26.3333
14	.50	27.2062,-22.7939	15.2683,-27.7317
14	.45	27.2496,-22.7504	13.6179,-29.6321
14	.40	27.1438,-22.8562	11.5134,-31.4867
14	.35	26.7824,-23.2176	8.4601,-34.5399
14	.30	25.3368,-24.6633	5.0000,-38.0000
14	.25	25.2301,-24.7699	5.0000,-38.0000
18	.90	27.2598,-22.7402	22.0000,-21.0000
18	.85	27.0957,-22.9043	22.0000,-21.0000
18	.80	26.9013,-23.0987	22.0000,-21.0000
18	.75	26.9586,-23.0414	20.9971,-22.0029
18	.70	26.9793,-23.0207	19.8341,-23.1659
18	.65	26.9669,-23.0331	18.5947,-24.4053
18	.60	26.8530,-23.1470	17.3436,-25.6564
18	.55	27.0466,-22.9534	15.9830,-27.0170
18	.50	27.1503,-22.8497	14.4367,-28.5633
18	.45	27.1075,-22.6925	12.5850,-30.4150
18	.40	26.9715,-23.0285	10.0985,-32.9015
18	.35	26.1469,-23.8531	6.4130,-36.5870

18	.30	25.0717,-24.9282	5.0000,-38.0000
22	.90	27.2262,-22.7738	22.0000,-21.0000
22	.85	27.0477,-22.9532	22.0000,-21.0000
22	.80	26.8873,-23.1127	21.8248,-21.1753
22	.75	26.9801,-23.0199	20.6028,-22.3972
22	.70	27.0164,-22.9836	19.3353,-23.6647
22	.65	27.0194,-22.9806	18.0135,-24.9865
22	.60	26.8667,-23.1333	16.6537,-26.3463
22	.55	27.0119,-22.9880	15.1578,-27.8422
22	.50	27.0199,-22.9801	13.5678,-29.5678
22	.45	26.9190,-23.0810	11.2427,-31.7573
22	.40	26.5847,-23.4153	8.2382,-33.7618
22	.35	25.3709,-24.6792	5.0000,-38.0000
22	.30	25.1478,-24.8523	5.0000,-38.0000
26	.90	27.1877,-22.8123	22.0000,-21.0000
26	.85	26.9906,-23.0094	22.0000,-21.0000
26	.80	26.9366,-23.0634	21.4198,-21.5802
26	.75	27.0291,-22.9709	20.1317,-22.8683
26	.70	27.1280,-22.8720	18.7323,-24.2677
26	.65	27.0930,-22.9170	17.3037,-25.6963
26	.60	26.8501,-23.1499	15.8139,-27.1861
26	.55	26.8977,-23.1023	14.1526,-28.8474
26	.50	26.8249,-23.1751	12.1327,-30.8673
26	.45	26.7082,-23.2918	9.5537,-33.4464
26	.40	25.7882,-24.2118	5.9549,-37.0451
26	.35	25.0313,-24.9687	5.0000,-38.0000
26	.30	25.1150,-24.8850	5.0000,-38.0000
30	.90	27.1405,-22.8595	22.0000,-21.0000
30	.85	26.9340,-23.0660	22.0000,-21.0000
30	.80	27.0269,-22.9731	20.9211,-22.0789
30	.75	27.1622,-22.8378	19.5016,-23.4984
30	.70	27.2342,-22.7658	17.9817,-25.0183
30	.65	27.1207,-22.8793	16.4251,-26.5749
30	.60	26.7404,-23.2596	14.7789,-28.2211
30	.55	26.6819,-23.3181	12.8383,-30.1617
30	.50	26.6237,-23.3767	10.4812,-32.5189
30	.45	26.0799,-23.9201	7.2889,-35.7111
30	.40	25.1127,-24.8873	5.0000,-38.0000
30	.35	24.9556,-25.0444	5.0000,-38.0000
34	.90	27.0970,-22.9030	22.0000,-21.0000
34	.85	26.9523,-23.0477	21.7643,-21.2357
34	.80	27.1475,-22.8525	20.3042,-22.6952
34	.75	27.3222,-22.6778	18.7056,-24.2944
34	.70	27.3322,-22.6678	17.0547,-25.9453

34	.65	27.0784,-22.9216	15.3424,-27.6576
34	.60	26.5003,-23.4997	13.4120,-29.5880
34	.55	26.4581,-23.5419	11.1563,-31.8437
34	.50	26.1650,-23.8349	8.2467,-34.7533
34	.45	25.2234,-24.7766	5.0000,-38.0000
34	.40	24.8747,-25.1254	5.0000,-38.0000
38	.90	27.0418,-22.9582	22.0000,-21.0000
38	.85	27.1003,-22.8997	21.1088,-21.8912
38	.80	27.3384,-22.6616	19.4861,-23.5136
38	.75	27.4664,-22.5336	17.7164,-25.2836
38	.70	27.3436,-22.6564	15.8939,-27.1061
38	.65	26.9336,-23.0665	13.8919,-29.1081
38	.60	26.2547,-23.7453	11.6644,-31.3356
38	.55	26.0784,-23.9316	8.9181,-34.0819
38	.50	25.2212,-24.7788	5.5550,-37.4450
38	.45	24.9137,-25.0863	5.0000,-38.0000

Appendix D

This Appendix presents the parameter vectors for the flight conditions specifically addressed in this thesis. Recall that the parameter vector is a set of parameters associated with a given flight condition that are used in the autoregressive difference equation form of the aircraft model.

Flight Condition: 10,000 ft, 0.35 Mach

$A_1 = -3.990568$ $\underline{B}_1 =$ 0.000842   0.001033
                                 -0.039268   0.000310

$A_2 = 5.971522$ $\underline{B}_2 =$ -0.002524   -0.003096
                                 0.117563   -0.000950

$A_3 = -3.971342$ $\underline{B}_3 =$ 0.002520   0.003092
                                 -0.117320   0.000969

$A_4 = 0.990387$ $\underline{B}_4 =$ -0.000838   -0.001029
                                 0.039025   -0.000329

Flight Condition: 10,000 ft, 0.40 Mach

$A_1 = -3.989059$ $\underline{B}_1 =$ 0.000957   0.001442
                                 -0.051883   -0.001841

$A_2 = 5.966940$ $\underline{B}_2 =$ -0.002871   -0.004321
                                 0.155263   0.005471

$A_3 = -3.966701$ $\underline{B}_3 =$ 0.002866   0.004315
                                 -0.154875   -0.005419

$A_4 = 0.988821$ $\underline{B}_4 =$ -0.000952   -0.001436
                                 0.051495   0.001789

Flight Condition: 10,000 ft, 0.50 Mach

$A_1 = -3.986201$ $\underline{B}_1 =$ 0.001149   0.001891
                                 -0.080647   -0.005754

$A_2 = 5.958298$ $\underline{B}_2 =$ -0.003451   -0.005664
                                 0.241174   0.017146

$A_3 = -3.957994$ $\underline{B}_3 =$ 0.003444   0.005655
                                 -0.240404   -0.017027

$A_4 = 0.985896$ $\underline{B}_4 =$ -0.001143   -0.001881
                                 0.079878   0.005636

Flight Condition: 10,000 ft, 0.65 Mach

A_1 = -3.981994 $\underline{B}_1$ =   0.001427   0.002386
                             -0.139296   -0.016365

A_2 = 5.945443 $\underline{B}_2$ =   -0.004298   -0.007146
                              0.416132   0.048754

A_3 = -3.944927 $\underline{B}_3$ =   0.004279   0.007130
                             -0.414375   -0.048414

A_4 = 0.981466 $\underline{B}_4$ =   -0.001417   -0.002370
                              0.137539   0.016024

Flight Condition: 10,000 ft, 0.75 Mach

A_1 = -3.977787 $\underline{B}_1$ =   0.001672   0.002931
                             -0.197434   -0.046029

A_2 = 5.932799 $\underline{B}_2$ =   -0.005032   -0.008782
                              0.589214   0.137196

A_3 = -3.932239 $\underline{B}_3$ =   0.005019   0.008757
                             -0.586125   -0.136303

A_4 = 0.977226 $\underline{B}_4$ =   -0.001658   -0.002908
                              0.194345   0.045136

Flight Condition: 10,000 ft, 0.80 Mach

A_1 = -3.975528 $\underline{B}_1$ =   0.001793   0.003139
                             -0.231040   -0.059402

A_2 = 5.926021 $\underline{B}_2$ =   -0.005404   -0.009403
                              0.689126   0.176989

A_3 = -3.925456 $\underline{B}_3$ =   0.005388   0.009376
                             -0.685132   -0.175772

A_4 = 0.974963 $\underline{B}_4$ =   -0.001778   -0.003112
                              0.227046   0.058185

Flight Condition: 10,000 ft, 0.90 Mach

A_1 = -3.970230 $\underline{B}_1$ =

0.002019	0.003569
-0.307304	-0.093715

A_2 = 5.911380 $\underline{B}_2$ =

-0.006103	-0.010695
0.915522	0.278993

A_3 = -3.910892 $\underline{B}_3$ =

0.006083	0.010660
-0.909132	-0.276841

A_4 = 0.970134 $\underline{B}_4$ =

-0.002000	-0.003534
0.300914	0.091562

Flight Condition: 14,000 ft, 0.80 Mach

A_1 = -3.978575 $\underline{B}_1$ =

0.001567	0.002800
-0.198759	-0.051639

A_2 = 5.935265 $\underline{B}_2$ =

-0.004720	-0.008388
0.593277	0.154001

A_3 = -3.934805 $\underline{B}_3$ =

0.004709	0.008367
-0.590276	-0.153085

A_4 = 0.978115 $\underline{B}_4$ =

-0.001555	-0.002779
0.195758	0.050722

Flight Condition: 18,000 ft, 0.45 Mach

A_1 = -3.990800 $\underline{B}_1$ =

0.000800	0.001234
-0.048047	-0.001312

A_2 = 5.972188 $\underline{B}_2$ =

-0.002400	-0.003699
0.143841	0.003898

A_3 = -3.971961 $\underline{B}_3$ =

0.002397	0.003694
-0.143541	-0.003859

A_4 = 0.905786 $\underline{B}_4$ =

-0.000797	-0.001229
0.047746	0.001274

Flight Condition: 18,000 ft, 0.80 Mach

A_1 = -3.981308 $\underline{B}_1$ =   0.001363   0.002486
                                          -0.170151   -0.044673

A_2 = 5.943556 $\underline{B}_2$ =   -0.004105   -0.007449
                                           0.508218   0.133337

A_3 = -3.943189 $\underline{B}_3$ =   0.004096   0.007433
                                          -0.505982   -0.132653

A_4 = 0.980940 $\underline{B}_4$ =   -0.001355   -0.002470
                                           0.167915   0.043990

Flight Condition: 22,000 ft, 0.45 Mach

A_1 = -3.992165 $\underline{B}_1$ =   0.000690   0.001052
                                          -0.040741   -0.001314

A_2 = 5.976305 $\underline{B}_2$ =   -0.002071   -0.003153
                                           0.122015   0.003916

A_3 = -3.976116 $\underline{B}_3$ =   0.002068   0.003149
                                          -0.121805   -0.003888

A_4 = 0.991975 $\underline{B}_4$ =   -0.000688   -0.001048
                                           0.040531   0.001286

Flight Condition: 22,000 ft, 0.65 Mach

A_1 = -3.987867 $\underline{B}_1$ =   0.000938   0.001573
                                          -0.086776   -0.008208

A_2 = 5.963342 $\underline{B}_2$ =   -0.002819   -0.004714
                                           0.259598   0.024513

A_3 = -3.963082 $\underline{B}_3$ =   0.002815   0.004706
                                          -0.258867   -0.024401

A_4 = 0.987607 $\underline{B}_4$ =   -0.000934   -0.001566
                                           0.086045   0.008096

255

Flight Condition: 22,000 ft, 0.90 Mach

A_1 = -3.992314

$\underline{B}_1$ =
| 0.001351 | 0.002570 |
| -0.194202 | -0.061218 |

A_2 = 5.976828

$\underline{B}_2$ =
| -0.004055 | -0.007702 |
| 0.581808 | 0.183375 |

A_3 = -3.976713

$\underline{B}_3$ =
| 0.004050 | 0.007692 |
| -0.581010 | -0.183095 |

A_4 = 0.992199

$\underline{B}_4$ =
| -0.001345 | -0.002559 |
| 0.193404 | 0.060938 |

Flight Condition: 26,000 ft, 0.70 Mach

A_1 = -3.988397

$\underline{B}_1$ =
| 0.000867 | 0.001382 |
| -0.087440 | -0.009880 |

A_2 = 5.964985

$\underline{B}_2$ =
| -0.002607 | -0.004142 |
| 0.261618 | 0.029530 |

A_3 = -3.964777

$\underline{B}_3$ =
| 0.002603 | 0.004137 |
| -0.260914 | -0.029421 |

A_4 = 0.988189

$\underline{B}_4$ =
| -0.000864 | -0.001376 |
| 0.086737 | 0.009770 |

Flight Condition: 30,000 ft, 0.50 Mach

A_1 = -3.993622

$\underline{B}_1$ =
| 0.000557 | 0.000771 |
| -0.035718 | -0.000740 |

A_2 = 5.980699

$\underline{B}_2$ =
| -0.001673 | -0.002313 |
| 0.107009 | 0.002205 |

A_3 = -3.980531

$\underline{B}_3$ =
| 0.001671 | 0.002311 |
| -0.106863 | -0.002189 |

A_4 = 0.993454

$\underline{B}_4$ =
| -0.000556 | -0.000769 |
| 0.035572 | 0.000724 |

Flight Condition: 34,000 ft, 0.60 Mach

A_1 = -3.988733 $\underline{B}_1$ =   0.000786   0.001548
                                       -0.099757   -0.030160

A_2 = 5.966067 $\underline{B}_2$ =   -0.002364   -0.004641
                                        0.298482   0.090220

A_3 = -3.965934 $\underline{B}_3$ =   0.002362   0.004636
                                       -0.297690   -0.089960

A_4 = 0.988600 $\underline{B}_4$ =   -0.000783   -0.001542
                                        0.098966   0.029899

Flight Condition: 34,000 ft, 0.85 Mach

A_1 = -3.993531 $\underline{B}_1$ =   0.000551   0.000905
                                       -0.042884   -0.000771

A_2 = 5.980380 $\underline{B}_2$ =   -0.001654   -0.002714
                                        0.128468   0.002292

A_3 = -3.980166 $\underline{B}_3$ =   0.001652   0.002711
                                       -0.128282   -0.002268

A_4 = 0.993317 $\underline{B}_4$ =   -0.000549   -0.000903
                                        0.042698   0.000748

Flight Condition: 38,000 ft, 0.60 Mach

A_1 = -3.994599 $\underline{B}_1$ =   0.000466   0.000745
                                       -0.035619   -0.001193

A_2 = 5.983623 $\underline{B}_2$ =   -0.001398   -0.002236
                                        0.106733   0.003562

A_3 = -3.983447 $\underline{B}_3$ =   0.001397   0.002234
                                       -0.106609   -0.003545

A_4 = 0.994423 $\underline{B}_4$ =   -0.000465   -0.000744
                                        0.035495   0.001176

Flight Condition: 38,000 ft, 0.65 Mach

A_1 = -3.994002 $\underline{B}_1$ =   0.000501   0.000786
                                        -0.042655   -0.002213

A_2 =   5.981814 $\underline{B}_2$ =   -0.001504   -0.002357
                                          0.127793   0.006616

A_3 = -3.981620 $\underline{B}_3$ =   0.001503   0.002355
                                        -0.127620   -0.006592

A_4 =   0.993808 $\underline{B}_4$ =   -0.000500   -0.000784
                                        0.042482   0.002189

Flight Condition: 38,000 ft, 0.70 Mach

A_1 = -3.993253 $\underline{B}_1$ =   0.000536   0.000814
                                        -0.050619   -0.003657

A_2 =   5.979562 $\underline{B}_2$ =   -0.001611   -0.002441
                                          0.151622   0.010938

A_3 = -3.979365 $\underline{B}_3$ =   0.001609   0.002439
                                        -0.151384   -0.010905

A_4 =   0.993056 $\underline{B}_4$ =   -0.000535   -0.000812
                                        0.050382   0.003624

Flight Condition: 38,000 ft, 0.80 Mach

A_1 = -3.991436 $\underline{B}_1$ =   0.000605   0.000946
                                        -0.070422   -0.012959

A_2 =   5.974184 $\underline{B}_2$ =   -0.001818   -0.002837
                                          0.210843   0.038788

A_3 = -3.974057 $\underline{B}_3$ =   0.001816   0.002835
                                        -0.210419   -0.038698

A_4 =   0.991310 $\underline{B}_4$ =   -0.000603   -0.000943
                                        0.069998   0.012869

Flight Condition: 38,000 ft, 0.90 Mach

$$A_1 = -3.989684 \qquad \underline{B}_1 = \begin{array}{cc} 0.000705 & 0.001424 \\ -0.095594 & -0.031531 \end{array}$$

$$A_2 = 5.968947 \qquad \underline{B}_2 = \begin{array}{cc} -0.002120 & -0.004271 \\ 0.286084 & 0.094348 \end{array}$$

$$A_3 = -3.968841 \qquad \underline{B}_3 = \begin{array}{cc} 0.002118 & 0.004267 \\ -0.285385 & -0.094101 \end{array}$$

$$A_4 = 0.989578 \qquad \underline{B}_4 = \begin{array}{cc} -0.000703 & -0.001420 \\ 0.094895 & 0.031285 \end{array}$$

Bibliography

1. Pineiro, L. A., Parameter-Adaptive Model Following for In-Flight Simulation. MS Thesis, GE/ENG/87M, School of Engineering, Air Force Institute of Technology, Wright Patterson AFB, OH, 1987.

2. Berens, T.J., Multiple Model Algorithm for In-Flight Simulation. MS Thesis, GE/ENG/86D, School of Engineering, Air Force Institute of Technology, Wright Patterson AFB, OH, 1987.

3. Porter, B., Jones, A. H.,"Design of Adaptive Digital Set Point Tracking Controllers Incorporating Recursive Step-Response Matrix Identifiers For Multivariable Plants", Fourth IASTED International Symposium on Modelling, Identification and Control, Grindelwald, Switzerland, February 1985.

4. Porter, B., "Design of Direct Digital Flight-Mode Control Systems for High Performance Aircraft Using Step-Response Matrices", Proceedings of the IEEE National Aerospace Conference, Dayton, OH, May 1985, pp 507-513.

5. Porter, B., "Self-Designing Digital Control Systems. Progress and Forecast Report", Grant AFOSR-85-0208, Department of Aeronautical and Mechanical Engineering, University of Salford, Salford, England, November 1985.

6. Porter, B., Manganas, A., "Design of Fast Non-interacting Digital Flight-Mode Control Systems for High Performance Aircraft", Proceedings of the AIAA Guidance, Navigation, and Control Conference, Snowmass, Colorado, August 1985.

7. Porter, B., Manganas, A., "Design of Adaptive Direct Digital Flight-Mode Control Systems Incorporating Recursive Step-Response Matrix Identifiers for High Performance Aircraft", Proceedings of the IEEE National Aerospace Conference, Dayton, OH, May 1986.

8. Porter, B., "Design of High Performance Tracking Systems", AFWAL-TR-82-3032, Air Force Wright Aeronautical Laboraties, Wright-Patterson AFB, OH,1982.

9. Maybeck, P. S.,Stochastic Models, Estimation and Control, Vol. 2, Academic Press, New York, 1982.

10. Markman, S. R., "Capabilities of Airborne and Ground Based Flight Simulation", SAE Aerospace Technology Conference and Exposition, Long Beach, California, Oct. 198£, pp 35-42.

11. Barry, J. and Schelhorn, A. E., "A Modest Proposal for a New Fighter In-Flight Simulator", AAIA 22nd Aerospace Sciences Meeting, Reno, Nevada, Jan. 1984.

12. Rynaski, E. G., Memorandum on Improved Model-Following. ARVIN/CALSPAN Fight Research Dept., Buffalo N.Y., 20 July 1984.

13. Hartman, U. and Krebs, V., "Command and Stability Systems for Aircraft: A New Digital Adaptive Approach", Automatica, Vol 16, 1981, pp 135-146.

14. Hagglund, T., "New Estimation Techniques for Adaptive Control", PhD Dissertation, Report LUTFD2/(TFRT-1025)/1-120/(1983), Department of Automatic Control, Lund Institute of Technology, Lund, Sweden, December 1983.

15. Astrom, K. J., "Theory and Applications of Adaptive Control-A Survey", Automatica, Vol 19, No.5, 1983, pp 471-486.

16. Isermann, R., "Parameter-Adaptive Control Algorithms - Tutorial", Automatica, Vol 18, No. 5, 1982, pp 513-528.

17. Ljung, L. and Sodestrom, T., Theory and Practice of Recursive Identification, MIT Press, Cambridge, Mass., 1983.

18. Maybeck, P. S., and Hentz K. P., "Investigati Moving Bank Multiple Model Adaptive Algorithms of 24th Conference on Decision and Control. F FL, December 1985.
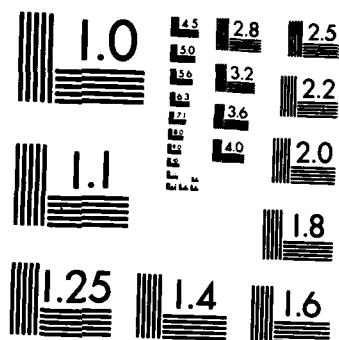
MICROCOPY RESOLUTION TEST CHART

NATIONAL BUREAU OF STANDARDS-1963-A

19. Athans, M., et. al., "The Stochastic Control of the F-8C Aircraft Using a Multiple Model Adaptive Control (MMAC) Method-Part 1: Equilibrium Flight", IEEE Trans. AC, Vol AC-22, No.5, pp 768-780, October 1977.

20. Eslinger, R. A., Multivariable Control Law for the AFTI/F-16 with a Failed Control Surface. MS Thesis, AFIT/GE/EE-84D-28.

21. Barfield, A., Multivariable Control Law Development for the AFTI F-16. MS Thesis, AFIT/GE/EE-84S-4. School of Engineering, Wright-Patterson AFB, OH, December 1982.

22. Kokotovic, P.V. and Haddad, A.H., "Controllability and Time Optimal Control of Systems with Slow and Fast Modes", IEEE Transactions on Automatic Control, Vol AC-20, Feb. 1975, pp 111-113.

23. Porter, B. and Shenton, A.T., "Singular Perurbation Analysis of the Transfer Function Matrices of a Class of Multivariable Linear Systems", International Journal of Control, Vol 21, No. 4, 1975, pp 655-660.

24. Wittenmark, B., "A Two-Level Estimator for Time Varying Parameters", Automatica, Vol 15, 1978, pp 85-89.

25. Iserman, R. and Lachman, K., "Parameter Adaptive Control with Configuration Aids and Supervision Functions", Automatica, Vol 21, 1985, pp 625-638.

26. Andersson, P., "Adaptive Forgetting and Recursive Identification through the Multiple Model Algorithm", International Journal of Control, No. 42, 1985, pp 1175-1193.

27. MATRIXx User's Guide, Integrated Systems Inc., Palo Alto, California, 1982.

28. Banda, S.S., and Ridgely, D.B., "Introduction to Robust Multivariable Control", AFWAL-TR-85-102, Wright Patterson AFB, Oh, Feb 1986.

VITA

Captain James R. Matthes was born on 23 March 1955 in Fairbanks, Alaska. He attended Troy State University, Troy, Alabama where he received the degree of Bachelor of Science in Mathematics in November 1978. Upon graduation, he received a commission in the USAF through the ROTC program and was assigned to the 3246th Test Wing, Air Force Systems Command at Eglin Air Force Base, Florida. At Eglin, he was a test engineer for the development, test, and evaluation phase of the Advanced-Medium-Range-Air-to-Air-Missile program. In September 1984, he attended Auburn University through a program sponsored by the Air Force Institute of Technology. In August 1986, he graduated from Auburn University with a Bachelor of Science degree in Electrical Engineering and was assigned to the Strategic Systems System Program Office, Air Force Systems Command at Wright Patterson Air Force Base, Ohio. At the program office he was the lead system integration engineer for the Air Launched Cruise Missile. In May 1986 he was assigned to the School of Engineering, Air Force Institute of Technology.

Permanent Address: 201 Priscilla Dr.

Ft. Walton Beach, Florida 32548

ADA189715

REPORT DOCUMENTATION PAGE

1a. REPORT SECURITY CLASSIFICATION	1b. RESTRICTIVE MARKINGS
UNCLASSIFIED	

2a. SECURITY CLASSIFICATION AUTHORITY	3. DISTRIBUTION/AVAILABILITY OF REPORT
	Approved for public release distribution unlimited
2b. DECLASSIFICATION/DOWNGRADING SCHEDULE	

4. PERFORMING ORGANIZATION REPORT NUMBER(S)	5. MONITORING ORGANIZATION REPORT NUMBER(S)
AFIT/GE/ENG87D-40	

6a. NAME OF PERFORMING ORGANIZATION	6b. OFFICE SYMBOL (If applicable)	7a. NAME OF MONITORING ORGANIZATION
School of Engineering	AFIT/ENG	

6c. ADDRESS (City, State, and ZIP Code)	7b. ADDRESS (City, State, and ZIP Code)
Air Force Institute of Technology Wright-Patterson AFB, OH 45433	

8a. NAME OF FUNDING/SPONSORING ORGANIZATION	8b. OFFICE SYMBOL (If applicable)	9. PROCUREMENT INSTRUMENT IDENTIFICATION NUMBER
Flight Dynamics Lab	AFWAL/FIGI	

8c. ADDRESS (City, State, and ZIP Code)	10. SOURCE OF FUNDING NUMBERS			
Wright-Patterson AFB, OH 45433	PROGRAM ELEMENT NO.	PROJECT NO.	TASK NO	WORK UNIT ACCESSION NO.

11. TITLE (Include Security Classification)

See Block 19

12. PERSONAL AUTHOR(S)
James R. Matthes, jr., B.S., Captain, USAF

13a. TYPE OF REPORT	13b. TIME COVERED	14. DATE OF REPORT (Year, Month, Day)	15. PAGE COUNT
MS Thesis	FROM _____ TO _____	1987 December	287

16. SUPPLEMENTARY NOTATION

17. COSATI CODES			18. SUBJECT TERMS (Continue on reverse if necessary and identify by block number)
FIELD	GROUP	SUB-GROUP	Multivariable Control, Flight Control Systems, Adaptive Control, Multiple Model Estimation
04	01		

19. ABSTRACT (Continue on reverse if necessary and identify by block number)

Title: MODEL SELECTION FOR THE MULTIPLE MODEL ADAPTIVE ALGORITHM FOR IN-FLIGHT SIMULATION

Thesis Chairman: John J. D'Azzo

20. DISTRIBUTION/AVAILABILITY OF ABSTRACT	21. ABSTRACT SECURITY CLASSIFICATION
☒ UNCLASSIFIED/UNLIMITED ☐ SAME AS RPT. ☐ DTIC USERS	UNCLASSIFIED

22a. NAME OF RESPONSIBLE INDIVIDUAL	22b. TELEPHONE (Include Area Code)	22c. OFFICE SYMBOL
Dr. John J. D'Azzo	513-255-2024	AFIT/ENG

Previous editions are obsolete.

    This thesis extends the research accomplished by Capt
Pineiro and Lt Berens in the area of adaptive algorithm imple-
mentation. Specifically, this thesis explores the performance
characteristics of the multiple model estimation algorithm and how
they influence the selection of aircraft models to allow the parameter
adaptive control system to maintain tracking performance over a
desired portion of the flight envelope. The aircraft dynamic
equations used are those of the AFTI/F-16 and the control law
design is based on the method developed by Professor Porter.
    Numerous fixed gain simulations are presented in order to
determine the performance robustness to plant variations of
selected flight conditions. From these simulations, performance
or robustness boundaries for each nominal are determined. Data
is then generated to ascertain the effect on the control surfaces'
responses of replacing the nominal model of a performance boundary
with another model within the same boundary. That leads to the
determination of the critical factors to be considered in choosing
an aircraft model to represent a specific set of performance
boundaries.
    Following the determination as to what factors are important
in establishing performance bounds for a fixed gain system, model
selection for the multiple model algorithm is evaluated. In attempt-
ing to select a set of aircraft models that would ensure an
acceptable level of tracking performance over the desired flight
envelope several two-, three-, and four-model configurations are
examined. Each configuration is evaluated to determine the amount
of overlap of performance bounds required for proper tracking
performance, the amount of the flight envelope that is covered,
and control surface performance.
    After selecting a set of aircraft models that results in the
best overall system response, the effect of adjusting the control
law gains on the performance of the multiple model estimation
algorithm is evaluated. By assuming that all states are access-
ible, sensor noise is them added to each of the longitudinal states
to study how noise impacts model selection. A set of models that
produces acceptable tracking performance over the desired flight
envelope and the most immunity to sensor noise is then selected.

END
DATE
FILM
4-88
DTIC